Université Blaise Pascal
(U.F.R. de recherche Scientifique et Technique)
ECOLE DOCTORALE DES SCIENCES FONDAMENTALE N°609
N°d´Ordre: D.U. 1940

&

University of Iceland
School of Engineering and Natural Sciences, Faculty of Earth Sciences
ISBN: 978-9979-9914-2-7

DISSERTATION FOR THE DEGREE OF DOCTOR OF PHILOSOPHY
Speciality: Volcanology

Holocene eruption history and magmatic evolution of the subglacial volcanoes, Grímsvötn, Bárdarbunga and Kverkfjöll beneath Vatnajökull, Iceland

By:

Bergrún Arna Óladóttir

Defended in Clermont-Ferrand on the 30th of June 2009

Rapporteurs: Patrick Bachelery – Université de la Réunion
Þorvaldur Þórðarson – University of Edinburgh
Examinateurs: Tim Druitt – Université Blaise Pascal Clermont-Ferrand
Sigurður Steinþórsson – University of Iceland
Supervisors: Guðrún Larsen – University of Iceland
Olgeir Sigmarsson – Université Blaise Pascal Clermont-Ferrand

Contents

Abstract

In order to study eruption history and magmatic evolution of the subglacial volcanoes, Grímsvötn, Bárdarbunga and Kverkfjöll, tephra layers have been sampled systematically from measured soil profiles around the Vatnajökull ice cap. In total 921 tephra samples have been analysed for major element composition by electron microprobe. Their provenance has been assessed by comparison with the chemical composition of products from each volcanic system as determined in previous studies. The major element compositions fall into three distinctive groups, each one featuring a compositional range reflecting a liquid-line-of descent. Although this grouping reinforces the compositional distinction between the three volcanic systems it also demonstrates that a slight overlap remains between the major element compositions. However, a more distinct grouping is obtained via in-situ trace element analyses by laser-ablation ICP-MS. Collectively, major and trace element compositions allow robust determination of provenance for basaltic tephra having similar major element composition, and consequently the Holocene tephra record around Vatnajökull is improved significantly.

On a regional scale the soil profiles are correlated using key tephra markers. The basaltic tephra between these markers are correlated via tephra stratigraphy and chemical composition. Approximately 70% of the tephra layers originate at Grímsvötn, Bárdarbunga or Kverkfjöll. The eruption frequency, calculated from tephra layer frequency in soil profiles around Vatnajökull, reveals Grímsvötn as the most active volcanic system followed by Bárdarbunga, but Kverkfjöll show episodic activity with repose periods of more than 1000 years. All three volcanic systems had lower eruption frequency 5-2 ka caused by decrease in volcanic activity traced to periodic magma generation and delivery from the mantle rather than changes in environmental factors such as changing ice load. During prehistoric time a 1-3 thousand years age difference is found between peak activities above the mantle plume (Grímsvötn and Bárdarbunga) and peak activities at volcanoes located farther SW on the non-rifting part of the Eastern Volcanic Zone (EVZ; e.g. Katla). This suggests that a significant increase could be expected in volcanism on this part of the EVZ in the future since the highest observed eruption frequency was only 2-1 ka in Grímsvötn and Bárdarbunga.

Magmatic evolution of the three volcanic systems is controlled by crystal fractionation and crustal contamination. Trace element systematic suggests similar source mineralogy beneath the three volcanoes. This allows an assessment of the relative magma source melting at depth: Bárdarbunga above the assumed centre of the Iceland mantle plume produces basalts formed by highest degree of melting whereas the smallest melt fraction is recorded in the Kverkfjöll basalts erupted farther away from the assumed plume centre. A deep magma source appears to have played an important role in the activity of both Grímsvötn and Bárdarbunga, with a sill and dyke complex most active beneath Grímsvötn during a period of highest eruption frequency. This complex evolved into a magma chamber approximately 1000 years ago with correspondingly lower eruption frequency. The compositional variations of basalts from both Grímsvötn and Bárdarbunga are consistent with the presence of active magma chambers in their plumbing systems at depth.

Útdráttur

Til að rannsaka gossögu og kvikuþróun eldstöðvakerfanna, Grímsvatna, Bárðarbungu og Kverkfjalla, hefur gjósku verið safnað kerfisbundið úr jarðvegssniðum umhverfis Vatnajökul. Aðalefni í gjóskusýnum hafa verið greind með örgreini og uppruni þeirra metinn með samanburði við áður birtar greiningar á gosefnum frá viðkomandi eldstöðvakerfum. Hinar nýju aðalefnagreiningar mynda þrjá hópa sem hver um sig stjórnast af eðlilegri kvikuþróun bergraða. Þrátt fyrir að hóparnir þrír auðveldi greiningu uppruna gjósku frá eldstöðvakerfunum þremur er enn örlítil skörun á efnasamsetningu þeirra. Snefilefna-greiningar voru framkvæmdar með "*laser ablation inductively coupled plasma mass spectrometry"* (LA-ICP-MS) til að skera úr um uppruna þeirra sýna sem skarast við aðalefnagreiningu. Samnýting aðal- og snefilefna við upprunagreiningu gjósku hefur bætt nútímagjóskutímatal umhverfis Vatnajökul umtalsvert.

Eftir greiningu uppruna gjósku og tengingu hennar milli jarðvegssniða má reikna gostíðni viðkomandi eldstöðvakerfa. Leiðarlög voru notuð við tengingu jarðvegssniða allt í kringum jökulinn og basísk gjóska milli leiðarlaganna var tengd út frá upphleðsluröð og efnasamsetningu. Grímsvötn, Bárðarbunga og Kverkfjöll hafa myndað 70% gjóskulaga sem finnast umhverfis Vatnajökul. Grímsvötn eru virkust bæði á sögulegum og forsögulegum tíma, næst kemur Bárðarbunga en Kverkfjöll reka lestina, en virknin þar einkennist af löngum goshléum (allt upp í 1200 ár). Öll eldstöðvakerfin þrjú höfðu hægt um sig á tímabilinu frá því fyrir 5000 til 2000 árum síðan en það er fremur rakið til djúpstæðra ferla í jarðskorpunni en til breytilegra umhverfisaðstæðna s.s. breytinga á jökulfargi og ísþekju. Á forsögulegum tíma sést eitt til þrjú þúsund ára munur á virknitoppum eldstöðva yfir íslenska möttulstróknum annars vegar og hins vegar á eldstöðvum á SV hluta Eystra gosbeltisins þar sem áhrif flekareks gætir ekki. Síðasti virknitoppur yfir möttulstróknum var fyrir tvö til eitt þúsund árum sem bendir til þess að aukinnar eldvirkni geti farið að gæta á SV hluta Eystra gosbeltisins.

Kvikuþróun eldstöðvakerfanna þriggja stjórnast af hlutkristöllun og skorpumengun. Kerfisferli snefilefna (trace element systematic) benda til svipaðrar steindasamsetningar djúpstæðrar "kvikuuppsprettu" undir öllum eldstöðvakerfunum sem leiðir af sér að hægt er að meta hlutfall kvikubráðar úr henni. Bárðarbunga, sem er staðsett yfir miðju möttulstróksins myndar basalt sem einkennist af mestu hlutfalli bráðar en Kverkfjallabasalt, sem myndast mun lengra frá áætlaðri miðju möttulstróksins, einkennist af mun minni bráðnun. Hin djúpstæða "kvikuuppspretta" virðist eiga töluverðan þátt í virkni bæði Grímsvatna og Bárðarbungu. Á því tímabili í sögu Grímsvötna kerfisins sem einkennist af mestri virkni þess samanstóð kvikuaðfærslukerfið af göngum og sillum. Fyrir um þúsund árum þróaðist kvikuhólf úr ganga- og sillukerfinu sem leiðir af sér lægri gostíðni. Efnasamsetning basalts frá Grímsvötnum og Bárðarbungu bendir til þess að í dag sé virkt kvikuhólf í aðfærslukerfi beggja eldstöðvanna.

Résumé

Dans le but d'étudier l'activité volcanique et l'évolution magmatique des volcans sous-glaciaires de Grímsvötn, Bárdarbunga and Kverkfjöll, des téphras ont été systématiquement échantillonnés au sein de profils établis dans des sols autour du glacier de Vatnajökull en Islande. La composition en éléments majeurs de 921 échantillons de téphra a été analysée par microsonde, ce qui a permis, par comparaison avec la composition chimique des différents produits émis par ces systèmes volcaniques, de déterminer leur provenance. Les nouveaux résultats indiquent trois groupes de composition distincts, présentant chacun des variations cohérentes avec une évolution cotectique. Si l'identification de ces groupes améliore la distinction compositionnelle entre les produits émis par les trois systèmes volcaniques étudiés, une légère superposition des compositions demeure néanmoins entre ces différents groupes.
L'analyse in-situ des teneurs en éléments traces par ICP-MS à ablation laser permet toutefois d'affiner leur distinction. Ensemble, l'analyse des teneurs en éléments majeurs et traces permet d'améliorer significativement l'identification de la provenance des téphras basaltiques Holocène qui peuvent avoir des compositions en éléments majeurs similaires autour de Vatnajökull.
Régionalement, les profils établis dans les sols sont corrélés les uns aux autres en utilisant des niveaux de téphras marqueurs clefs, et les unités intermédiaires sont corrélées grâce à des outils stratigraphiques et à leur composition chimique. Approximativement, 70% des couches de téphras viennent de Grímsvötn, Bárdarbunga ou Kverkfjöll. La fréquence éruptive de Grímsvötn indique que c'est le système volcanique le plus actif, suivi par Bárdarbunga. En revanche, Kverkfjöll présente une activité épisodique avec des périodes de repos supérieures au millier d'années. La diminution de la fréquence éruptive observée il y a 2000-5000 ans dans les trois systèmes volcaniques, est liée à une diminution de l'activité volcanique et non à des facteurs environnementaux. Pendant la préhistoire, une différence d'âge de 1000-3000 ans a été observée entre les pics d'activité à l'aplomb du panache mantellique (Grímsvötn and Bárdarbunga) et les pics d'activité des volcans localisés au Sud-ouest, dans la partie hors-rift de la Zone Volcanique Est (ZVE; e.g. Katla). Ceci suggère qu'une importante augmentation de l'activité volcanique dans cette partie du ZVE est attendue dans un futur proche car la fréquence éruptive maximum a été observée il y a 1000-2000 ans à Grímsvötn et Bárdarbunga.
L'évolution magmatique des trois systèmes volcaniques étudiés est contrôlée par les processus de cristallisation fractionnée et de contamination crustale. Les teneurs en éléments traces indiquent des minéralogies similaires dans les différentes sources magmatiques sous les trois volcans. Ceci permet alors d'accéder aux conditions relatives de fusion partielle du manteau source: Bárdarbunga à l'aplomb du centre du panache mantellique islandais produit des basaltes issus de plus forts degrés de fusion alors que les plus faibles degrés de fusion sont atteint sous Kverkfjöll, plus loin du centre du panache. Une source magmatique profonde semble avoir joué un rôle important dans l'activité de Grímsvötn et Bárdarbunga, avec un système de sills et dykes plus actif sous le système volcanique de Grímsvötn pendant la période de plus forte fréquence éruptive. Ce système a évolué en chambre magmatique il y a environ 1000 ans, ce qui explique les plus faibles fréquences éruptives observées à cette période. Un lien direct semble lié la fréquence éruptive à l'architecture de la chambre magmatique. Les variations de composition des basaltes issus de Grímsvötn et Bárdarbunga sont consistantes avec la présence d'une chambre magmatique active en profondeur.

Acknowledgement

When looking back over the last four years of my life I realise that there is a large group of people that have helped me and supported in many ways during my studies. I would like to express my thanks to all of them for helping me realizing this dissertation.

First and foremost I want to thank both of my excellent supervisors, Guðrún Larsen and Olgeir Sigmarsson for their help and I believe endless patience towards me. Guðrún, who has supervised me not only during this PhD work but also for my bachelors and masters degree, I specially thank for teaching me to understand tephra during numerous field trips and for the countless amusing stories told around Vatnajökull and in the south of Iceland during the last six years. It is mostly due to you that I am beginning to get to know my own country, at least from the geological point of view. Olgeir has also supervised my longer than just during this PhD study as he also supervised my masters study. I specially thank Olgeir for all the discussions we have had, both scientific and completely unscientific, for his field "assistance" and last but not least to opening my eyes to study in France.

During my stay in France I am especially indebted to Olgeir and his family, Hildur, Logi and Kári, for their enormous hospitality and goodwill in my behalf, inviting me to their home in La Roche Blance for countless suppers, dinners and days, for carrying e.g. my washing machine up and down narrow stairs in French houses and storing all my furniture when I went back to Iceland for field summers.

Karen Pascal is genuinely thanked for finding two apartments for us in Clermont, for making me laugh and sometimes cry, for improving my French and being a friend for the two years we rented together. The stay in Clermont would not have been the same without you.

I thank Marie-Claire Comte-Rome at the Service d´Accueil et de gestion des Boursiers Internationaux in Clermont-Ferrand from the bottom of my hart for her hospitality, kindness and general interest.

Erwan Martin helped translating the English abstract to a French "résumé" and is genuinely thanked for that as well as his good company in Iceland, France and California.

I thank all of the people at Laboratoire Magmas et Volcans, especially Sébastian Loock and Guillaume Bertrand whom I shared office with during three years and all the other PhD students that showed great patience listening to my sometimes invented French. Last but not least I am particularly thankful to Jean-Luc Devidal for interesting discussions and his help and endless tolerance during microprobe analyses. Since October 2005 he has calibrated the microprobe at least 60 times for me and allowed me to acquire about 8000 point analyses

during which I managed to make a part of the A99 standard disappear and analyse the sample holder to mention but a few small struggles I ran into and he solved one handed.

Several people have assisted me during field work in Iceland, Guðmundur Óli Sigurgeirsson, Ester Anna Ingólfsdóttir, Sóley Unnur Einarsdóttir, Gustav Pétursson and Tenley Banik all helped during measuring and sampling in different places. The members of the rescue team Kyndill, Jón Þorbergsson and Guðmundur Vignir Steinsson helped me get across the Núpsvötn glacial river using the huge four wheel drive vehicles of Kyndill when the water was too high for my "Barbie jeep", as did Ármann Höskuldsson who provided his own all terrain jeep. Fjölnir Torfason at Hali in Suðursveit showed us the Steinadalur profile and Ragnar Frank Kristjánsson and Hafdís Roysdóttir at the Skaftafell National Park made work inside the park easier.

I want to thank my fellow PhD students at the University of Iceland for discussion and support, especially Esther Ruth Guðmundsdóttir a fellow tephra student and Hrafnhildur Hannesdóttir who guarded my desk in Askja while I was away in France; I also thank the members of the Earth science Institute for fruitful discussion and comments on this work during the years. Thanks to Anna Eiríksdóttir for her help with financial matters.

For financial support I am thankful to: the Icelandic Science Foundation, the National Power Company Landsvirkjun, Eimskip Fund of the University of Iceland, the French government through a student's grant and the French-Icelandic collaboration programme Jules Verne.

Last but not least I thank all of my friends and family for supporting me during these years, for welcoming me every time I came back home and remembering me during my months away. My special thanks go to my parents that have encouraged me in every thing I strangely decide to do, to my mother for teaching me to like and love the nature and all of its creatures, to my father for his endless interest in my geology work and unlimited optimism in all fields of live. Gustav Pétursson and his daughter Katrín Valgerður are thanked for reintroducing me to regular hot meals and normal family live rhythm as well as teaching me to respect one unscientific rule: Holidays mean time off!

1. Introduction

This doctoral thesis is based on three manuscripts of scientific papers, included as chapters, preceded by a short overview of the geology of Iceland, field methods and analytical methods. A short summary of the work obtained during the three and a half year covering the PhD project follows as general conclusions. The paper manuscripts are the following:

1. Provenance of basaltic tephra in soil profiles around the Vatnajökull ice cap, Iceland, by Bergrún Arna Óladóttir, Olgeir Sigmarsson, Guðrún Larsen and Jean-Luc Devidal. **Chapter 4**
2. Holocene activity at the Grímsvötn, Bárdarbunga and Kverkfjöll subglacial volcanoes of Vatnajökull, Iceland, by Bergrún Arna Óladóttir, Guðrún Larsen and Olgeir Sigmarsson **Chapter 5**
3. Origin and ascent of basaltic magma at the subglacial volcanoes beneath northwest Vatnajökull, Iceland, by Bergrún Arna Óladóttir, Olgeir Sigmarsson and Guðrún Larsen **Chapter 6**

1.1 Project background

The first thing you learn when beginning to study geology is that the present is the key to the past. In order to understand volcanoes and their behaviour in the present and in the unforeseen future it is vital to know and understand their behaviour in the past. Being brought up in the vicinity of the Vatnajökull ice cap made me understand the importance of hazard prediction related to the glacier itself and the volcanoes it covers. By studying the prehistoric and historical activity of three volcanoes covered by Vatnajökull their future activities can be predicted more confidently than before.

The eruption history of Icelandic volcanoes is well known during historical time or since the Vikings came across the Atlantic Ocean and settled in Iceland in ~870 AD. Many of the largest eruptions that have taken place during these ~1100 years are mentioned in written documents but knowledge about the smaller eruptions has been obtained through studies of tephra preserved in glaciers, soils and lakes (e.g. Thorarinsson 1944; 1958; 1961; 1967; 1974; Thorarinsson and Sæmundsson 1979; Thorarinsson 1980; 1981; Larsen 1982; 1984; Haflidason et al. 1992; Larsen 1996; Larsen et al. 1998; 1999; Larsen 2000; Óladóttir et al. 2005; 2008).

The tephra composition holds important information on its provenance and magmatic evolution in part controlled by the type of plumbing system feeding the volcanoes. By

combining information on eruption frequency and magmatic evolution through tephra series throughout the Holocene, information on volcanic behaviour and magmatic evolution, otherwise difficult or even impossible to approach, become easily accessible. This greatly improves knowledge on volcano behaviour in the past and allows further assessment of potential volcanic hazards at the volcano of interest.

1.2. Brief overview of the geology of Iceland

Iceland (63°23'N to 66°30'N) is located at the junction between the Reykjanes Ridge in the south and the Kolbeinsey Ridge in the north, where the Mid-Atlantic Ridge is superimposed on the Iceland mantle plume (Fig. 1). This location explains the high magma production and eruption frequency in Iceland. In historical time (i.e. last ~1100 years) 205 eruptions are known to have occurred (Thordarson and Larsen 2007) or one eruption every ~5 years.

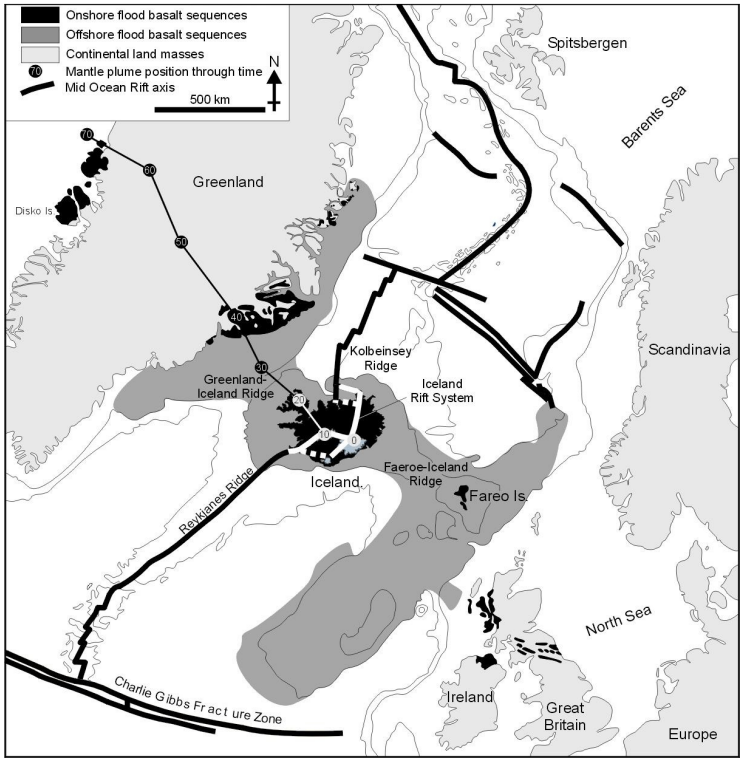

Figure 1 Iceland is situated in the middle of the North Atlantic at the junction between the Reykjanes and Kolbeinsey Ridge segments. The dotted line shows the Iceland mantle plume position for the last 65 million years. From Thordarson and Höskuldsson (2002) after Saunders et al. (1997)

Volcanism on the island is confined to three axial rifts and two intra-plate volcanic belts (Fig. 2). The axial rift zones, which correspond to the plate boundary across Iceland, are the focus of active spreading and characterized by tholeiitic volcanism (Jakobsson 1979a; Óskarsson et al. 1982). The axial rifts zones are divided into three zones, the Western, Northern and Eastern Volcanic Zones (WVZ, NVZ, EVZ, respectively). The first two are thought to represent the main rifts in Iceland, whereas the last one (i.e. the EVZ) is a rift in making via southwest propagation through older crust (Meyer et al. 1985; Óskarsson et al. 1985; Hardarson et al. 1997). Most of the volcanic activity in the country occurs on these volcanic zones, although the Eastern Volcanic Zone is by far the most active today (e.g. Sæmundsson 1979; Thordarson and Larsen 2007).

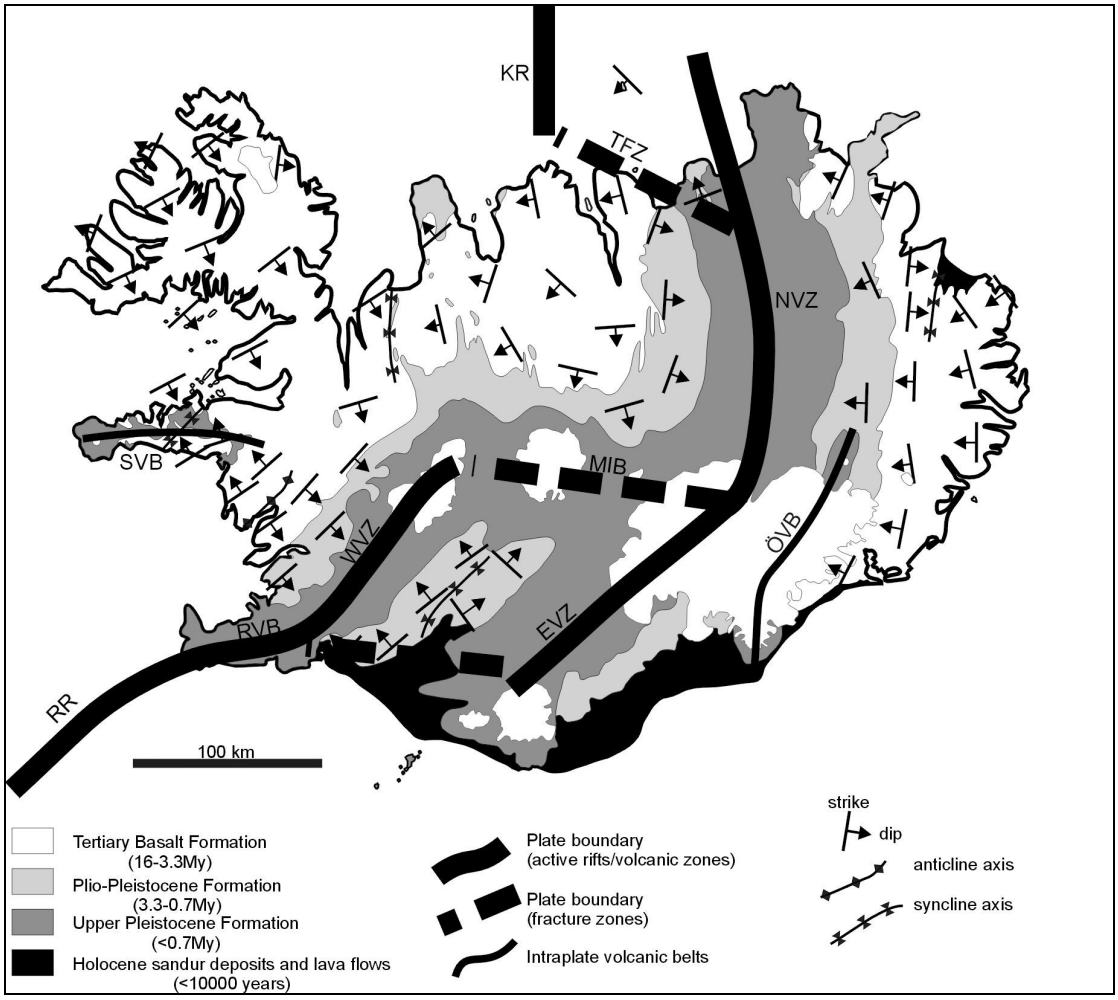

Figure 2 The principal elements of the geology in Iceland, outlining the distribution of the major geological subdivisions, including the main fault structures, volcanic zones and belts. RR: Reykjanes Ridge, RVB: Reykjanes Volcanic Belt, WVZ: Western Volcanic Zone, MIB: Mid-Iceland Belt, EVZ: Eastern Volcanic Zone, NVZ: Northern Volcanic Zone, TFZ: Tjörnes Fracture Zone, KR: Kolbeinsey Ridge, ÖVB: Öræfi Volcanic Belt and SVB: Snæfellsnes Volcanic Belt. After Thordarson and Höskuldsson (2002) as modified from Jóhannesson and Sæmundsson (1998a).

The volcanic belts of Öræfi and Snæfellsnes are characterized by mildly alkalic magmatism where young (<2 million years) volcanic rocks rest unconformably on older tholeiite rock formations (Meyer et al. 1985; Steinthórsson et al. 1985). The Öræfi Volcanic Belt is situated to the east of the plume centre as well as the current plate margins and may represent an embryonic rift. The Snæfellsnes Volcanic Belt is located in west Iceland (Fig. 2).

The volcanic zones and belts feature discrete volcanic systems, which are the principal geological structure in Iceland (Fig. 3; Sæmundsson 1978; Jakobsson 1979b; Meyer et al. 1985). A volcanic system consists of a fissure swarm, a central volcano, or both. These structures are interpreted as being the surface expressions of two different types of subsurface magma holding structures: the first a deep-seated magma reservoir, the second a shallower crustal magma chamber (Gudmundsson 1995; 2000). Each volcanic system is characterised by conspicuous tectonic architecture and distinct magma composition and typically has a

lifetime between 0.3-0.5 million years (Sæmundsson 1978) and some system are known to have been active for 2-2.5 million years (Jóhannesson 1975). All together there are 30 active volcanic systems in Iceland (Jóhannesson and Sæmundsson 1998a).

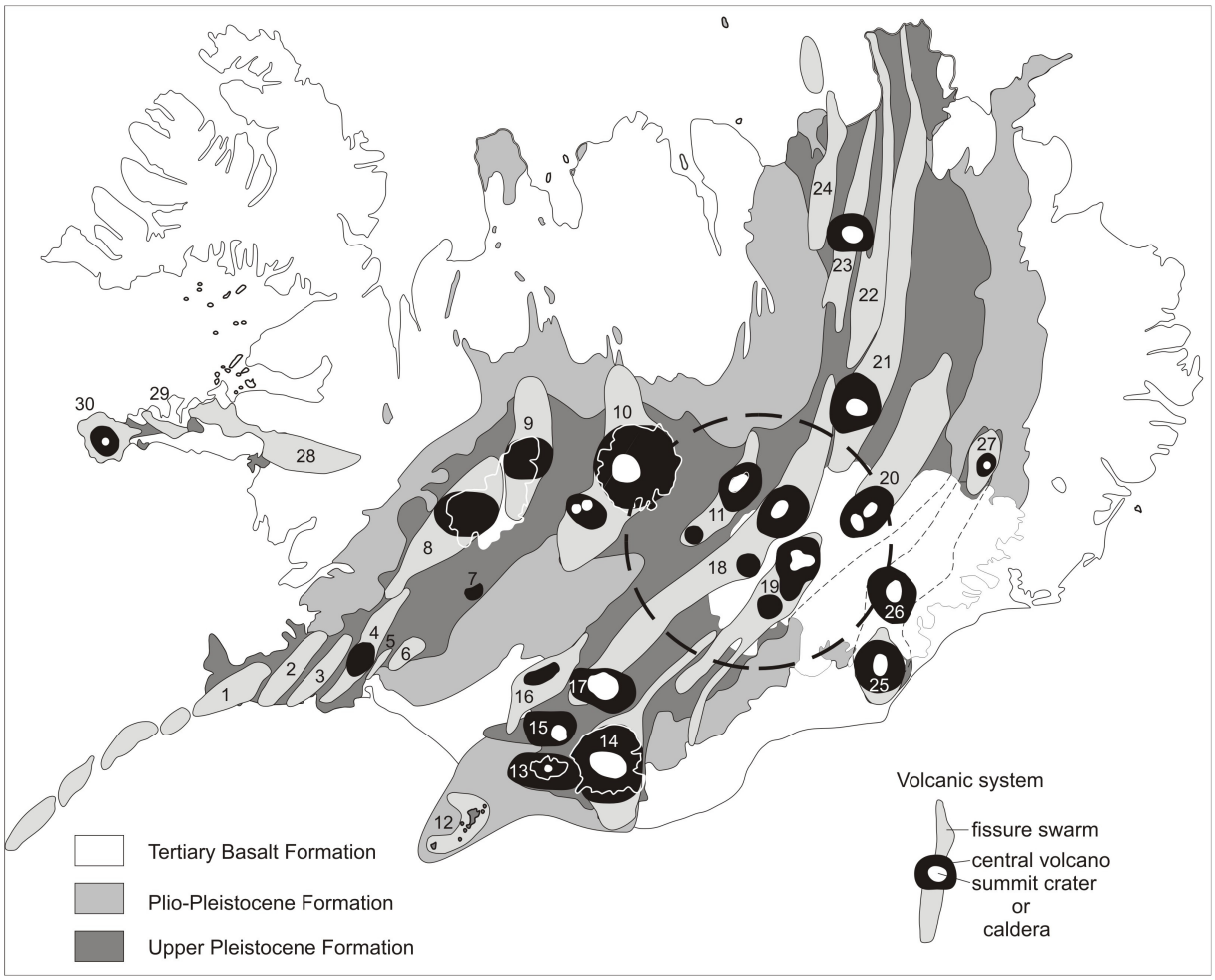

Figure 3 Volcanic systems in Iceland. 1. Reyjanes, 2. Krýsuvík, 3. Brennisteinsfjöll, 4. Hengill, 5. Hrómundartindur, 6. Grímsnes, 7. Hrafnabjörg, 8. Prestahnjúkur, 9. Kjölur, 10. Hofsjökull, 11. Tungnafellsjökull, 12. Vestmannaeyjar, 13. Eyjafjallajökull, 14. Katla, 15. Tindfjöll, 16. Hekla, 17. Torfajökull, 18. Bárdarbunga, 19. Grímsvötn, 20. Kverkfjöll, 21. Askja, 22. Fremrinámur, 23. Krafla, 24. Þeistareykir, 25. Öræfajökull, 26. Esjufjöll, 27. Snæfell, 28. Ljósufjöll, 29. Lýsuskarð, 30. Snæfellsjökull. From Thordarson and Larsen (2007) modified from Jóhannesson and Sæmundsson (1998a).

1.3 The volcanic system Grímsvötn

The Grímsvötn volcanic system is located on the northern part of the EVZ but this part of the volcanic zone is considered to be part of the main rifting zone whereas the southern part of the EVZ is a rift in making that might be taking over as the main rift in South Iceland (Sæmundsson 1978; Gudmundsson 2000; Einarsson 2008). Grímsvötn produce magma of tholeiitic composition and the system is mostly covered by the Vatnajökull ice cap (no. 19 on Fig. 3). As a result explosive basaltic eruptions are frequent due to water-magma interaction.

The Grímsvötn volcanic system is 100 km long and up to 23 km wide and covers an area of 1350 km^2, of which the central volcano and 2/3 of the fissure swarm are covered by the ice cap (Sæmundsson 1978; Jakobsson 1979b; Jóhannesson and Sæmundsson 1998a). It consists of an embryonic fissure swarm and a central volcano, Grímsvötn, with a composite caldera and extensive geothermal activity therein. Þórdarhyrna has been proposed as a second central volcano in this volcanic system (Björnsson and Einarsson 1990; Jóhannesson and Sæmundsson 1998a; Thordarson and Larsen 2007). The Laki flood lava eruption that took place in 1783-1784 on a 27 km long fissure is the only historical eruption that has taken place on the ice free part of the Grímsvötn system. It produced ~14.7 km^3 of lava and ~0.4 km^3 (DRE) of tephra (Thordarson and Self 1993; Thordarson and Larsen 2007).

Several studies aimed at better comprehension of the internal structure of Grímsvötn have been undertaken. These include gravity and magnetic studies (Gudmundsson and Milsom 1997; Gudmundsson and Högnadóttir 2007) as well as teleseismic earthquake data analyses (Alfaro et al. 2007) revealing a magma chamber at ~3 km depth underneath the central volcano (Alfaro et al. 2007). GPS measurements also showed uplift in Grímsvötn due to inflation prior to the 1998 eruption followed by subsidence after the eruption due to a pressure drop in the assumed magma chamber (Sturkell et al. 2003).

1.4 The volcanic system Bárdarbunga

The Bárdarbunga volcanic system (also referred to as the Veidivötn system or Bárdarbunga-Veidivötn system) produces basalts of tholeiitic composition and is considered as one of the volcanic systems on the EVZ although its northern part extends into the NVZ (no. 18 on Fig. 3). It is part of the main rifting section of the EVZ.

The Bárdarbunga volcanic system is 190 km long and up to 28 km wide, covering about 2500 km^2 which makes it Iceland's most extensive volcanic system (Thordarson and Larsen 2007). About 60 km, out of the 190 km, are partly ice covered (Sæmundsson 1978). The system has a well-developed fissure swarm and two proposed central volcanoes located under the ice cap, Bárdarbunga that contains a 700 m deep caldera and Hamarinn (Björnsson and Einarsson 1990; Jóhannesson and Sæmundsson 1998a). Three of the historical eruptions occurred on the ice free part of the volcanic system (Larsen 1984).

The internal structures of Bárdarbunga are not as well studied as in Grímsvötn but gravity data show density anomalies indicating high density body underneath Bárdarbunga (Gudmundsson and Högnadóttir 2007) that have been interpreted as cumulates of gabbro from an overlying magma chamber (e.g. Melengreu et al. 1999; Ablay and Kearey 2000).

Bárdarbunga has been one of the most seismically active volcanoes in Iceland showing an abrupt increase in activity in 1974 that lasted for 22 years ending with the Gjálp eruption in 1996. This activity has been interpreted by Einarsson (1991) as a response to decreasing pressure in a magma chamber. During the Gjálp eruption in 1996, that took place midway between Bárdarbunga and Grímsvötn, deflation was observed on InSAR images (Pagli et al. 2007) also interpreted as a result of an underlying magma chamber beneath Bárdarbunga but incompatible trace element ratios as well as $\delta^{18}O$ and $^{87}Sr/^{86}Sr$ of the magma erupted at Gjálp eliminate the possibility of an origin at Bárdarbunga but strongly suggest that the magma were produced at Grímsvötn volcano (Sigmarsson et al. 2000).

1.5 The volcanic system Kverkfjöll

The Kverkfjöll volcanic system, named after its central volcano, is located on the NVZ and produces evolved tholeiitic magma. The Kverkfjöll system is 120 km long and 20 km wide, covering 1600 km^2, most of which are ice free (no. 20 on Fig. 3). It contains a mature fissure swarm and a central volcano with two calderas and considerable geothermal activity is associated with the northern one (Björnsson and Einarsson 1990; Jóhannesson and Sæmundsson 1998a; Thordarson and Larsen 2007). Not much is known about this volcanic system and no historical eruption is known with certitude. It has still not been studied with geophysical methods but the considerable geothermal activity points towards the presence of shallow magma intrusions or a magma chamber.

1.6 Tephra and tephrochronology

A substantial part of the Holocene volcanism in Iceland is manifested in explosive eruptions (e.g. Thordarson and Höskuldsson 2008) where the products are partly or solely tephra. Hydromagmatic basaltic eruptions are the characteristic explosive style, the reason being the presence of ice caps and high water table in the volcanic areas, and the majority of tephra layers in Icelandic soils and sediments are of basaltic composition (Larsen and Eiríksson 2008a).

Tephra layers can be regarded as archives of the eruption history for volcanic systems where it has been demonstrated that explosive eruptions dominate the activity. Individual tephra layers are records containing information on (1) the type of activity, (2) the intensity and mechanism of the eruption that produced the deposit, (3) the magnitude of the explosive eruption or explosive phase and (4) the course of eruptive events. It also holds information on the melt composition at the time of eruption and the vigour with which the magma was

erupted. Tephra layer sequences extending over thousands of years can provide information on eruption frequency and on magma evolution with time in a volcanic system (e.g. Óladóttir et al. 2005; Óladóttir et al. 2008).

Individual tephra layers can be used as isochrons or time-parallel marker horizons within the area affected by the tephra-fall, which may cover several hundred thousand km^2. Magma composition and type of explosive activity determine the characteristics of the tephra and thereby the potential to identify and correlate the tephra horizons. Once a tephra layer has been dated, that particular date applies to all the area where the individual tephra layer is found. In the 1930's Sigurdur Thorarinsson began his pioneering research to develop tephrochronology as a tool for dating, a method now used world wide in various branches of environmental sciences as well as in geosciences (Thorarinsson 1944; 1981).

The application of tephra layers as a tool in research began in the late 1920's and 1930's in New Zealand, Japan, Iceland (Grange 1931; Uragami et al. 1933; Thorarinsson 1944) and South America where Auer and Sahlstein, two Finnish geologists, used tephra as marker horizons when studying Tierra del Fuego (e.g. Alloway et al. 2007). Tephra is the Greek word for ash adopted by Thorarinsson (1944) to describe all pyroclasts erupted explosively and leaving the volcanic source by air, regardless of size, shape and type. Tephrochronology is also a term introduced by Thorarinsson (1944) in his doctoral thesis from Stockholm University and he defined the term in English (1981) as a dating method based on the identification, correlation and dating of tephra layers. Until the 1970's it was uncommon to do geochemical analyses on single small grains and Waagstein and Jóhansen (1968) as well as Persson (e.g. 1971), among the first to apply Thorarinsson's techniques outside Iceland, correlated tephra layers found in Scandinavia to their provenance in Iceland using refractive indices of glass shards and grain size distribution (Wastegard 2005 and references therein). Today, analytical methods have developed so that major and trace element composition in single tephra grains can be measured by electron microprobe and laser ablation ICP-MS, making fingerprinting and correlation of tephra much easier than during the pioneer days of tephrochronology when mapping of tephra dispersal was the main tool for finding tephra origin.

Today, 65 years after the introduction of the two terms, they have grown a part of geological terms widely used and to a new field of study used in many parts of the world such as Europe (e.g. Dugmore 1989a; Dugmore et al. 1995; Haflidason et al. 2000; Wastegard et al. 2000; van den Bogaard and Schminke 2002; Wastegard 2005), New Zealand (e.g. Shane 2000) and Africa (e.g. Pyle 1999). In Iceland the field of tephrochronology has added a vast

amount of information on the volcanic history of the country. In fact great parts of the volcanic history of Iceland are inaccessible without tephra studies as many of the largest volcanoes are covered by glaciers making lava production considerably less important and partly unreachable if and where lava has formed. Tephra layers originating in Iceland are nowadays correlated over the Atlantic Ocean (e.g. Dugmore et al. 1995; Haflidason et al. 2000) by tephra invisible to the naked eye but detected with different techniques such as x-ray photography and magnetic susceptibility (e.g. Gehrels et al. 2006).

The present study utilizes multiple identities of tephra layers, such as chemical composition, colour, thickness, and grain size, as data-archives on the eruption history of the parent volcanic systems. The tephra is also used as isochrons that allow correlation and synchronization between areas spaced tens to hundreds of km apart to unravel the eruption frequency and magma evolution of the three volcanic systems Grímsvötn, Bárdarbunga and Kverkfjöll.

1.7 Volcanic glass

Volcanic glass is amorphous natural material, formed if a liquid is cooled very rapidly without any crystallisation (e.g. Spudis 2000; Wallace and Anderson Jr. 2000). Basaltic glass is divided in two types (Fig. 4), sideromelane, light brown to brown homogeneous translucent glass and tachylite, an opaque magnetic glass with abundant microlites. Tachylite results from slightly slower quenching than sideromelane. Palagonite is produced upon hydration of sideromelane but the term sideromelane was first used by Robert Bunsen and Sartorius von Walterhausen in 1846 when they were studying palagonite in Iceland. They noted that the palagonite core often contained a water-free glass like material similar to obsidian and named it sideromelane. Microprobe analyses are obtained on fresh sideromelane glass cores rather than tachylite as they produce better totals, partly due to the fact that sideromelane is purer glass.

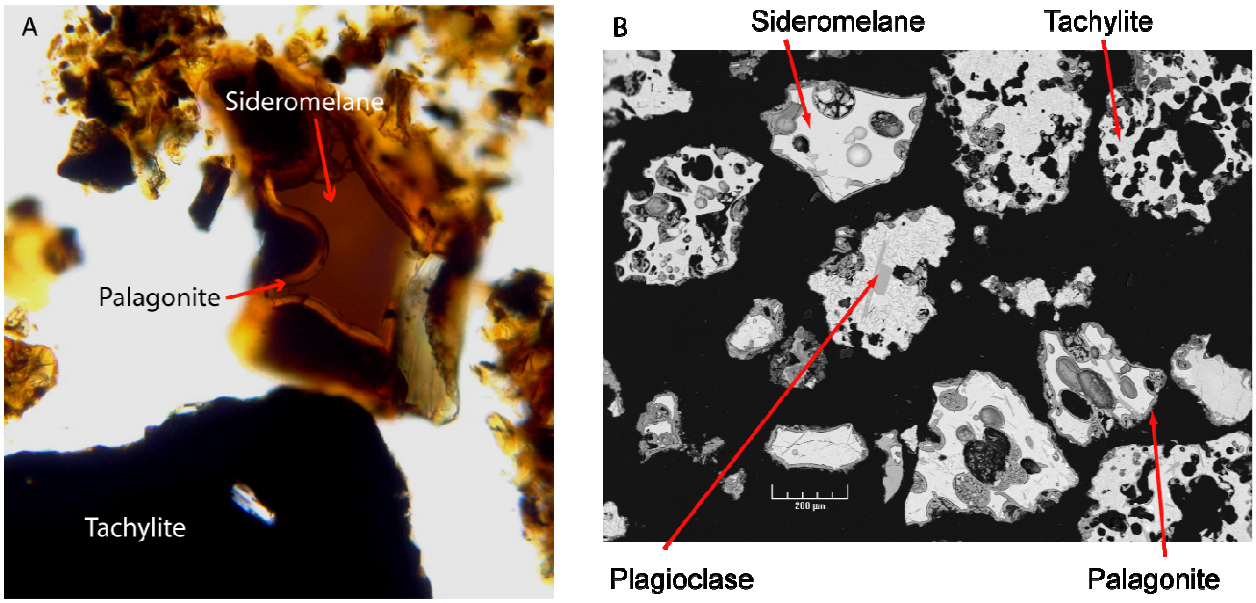

Figure 4 Sideromelane, tachylite and palagonite. A) Photo taken through a microscope with transmitted light. The sideromelane is light brown to brown with a lighter rim of palagonite whereas the tachylite is completely black due to its opaque character. B) Photo taken with a Scanning Electron Microscope (SEM) by S. Bonnefoy. The sideromelane is clear and light grey with spherical bubbles and the palagonite rime is presented in a darker grey tone. The tachylite is full of microlites and the bubbles have much more irregular forms.

2. Methods

2.1 Field methods and criteria (chapter from Óladóttir et al. 2005)

In order to obtain a representative composite tephra section, selection of suitable soil profiles is critical. Firstly, such profiles have to be located at an appropriate distance from the source volcano. Close to a volcano the tephra is often deposited on barren ground, increasing the likelihood of erosion and reworking of the primary fall. This decreases the preservation potential of individual layers and may also result in significant contamination between adjacent tephra layers. On the other hand, a soil section too far from the source volcano will not include tephra fall from low-intensity eruptions due to their limited dispersal. Secondly, the topography has to be favourable. Tephra layers are best preserved in topographic lows which commonly act as sediment traps ensuring rapid burial of the tephra. Thirdly, the sections should contain tephra layers that show minimal post-depositional reworking and disturbance, i.e. contain the primary facies of the tephra fall.

The macroscopic characteristics that are used to distinguish individual tephra layers are a function of several factors. The colour of the tephra is a direct function of chemical composition, in general changing from black to white with increasing silica. Properties such as grain size and size distribution, sorting and clast shapes are symptomatic of the nature of the explosive activity that produced the layer. The type and content of crystals and lithics are also diagnostic features in some tephra layers (Table 1). Silicic tephra layers are readily identified in Icelandic soils by their light colour and are therefore ideal key marker horizons for correlation between profiles.

When measuring and sampling soil profiles the sampling is done last, both to double check the measurement and to have the over all picture of the section before sampling tephra from it. To reduce risk of contamination from overlying tephra layers during sampling it is best to begin at the top and work down the section. To ensure representative sampling of each layer, a bulk sample is required, i.e. equal amount is taken across each layer from top to bottom. It is also important to clean the tools thoroughly after each sampled layer to avoid contamination between layers. The objective of the study controls the minimum thickness of sampled tephra layers. This study focuses on the over all eruption frequency of three volcanoes, hence even the thinnest tephra layers are sampled when possible.

Table 1 Criteria used during field measurements. Key parameters used for describing tephra layers in a soil profile

Parameters	Description
Thickness	Three to five thickness measurements are made on each layer to obtain a meaningful average value and information on minimum and maximum thickness for each tephra layer in a section. Tephra thicknesses are a function of eruption intensity, distance downwind from source and distance from the dispersal axis.
Contacts	Pristine sub-aerial tephra fall deposits typically have sharp and non-erosional contacts. Deviations may suggest post-depositional modification by reworking or soil creep.
Colour	Colour of tephra layers reflects their composition. Basaltic tephra layers are typically black, brownish-black, or greyish black, whereas tephra layers of intermediate compositions are commonly brown to greyish brown. Silicic layers are typically light coloured, with colours changing from olive-grey to light-grey to yellowish-white to white in accordance with increasing SiO_2 contents.
Grain size	Estimates of mean grain size and sorting for each layer, classification of grain types and measurements of five largest grains were used to obtain qualitative information on eruption type and intensity.
Depositional structures	Internal bedding (stratification), bed-forms, size grading and fabric provided information on modes of transport and deposition (i.e. to establish primary versus secondary origin). In case of primary tephra fall deposits internal stratification may reflect changes in eruption style or periodicity of activity, whereas size grading may reflect changes in eruption intensity or change in tephra dispersal direction.
Components	The relative abundance of pyroclasts and accessory components (i.e. wall-rock lithics and crystal fragments) is documented as it is a good indicator of eruption type and style.
Other observations	Any other observations that provide additional information about the tephra layer and its impact on the local environment (i.e. presence of tree trunks/molds or material of archaeological significance, etc.)

2.2 Sample handling

The samples were air dried and cleaned by handpicking and sieving in steel mesh sieves. The 125 µm size fraction was preferred for 100 µm thick polished thin sections for in-situ measurements but supplemented if necessary by the 63 and/or 250 µm size fractions. The 125 µm was chosen as it most commonly represents the main size fraction of a tephra deposit in the soil profiles deemed to be at a suitable distance from the volcanic source (see chapter 2.1). This size fraction is also straightforward to work with during cleaning and sieving. Additionally, the number of grains that fit into a standard tephra thin-section is right for obtaining representative number of chemical analyses. Last but not least in order to analyse trace elements a solid tephra core of 60 µm is required and as the tephra grains are often vesicular, grains of diameter ≥125 µm are necessary for trace element analyses.

3. Analyses

3.1 Electron microprobe analysis – technique

Electron microprobe analysis is a technique that has been developed since the middle of the 20th century using an electronic beam to excite atoms in a sample. The source of electrons is a tungsten wire placed in an electron gun. Electric current is passed through the wire and heats it up until it emits electrons that are accelerated from the gun. The electrons are directed through a column containing several lenses to focus the beam on the sample. When the sample is bombarded with electrons the atoms of individual elements are excited to higher energy states and as they relax to regain their initial lower energy state, characteristic x-rays are emitted. These x-rays are directed to spectrometers, where the number of x-rays created by each element to be measured is counted. The counts for individual element are compared to counts for the same element on a standard of known composition, which in turn is used to calculate the amount of each element in atomic per cents or weight per cents in the sample. The diameter of the electron beam can be made as small as one micron-meter (μm) making the instrument ideal for point analyses (Potts 1987) even though better results are obtained using larger beam but the beam size must be chosen in accordance to what material is being analysed.

There are two types of spectrometers used to measure x-rays, energy dispersive spectrometer (EDS) and wave dispersive spectrometer (WDS). The EDS measures the whole spectrum of x-ray energies emitted from the sample but the WDS only measures x-ray energies of specific elements (Potts 1987). The EDS is closer to the sample and counts faster than the WDS allowing a lower probe current to be used, which can be an advantage when measuring light elements that may be volatilised during analysis. The WDS uses a diffracting crystal that deflects the x-rays to the spectrometers using the Bragg equation ($n\lambda=2d\sin\theta$; λ: wavelength, n: integer, d: lattice spacing between individual layers of atoms in the crystal, θ: angle of incidence) to calculate their wavelengths and thereby determine the elements that initially created the x-rays. This is why it is very important to set the beam focus right so the same calculation applies both to samples and standards (Reed 1996).

The microprobe is calibrated using standards and it is essential to use standards of known, and uniform, composition because the weight percent of each element or oxide is calculated from the ratio between counts of x-rays from the sample and the standards. Ideally,

standards of similar composition as the sample should be used to reduce matrix corrections and minimize the potential errors associated with such corrections (Reed 1996).

The most frequently used matrix correction has been the ZAF correction. It takes into account the influence of the atomic number (Z), the x-ray absorption (A) and the secondary fluorescence (F) and is used to correct for the non-linearity between the current and concentrations of elements measured by the microprobe. The correction related to the atomic number (Z) accounts for two phenomena:

(1) Heavier elements backscatter incoming electrons more easily and thus decrease the amount of x-rays that should otherwise be created.

(2) Lighter elements absorb more energy than the heavier ones, having a higher proportion of orbital electrons per unit volume, and therefore they have a greater probability of creating x-rays.

The x-ray absorption factor (A) corrects for x-rays created inside the sample and thus have to travel through a part of the sample before arriving at the spectrometers. The third and last correction factor, the fluorescence (F), corrects the fluorescence of one element caused by a second element that emits a characteristic x-ray of the absorption edge of the first, i.e. overlapping x-rays. Having corrected for these factors the microprobe gives the "true" concentration of each element (Potts 1987). The ZAF correction procedure has evolved and additional correction have been added especially on distribution of ionisation at depth in the sample, correction program called X-PHI takes this into account (e.g. Merlet 1994).

Before analysis can take place the sample must be polished so that the x-rays wont be attenuated by scratches or "rough" surfaces (Potts 1987) resulting in inadequate x-ray detection and an underestimation in the concentration of individual elements in the sample. The sample must also be carbon coated but the carbon film conducts the electron charges from the electron beam to earth so they do not build up in the sample. It is critical that the thickness of the carbon coating is correct because otherwise it can behave as an adsorber (Hunt and Hill 1993).

The points to be analysed are selected in accordance with the objective of each study. When selecting a point it should be kept in mind that the electron beam does not only affect the surface of the sample but a thin surface layer of thickness dependent on the accelerating voltage of the electron beam (Potts 1987). The beam size must be chosen in accordance to what material is being analysed, if the beam diameter is set to small (<8 μm) when analysing glass it may result in loss of Na, and to a lesser extent K, Ca and Ba, due to localized mobilization of these elements, which are unstable and migrate away from the heat created by

the beam (Nielsen and Sigurdsson 1981). These elements are usually measured first in order to minimize the chances of element-loss from heating of the sample (Hunt and Hill 1993).

3.2 Electron microprobe analysis – procedure

All of the tephra samples used in this study have been analysed for major elements using the WDS Cameca SX 100 electron microprobe at Laboratoire Magmas et Volcans (LMV), Clermont-Ferrand and the X-PHI correction procedure. Point analyses were made on at least five fresh sideromelane glass grains from each tephra sample. Inter-laboratory check was performed on the international glass standard A99 (Kilauea basalt glass; Jarosewich et al. 1979; Thornber et al. 2002). Ten points were analysed before and after every analytical session and two points after every ~30 unknown analyses. In total the A99 standard was analysed 1536 times over three years yielding information of its homogeneity and overall instrumental stability during this period (Fig. 5). For further discussion on analytical conditions, calibration and procedure see Óladóttir et al. Manuscript 1.

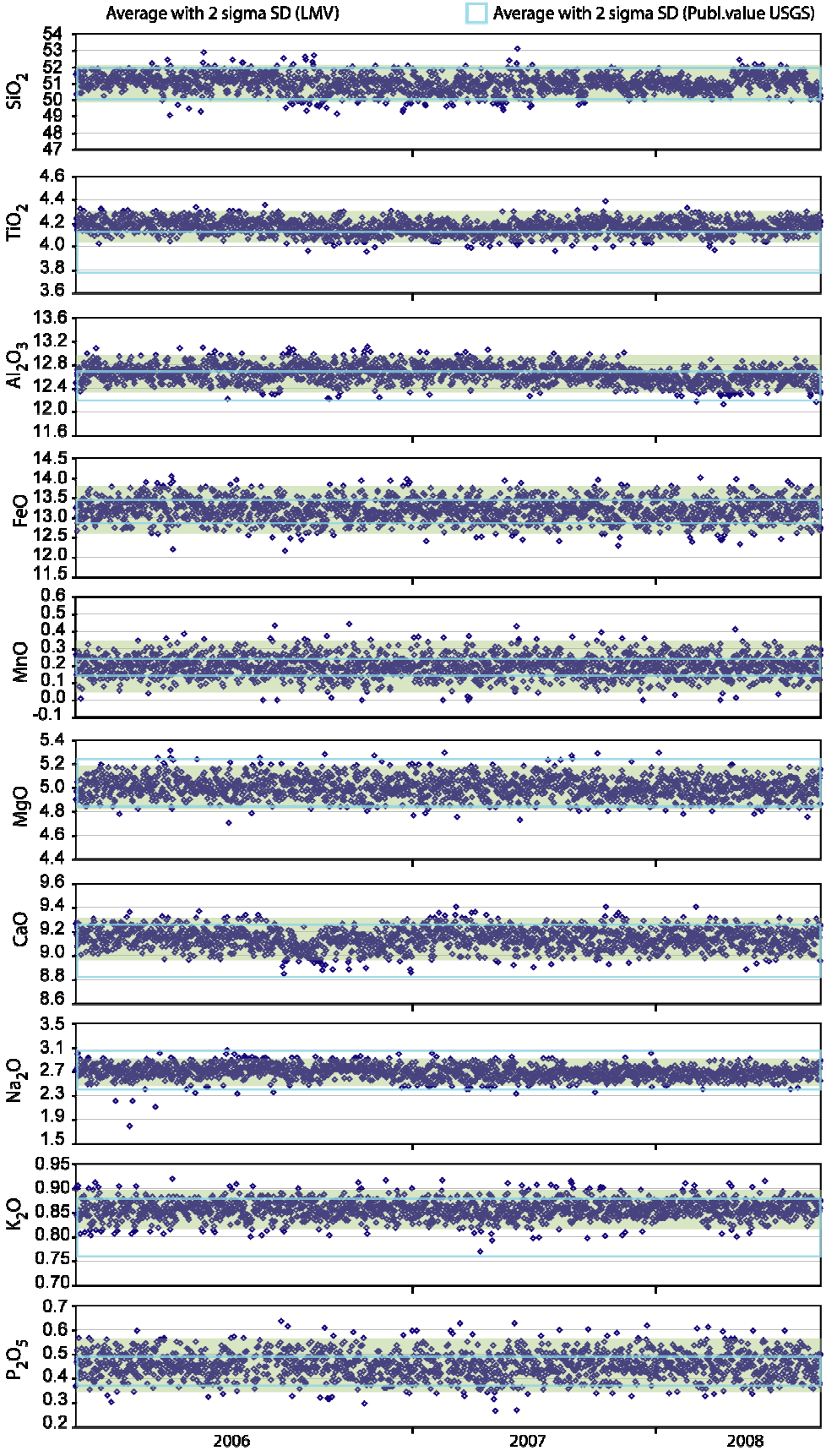

Figure 5 All analyses of the international standard A99 analysed in Laboratoire Magmas et Volcans (LMV) during the three years covered by the PhD project. The shaded area shows calculated average and 2 sigma standard deviation (SD) after 1536 analyses. Light blue square shows average and 2 sigma SD published by USGS (Thornber et al. 2002). The results are compatible with those reported elsewhere except for titanium that is systematically higher in LMV but nevertheless within 2 SD of accepted values.

3.3 Laser ablation ICP-MS – technique

Laser ablation inductively coupled plasma mass spectrometry (LA-ICP-MS) was first introduced in 1985 and has since then developed as an important in-situ analytical tool in the Earth sciences. LA-ICP-MS has filled the void left by the electron microprobe with in-situ measurements of many elements with concentrations as low as few ppm or less. A high power laser beam is directed to the sample surface and physically ablates the region of interest forming aerosols particles that are carried by a stream of inert gas (He or Ar or ideally a blend thereof) into the argon plasma where the particles are ionised.

Mass spectrometers can be divided in four separate parts, the vacuum system, ion source, analyser and detector, but each part can be built in a slightly different manner. Here we will focus on the ion source ICP and a quadrupole analyser as these are the instrumentation in the machine used in this study, all of the information in the following discussion is from Longerich and Diegor (2001).

The vacuum system is fundamental for a mass spectrometer as the ions created in the plasma cannot travel far before colliding with other particles, loosing energy and thus interfere with elements of lower atomic mass. Different pumps are used to obtain the vacuum needed for the machine.

The ion source ionises the sample particles, accelerates them in the desired direction and focuses them to increase the ion beam current. The temperature of the plasma is ~8000 K or close to the apparent temperature of the sun's surface. All lithophile and siderophile elements are almost entirely ionised but chalcophile elements are only partly ionised in the plasma. In order to get the ions from atmospheric pressure in the plasma into the vacuum in the analyser the pressure decrease is done stepwise. During the first step the plasma is "sucked" through an orifice, 1 mm in diameter, in a metal disc called s*ampler*. It is usually made of Ni but Al, Cu and Pt can also be used, the metal has to have good thermal conductivity to dissipate the heat from the plasma. The gas flow through the sampler is 1-2 l/min and after passing the first orifice the gas reaches supersonic velocities carrying the ions towards the analyser. Before getting there the ions have to pass through another orifice of similar diameter (1 mm), this one is a metal disc called s*kimmer* made of the same metal as the sampler. The skimmer only allows ~1% of the sample to pass through and on the inner side of the skimmer the pressure is kept significantly lower. Various lenses are used to focus the ion beam and at the same time remove unwanted photons from the sample. The analyser and detector region is behind one more orifice, larger than the other two as the pressure decrease is not as intense as before.

In the analyser the ions are separated according to mass to charge ratio (m/e) although the term "mass" is applied. Magnetic field is used to change the paths of different "masses" and thereby separate them. A quadrupole analyser contains four rods of hyperbolic shape arranged in a perfect square. Opposite pairs are electrically connected and the connections are brought out of the vacuum and connected to a radio frequency (RF) and a direct current (DC) electrical supply. The ions that have passed the skimmer reach the region between the four rods become affected by the RF oscillations and only ions of a selected "mass" (m/e) can pass this area. The "mass" is selected by applying different values of RF and DC. Since the quadrupole analyser is selective only measurements of one element at a time is possible but the change between masses allowed to pass the four rods is short so it is possible to analyse many elements during a short amount of time. The ions that pass the quadrupole analyser enter the detector.

The detector converts an ion beam into a computer usable number either in digital mode (pulse counting, i.e. ions counted) or analogue mode (ion beam current is converted to a potential, voltage, that is later converted to a number using special hardware. The digital mode is optimum in analyses of low signal intensities whereas stronger signals must be measured in the analogue mode due to impractical detectors dead-time corrections at high ion-currents.

3.4 Laser ablation ICP-MS – procedure

In order to analyse the trace elements in tephra samples of this study, two ICP-MS-Laser ablation sessions of four days were needed. The instrument at the Utrecht University in the Netherlands was selected and the samples analysed using a Micromass Platform ICP behind a Geolas 193 nm eximer laser ablation system and a quadrupole analyser. The first session was from 6th-9th February 2007 and the second one from 25th-28th of March 2008. In both sessions the pulse repetition rate was 10 Hz and the laser beam size was 60 µm in diameter. The laser energy in the first session was 9 J/cm^2 and 12 9 J/cm^2 in the second session except for several analyses done in the morning of 25th of March 2008 where the energy was set to 20 J/cm^2, which showed to be to high for the tephra samples. The NIST-612 standard was used for calibration. Inter-laboratory check was performed on the international glass standard BCR-2G (Colombia River basalt; Wilson 1997), two points were analysed before unknown tephra glasses and two in the end, adding to a total of 29 analyses. The weighted mean of BCR-2G for 2007 and 2008 and its associated 1 sigma error (SD) show less than 2% drift in the BCR-2G analyses for all elements, and the average values are within 10% from those published

(see Table 2, Óladóttir et al. Manuscript 1). For further discussion on analytical conditions see Óladóttir et al. Manuscript 1.

Figure 6 shows the percentage error calculated for every point analysed in 2007 (Fig. 6a) and 2008 (Fig. 6b), including external standards and the NIST-612 standard. It is obvious that the error associated with each analysed point increases during the day in both sessions. This is partly explained by decrease in count rates (cps) observed on the NIST-612 standard (Fig. 7). Nevertheless this increase in analytical error is systematic and also detected on days when no fall in count rate on the NIST-612 standard is observed (e.g. day 6/2/2007; Fig. 7). The increasing analytical error is an effect of laser energy density decease during the day as observed by the absolute decrease in count rates on the NIST-612 standard whilst the transience of the signal increases. However, the external precision does not seem to be affected by this decrease in internal precision observed by the good reproducibility of the external standard BCR-2G (see Table 2, Óladóttir et al. Manuscript 1).

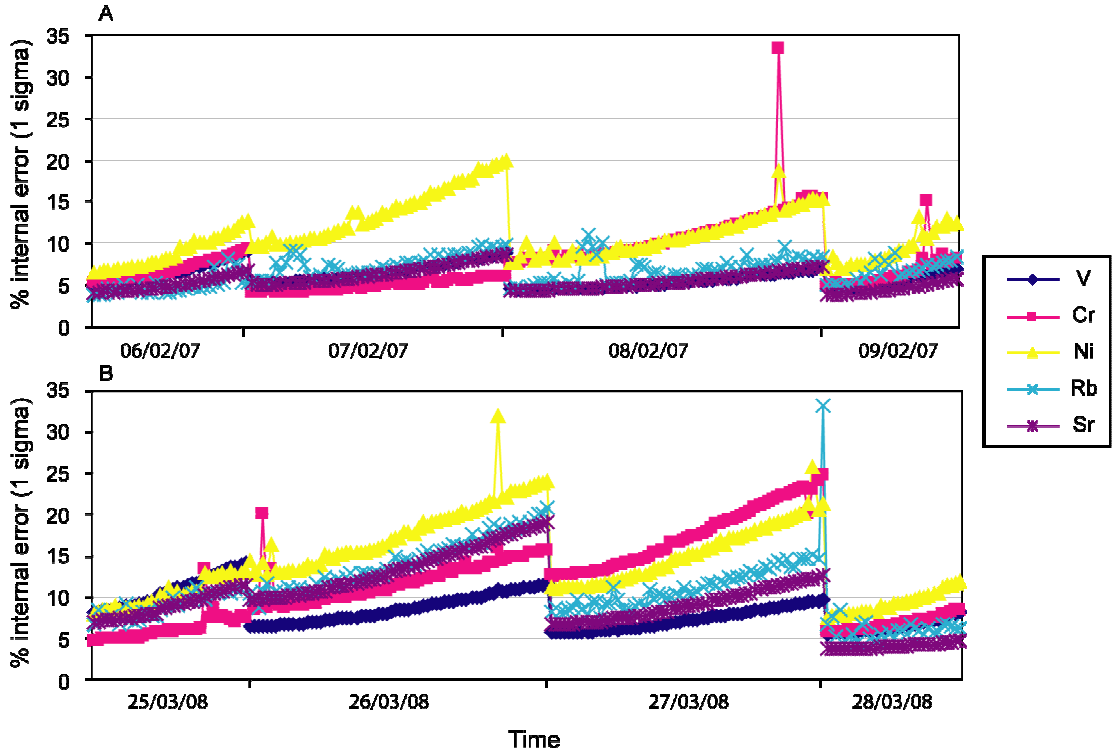

Figure 6 Internal error (1 sigma) calculated as % of element's concentration for every point analysis in the LA-ICP-MS sessions in 2007 (A) and 2008 (B) including the external standard BCR-2G and the NIST-612 standard. Elements shown are V, Cr, Ni, Rb and Sr but the same trend is observed for other elements see text for further discussion

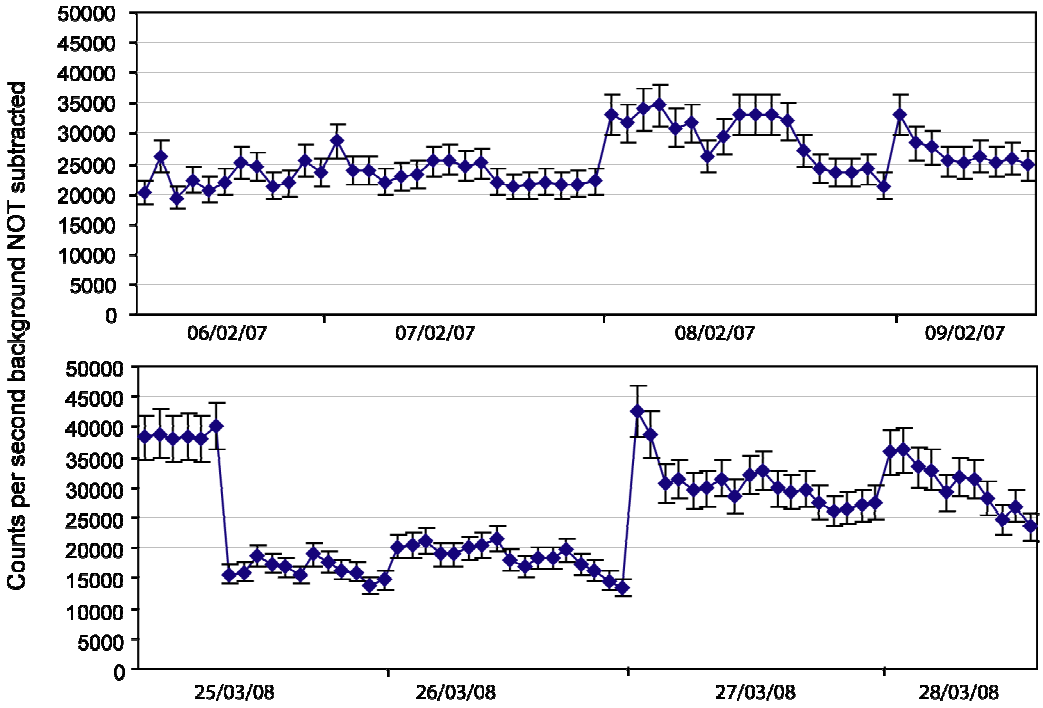

Figure 7 LA-ICP-MS analyses sessions in 2007 and 2008 show fall in count rate (counts per second) on the NIST-612 standard during all days except 06/02/07 and 07/02/07. The abrupt fall in cps on the 25/03/08 is due to decrease in energy (from 20 J/cm^2 down to 12 J/cm^2). Element shown is Y, randomly chosen as all elements show the same behaviour during all days.

In order to trace tephra layers to their source volcanoes, reference compositional fields (RCF) were drawn using both published trace element analyses from different volcanic systems (Meyer et al. 1985; Hémond et al. 1993; Chauvel and Hémond 2000; Kokfelt et al. 2006) as well as reference samples analysed during this study. As the internal precision of each analysis degrades during the day, only reference samples with internal error less than 10% (1 sigma) were used in the RCF-construction. Nevertheless, since the external standard BCR-2G shows good reproducibility and therefore accuracy, analyses of samples with somewhat higher precision than 10% were used for fingerprinting of provenance rather than reanalysing each sample (see Óladóttir et al. Manuscript 1 for fingerprinting of provenance).

4. Manuscript 1: Provenance of basaltic tephra in soil profiles around the Vatnajökull ice cap, Iceland

Provenance of basaltic tephra in soil profiles around the Vatnajökull ice cap, Iceland

Bergrun Arna Óladóttir[1,2], Olgeir Sigmarsson[1,2], Gudrun Larsen[2] and Jean-Luc Devidal[1]

1) Université Blaise Pascal, OPGC and CNRS, 5 rue Kessler, 63038 Clemont-Ferrand, France

2) Institute of Earth Sciences, University of Iceland, 101 Reykjavík, Iceland

4.1 Abstract

The formation of a tephra layer can be considered instantaneous and its potential wide-spread distribution forms a very useful time marker for volcanological, environmental and archaeological studies. The source of a tephra layer can be established by mapping its distribution or inferred via compositional fingerprinting. Major element analyses of volcanic glass have proven reliable for tephra fingerprinting. However, distinguishing between basaltic tephra is not always straight forward. In order to improve provenance determinations for Grímsvötn, Bárdarbunga and Kverkfjöll volcanic systems, tephra has been systematically sampled from soil profiles around the Vatnajökull ice cap. Only basaltic magma is known to erupt from these volcanic systems, and within each system the tephra is often of very similar composition. In total 921 tephra samples have been analysed for major elements by electron probe microanalysis (EPMA) and their provenance has been assessed by comparison with chemical composition of previously analysed products from each volcanic system. Several discriminating major element plots allow identification of the tephra source. However, some of the analysed samples fall outside the reference compositional fields established from the published major element analyses. The major element results fall into three distinctive compositional groups, all of which show regular decrease of MgO with increasing K_2O concentrations, as expected from frequently observed differentiation of a magma suite. Although these groups improve the compositional distinction between products of the three volcanic systems, a slight overlap still remains. In-situ trace element analyses by laser-ablation inductively-coupled-plasma mass-spectrometry (LA-ICP-MS) were applied for better provenance identification for tephra layers of similar major element composition. Three element to element concentration ratios, Rb/Y, La/Yb and Sr/Th, are particularly useful as they are markedly different in the products of the three volcanic systems. Significantly higher La/Yb distinguishes the Grímsvötn basalt products from those of Bárdarbunga and Rb/Y values differentiates the basalt products of Grímsvötn and Kverkfjöll. The products of Bárdarbunga, Grímsvötn and Kverkfjöll volcanic systems form distinct compositional fields on a Sr/Th versus Th plot and further help identifying the source of the tephra. Taken together, the combined use of major and trace element analyses in delineating the provenance of basaltic tephra having similar major element composition significantly improves the Holocene tephra record around Vatnajökull ice cap.

4.2 Introduction

In tephrochronology the age of the tephra to be used for dating purposes must be known as accurately and precisely as possible. This is straight forward for tephra-forming eruptions witnessed by man and concisely recorded. The written record for historical eruptions is reliable for the last centuries and the tracing of a given tephra to an eruption of a known age is trivial if the tephra bear some physical or chemical characteristics allowing its provenance to be determined. On of the most reliable means for such fingerprinting is the chemical composition of the tephra. Distinguishing the potential sources for silicic tephra appears relatively straight forward whereas basaltic tephra is often much harder to trace to a single volcano or volcanic system. With improved analytical developments and careful standardisation procedure the determination of basaltic tephra provenance is becoming less difficult than before. In Iceland, most Holocene silicic tephra can be recognized by its major element composition (e.g. Dugmore et al. 1995; Larsen et al. 1999; Larsen et al. 2001) and stratigraphy, whereas basaltic tephra, especially from volcanoes producing the same magma series are less readily identified (e.g. Jakobsson 1979; Larsen 1981).

Due to Iceland's location in the north Atlantic between the 63° and 66° north, many of its volcanoes are capped by glaciers, leading to explosive basaltic eruptions. During historical time (the last ~1100 years) 75% of eruptions taking place in Iceland have produced tephra (Larsen and Eiríksson 2008). Several silicic tephra from Iceland are known to have been transported to Europe (see e.g. Persson 1971; Dugmore 1989; Haflidason et al. 2000; van den Bogaard and Schminke 2002 and references therein), whereas the explosive basaltic products are more localised. However, exceptionally, basaltic products of Icelandic volcanoes such as the Vedde ash (basaltic component) and the Saksunarvatn ash cover areas significantly greater than Iceland and are observed in lake sediments and soil profiles in N-Europe and in Greenland's ice cores (Mangerud et al. 1984; 1986; Björck et al. 1992; Norddahl and Haflidason 1992; Grönvold et al. 1995; Ingólfsson et al. 1995; Lacasse et al. 1995). Correct identification of basaltic tephra from Iceland is thus of interest for all tephra studies of the North-Atlantic area as well as i.e. paleo-climatology, paleo-oceanography, and archaeology.

Volcanoes above the assumed centre of the Iceland mantle plume, and part of their associated volcanic systems, are covered by the Vatnajökull ice cap resulting in phreatomagmatic activity and formation of abundant tephra. The aim of this study is to better constrain major and trace element composition for three of these volcanic systems, Grímsvötn, Bárdarbunga and Kverkfjöll and thus improve identifications of their eruptive

products in Holocene soil and sediment archives. This goal is achieved by analysing tephra identified and sampled in soil profiles around the Vatnajökull ice cap. One of the outcomes of this study is improved tephra record for these three volcanic systems, which in turn will have direct applications for studies within other scientific fields, such as soils science and environmental studies.

4.3 Geological context

The neovolcanic zones of Iceland represent the Mid-Atlantic Ridge and its interaction with the Iceland mantle plume (White et al. 1995; Bjarnason et al. 1996; Wolfe et al. 1997). They are made up of individual volcanic systems (Sæmundsson 1978; Jakobsson 1979) that appear to have characterised volcanism in Iceland through its history (Fig. 1; Sæmundsson 1979; Jóhannesson and Sæmundsson 1998a). The volcanic systems include a central volcano, where the magmatic productivity is highest, and/or surrounding fissure swarms (Sæmundsson 1978; Jakobsson 1979). Tectonic settings appear to control the magma types produced at individual volcanic systems. Three igneous magma series are found (1) tholeiitic series, characterised by relatively high Fe and Ti and low Al and Ca contents, (2) transitional alkalic series, characterised by high Fe, Ti, and alkali metals for a given SiO_2

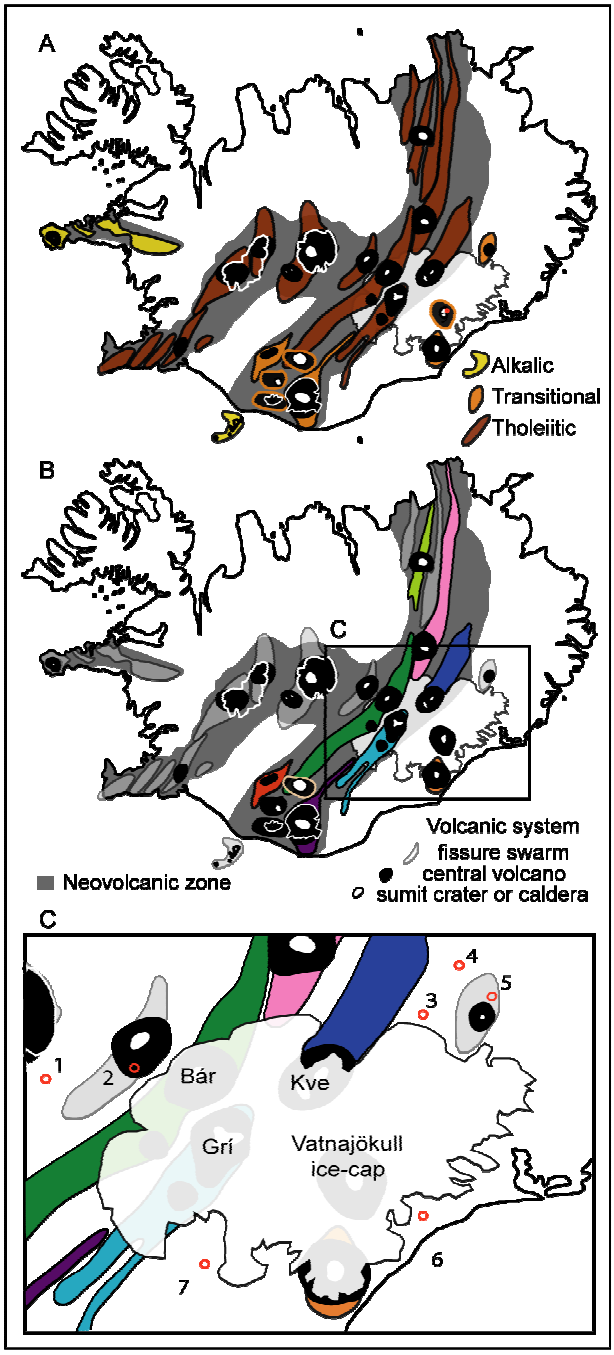

Figure 1. The neovolcanic zone and volcanic systems in Iceland. A) Colour indicates the igneous magma series of Iceland. Yellow: alkalic series, light-brown: transitional alkalic series and brown: tholeiitic series. B) Volcanic systems discussed. Main focus is on Grímsvötn in sky blue, Bárdarbunga in green and Kverkfjöll in blue. Other coloured volcanic systems are Askja (rose), Krafla (lime), Hekla (red), Katla (violet), Torfajökull (tan) and Öræfajökull (orange). C) Area of study and location soil sections. In total seven soil profiles have been measured and sampled: 1: Hreysiskvísl; 2: Nýidalur; 3: Hraukahreppur; 4: Kárahnjúkar; 5: Snæfell; 6: Steinadalur and 7: Núpsstadarskógar. Abbreviations are as follows: Bár Bárdarbunga; Grí Grímsvötn; Kve Kverkfjöll. Modified after Jóhannesson and Sæmundsson (1998a), Jakobsson et al. (2008) and Thordarson and Larsen (2007).

concentration but low Al contents and (3) alkalic series, characterised by significantly higher Na and K contents than the other two series; the first two series are hy-normatives (Jakobsson 1979). Volcanic systems located in the rift zone produce magma of the tholeiitic series and the other two series are in the flank zones or non-rifting zones (Jakobsson et al. 2008; Fig. 1a). As a result, most of the volcanic products of Iceland are of tholeiitic origin (80%), 12% are of transitional alkalic origin and the missing 8% are alkalic (Jakobsson et al. 2008).

The partly subglacial volcanic systems, Grímsvötn, Bárdarbunga and Kverkfjöll (Fig. 1b), are all located in the rift zone, above the assumed centre of the Iceland mantle plume. They all produce predominantly basaltic tephra of similar tholeiitic composition.

4.4 Methods

Field work and sample preparation

Seven soil profiles were measured and sampled around the Vatnajökull ice cap, all within 30 km from the ice margin (Fig 1c). They vary in thickness from 3.2-6.5 m, cover ~2500 up to ~7300 years and contain from 50 to 169 visible tephra units separated by soil. Criteria such as colour of tephra, thickness, grain size, depositional structures and contacts with the soil was recorded, as well as observations concerning the impact the tephra had on its local environment. Samples were collected from tephra down to less than 1mm in thickness (see Óladóttir et al. 2005 for further information on field methods). In total, 921 samples were prepared for thin sections by sieving. The 125 µm size fraction was preferred for the 100 µm thick polished thin sections for in-situ measurements in order to have enough material for trace element analyses, but supplemented if necessary by the 63 and/or 250 µm size fractions.

Defining primary tephra

Occasionally, parts of soil sections contain irregular units that can be considered a single tephra unit if analyses yield a homogeneous composition and field observations concur, i.e. when soil between layers is very thin or even absent possibly related to soil creep, frost and thaw upheaval or bioturbation. In other cases closer inspection is needed to distinguish between reworked material and primary tephra. The three following field observations have proved useful: (1) Thickness. To provide material for aeolian reworking the base unit in a series has to be of considerable thickness. Thick tephra can cover vegetation completely which then cannot prevent wind erosion, increasing the possibilities of tephra reworking. (2) Colour and contacts. The colour of the tephra and its contacts with the surrounding soil hold important information. Sharp contacts indicate primary undisturbed tephra rather than

reworked material since tephra is deposited rapidly whereas re-deposited tephra often have diffuse contacts because of progressive reworking by the wind. Primary tephra also has distinct colour as it is not contaminated by soil and unrelated tephra grains. Laterally continuous bedding can also be diagnostic. (3) Grain size and shape. Grains are exposed to abrasion during reworking by wind and consequently their roundness increases. The wind also sorts out grains based on their bulk densities. This leads to decreasing grain size and increased sorting in reworked material compared to primary tephra.

If a tephra sample is comprised of glasses having two chemical compositions in similar proportions, originating from different volcanic systems, and neither of these can be assigned to contamination, contemporaneous eruptions at two volcanic systems should be considered. Examination of nearby soil profiles, especially those exhibiting higher soil accumulation rates, may provide a section were these tephra layers are separated by soil and hence the evidence being sought, emphasising the importance of inspecting the lateral extension of any given tephra.

If a tephra unit contains grains of three or more different chemical compositions present in roughly equal proportions, origin by reworking is assumed and such layers are not considered any further in this study.

Analytical techniques

Major element analyses - Electron Probe Microanalyses (EPMA)

Electron probe microanalyses (EPMA) of glasses were obtained on a WDS Cameca SX100 at the Laboratoire Magmas et Volcans (LMV), Clermont-Ferrand. The instrument was calibrated on natural and synthetic mineral standards and glasses. The analytical conditions used are 15 kV accelerating voltage and 8 nA beam current with a beam diameter of preferably 20 µm but 10 µm where grains were too small for the 20 µm beam. The counting time was 10 s for Na, Ca, Ti, P and Si; 20 s for Mg and Al; 30 s for Mn and finally 40 s for Fe and K, adding up to a total analyses time of 3 min and 40 s for each spot. For analyses of silicic glass the beam current was reduced to 4 nA to reduce Na loss and the beam diameter to either 10 or 5 µm (see further discussion below). Raw data were corrected by the X-PHI correction procedure (Merlet 1994; for overview on analytical techniques see Table 1).

Inter-laboratory check was performed on the international glass standard A99 (Kilauea basalt glass; Jarosewich et al. 1979; Thornber et al. 2002). Ten points were analysed before and after every analytical session and two points after every ~30 unknown analyses. In total the A99 standard was analysed 1536 times over three years yielding a very narrow

compositional range (Table 1). The results are indistinguishable from those reported elsewhere except for titanium that is systematically higher but nevertheless within the 95% confidence limits (Table 1; Jarosewich et al. 1979; Thornber et al. 2002).

Point analyses were made on at least five fresh sideromelane glass grains from each tephra sample. If the analysed points did not show homogeneous major element composition or totals were lower than 96.5% additional analyses were performed to fulfil the criteria that at least five homogeneous point analyses with acceptable totals are needed for calculating an average but five grains has shown to be enough for assigning a tephra to its source system (Óladóttir et al. 2008). Samples composed of heterogeneous tephra grains were inspected further and based on field observations such as colour, grain size, contact to the surrounding soil and adjacent tephra some were declared reworked material, e.g. windblown material (further discussion below).

Table 1 Electron microprobe calibration, analytical condition, published values of the external international standard A99 and its mean value from Laboratoire Magmas et Volcans (LMV), Clermont-Ferrand.

Major element	*Calibration*	*Counting time (s)*	*Crystal*	*A99 (USGS) n=418**	*A99 (USNM)*	*A99 (LMV) n=1536**
SiO_2	A-THO	10	TAP	51.06 (0.46)	50.94	51.00 (0.54)
TiO_2	$TiMnO_3$	10	LPET	3.95 (0.09)	4.06	4.17 (0.06)
Al_2O_3	VG2	20	TAP	12.44 (0.13)	12.49	12.65 (0.15)
FeO	Fe_2O_3	40	LIF	13.15 (0.16)	13.30	13.20 (0.29)
MnO	$TiMnO_3$	30	LIF	0.19 (0.02)	0.15	0.20 (0.07)
MgO	MgO	20	TAP	5.04 (0.10)	5.08	5.01 (0.09)
CaO	Wollastonite	10	LPET	9.04 (0.11)	9.30	9.14 (0.09)
Na_2O	Albite	10	TAP	2.72 (0.16)	2.66	2.69 (0.11)
K_2O	Orthoclase	40	LPET	0.82 (0.03)	0.82	0.86 (0.02)
P_2O_5	Apatite	10	LPET	0.43 (0.03)	0.38	0.46 (0.02)
Total				98.84	99.18	99.35

*Numbers in brackets are one sigma standard deviations. (USNM: Jarosewich et al. 1979; USGS: Thornber et al. 2002). *n* denotes the number of analyses.

Sodium loss during electron probe microanalyses (EPMA) of silicic tephra grains

Sodium loss during EPMA is widely recognised and several methods have been introduced in order to reduce it, such as increasing beam sizes, rastering and sample's cooling during analyses (Keller 1981; Nielsen and Sigurdsson 1981; Hunt and Hill 2001). Silicic Hekla tephra is extremely vesicular with particularly thin vesicle walls (Fig. 2), limiting the beam size used for analyses with resulting Na loss. Several analytical conditions were assessed on Hekla tephra having independently measured Na concentration (whole rock analyses; Sigmarsson et al. 1992; Schuessler et al. 2009). The best combination for Hekla tephra analyses was found to be 15 kV accelerating voltage and a beam current of 4 nA for a defocused 5 µm beam. Nevertheless, the Hekla samples showed a systematic 10% sodium

loss induced by the electron microprobe. This demonstrates that analyses of thin silicic glass using a beam <5 µm need to be corrected for Na-loss (Devidal et al. 2008).

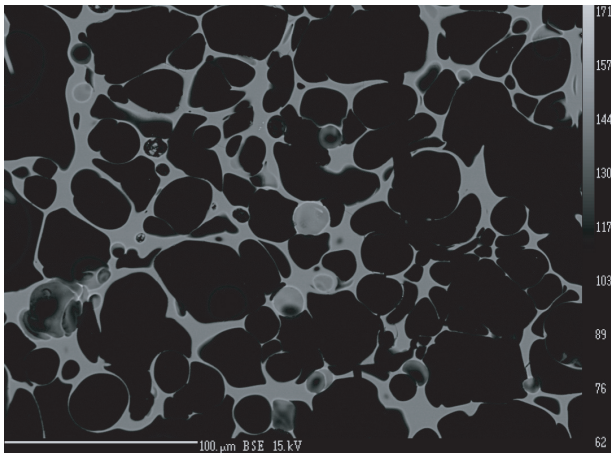

Figure 2. Back scattered electron (BSE) photo of a Hekla sample, obtained at 15 kV with the Cameca SX100 electron microprobe at LMV, emphasising the small analysable glass rims in silicic and highly vesicular Hekla tephra. Scale is 100 µm (photo by J.L. Devidal).

Trace element analyses with Laser ablation ICP-MS

Trace elements were analysed at the Utrecht University, in the Netherlands, with a Micromass Platform ICP (ICP-MS with collision cell technique) and a Geolas 193 nm eximer laser ablation system. The laser energy was 9-12 J/cm^2, the pulse repetition rate 10 Hz and the laser beam size was set at 60 µm in order to maximize signal strength and thus precision. The instrument was tuned and calibrated relative to the NIST-612 glass, and all analyses were assessed with the Glitter© program (van Achterbergh et al. 2001). Inter-laboratory check was performed on the international glass standard BCR-2G (Colombia River basalt; Wilson 1997), two points were analysed before unknown tephra glasses and two at the end, adding to a total of 29 analyses. The weighted mean of BCR-2G for 2007 and 2008 and its associated 1 sigma error show less than 2% drift in the analyses for all elements, and the average values are within 10% of those published (Table 2).

Point analyses were usually made on the 5 grains in each sample that had been previously analysed by the electron microprobe. In a few cases, there were only 3 grains analysed for trace elements due to small grain sizes and therefore lack of suitable material, and up to 7 grains were analysed in samples of heterogeneous major element composition. Weighted mean was calculated from the analysed points representing the trace element composition of a given tephra sample.

Table 2 Published values of the external international standard BCR-2G and its mean value obtained during analyses at Utrecht University in 2007 and 2008.

Trace element	*BCR-2G (USGS)**	*BCR-2G Utrecht 2007*		*BCR-2G Utrecht 2008*		*BCR-2G Utrecht 2007+2008*		
		Mean (ppm)	*1σ SD*	*Mean (ppm)*	*1σ*	*Mean (ppm)*	*1σ*	*% error RSD*
V	416	418.8	6.7	408.2	6.7	413.49	4.72	1.14
Cr	18	17.2	0.4	16.5	0.3	16.77	0.24	1.42
Rb	48	47.5	0.8	48.0	0.8	47.74	0.58	1.22
Sr	346	320.8	4.8	322.5	4.5	321.70	3.30	1.02
Y	37	34.5	0.7	31.4	0.5	32.41	0.40	1.25
Zr	188	171.9	3.6	161.6	2.9	165.57	2.24	1.35
Nb	13.1	11.8	0.2	12.0	0.2	11.94	0.14	1.15
Ba	683	642.9	10.9	624.1	11.1	633.70	7.77	1.23
La	25	25.2	0.4	24.2	0.4	24.69	0.26	1.07
Ce	53	53.0	0.8	51.2	0.8	52.09	0.55	1.06
Pr	6.8	6.6	0.1	6.5	0.1	6.56	0.07	1.14
Nd	28	28.9	0.6	27.7	0.5	28.22	0.40	1.43
Sm	6.7	6.5	0.1	6.2	0.1	6.34	0.06	0.99
Eu	2	1.84	0.03	1.91	0.04	1.87	0.02	1.29
Gd	6.8	6.6	0.1	6.5	0.1	6.56	0.09	1.35
Dy	6.38	7.2	0.1	6.4	0.1	6.62	0.07	1.10
Er	3.66	3.9	0.1	3.5	0.0	3.59	0.03	0.96
Yb	3.5	3.8	0.1	3.5	0.0	3.56	0.03	0.93
Lu	0.51	0.58	0.01	0.51	0.01	0.53	0.01	1.45
Hf	4.8	4.9	0.1	4.4	0.1	4.51	0.07	1.56
Ta	0.78	0.87	0.02	0.84	0.01	0.85	0.01	1.37
Pb	11	10.9	0.2	11.0	0.2	10.96	0.16	1.45
Th	6.2	5.96	0.14	5.73	0.08	5.78	0.07	1.18
U	1.69	1.72	0.03	1.69	0.03	1.70	0.02	1.16

*(Wilson 1997)

4.5 Results

Field observations and sample description

The tephra samples are mostly basaltic, made up of two glass types in different proportions, (1) sideromelane, displaying different brown tones in transmitted light reflecting changing chemical composition, and (2) tachylite, which is opaque in transmitted light. Samples may include phenocrysts and/or microcrystals, mostly plagioclase, pyroxene and olivine, lithics and silicic glass grains. Only about 8% of the analysed tephra are silicic and may or may not include crystals and lithics. The tephra glass varies from non- to highly vesicular grains, with highest porosity in the silicic glass grains.

Electron microprobe

In total 7945 point analyses were made. Thereof 1536 are analyses of the external standard A99. The remaining 6409 points are analyses of basaltic and silicic glasses in 921 tephra samples. Of these, 895 samples represent 749 primary tephra units where 89.5% are basaltic (the emphasis of this paper), 7.8% silicic and 2.7% intermediate in composition (Fig. 3; note

that intermediate grains observed in predominantly silicic samples are not included in these percentages). The remaining 26 samples were defined as reworked (see below). Of the 749 primary tephra units, 280 come from the Grímsvötn system, 214 originated from Bárdarbunga, 34 from Kverkfjöll, 115 from Katla, 42 from Hekla, 8 from Öræfajökull, 6 from Torfajökull, 2 from Askja and 48 are of unidentified origin. Of the unidentified ones 27 are basaltic in composition, 18 intermediate and three silicic. The method for fingerprinting tephra from Grímsvötn, Bárdarbunga and Kverkfjöll is based on Fig. 4 as discussed below.

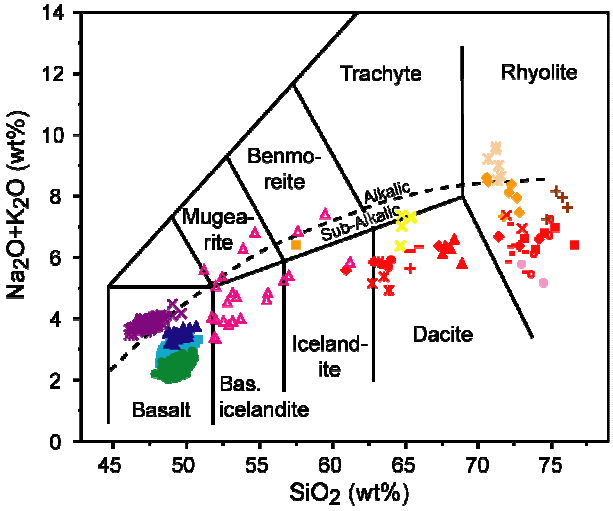

Figure 3. Total alkalis vs. silica diagram with rock classification boundaries from Le Bas et al. (1986). The dashed line (based on Miyashiro 1978) separates alkalic and sub-alkalic fields. All analysed samples representing primary tephra are shown except those 27 basalts that are of unidentified provenance. Colour use is the same as in Fig. 1b, but in addition yellow symbols represent silicic Katla tephra, brown and pink symbols are silicic and intermediate tephra, respectively, of unidentified provenance.

Table 3a Range of major elements analysed by the electron microprobe and calculated mean values for tephra from Bárdarbunga, Grímsvötn and Kverkfjöll tephra.

	Bárdarbunga		*Grímsvötn*		*Kverkfjöll*	
	Range	*Mean n=236*	*Range*	*Mean n=300*	*Range*	*Mean n=35*
SiO_2	47.97-50.61	49.44	48.23-50.85	49.50	48.72-50.72	49.54
TiO_2	1.34-2.13	1.70	1.89-3.62	2.68	2.92-3.69	3.20
Al_2O_3	13.66-14.94	14.24	12.78-14.95	13.73	12.62-14.23	13.39
FeO	10.10-13.34	11.63	10.55-15.2	12.94	13.83-15.45	14.41
MnO	0.12-0.38	0.21	0.14-0.49	0.22	0.17-0.32	0.25
MgO	5.91-8.16	7.19	4.45-7.49	5.92	4.26-5.13	4.76
CaO	10.38-13.10	12.03	8.73-12.37	10.47	8.48-9.66	9.13
Na_2O	1.89-2.61	2.21	2.18-2.99	2.68	2.64-3.03	2.85
K_2O	0.12-0.33	0.19	0.23-0.57	0.39	0.51-0.75	0.63
P_2O_5	0.09-0.23	0.15	0.15-0.48	0.28	0.30-0.48	0.39

n denotes number of tephra layers included in the calculated mean.

The MgO concentration in Grímsvötn tephra ranges from 4.45-7.49 wt% with an average of 5.92 wt%. K_2O varies from 0.23-0.57 wt% with an average value of 0.39 wt%, the TiO_2 range is from 1.89-3.62 wt% averaging at 2.68 wt% and FeO concentration is 10.55-15.20 wt% with an average of 12.94 wt%. The Bárdarbunga tephra has MgO average of 7.19

wt% and a range from 5.91-8.16 wt%. Concentrations of K_2O, TiO_2 and FeO fall in the range 0.12-0.33, 1.34-2.13 and 10.10-13.34 wt%, respectively, with averages in the same major element order of 0.19, 1.70 and 11.63 wt%. Finally the Kverkfjöll tephra has MgO range from 4.26-5.13 wt% and an average of 4.76 wt%. K_2O average is 0.63 wt%, TiO_2 average 3.20 wt% and FeO average in Kverkfjöll is 14.41 wt%. The concentrations ranges are 0.51-0.75, 2.92-3.69 and 13.83-15.45 wt%, respectively (Table 3a&b, Fig 4).

Table 3b Selected major element compositions of tephra from Bárdarbunga, Grímsvötn and Kverkfjöll. The tephra were chosen to show the maximum compositional range within each volcanic system.

Log #	*Age*[+]	*SiO_2*	*TiO_2*	*$Al2O_3$*	*FeO*	*MnO*	*MgO*	*CaO*	*Na_2O*	*K_2O*	*P_2O_5*	*Total*
Bárdarbunga												
Hrau53	3920	49.37	1.34	14.41	10.52	0.19	8.00	13.01	1.93	0.12	0.09	98.99
Hrau9	5840	49.30	1.35	14.67	10.10	0.20	8.16	13.09	1.93	0.13	0.11	99.05
Snæ85	5750	47.97	1.42	14.54	10.55	0.29	7.87	12.82	2.03	0.15	0.14	97.78
Hrey41a	2750	49.00	1.63	14.44	11.12	0.13	7.46	12.24	2.19	0.17	0.14	98.52
Hrey57	3700	48.69	1.54	14.76	10.93	0.23	7.75	12.64	2.07	0.17	0.14	98.91
He22	6700	48.60	1.73	14.29	11.50	0.22	7.21	12.02	2.20	0.23	0.15	98.16
Kár82	2620	49.41	1.85	14.20	12.17	0.22	7.03	11.73	2.29	0.19	0.18	99.28
Nup45	2430	49.09	1.92	13.66	12.57	0.19	6.60	11.50	2.31	0.22	0.19	98.26
HKV31	1760	50.46	2.01	14.02	12.66	0.22	5.96	10.40	2.61	0.32	0.23	98.89
Kár111	1440	49.84	2.07	13.94	13.34	0.29	6.01	10.64	2.54	0.27	0.22	99.16
S3-29	1740	50.55	2.09	13.83	12.89	0.22	5.91	10.38	2.56	0.33	0.22	98.98
S3-18	1580	49.19	2.13	13.79	12.99	0.22	6.14	10.67	2.45	0.27	0.21	98.07
Grímsvötn												
Sau1	7330	48.80	1.89	14.95	10.70	0.20	7.49	12.10	2.27	0.23	0.17	98.82
Hrey83	4540	48.23	1.99	14.35	11.02	0.21	7.39	12.21	2.28	0.27	0.17	98.12
Kár23	6510	49.23	2.08	14.38	11.71	0.23	6.87	11.36	2.43	0.27	0.18	98.75
Hrau31	4740	49.17	2.21	14.13	11.47	0.22	6.96	11.73	2.31	0.30	0.24	98.73
Sau92	1470	49.07	2.32	14.03	11.99	0.19	6.40	10.99	2.56	0.34	0.23	98.13
Hrey55	3650	48.67	2.40	14.11	12.16	0.22	6.41	11.10	2.50	0.34	0.22	98.13
Snæ90	6140	49.04	2.55	13.85	12.72	0.23	6.16	10.72	2.58	0.35	0.24	98.46
Snæ2.27	1630	50.85	2.60	13.64	12.70	0.23	5.32	9.65	2.81	0.52	0.22	98.53
Saud4	460	49.65	2.78	13.47	13.11	0.27	5.79	10.27	2.63	0.43	0.28	98.68
Nups4	1190	49.93	3.47	13.01	15.01	0.22	4.68	8.88	2.90	0.57	0.37	99.04
HKV25	1510	49.23	3.51	13.01	14.87	0.27	4.52	8.77	2.99	0.52	0.38	98.08
S3-19	1620	48.96	3.62	12.78	15.20	0.24	4.45	8.73	2.96	0.53	0.34	97.80
Kverkfjöll												
Kár44	4770	49.90	2.92	13.66	13.83	0.19	5.11	9.62	2.78	0.59	0.32	98.92
Sau6	6900	50.08	3.02	14.23	14.32	0.29	4.88	9.18	2.83	0.60	0.38	99.79
Kár75	2810	49.49	3.07	13.53	14.07	0.22	5.13	9.62	2.81	0.56	0.30	98.81
Hrau33	4690	50.13	3.09	13.45	14.05	0.24	4.78	9.06	2.90	0.66	0.38	98.75
Kár8	7280	49.84	3.20	13.49	13.83	0.24	4.74	9.09	3.03	0.69	0.36	98.52
Hrau13	5680	48.72	3.28	13.36	14.36	0.32	4.69	9.16	2.88	0.65	0.34	97.75
Stein5	4940	49.05	3.31	13.19	14.27	0.23	5.03	9.66	2.70	0.63	0.41	98.47
Kár27	6180	49.92	3.36	13.17	14.53	0.21	4.61	8.80	2.88	0.63	0.42	98.54
Stein14	2980	50.72	3.37	13.19	14.59	0.23	4.26	8.48	3.01	0.75	0.48	99.08
Sau76	2240	49.43	3.38	13.27	14.35	0.31	4.56	8.96	2.90	0.57	0.41	98.14
Snæ75	5060	48.87	3.48	12.89	14.66	0.25	4.90	9.09	2.70	0.51	0.40	97.76
Hrau22	5390	49.24	3.69	12.62	15.45	0.23	4.82	9.02	2.64	0.52	0.38	98.61

[+]Age is calculated from soil accumulation rate (Óladóttir et al. 2005; Óladóttir et al. Manuscript 2)

Our major element results show that each volcanic system is characterized by a distinct evolutionary trend. However, small but significant overlaps exist for all major element compositions between Bárdarbunga and Grímsvötn as well as between Grímsvötn and Kverkfjöll whereas between Bárdarbunga and Kverkfjöll there is only an overlap in three elements, SiO_2, Al_2O_3 and MnO. In spite of this overlap, Bárdarbunga has systematically lower TiO_2, Al_2O_3, MgO, CaO, P_2O_5 and higher FeO and Na_2O concentration than Grímsvötn has for the same K_2O value. Notably, the FeO/TiO_2 of 6 clearly distinguishes between these

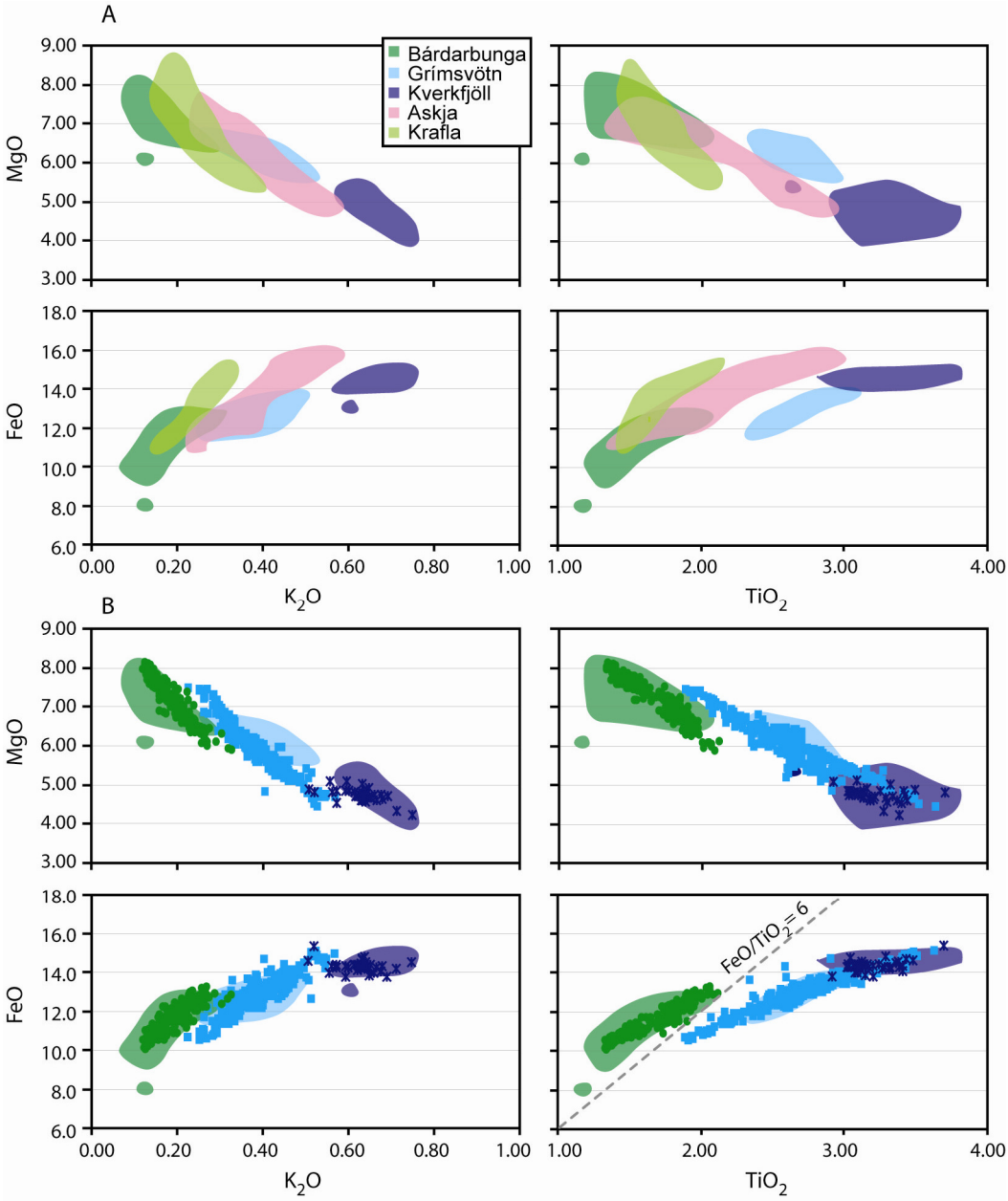

Figure 4. Reference compositional fields (RCF) from the literature form the basis for fingerprinting of tephra. Colours used are the same as in Fig. 1b. All units are wt%. A) RCF of the Grímsvötn, Bárdarbunga, Kverkfjöll, Askja and Krafla volcanic systems (whole rock analyses: Jakobsson 1979; Nicholson 1990; Hémond et al. 1993; Kokfelt et al. 2006 EPMA: reference samples, this study). B) Analytical results from this study are shown with individual symbols on top of the RCF for Grímsvötn, Bárdarbunga and Kverkfjöll. Broken line on FeO vs. TiO_2 shows FeO/TiO_2 of six that clearly distinguishes between Bárdarbunga and Grímsvötn provenance

two systems. Distinction between Grímsvötn and Kverkfjöll is somewhat more problematic as their chemical compositions exhibit a significant overlap (Fig. 4). Nevertheless, Kverkfjöll products are characterized by slightly higher K_2O concentration than Grímsvötn at the same MgO and FeO values as well as slightly lower TiO_2 concentration than that of Grímsvötn tephra for the same MgO value.

ICP-MS Laser ablation

Trace elements were analysed in 53 samples. In order to form a good reference compositional base, 27 tephra of known origin according to their major element composition, were selected, 11 from Grímsvötn, 6 from Bárdarbunga and 10 from Kverkfjöll. The remaining 26 samples were unknown since they plot inconsistently in relevant major element compositional fields.

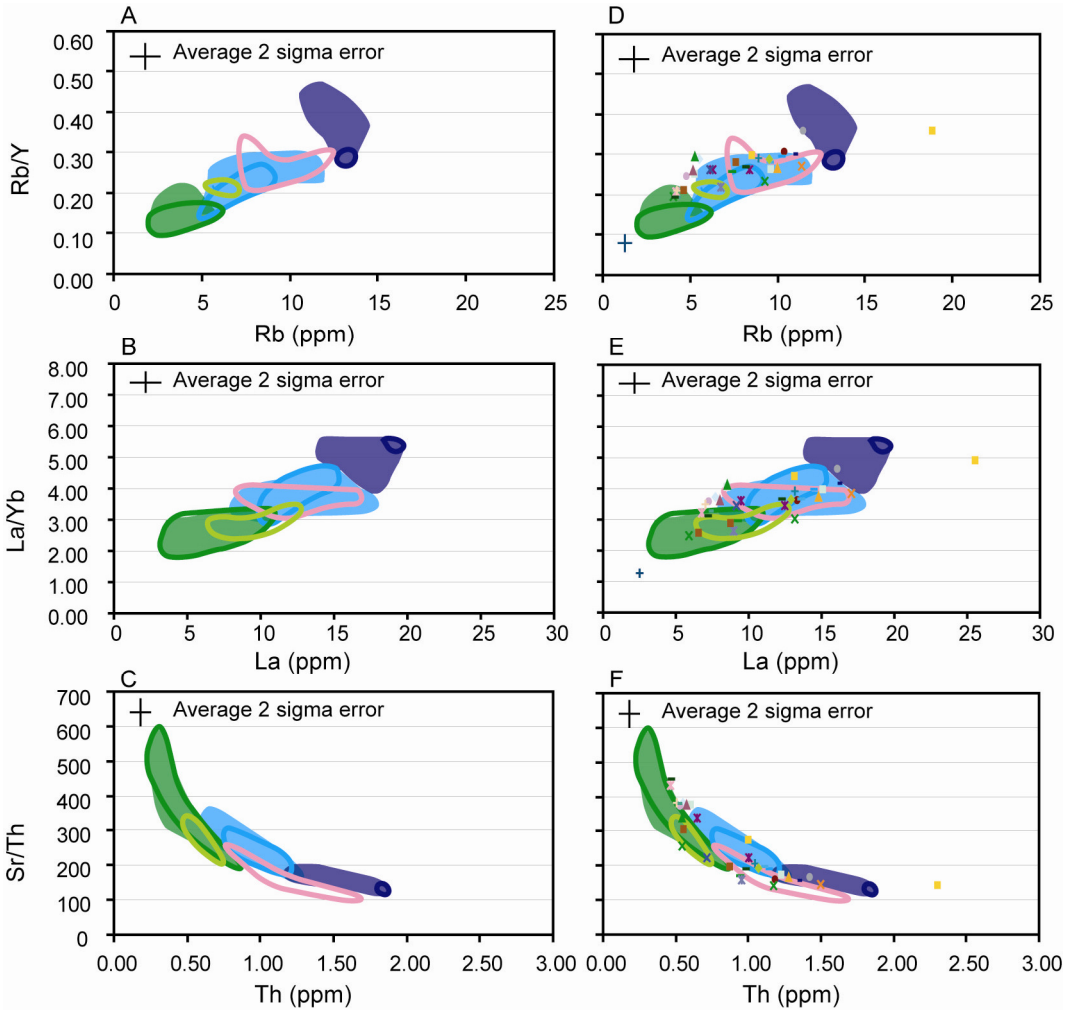

Figure 5. Trace element reference compositional fields. A-C) The coloured fields show a conservative estimate (enveloping the present results and associated 2 sigma error) of trace element composition for Bárdarbunga, Grímsvötn and Kverkfjöll tephra (colour scheme as in Fig. 1b). Open fields show published results (Meyer et al. 1985; Hémond et al. 1993; Chauvel and Hémond 2000; Kokfelt et al. 2006) from the three previously mentioned volcanic systems as well as Askja (pink) and Krafla (lime). The published values plot well within the compositional field obtained in this study. D-F) The coloured symbols show samples with unidentified source following major element analyses.

The compositional fields of Bárdarbunga, Grímsvötn and Kverkfjöll are relatively well separated by three trace element ratios, Rb/Y, La/Yb and Sr/Th although some overlap still exists between (1) Bárdarbunga and Grímsvötn and (2) Grímsvötn and Kverkfjöll (Fig. 5, Table 4). Tephra from the Bárdarbunga system has the lowest Rb, La and Th concentrations; range Rb: 2.98-4.61 ppm, La: 4.48-7.03 ppm, and Th: 0.31-0.62 ppm. Tephra of the Grímsvötn system has Rb, La and Th concentrations in the range of 5.71-11.3 ppm, 8.65-16.9 ppm and 0.59-1.26 ppm, respectively. Finally, Kverkfjöll tephra is characterized by the highest concentrations of Rb (11.0-14.1 ppm), La (14.8-18.5 ppm) and Th (1.17-1.57 ppm). Bárdarbunga tephra also has the lowest Rb/Y (range 0.13-0.20) and La/Yb (range 2.00-2.59) values and the highest Sr/Th values (range 242-461) whereas tephra from the Grímsvötn system ranges from 0.23-0.27 in Rb/Y, 3.37-3.88 in La/Yb and 157-365 in Sr/Th. Tephra from Kverkfjöll displays the highest Rb/Y (range 0.32-0.44) and La/Yb (range 4.05-5.12) and the lowest Sr/Th values (range 136-183; Fig. 5 and Table 4).

Table 4 Range and mean value of selected trace elements obtained by LA-ICP-MS analyses on identified tephra grains from Bárdarbunga, Grímsvötn and Kverkfjöll volcanic systems

	Bárdarbunga		***Grímsvötn***		***Kverkfjöll***	
	Range	***Mean***	***Range***	***Mean***	***Range***	***Mean***
Rb (ppm)	2.98-4.61	3.75	5.71-11.3	7.79	11.0-14.1	12.6
Y (ppm)	16.7-26.3	22.0	22.7-42.5	30.8	25.8-41.3	34.0
Rb/Y	0.13-0.20	0.17	0.23-0.27	0.25	0.32-0.44	0.38
La (ppm)	4.48-7.03	5.75	8.65-16.9	11.7	14.8-18.5	16.6
Yb (ppm)	1.99-2.91	2.47	2.50-4.69	3.27	2.89-4.56	3.68
La/Yb	2.00-2.59	2.33	3.37-3.88	3.59	4.05-5.12	4.56
Sr (ppm)	141-161	149	198-224	213	207-248	228
Th (ppm)	0.31-0.62	0.42	0.59-1.26	0.87	1.17-1.57	1.41
Sr/Th	242-461	375	157-365	260	136-183	163

The Grímsvötn tephra can be further divided into two groups, G-II and G-I, with and without a relative Sr depletion, respectively. No difference is observed between the spectra from the G-II group and that of Kverkfjöll except that tephra from the latter display higher element concentration. The less evolved Grímsvötn group (G-I) shows spectra comparable to the Bárdarbunga spectra, although systematically having higher concentrations of incompatible elements (e.g. HFSE, REE, LILE; Fig. 6). The volcanological implications of the compositional differences between G-I and G-II will be discussed elsewhere.

The trace element compositions of the 26 unknown tephra samples indicate that 13 come from Grímsvötn, four originated at Bárdarbunga and one is from Kverkfjöll (Fig. 5 and 6), leaving only eight samples of unidentified provenance. Hence, the trace element chemistry confirmed and permitted identification of 85% of the analysed tephra samples. Further

knowledge of trace element systematic in volcanics from neighbouring volcanic systems, such as Askja, is needed for further tephra identification in the soil north of Vatnajökull.

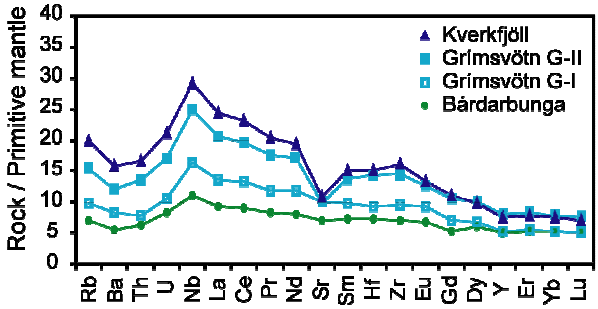

Figure 6. Primitive-mantle normalized multi-element diagram (Sun and McDonough 1989) for average Kverkfjöll (blue), Grímsvötn (sky blue, G-II and G-I filled and open squares, respectively) and Bárdarbunga (green) tephra composition. Element order is from Martin and Sigmarsson (2007). Grímsvötn tephra forms two groups, G-I with a spectra comparable with the Bárdarbunga spectra and G-II with a relative Sr depletion and follows the Kverkfjöll spectra, the only difference is higher element concentrations in the Kverkfjöll basalts.

Number of primary tephra

The great majority of the analysed samples, or 895 out of 921, represent primary tephra whereas 26 units (~3%) represent reworked material. However, the tephra units are not always uniform in their composition. Many units contain 5 grains of identical composition but include one or more grains of different composition. These grains appear to represent contamination from adjacent tephra units or volcanogenic soil, as the chemical composition is often indistinguishable from tephra units either below or above the sample of consideration.

4.6 Discussion

Tephra homogeneity

A few of the tephra samples contain glasses that exhibit clearly different compositions, although both plot within the same compositional field and thus indicate origin at the same volcanic system (Fig. 4). These samples may represent tephra produced by one event involving eruption producing magma of variable composition, possibly from a zoned magma chamber. This occurrence is not common but during the Krafla Fires of 1974-84, basalts erupted outside the caldera were of more primitive composition than basalts from within the caldera (Grönvold and Makipaa 1978). As wind directions can change throughout an eruption, this may result in deposition of tephra with different composition at different location around the volcanic edifice in the same eruption such as was observed during the Vatnaöldur 870 AD eruption (Larsen 1984). Other known eruptions that have continued over long periods exhibit exceptionally uniform magma composition throughout the whole eruption, such as the 8-month-long Laki eruption, (Sigmarsson et al. 1991).

Identifying basaltic tephra provenance from major element composition

When the primary tephra has been distinguished from those of secondary origin, their provenance can be traced using the criteria of chemical fingerprinting. The chemical composition of the tephra is compared to the characteristic compositional fields of the Grímsvötn, Bárdarbunga and Kverkfjöll volcanic systems, as well as those of Askja and Krafla, as they are defined by chemical composition determined in previous studies (Fig. 4; Jakobsson 1979; Nicholson 1990; Hémond et al. 1993; Kokfelt et al. 2006; this study). The Askja and Krafla volcanic systems are located somewhat north of the study area (Fig. 1) and both have been active during the Holocene.

Whole rock analyses (wet chemistry, XRF, ICP-MS) from Jakobsson (1979), Nicholson (1990), Hémond et al. (1993) and Kokfelt et al. (2006) on lavas from these five volcanic systems, along with electron microprobe analyses on reference samples from this study, are used to establish the reference compositional fields (RCF) shown in Figure 4. These studies yield rather homogeneous major element composition for a given volcanic system (Fig. 4a) although the compositional fields of individual systems often overlap (e.g. Grímsvötn and Askja on both plots of MgO and FeO vs. K_2O). Nevertheless, it is possible to confidently establish provenance for a tephra on basis of major elements alone by using specific discrimination graphs (e.g. Askja is distinguished from Grímsvötn on MgO vs. TiO_2 and FeO vs. TiO_2 graphs).

On Figure 4b the RCF for Askja and Krafla have been excluded since no confirmed tephra from these systems have been analysed. This may seem surprising; especially in relation to the proximity of Askja to the three soil profiles on the north side of Vatnajökull. However, not many explosive basalt eruptions within these volcanic systems are recorded in the literature and it is likely that Holocene activity at these systems has been dominated by effusive eruptions as they are ice-free. Still, at least one large basaltic explosive eruption is known on the Krafla volcanic system during the time period from 6800 years ago until today, the Hverfjall eruption, ~2900 years old (Thorarinsson 1952; Sæmundsson 1991). Tephra from this eruption has been mapped around the volcanic edifice and it was principally dispersed to the north and south (Sæmundsson 1991).

The results of the electron microprobe tephra analyses are shown in Figure 4. Discriminating diagrams such as K_2O and TiO_2 versus both FeO and MgO allow source identification for most of the tephra units as they fall into three distinctive groups, each showing a distinct trend of decreasing MgO with increasing K_2O (Fig. 4a&b). However, some

analysed samples in these groups plot outside the fields of published results. The extended compositional range of these samples is partly due to larger data set in the present study and the wider published RCF (larger variability in MgO and FeO for a given K_2O; shaded field on Fig. 4b) could result from potential inter-laboratory analytical bias due to different instrumental set-up and calibration schemes in the numerous laboratories from which the published result come from. The result is narrowing and extension of the compositional fields for the volcanic systems Grímsvötn, Bárdarbunga and Kverkfjöll.

Although these improved compositional fields better represent products of the relevant volcanic systems, a slight overlap still remains between compositions from different systems. This overlap is most pronounced between the fields of evolved basalts from Grímsvötn and Kverkfjöll, but is also present for a fraction of less evolved Grímsvötn and Bárdarbunga basalts. Nevertheless, the FeO/TiO_2 of 6 distinguishes between the two systems, Grímsvötn and Bárdarbunga, with the latter having higher ratio than 6. To further address this remaining overlap and better distinguish the compositional field of the volcanic systems, trace element compositions can be utilised.

Improving tephra provenance by trace element composition

The same process was applied on trace element results as the major elements. Correspondingly, RCF was drawn using published results (Meyer et al. 1985; Hémond et al. 1993; Chauvel and Hémond 2000; Kokfelt et al. 2006) and reference samples from this study (Fig. 5a-c). Askja and Krafla were included in the RCF even though major elements do separate them from Grímsvötn and Bárdarbunga. This was done to test if trace element concentrations offer higher resolving power for distinguishing between the volcanic systems. Clearly, the Rb/Y is significantly different and thus offers the possibility to distinguish between tephra originating at Bárdarbunga, Krafla, Askja and Kverkfjöll. Grímsvötn overlaps in Rb/Y with both Krafla and Askja, whereas the Sr/Th is generally higher in Grímsvötn tephra for a given Th concentration. Although published results for Krafla and Askja have La/Yb overlapping with the field of Grímsvötn and Bárdarbunga, this ratio is useful for distinguishing between tephra from the three Vatnajökull volcanoes.

On Figure 5 (d-f) the tephra units that remained unknown after discrimination based on major elements, shown as individual symbols, are compared to the RCF for Grímsvötn, Bárdarbunga and Kverkfjöll. Please note that Askja and Krafla fields are excluded from these plots. Most of the units do fall into the RCF as was observed for the major elements. However, some points fall outside of the published fields but the majority can be traced to

provenance based on logical trace element behaviour during magma evolution. During crystal fractionation of magma the La/Yb value does not change as both elements are incompatible in the major mineral phases found in the magmas produced by these systems and thus are concentrated in the derived melt. This simple fact is used to confidently trace the origin of most of the samples that fall outside of the RCF. However, since the trace element RCF for Grímsvötn and Bárdarbunga and Grímsvötn and Kverkfjöll do slightly overlap, eight tephra samples cannot be assigned to a volcanic system with confidence and further inspections is needed such as measurements of isotope ratios.

Possible sources for the basaltic tephra of uncertain provenance

In addition to the unidentified eight tephra samples, additional 19 basaltic tephra units out of the total 749 are of unidentified origin, or only 3.6%. Of the 27 unidentified units, 23 are of tholeiitic and four of transitional alkali basalt compositions (Table 5). The four transitional alkalic units are found in the soil section close to the Snæfell volcano. This volcano has produced magmas of similar composition (Hards 1995), although it is not known whether it has produced any mid- to late-Holocene eruptions. The age of the last volcanic activity at Snæfell, being either Holocene or Pleistocene, is debated (Hards 1995; Höskuldsson and Imsland 1998). However, since the age of the four transitional tephra falls in the period ~4700 to ~7000 and that their composition concurs with that of the eruption products from Snæfell this volcano still should be considered a potentially active volcano.

Six of the unknown basaltic tephra have tholeiitic composition with very low TiO_2 contents (1.12-1.27 wt%) pointing towards a possible origin at Hofsjökull (Kokfelt et al. 2006; Jakobsson et al. 2008) or Gígöldur (east of Dyngjuháls, reference samples, this study). The Gígöldur crater complexes have been assigned to Askja volcanic system by Jóhannesson and Sæmundsson (1998a). Of these six tephra, three are found in Hreysiskvísl, two of which are of historical age, ~770 and ~970 years old; and one ~1920 years old (profile nr. 1; Fig. 1c). One of these tephra, ~6950 years old, is found in Kárahnjúkar (profile nr. 4; Fig 1c) and the remaining two in the Snæfell profile, 6950 and 7000 years old (profile nr. 5; Fig. 1c). According to Jóhannesson and Sæmundsson (1998b), seven Holocene lavas have been erupted in the Hofsjökull volcanic system and some Holocene age volcanic formation are in the Gígöldur area, all of which may be at the origin of these unidentified tephra.

Four of the unknown tephra may be from Krafla. They exhibit TiO_2 contents similar to Bárdarbunga (i.e. 1.67-1.80 wt%), but the corresponding K_2O concentrations (i.e. 0.28-0.32 wt%) is significantly higher than in Bárdarbunga tephra . These four units are found in the

profiles at Snæfell and Kárahnjúkar (two in each) and are ~6300-6700 years old. These calculated ages do not support Krafla origin because according to Sæmundsson (1991), at this time there was lull in the activity at Krafla and even the soils close to Krafla are deprived of tephra from this period.

Table 5 Average values for electron microprobe glass analyses of tephra of unidentified provenance.

*	Log #	Age+	SiO_2	TiO_2	Al_2O_3	FeO	MnO	MgO	CaO	Na_2O	K_2O	P_2O_5	Total
1	**HKV32**	1920	48.90	1.12	15.32	10.36	0.16	8.39	12.95	2.03	0.11	0.10	99.43
1	**HKV5**	770	49.01	1.13	14.99	10.42	0.20	7.94	12.76	2.08	0.14	0.07	98.76
1	**HKV11**	970	48.32	1.17	14.90	10.56	0.18	8.21	12.88	2.00	0.10	0.09	98.41
1	**Kár12**	6950	48.90	1.17	14.99	10.03	0.18	8.24	13.25	1.92	0.10	0.10	98.88
1	**Snæ105**	6970	49.59	1.25	14.86	10.14	0.21	8.07	12.91	1.91	0.12	0.11	99.17
1	**Snæ108**	6997	49.83	1.27	14.83	10.17	0.18	7.91	12.87	1.92	0.14	0.07	99.17
2	**Snæ109**	7000	51.40	1.36	14.70	10.21	0.23	7.09	11.82	2.24	0.26	0.10	99.41
3	**Kár22**	6540	49.76	1.67	14.15	11.53	0.17	6.99	11.73	2.29	0.28	0.19	98.75
3	**Snæ95**	6330	50.26	1.70	14.20	11.74	0.20	6.70	11.15	2.38	0.32	0.16	98.83
3	**Snæ97**	6400	49.82	1.76	14.21	12.07	0.19	6.68	11.26	2.34	0.30	0.18	98.82
3	**Kár18**	6730	50.07	1.80	14.12	12.06	0.19	6.75	11.40	2.32	0.32	0.18	99.22
4	**Snæ111**	7070	49.03	1.82	14.76	10.90	0.15	7.54	12.18	2.19	0.23	0.14	98.95
4	**Stein12**	3220	49.87	1.83	13.99	11.83	0.16	7.03	11.68	2.26	0.22	0.18	99.04
4	**Sau51**	3480	49.76	1.84	14.69	11.53	0.19	6.78	11.52	2.51	0.26	0.19	99.27
4	**Stein9**	3440	50.05	1.90	14.56	11.79	0.27	6.51	11.26	2.48	0.28	0.25	99.35
4	**Hre106**	7125	49.87	1.99	13.86	12.86	0.23	5.90	10.29	2.50	0.43	0.20	98.14
4	**Snæ112**	7080	49.21	2.00	14.36	11.39	0.13	7.18	11.76	2.41	0.24	0.15	98.84
4	**Sau14**	6240	49.56	2.01	14.66	11.91	0.20	6.58	11.30	2.36	0.36	0.18	99.13
4	**Kár112**	1410	50.21	2.14	13.83	13.12	0.25	5.77	10.27	2.60	0.33	0.22	98.75
4	**Sau75**	2280	50.16	2.17	14.33	12.24	0.21	5.17	9.66	2.84	0.42	0.32	97.52
5	**Snæ101**	6880	47.40	2.51	15.44	11.25	0.19	6.43	11.30	2.66	0.76	0.27	98.23
5	**Snæ106**	6990	47.93	2.53	15.45	11.19	0.17	6.50	11.15	2.62	0.75	0.26	98.54
5	**Snæ103**	6940	47.79	2.62	15.16	11.22	0.21	6.26	11.09	2.72	0.77	0.30	98.12
5	**Snæ73**	4710	47.60	2.63	15.14	11.44	0.21	6.31	11.13	2.68	0.78	0.32	98.24
2	**Sau76**	2240	50.90	3.24	13.32	13.98	0.28	3.76	7.96	3.33	0.84	0.57	98.17
2	**Kár92**	2260	51.17	3.26	13.23	13.87	0.25	3.84	8.00	3.30	0.80	0.59	98.32
2	**Hreys90**	5400	46.64	3.90	13.51	14.06	0.27	5.42	10.43	2.86	0.63	0.42	98.14

*Number denotes possible origin 1: Hofsjökull/Dyngjuháls; 2: unidentified origin; 3: Krafla; 4: Grímsvötn/Bárdarbunga/other; 5: Snæfell/Öræfajökull/other. + Age see Table 3b

Of the remaining 13 tephra units that have not been assigned to a source system, three exhibit compositions that are not compatible with established chemical signature for any known volcanic system (SiO_2: 46.64-51.17 wt%; TiO_2: 3.24-3.9 wt%; MgO: 3.76-5.42 wt%; K_2O: 0.63-0.84 wt%). One of these 13 units is marginally a basaltic icelandite (SiO_2: 51.40 wt%). Nine samples exhibit a mixed Grímsvötn and Bárdarbunga characteristics both in terms of their major and trace element signatures. They may originate from a specific volcanic system or segment of a known volcanic system yet to be chemically fingerprinted, but grouped here as from an unidentified source. Mapping and chemical fingerprinting of

volcanic systems in central Iceland is still in its infancy and is essential in order to improve provenance identification of Holocene basaltic tephra.

4.7 Conclusions

Field observations, combined with chemical composition of tephra, determine primary volcanic or secondary aeolian origin of the sampled tephra. Measurements of major element composition of primary tephra is sufficient for identifying provenance for most basaltic tephra from the Grímsvötn, Bárdarbunga and Kverkfjöll volcanic systems. The provenance of individual tephra is determined by comparison with improved reference compositional fields (RCF) for each system, established from published data as well as new reference data obtained in this study. Of the tephra that were of uncertain provenance on basis of major element criteria, the source volcanic system was confirmed and identified for 85% on basis of their trace element compositions. Both major and trace elements RCF provide a robust method for determining the provenance of tephra and the added tephra analyses from this study, covering the last ~7.6 ka of activity, have greatly improved our knowledge of the compositional range within each volcanic system.

Four major elements, K_2O, TiO_2, MgO and FeO, and their ratios are the best discriminators of tephra from the Grímsvötn, Bárdarbunga and Kverkfjöll volcanic systems, although the chemical compositional fields defined by these elements slightly overlap. Three trace element ratios, Rb/Y, La/Yb and Sr/Th, further improve the fingerprinting of the tephra. The results of this study demonstrate the usefulness of combined major and trace element analyses in delineating the provenance of basaltic tephra in Iceland.

4.8 Acknowledgements

This paper is based on a PhD-study at the Laboratoire Magmas et Volcans (LMV), CNRS-Université Blaise Pascal in Clermont-Ferrand and the University of Iceland. It was financed by the Icelandic Science Foundation, Landsvirkjun, Eimskip Fund of The University of Iceland, the French government through a student's grant and the French-Icelandic collaboration programme Jules Verne. Paul Mason and Gijs Nobbe at the Utrecht University are genuinly thanked for their help during and after LA-ICP-MS analyses.

4.9 References

Bjarnason IT, Wolfe CJ, Solomon SC, Gudmundson G (1996) Initial results from the ICEMELT experiment: Body-wave delay times and shear-wave splitting across Iceland. Geophysical Research Letters 23(8):903-903.

Björck S, Ingólfsson Ó, Haflidason H, Hallsdóttir M, Anderson NJ (1992) A high resolution record of the North Atlantic ash zone 1 and the last glacial-interglacial environment changes in Iceland. Boreas 21:15-22.

Chauvel C, Hémond C (2000) Melting of a complete section of recycled oceanic crust: Trace element and Pb isotopic evidence from Iceland. Geochemistry, Geophysics, Geosystems 1, Paper number 1999GC000002.

Devidal JL, Sigmarsson O, Óladóttir BA, Larsen G (2008) Sodium loss during electron microprobe analysis of Hekla tephra and empirical corrections. In: IAVCEI 2008 General Assembly. Reykjavík, Iceland, 17-22 August.

Dugmore AJ (1989) Iceland volcanic ash in late-Holocene peats in Scotland. Scottish Geographical Magazine 105:169-172.

Dugmore AJ, Shore JS, Cook GT, Newton AJ, Edwards KJ, Larsen G (1995) The radiocarbon dating of Icelandic tephra layers in Britain and Iceland. Radiocarbon 37(2):379-388.

Grönvold K, Makipaa H (1978) Chemical composition of Krafla lavas. In: Nordic Volcanological Institude Rep. 7816.

Grönvold K, Óskarsson N, Johnsen SJ, Clausen HB, Hammer CU, Bond G, Bard E (1995) Ash Layers from Iceland in the Greenland Grip Ice Core Correlated with Oceanic and Land Sediments. Earth and Planetary Science Letters 135(1-4):149-155.

Haflidason H, Eiríksson J, Van Kreveld S (2000) The tephrochronology of Iceland and the North Atlantic region during the Middle and Late Quaternary: a review. Journal of Quaternary Science 15(1):3-22.

Hards VL (1995) The evolution of the Snæfell volcanic centre, Eastern Iceland. Unpublished PhD theses from the University of Durham, Durham, p 324.

Hémond C, Arndt NT, Lichtenstein U, Hofmann AW, Óskarsson N, Steinthórsson S (1993) The Heterogeneous Iceland Plume - Nd-Sr-O Isotopes and Trace-Element Constraints. Journal of Geophysical Research-Solid Earth 98(B9):15833-15850.

Hunt JB, Hill PG (2001) Tephrological implications of beam size-sample-size effects in electron microprobe analysis of glass shards. Journal of Quaternary Science 16(2):105-117.

Höskuldsson Á, Imsland P (1998) Snæfell - Eldfjall á gosbelti framtíðar (Geology of Snæfell, an intraplate volcano in Eastern Iceland). Glettingur 8(2-3):22-30.

Ingólfsson Ó, Norddahl H, Haflidason H (1995) Rapid Isostatic Rebound in Southwestern Iceland at the End of the Last Glaciation. Boreas 24(3):245-259.

Jakobsson SP (1979) Petrology of recent basalts of the Eastern Volcanic zone, Iceland. Acta Naturalia Islandica 26:1-103.

Jakobsson SP, Jónasson K, Sigurdsson IA (2008) The three igneous rock series of Iceland. Jökull 58:117-138.

Jarosewich E, Nelen JA, Borberg JA (1979) Electron microprobe reference samples for mineral analysis. In: Fudali RF (ed) Smithsonian Institution Contributions to the Earth Sciences No. 22. Smithsonian Institution Press, Washington, D.C., pp 68-72.

Jóhannesson H, Sæmundsson K (1998a) Geological map of Iceland, 1:500,000. Tectonics. Icelandic Institute of Natural History and Iceland Geodetic Survey, Reykjavík.

Jóhannesson H, Sæmundsson K (1998b) Geological map of Iceland, 1:500,000. Icelandic Institute of Natural History and Iceland Geodetic Survey, Reykjavík.

Keller J (1981) Quaternary tephrochronology in the Mediterranean. In: Self S, Sparks RSJ (eds) Tephra studies. D. Reidel, Dordrecht, pp 227-244.

Kokfelt TF, Hoernle K, Hauff F, Fiebig J, Werner R, Garbe-Schonberg D (2006) Combined trace element and Pb-Nd-Sr-O isotope evidence for recycled oceanic crust (upper and lower) in the Iceland mantle plume. Journal of Petrology 47(9):1705-1749.

Lacasse C, Sigurdsson H, Jóhannesson H, Paterne M, Carey S (1995) Source of Ash-Zone-1 in the North-Atlantic. Bulletin of Volcanology 57(1):18-32.

Larsen G (1981) Tephrochronology by microprobe glass analysis. In: Self S, Sparks RSJ (eds) Tephra Studies. D. Reidel, Dordrecht, pp 95-102.

Larsen G (1984) Recent volcanic history of the Veidivötn fissure swarm, Southern Iceland. An approach to volcanic risk assessement. Journal of Volcanology and Geothermal Research 22:33-58.

Larsen G, Eiríksson J (2008) Late Quaternary terrestrial tephrochronology of Iceland - frequency of explosive eruptions, type and volume of tephra deposits. Journal of Quaternary Science 23(2):109-120.

Larsen G, Dugmore A, Newton A (1999) Geochemistry of historical-age silicic tephras in Iceland. Holocene 9(4):463-471.

Larsen G, Newton AJ, Dugmore AJ, Vilmundardóttir EG (2001) Geochemistry, dispersal, volumes and chronology of Holocene silicic tephra layers form the Katla volcanic system, Iceland. Journal of Quaternary science 16:119-132.

Le Bas MJ, Le Maitre RW, Streckeisen A, Zanettin B (1986) A chemical classification of volcanic rocks based on the total alkali-silica diagram. Journal of Petrology 22:745-750.

Mangerud J, Furnes H, Johanssen J (1986) A 9000year old ash bed on the Faroe Islands. Quaternary Research 26:262-265.

Mangerud J, Lie SE, Furnes H, Kristianssen IL, Lomo L (1984) A Younger Dryas ash bed in western Norway and its possible correlation with tephra in cores from the Norwegian Sea and the North Atlantic. Quaternary Research 21:85-104.

Martin E, Sigmarsson O (2007) Low-pressure differentiation of tholeiitic lavas as recorded in segregation veins from Reykjanes (Iceland), Lanzarote (Canary Islands) and Masaya (Nicaragua). Contributions to Mineralogy and Petrology 154(5):559-573.

Merlet C (1994) An Accurate Computer Correction Program for Quantitative Electron-Probe Microanalysis. Mikrochimica Acta 114:363-376.

Meyer PS, Sigurdsson H, Shilling JG (1985) Petrological and geochemical variations along Iceland's Neovolcanic zones. Journal of Geophysical Research 90:10043-10072.

Miyashiro A (1978) Nature of alkalic volcanic rock series. Contributions to Mineralogy and Petrology 66:91-104.

Nicholson H (1990) The magmatic evolution of Krafla, NE Iceland. Unpublished PhD theses from the University of Edinburgh, Edinburgh, p 286.

Nielsen CH, Sigurdsson H (1981) Quantitative Methods for Electron Micro-Probe Analysis of Sodium in Natural and Synthetic Glasses. American Mineralogist 66(5-6):547-552.

Norddahl H, Haflidason H (1992) The Skógar Tephra, a Younger Dryas Marker in North Iceland. Boreas 21(1):23-41.

Óladóttir BA, Larsen G, Thordarson T, Sigmarsson O (2005) The Katla volcano S-Iceland: Holocene tephra stratigraphy and eruption frequency. Jökull 55:53-74.

Óladóttir BA, Sigmarsson O, Larsen G, Thordarson T (2008) Katla volcano, Iceland: magma composition, dynamics and eruption frequency as recorded by Holocene tephra layers. Bulletin of Volcanology 70(4):475-493.

Persson C (1971) Tephorchronological investigation of peat deposits in Scandinavia and on the Faroe Islands. Geological Survey of Sweden C 656:34.

Schuessler JA, Schoenberg R, Sigmarsson O (2009) Iron and lithium isotope systematics of the Hekla volcano, Iceland - Evidence for Fe isotope fractionation during magma differentiation. Chemical geology 258:78-91.

Sigmarsson O, Condomines M, Fourcade S (1992) A Detailed Th, Sr and O Isotope Study of Hekla - Differentiation Processes in an Icelandic Volcano. Contributions to Mineralogy and Petrology 112(1):20-34.

Sigmarsson O, Condomines M, Grönvold K, Thordarson T (1991) Extreme Magma Homogeneity in the 1783-84 Lakagígar Eruption - Origin of a Large Volume of Evolved Basalt in Iceland. Geophysical Research Letters 18(12):2229-2232.

Sun SS, McDonough WF (1989) Chemical and isotopic systematics of oceanic basalts: Implication for the mantle composition and processes. Geological Society, Special Publications 42:313-345.

Sæmundsson K (1978) Fissure swarms and central volcanoes of the neovolcanic zones of Iceland. Geological Journal Special Issue 10:451-432.

Sæmundsson K (1979) Outline of the geology of Iceland. Jökull 29:7-29.

Sæmundsson K (1991) Jarðfræði Kröflukerfisins (Geology of the Krafla volcanic system). In: Garðarsson AÓ, Einarsson Á (eds) Náttúra Mývatns. Hið Íslenska náttúrufræðifélag, Reykjavík.

Thorarinsson S (1952) Hverfjall II. Aldur Hverfjalls og myndun (Hverfjall: Age and formation). Náttúrufræðingurinn 22(4):146-172.

Thordarson T, Larsen G (2007) Volcanism in Iceland in historical time: Volcano types, eruption styles and eruptive history. Journal of Geodynamics 43(1):118-152.

Thornber CR, Sherrod DR, Siems DR, Heliker CC, Meeker GP, Oscarsson RL, Kauahikaua JP (2002) Whole rock and glass major-element geochemistry of Kilauea Volcano, Hawaii, near-vent eruptive products: September 1994 through September 2001. In: USGS, open file report 02-17.

van Achterbergh E, Ryan CG, Jackson SE, Griffin W (2001) Data reduction software for La-ICP-MS. In: Sylvester P (ed) Laser ablation ICP-MS in Earth Science Principles and Applications. Mineralogical Association of Canada, pp 239-243.

van den Bogaard C, Schminke HU (2002) Linking the North Atlantic to central Europe: a high-resolution Holocene tephrochronological record from northern Germany. Journal of Quaternary science 17:3-20.

White RS, Bown JW, Smallwood JR (1995) The Temperature of the Iceland Plume and Origin of Outward-Propagating V-Shaped Ridges. Journal of the Geological Society 152:1039-1045.

Wilson SA (1997) The collection, preparation, and testing of USGS reference material BCR-2, Columbia River, Basalt. In: U.S. Geological Survey Open-File Report 98-xxx.

Wolfe CJ, Bjarnason IT, VanDecar JC, Solomon SC (1997) Seismic structure of the Iceland mantle plume. Nature 385(6613):245-247.

5. Manuscript 2: Holocene activity at the Grímsvötn, Bárdarbunga and Kverkfjöll subglacial volcanoes of Vatnajökull, Iceland

Holocene activity at the Grímsvötn, Bárdarbunga and Kverkfjöll subglacial volcanoes of Vatnajökull, Iceland

Bergrun Arna Óladóttir[1,2], Gudrun Larsen[2] and Olgeir Sigmarsson[1,2]

1) Université Blaise Pascal, OPGC and CNRS, 5 rue Kessler, 63038 Clemont-Ferrand, France

2) Institute of Earth Sciences, University of Iceland, 101 Reykjavík, Iceland

5.1 Abstract

Assessment of future eruptions and eruptive behaviour of active volcanoes relies strongly on knowledge of their activity in the past, including information on eruption frequency, magnitude and repose time. The eruption history of Grímsvötn, Bárdarbunga and Kverkfjöll central volcanoes is studied via tephra collected from soil sections around Vatnajökull ice cap, which collectively cover the last 7.6 ka. Major and trace element composition of tephra allows correlation to source volcanoes and between measured soil profiles. Altogether 749 tephra units were measured and sampled from seven profiles. Well-known regional Holocene marker tephra, such as H3, H4 and H5, were utilized to correlate the profiles. Then stratigraphic position and chemical composition was used for fine scale correlation of basaltic tephra in order to reconstruct the eruption history at each volcano as it is preserved in the soil cover. On basis of these correlations we identify 348 tephra layers, each representing an explosive eruption, in the soil cover around Vatnajökull, of which 70% come from the subglacial central volcanoes beneath Vatnjökull, Grímsvötn, Bárdarbunga and Kverkfjöll. The eruption frequency of each volcanic system is estimated and it reveals Grímsvötn as the most active volcanic system of the three during prehistoric as well as historical time, with an average of ~7 eruptions per century (range of 4-14) during the prehistoric time and no obvious repose periods during the last 7.6 ka. Its eruption frequency during the last 1 ka is lower than it was during the period 1-2 ka when activity was at its peak, but markedly higher than what it was in the period 2-8 ka. Bárdarbunga is the second most active during both historical and prehistoric time with ~5 eruptions per century and a range of 1-8 eruptions per century during the prehistoric era but the eruption frequency during the last millennium is the lowest one observed in the last ~6000 years. The Kverkfjöll volcanic system has remained calm with 0-3 eruptions per century and on average ~1 eruption per 100 years but the activity is periodic with typical repose time of >1000 years, including the current one that has lasted for ~1200 years. All three volcanic systems show a lull in activity between 5 and 2 ka. This period is referred to here as “the Mid Holocene low”, and appears to result from decrease in the overall eruption frequency caused by periodic decrease in magma generation and delivery from the mantle plume rather than from changes in climatic factors (i.e. changes in the ice load/glacier thickness). In prehistoric time, a 1-3 thousand years time lag is observed between peak of activity at the volcanoes directly above the mantle plume (Grímsvötn and Bárdarbunga) and that at volcanoes located farther away and in the non-rifting part of the Eastern Volcanic Zone (i.e. Katla). This may suggest that a significant increase could be expected in volcanism on

this part of the EVZ in the future since the highest observed eruption frequency was only 2-1 ka in Grímsvötn and Bárdarbunga.

5.2 Introduction

Plate boundaries are the most volcanically active places on Earth and diverse tectonic settings cause different types of volcanism. Most of the historically documented eruptions take place on subduction zones (~85%; Simkin and Siebert 1994), whereas intraplate volcanism accounts for ~10% of all historically documented eruptions (Simkin and Siebert 1994) which leaves only ~5% of documented eruptions to take place on the ocean ridges. However, budged calculations of new lava reaching the surface, calculated from relative plate motion, show that ocean ridge volcanism clearly dominates the planet accounting for ~75% of new lava production (Simkin and Siebert 2000).

Iceland is one of few places on Earth where an oceanic ridge rises above sea level and it is possible to monitor the eruptive behaviour on the ridge. Even though the crustal spreading is steady (~2 cm/year; Hreinsdóttir et al. 2001) the rift zone response to it seems to be episodic (e.g. Björnsson 1985; Simkin and Siebert 2000; LaFemina et al. 2005). If the magma production rate remains constant, even though eruptions are periodic, about 6 m^3/s of magma have to be produced to account for the volume needed to construct the volcanic island and its crust (Sigmundsson 2006). Previous studies show that eruptions are not spread evenly over time and their occurrence exhibits certain degree of episodicity (e.g. Sigvaldason et al. 1992; Larsen et al. 1998; Maclennan et al. 2002; Óladóttir et al. 2005). This implies that magma production is a periodic process or if production is steady then its delivery to the surface is delayed by temporary storage within the plumbing systems and/or magma chambers.

The frequency of explosive volcanism has been shown to be different between interglacial and glacial periods where an increase in activity is noted during the former ones (e.g. Sigurdsson and Loebner 1981; Sejrup et al. 1989; Sjoholm et al. 1991). This change has been attributed to glacio-isostatic processes related to the deglaciation of the large ice sheet after the last glacial period (Sejrup et al. 1989; Sjoholm et al. 1991; Jull and McKenzie 1996; Lacasse et al. 1998; Haflidason et al. 2000) and Gudmundsson (2000) explains the difference by magma chamber formation during glacial periods due to deflection of the crust causing stress barriers that trap magma. Sigvaldason et al. (1992) also report a 30 fold increase in lava production rates compared to present time during the millennia following the deglaciation and link it to decreasing lithostatic pressure due to unloading. This pulse of high production rates

lasted for less than 2000 years after the end of deglaciation (Maclennan et al. 2002). The effect of ice deloading on the magma output rate recently has been questioned by Thordarson and Höskuldsson (2008) and improved estimates on eruption frequency are clearly needed for the early Holocene.

The eruption frequency in Iceland during historical time (last ~1100 years) has been calculated to an average of 20 eruptions per century or an eruption every ~5 years (Thorarinsson and Sæmundsson 1979). Prehistoric time has received less attention but Jakobsson (1979) reported periodic volcanism on the Eastern Volcanic Zone (EVZ) during the Holocene peaking from ~9-7 ka and again ~3-1 ka. The volcanic history of the Katla volcano, on the EVZ, during the last 8.4 ka has also been thoroughly studied showing two tephra layer frequency (TLF) peaks, 8-7 ka and 4-2 ka (Óladóttir et al. 2005; 2008) and the silicic Holocene activity shows about the same peaks 8-7 ka and 3-1 ka (Larsen and Eiríksson 2008a;b).

Although the knowledge on prehistoric volcanic history of Icelandic volcanoes is improving, very little work has been done on the subglacial Vatnajökull volcanoes, which are amongst the most active volcanoes in the country during historical time (e.g. Thordarson and Larsen 2007). The aim of this study is to evaluate the eruption frequency and volcanic history of three tholeiitic Vatnajökull volcanoes, Grímsvötn, Bárdarbunga and Kverkfjöll during the last 7.6 ka based on the tephra stratigraphy around the Vatnajökull ice cap. The key question to be addressed is: Have they always been as active as during the last millennium or does their activity exhibit periodic or other systematic long term changes?

5.3 Geological context

Volcanism in Iceland follows distinct volcanic zones, further divided into volcanic systems (e.g. Sæmundsson 1978; Jakobsson 1979), of which the majority produces magma of tholeiitic composition. The main part, or 75-79% of eruptions, are basaltic (Thordarson and Larsen 2007; Jakobsson et al. 2008) and the same authors estimate that silicic eruptions constitute 5-11% of the total production. Volcanic activity in Iceland is high as a result of the peculiar geological setting, where the North Atlantic ridge system is superimposed on the Iceland mantle plume (e.g. Óskarsson et al. 1985).

Grímsvötn, Bárdarbunga and Kverkfjöll volcanic systems

Three central volcanoes, Grímsvötn, Bárdarbunga and Kverkfjöll, and parts of their associated fissure swarms, all characterised by basaltic eruptive products, are located under the NW-part of the Vatnajökull ice cap (Fig. 1). The Grímsvötn volcanic system, 100 km long and up to 23 km wide, has an area of 1350 km^2, of which 2/3 are covered by the ice cap (Sæmundsson 1978; Jóhannesson and Sæmundsson 1998; Thordarson and Larsen 2007). It consists of an embryonic fissure swarm and a central volcano, Grímsvötn, with a composite caldera and extensive geothermal activity therein. Þórdarhyrna has been proposed as a second central volcano in this volcanic system (Björnsson and Einarsson 1990; Jóhannesson and Sæmundsson 1998; Thordarson and Larsen 2007).

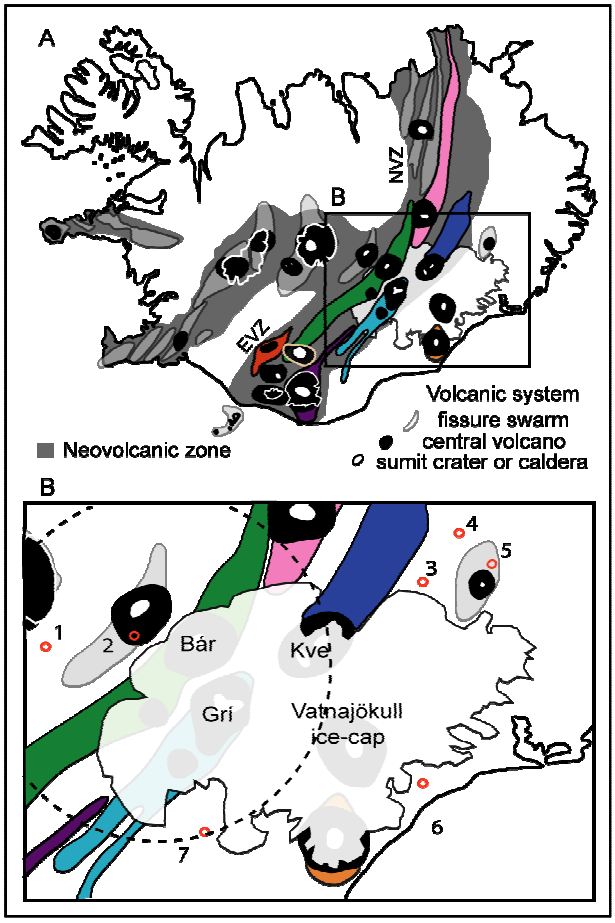

Figure 1 A) Map showing the position of the neovolcanic zone and volcanic systems in Iceland. The systems of concern in this study are colour coded: Grímsvötn (sky blue), Bárdarbunga (green), Kverkfjöll (blue), Hekla (red), Katla (violet), Torfajökull (tan), Askja (rose) and Öræfajökull (orange). The box outlines study area. B) Map of the study area, showing the location of the seven measured and sampled soil profiles around the Vatnajökull ice-cap: 1: Hreysiskvísl; 2: Nýidalur; 3: Saudárhraukar; 4: Kárahnjúkar; 5: Snæfell; 6: Steinadalur and 7: Núpsstadarskógar. Other abbreviations are: EVZ Eastern volcanic zone; Bár Bárdarbunga central volcano; Grí Grímsvötn central volcano; Kve Kverkfjöll central volcano. The circle outlines the mantle plume at 125 km depth (Wolfe et al. 1997). Modified after Jóhannesson and Sæmundsson (1998) and Thordarson and Larsen (2007).

The Bárdarbunga system, also referred to as the Veidivötn or Bárdabunga-Veidivötn system, is 190 km long and up to 28 km wide, covering about 2500 km^2 which makes it Iceland's most extensive volcanic system. About 60 km, out of the 190 km, are ice covered (Sæmundsson 1978; Thordarson and Larsen 2007). The system has a mature fissure swarm and two proposed central volcanoes located under the ice cap, Bárdarbunga, which contains a 700 m deep caldera, and Hamarinn (Björnsson and Einarsson 1990; Jóhannesson and Sæmundsson 1998; Thordarson and Larsen 2007).

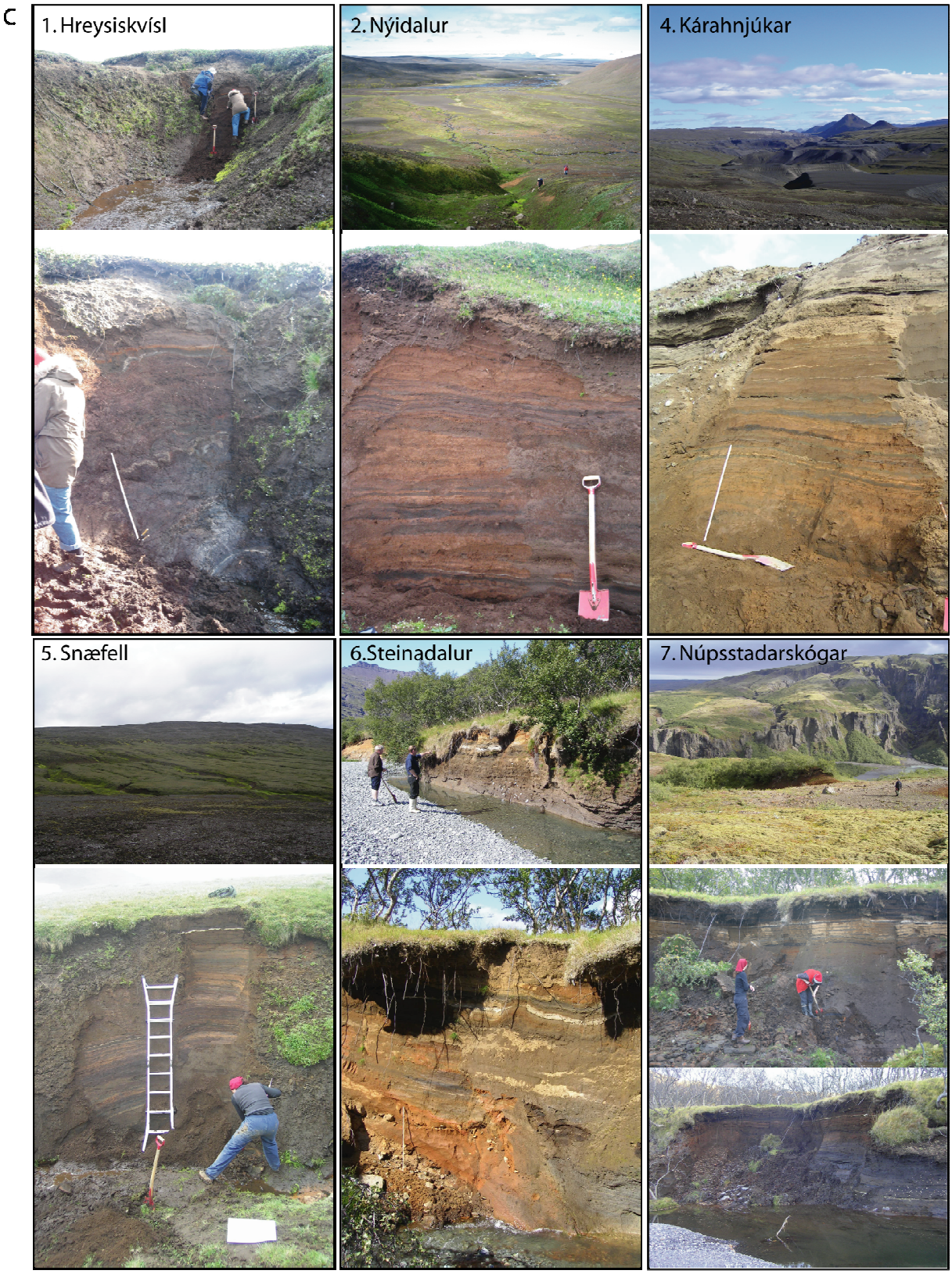

Figure 1C) Photos of the outcrops and their surroundings. No photos are shown from the Saudárhraukar outcrop (no. 3).

The Kverkfjöll system is 120 km long and 20 km wide, covering 1600 km^2, most of which are ice free (Fig. 1). It consists of a mature fissure swarm and a central volcano with

two calderas and considerable geothermal activity is associated with the northern one (Björnsson and Einarsson 1990; Jóhannesson and Sæmundsson 1998; Thordarson and Larsen 2007).

Two of the three central volcanoes, Grímsvötn and Bárdarbunga, are located on the EVZ, which is a propagating rift zone (Óskarsson et al. 1982), and close to the assumed centre of the Iceland mantle plume, whereas Kverkfjöll lies farther from the plume centre (Wolfe et al. 1997) and on the NVZ, which is on the axial rift zone (Óskarsson et al. 1982). The eruption frequency at Grímsvötn and Bárdarbunga is high and as a consequence of an extensive ice cover explosive eruptions are common, despite basaltic magma composition.

In historical time the eruption frequency of the most active volcanoes below Vatnajökull has been periodic, peeking every 130-140 years. The period is divided in 50-80 year long episodes of high eruption frequency, during which 6-11 eruptions are observed per 40 years, and equally long episodes of low eruption frequency, with only 0-4 eruptions per 40 years (Larsen et al. 1998).

Activity at Grímsvötn, Bárdarbunga and Kverkfjöll in historical time - a brief overview

The Grímsvötn volcanic system has been the most active system in Iceland during historical time, accounting for ~38% of all confirmed eruptions (Thordarson and Larsen 2007). All historical eruptions except the Laki eruption in 1783-84 took place on the ice covered part of the system and their majority is thought to have occurred within the domain of the central volcano (Thorarinsson 1974; Gudmundsson and Björnsson 1991). Over 70 eruptions are confirmed and/or reported, but since 1200 AD only one out of every five historical Grímsvötn eruptions have deposited detectable tephra outside of the Vatnajökull ice cap and the barren highlands (Larsen and Eiríksson 2008a). The observed periodicity in eruption frequency during historical time is mostly due to activity at Grímsvötn (Larsen et al. 1998).

The Bárdarbunga system is the second to third most active in historical time, along with Hekla, producing ~14% of confirmed eruptions. Even though about 70% of the system is ice free (Sæmundsson 1978), only 3 out of 23 confirmed eruptions have occurred out on the ice free fissure swarm (Larsen 1984; Thordarson and Larsen 2007). This system appears to have significantly lower eruption frequency than the Grímsvötn system but during historical time peaks of activity concur (Larsen et al. 1998). In the last 800 years, tephra from one out of four eruptions at Bárdarbunga are preserved in the soil cover outside of the Vatnajökull ice cap and the barren highlands (Larsen and Eiríksson 2008a), which is a higher preservation

ratio than observed for Grímsvötn tephra, most likely due to a location closer to the glacier margins.

The third volcanic system, Kverkfjöll, has not erupted during historical time. However, several eruptions have incorrectly been assigned to this volcano based on historical records, including the eastern sector of the tephra from the 1477 AD Veidivötn eruption of the Bárdarbunga system (Larsen 1982). Despite its quiescence in historical time (i.e. the last 1100 years), Kverkfjöll central volcano still features vigorous geothermal activity (Friedman et al. 1972; Björnsson and Einarsson 1990).

In the following chapters the names Grímsvötn, Bárdarbunga and Kverkfjöll will refer to the central volcanoes and the ice covered parts of the volcanic systems.

Volcanic systems producing silicic tephra marker layers

Volcanoes that have formed wide-spread silicic tephra layers of importance for this study are Hekla, Torfajökull, Askja, and Öræfajökull (see Fig. 1 for volcanic system locations), all of which produce transitional alkalic magma except Askja, which is also the only one located in the axial rift. Hekla is by far the most productive volcano in terms of production of intermediate to silicic tephra and is the second to third most active system in Iceland during historical time along with Bárdarbunga (Thordarson and Larsen 2007). Hekla is also known for its wide-spread prehistoric silicic tephra, i.e. H3, H4 and H5 (e.g. Larsen and Thorarinsson 1977).

Icelandic soils

The most common soil type in Iceland is Andosol, rich in volcanic material, although Histosol, rich in organic material, is present in significant abundances (e.g. Arnalds 2004). Large inputs of aeolian material make Icelandic topsoils young and the formation of both Andosol and Histosol in Iceland is unusually rapid (e.g. Arnalds 2004). As a result, tephra of similar age can be told apart and thus provide an exceptional high resolution archive to be measured and sampled (e.g. Óladóttir et al. 2005). The pH value of uncultivated Icelandic soils (normally ~5-6; Gudmundsson et al. 2004 and references therein) is also ideal for preservation of basaltic tephra as experimentally determined dissolution rates for basaltic glass are lowest between pH value of ~5-8 (Gíslason and Oelkers 2003).

5.4 Methods

Field work and sample preparation

The terrain around Vatnajökull is barren lava fields and sandur areas where continuous, undisturbed soil sections are not abundant. Nevertheless, seven soil profiles, located in a favourable topography for tephra deposition and preservation, containing extensive tephra record of Holocene volcanism at Grímsvötn, Bárdarbunga and Kverkfjöll, were measured and sampled around the Vatnajökull ice cap (Fig. 1b&c) with emphasis on prehistoric time (i.e. before ~870 AD). The profiles were all >2 m wide and thus allow for examination of lateral variations in appearance of the tephra. All primary and suspected tephra as well as layers of non-volcanic origin and the soils separating them, were measured with mm precision. Also, their characteristics, such as colour, grain size and other observations providing information on eruption mechanism and depositional environment, were described (for further information on field work and criteria see Óladóttir et al. 2005). No soil profiles were measured in the areas between profiles 7, 2 and 3 due to lack of adequate soil sections.

All volcanic and suspected volcanic layers were sampled, except those strongly contaminated by soil. The samples were air dried and clean fractions obtained by handpicking and sieving using steel mesh sieves. The 125 µm size fraction was preferred for the 100 µm thick polished thin sections for in-situ measurements of major and trace element chemical composition in the glass (see *Analyses* section below). If necessary, this sample fraction was supplemented by the 63 and/or 250 µm size fractions.

Correlation between soil profiles

The soil profiles were correlated by tephra marker layers (Table 1, Fig. 2, Fig. 3) most of which originate at the Hekla volcano (9). Other tephra marker layers used for correlation are from Öræfajökull (1), Torfajökull (1), Askja (1), Katla (2) and Bárdarbunga (2). The tephra marker layers are mostly wide-spread silicic tephra layers that are easily recognisable in the field due to their distinct macroscopic characteristics such as colour (i.e. white or yellowish white), bedding or crystal content. Individual basaltic layers are on the other hand more difficult to recognize in the field and therefore series of two or more such layers are better markers. However, occasionally distinctive basaltic tephra are good markers because they display readily identifiable characteristics. Examples of those are the coal black Katla tephra, found far away from its source as well as the so-named “Settlement Layer” from the Vatnaöldur phreato-Plinian fissure eruption in ~870 AD (V-871) on the Bárdarbunga volcanic

system (Larsen 1984; Grönvold et al. 1995; Zielinski et al. 1997). It is readily recognised by its colour of greenish-grey to greenish-black and its abundant plagioclase crystal fragments (e.g. Óladóttir et al. 2005). In addition to field criteria chemical composition of tephra marker layers is compared to published values and used for secure identification (e.g. Dugmore et al. 1995; Dugmore and Newton 1998; Larsen et al. 1999; 2001; 2002; Boygle 2004; Eiríksson et al. 2004; Kristjánsdóttir et al. 2007; Óladóttir et al. 2008).

The major element composition is used to determine the provenance of basaltic tephra and trace element concentrations were measured in a selected suite of samples to further improve fingerprinting. Tephra stratigraphy and chemical composition of the basaltic tephra is the main tool for correlation of individual or package of tephra between soil profiles. These correlations enable acquisition of the actual number of basaltic tephra originating in Grímsvötn, Bárdarbunga and Kverkfjöll present in the seven soil profiles.

Table 1 Tephra marker layers in the study area, their source volcanic systems and ages obtained from written documents, ice core dates, ^{14}C dates and SAR calculations.

Marker layer	*Volcanic system*	*Present in soil sec.*	*^{14}C dates*	*Calibrated/ calender yrs[1]*	*Bf 2005 AD*	*Reference*
K-1918	Katla	7		1918 AD	87	(e.g. Thorarinsson 1958)
Ö-1727	Öræfajökull	7		1727 AD	278	(Thorarinsson 1958)
V-1477	Bárdarbunga	2-7		1477 AD	528	(Larsen 1984)
Ö-1362	Öræfajökull	1-7		1362 AD	643	(Thorarinsson 1958)
H-1158	Hekla	1-5		1158 AD	847	(Larsen 1982)
H-1104	Hekla	1,4		1104 AD	901	(Thorarinsson 1967; 1968)
Eldgjá	Katla	1,7		934 AD	1071	(Hammer et al. 1980)
V-871	Bárdarbunga	1-7		871 AD	1134	(Grönvold et al. 1995)
Hrafnkatla	Katla	1-7		*760 AD	1250	Mean SAR age, this study
Grákolla (G)	Torfajökull	1,3,4,5,7	1995±30	10 AD	1995	(Larsen and Eiríksson, unpubl. data 2009)
Askja (A)	Askja	2,6	1995±30	10 AD	1995	Same age as Grákolla^
HY	Hekla	3,5		°~650 BC	2650	(Larsen unpubl. data 2009)
HZ	Hekla	3,4		°~750 BC	2750	(Larsen unpubl. data 2009)
UN$^{\Delta}$	Katla	7	2660±50 BP	845 BC	2850	(Larsen et al. 2001)
H3	Hekla	1-5	2879±34 BP	1050 BC	3055	(Dugmore et al. 1995)
LN	Katla	1,3	3139±40 BP	1430 BC	3435	(Larsen et al. 2001)
HS	Hekla	6,7	3515±55 BP	1855 BC	3860	(Larsen et al. 2001)
H4	Hekla	1,3,4,5,6,7	3826±12 BP	2250 BC	4255	(Dugmore et al. 1995)
N1	Katla	1		3200 BC	5200	(Larsen et al. 2001)
HÖ	Hekla	1,3,4,5,7		*4150 BC	6155	SAR age from soil section 5
HÖ	Hekla	1,3,4,5,7	5295±42 BP	"4120 BC	6125	(Larsen & Eiríksson, unpubl. data 2009)
H5	Hekla	1,3,4,5	6185±90 BP	5120 BC	7125	(Thorarinsson 1971)

[1]Mean calendar age, calibrated after (Stuiver et al. 1998)

$^{\Delta}$Tephra marker layer not used for correlation only SAR age calcualtions

*Calculated SAR ages, this study.

°Unpublished SAR ages, Hekla area.

"Age measurement realised subsequent to this study, it supports the calculated SAR age used.

^Grákolla and Askja marker layers are present as separate layers in some profiles, but were their distribution overlaps they occur as a single layer consisting of a mixture of the two. This suggests a near synchronous deposition of these layers and therefore they have been allocated the same age

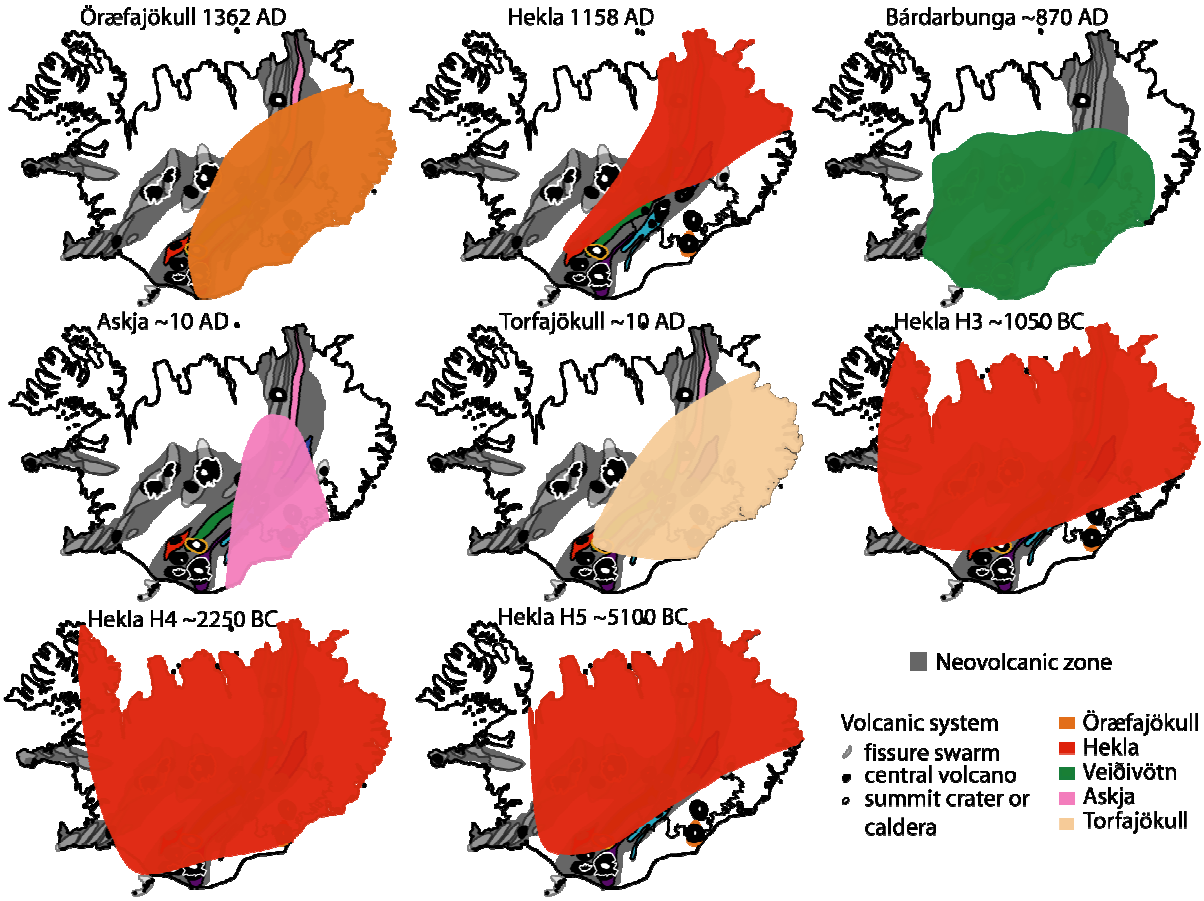

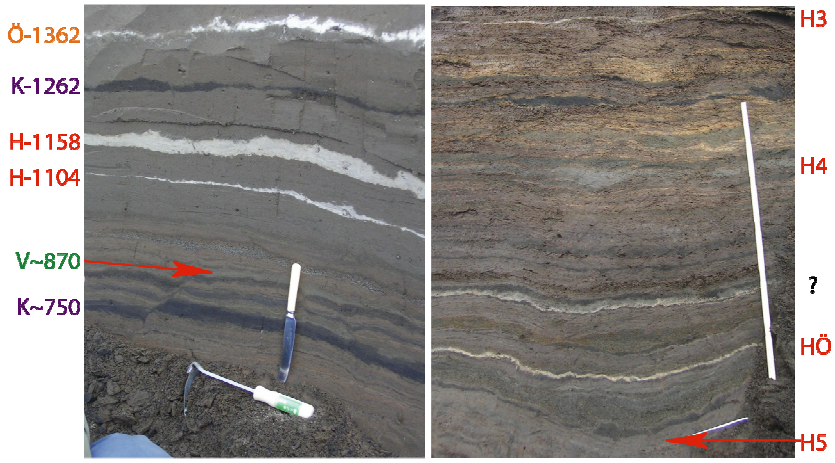

Figure 2 On land distribution of key marker tephra layers that underpin the correlation of the soil profiles around Vatnajökull ice cap. Not shown are the V-1477, Hrafnkatla and HÖ. Colour code is the same as in Fig. 1. Based on Thorarinsson (1958), Larsen and Thorarinsson (1977), Larsen (1984), Larsen (1992) and Larsen unpublished data. Photos show Öræfajökull 1362, Hekla 1158, Bárdarbunga ~870 (V-870), Hekla 3, Hekla 4 and H5 amongst other tephra layers as they are represented in the Kárahnjúkar and Saudárhraukar outcrops (no. 3, 4).

Analyses

Major element analyses on individual glass grains were obtained with a WDS Cameca SX100 electron microprobe at the Laboratoire Magmas et Volcans (LMV), Clermont-Ferrand, France. The instrument was calibrated on natural and synthetic mineral standards and glasses. The analytical conditions used are 15 kV accelerating voltage and 8 nA beam current with a

beam diameter of preferably 20 µm but 10 µm for the smallest grains. The counting time was 10 s for Na, Ca, Ti, P and Si; 20 s for Mg and Al; 30 s for Mn and finally 40 s for Fe and K, adding up to a total analyses time of 3 min and 40 s. For felsic grains the beam current was reduced to 4 nA to reduce Na loss and the beam diameter to either 10 or 5 µm. Raw data were corrected by the X-PHI correction procedure (Merlet 1994).

Trace elements were analysed at the Utrecht University, in the Netherlands, with a Micromass Platform ICP (ICP-MS with collision cell technique) and a Geolas 193 nm eximer laser ablation system. The laser energy was 9-12 J/cm^2, the pulse repetition rate 10 Hz and the laser beam size 60 µm (for further information on major and trace element analyses and standards see Óladóttir et al. Manuscript 1).

Soil accumulation rate (SAR) age model

Previously ^{14}C dated tephra marker layers form the base of the SAR age model (using calibrated age; Table 1). The SAR is calculated for each time period using the age difference of two dated tephra markers and the soil thickness separating them. An approximate age with an accuracy of ±250 years (Óladóttir et al. 2005) can thus be calculated for each tephra layer in all profiles based on soil thickness between individual layers and the calculated SAR for each time period. It is important to have several dated markers at relatively short time intervals in each soil section, because of the critical assumption that the SAR stays constant between the dated tephra marker layers (for further SAR information see Óladóttir et al. 2005).

Environmental factors controlling tephra deposition and preservation

Several factors influence tephra deposition and preservation in a soil profile. Therefore, in order to obtain reliable estimates of the "true" eruption frequency for individual volcanoes it is necessary to measure the tephra stratigraphy in several profiles covering the circumference around a volcano under consideration. The prime factors are distance from volcanic source, prevailing wind direction at the time of eruption as well as eruption magnitude and duration that influence tephra dispersal. Presence of a peak in tephra layer frequency (TLF) from an individual volcano in all sections over the same time interval is a strong indicator of high eruption frequency at the volcano in question. Equally, a synchronous TLF low in all sections must represent a lull in eruption frequency. Inverse relationship in profiles at opposite sides of a volcano, i.e. a low and a peak in TLF during the same time period, may indicate influence of prevailing winds whereas absence of tephra may, in some cases, be explained by distance

from the source volcano. It should be kept in mind that the effects of the external factors will be less conspicuous during intervals of high eruption frequency than during lows. Hence, individual profiles in the soil cover surrounding a volcanic source are likely to record different aspects of its (explosive) eruption history, but collectively they should provide a reasonable picture of the overall story, by indicating the minimum eruption frequency.

5.5 Results

Soil profiles and tephra provenance

Historical and prehistoric tephra layers were measured in seven soil profiles around the Vatnajökull ice cap. The soil profiles vary in thickness from 325-652 cm and cover 2530-7330 years (Table 2). The Katla 1918 AD is the youngest identified tephra layer and is found near the top of the Núpsstadarskógar profile. The oldest layer is from Grímsvötn and its position at the base of the Kárahnjúkar profile implies age in excess of 7600 years.

Table 2 Soil profile information

Profile no.	***1***	***2***	***3***	***4***	***5***	***6***	***7***
Profile length (cm)	460	325	447	560	452	327	652
Soil thickness (cm)	214.7	211.8	209.7	377	294	203.5	282.3
Soil % in profile	46.7	65.2	46.9	67.3	65.0	62.2	43.3
No. of SAR periods	9	5	8	9	10	6	12
Duration (yrs)	6570	2530	7000	7330	6840	5810	6160
No. of layers	104	62	193	181	126	52	163
Youngest tephra	Ö1362	V14771	V1717 +1	V1717 +1	V1717	K1755	K1918
Oldest tephra	H5 +3	H3	H5 +2	H5 +9	H5 +1	H4 +10	HÖ +2
No. of tephra	97	56	169	139	109	50	129
Tephra per 1000 yrs	14.8	22.1	24.1	19.0	15.9	8.6	20.9
Division of tephra units							
Grímsvötn	26	19	62	54	34	28	57
Bárdarbunga	30	20	58	44	32	9	21
Kverkfjöll	0	0	14	11	6	2	1
Katla basaltic	20	11	15	10	13	5	36
Kalta silicic	3	0	1	0	0	0	1
Hekla basaltic	3	0	0	0	0	0	0
Hekla silicic	6	2	7	7	6	2	6
Hekla T-layer	1	1	1	1	0	0	0
Öræfajökull	1	1	1	1	1	1	2
Torfajökull	1	0	2	1	1	0	1
Askja	0	1	0	0	0	1	0
Intermediate	1	1	3	4	4	0	4
Basaltic (unknown)	5	0	4	5	11	2	0
Silicic (unknown)	0	0	1	1	1	0	0

Profile no. are as follows: 1 Hreysiskvísl, 2 Nýidalur, 3 Saudárhraukar, 4 Kárahnjúkar, 5 Snæfell, 6 Steinadalur, 7 Núpsstadarskógar.
No. of layers shows the total amount of layers in soil sections including un-sampled ones and layers of non volcanic origin.
Youngest and oldest tephra layers are given as the last known tephra layers and +no. shows how many younger/older layers are found, respectively. Intermediate layers have not been traced to provenance.

Counting each primary tephra in these seven soil profiles as a separate unit, the total is 749 and the source volcano has been identified for 701 units, or 93.6%. The source volcanoes for the remaining 48 units (6.4%) cannot be determined with certainty (see also Óladóttir et al. Manuscript 1). Most of the source-identified tephra units originate at Grímsvötn (280) and Bárdarbunga (214). Kverkfjöll trails behind Katla and Hekla with 34 identified units. Consequently, Grímsvötn, Bárdarbunga and Kverkfjöll account for more than two-thirds (70%) of tephra measured in soil profiles around the Vatnajökull ice cap (Table 2). However, these profiles have to be correlated on a layer to layer basis before the actual number of eruptions represented by these tephra units can be determined. It is logical to begin this correlation with the key marker layers.

Tephra marker layers

A total of 21 regional and local marker tephra layers are present in soil profiles around Vatnajökull ice cap (Table 1). Of those nine silicic layers were produced by sub-Plinian to Plinian eruptions at the Hekla volcano. Five of the Hekla layers (H-1158, H3, H4, HÖ, H5) are present in at least four soil profiles and underpin the first-order correlation of the measured profiles. Four Hekla layers (H-1104, Hy, Hz, HS) occur in less than four profiles and are therefore used as local tephra markers.

The remaining marker tephra layers come from the Öræfajökull (Ö-1362, Ö-1727), Torfajökull (G), Askja (A), Katla (K-1918, Eldgjá 934, Hrafnkatla, UN, LN, N1) and the Bárdarbunga system (V-1477, V-871). The silicic Ö-1362, G tephra, the basaltic V-1477, V-871 and Hrafnkatla are present in four or more soil profiles. The other tephra occur in less than four soil profiles. The tephra G (from Torfajökull) and A (from Askja) were erupted near-simultaneously about 2000 years ago. In certain parts of the research area they overlap and merge to form a single horizon and are therefore referred to as G+A. Thus, ten layers (V-1477, Ö-1362, H-1158, V-871, Hrafnkatla, G+A, H3, H4, HÖ, H5) can be used as regional marker layers and of those Ö-1362, V-871, Hrafnkatla and G+A are present in all seven soil profiles.

The ten regional tephra markers are fairly evenly distributed through time (Table 1), separated by 115-287 years in historical time and 860-1900 years in the prehistoric era. The longest period between tephra markers is that of H4 to HÖ (i.e. 1900 years).

SAR age model

The regional and local marker tephra layers used in the SAR age model are shown in Table 3. Regional and local tephra markers are used in the model in order to make it as accurate as possible, causing different SAR periods to be calculated for different profiles, e.g. the Núpsstadarskógar profile covers 6160 years and is divided in 12 SAR periods whereas the Kárahnjúkar profile covers 7330 years and has nine SAR periods (Table 2 & 3). The calculated SAR for the same periods also differs between profiles (Table 3) as it is affected by environmental variables such as climate, topography, drainage and vegetation (e.g. Thorarinsson 1961). Different SAR values for the same time slice in the seven profiles have little effect on age calculations but some variations in SAR age of tephra units are to be expected if the time slices are of different length (Appendix 1).

The SAR age calculations are presented in Figure 3. This data enables assessment of the TLF for Grímsvötn, Bárdarbunga and Kverkfjöll in individual profiles. On the other hand, the actual eruption frequency at these three volcanoes can only be estimated after correlation and construction of a composite TLF.

Table 3. SAR calculations. Time periods, soil thickness and SAR for every SAR period in each profile.

		Hreysikvísl		*Nýidalur*		*Saudárhraukar*		*Kárahnjúkar*		*Snæfell*		*Steinadalur*		*Núpsstaðarsk.*	
Tephra marker layer	*Time range*	*Soil (cm)*	*SAR (cm/yr)*	*Soil (cm)*	*SAR (cm/yr)*	*Soil (cm)*	*SAR (cm/yr)*	*Soil (cm)*	*SAR (cm/yr)*	*Soil (cm)*	*SAR (cm/yr)*	*Soil (cm)*	*SAR (cm/yr)*	*Soil (cm)*	*SAR (cm/yr)*
K1918-Ö1727	191													14.25	0.0746
Ö1727-K1625	102													5.50	0.0539
V1717-K1625	92									2	0.0217				
K1625-V1477	148									3.85	0.0260			9.04	0.0611
K1755-V1477	278											37.35	0.1344		
H1636-V1477	159							20.76	0.1305						
V1477-Ö1362	115			31.00	0.2696	16.5	0.1435	9.5	0.0826	1.6	0.0139	3.25	0.0283	5.26	0.0457
Ö1362-K1262	100													5.50	0.0550
Ö1362-H1158	204	8.75	0.0429	10.75	0.0527	23.55	0.1154	16.73	0.0820	5.35	0.0262				
Ö1362-V871	491											10	0.0204		
K1262-Eldgjá	328													17.42	0.0531
Eldgjá-V871	63													3.44	0.0545
H1158-H1104	54	0.75	0.0139					5.67	0.1050						
H1158-V871	287			34.75	0.1211	4.6	0.0160			5.6	0.0195				
H1104-V871	233	8.85	0.0380					12.51	0.0537						
V871-G+A	861	28.19	0.0327	85.28	0.0990	17.77	0.0206	41.1	0.0477	22.15	0.0257	14.77	0.0171	58.68	0.0682
G+A-UN	855													18.87	0.0221
G+A-H3	1060	17.67	0.0167	28.03	0.0264	22.41	0.0211	29.38	0.0277	15.75	0.0149				
G+A-HS	1865											31.35	0.0168		
UN-HS	1010													32.60	0.0323
H3-H4	1200	22	0.0183			40.43	0.0337	29.94	0.0250	24.95	0.0208				
HS-H4	395											5	0.0127	10.85	0.0275
H4-N1	945	25.1	0.0266												
H4-HÖ	1905					29.05	0.0152			50.68	0.0266			68.05	0.0357
H4-H5	2870							48.47	0.0169*						
N1-HÖ	960	54.75	0.0570												
HÖ-H5	965	40.1	0.0416			12.83	0.0133			106.09	0.1099				

For further information on tephra layers see Table 1.

* In Kárahnjúkar the calculated SAR from H4 to H5 was used as the ^{14}C age from the area had not been measured. The measured ^{14}C age was found to be the same as the calculated SAR age (see Table 1).

	Hreysiskvísl			Nýidalur			Saudárhraukar I			Saudárhraukar II			Kárahnjúkar			Snæfell			Steinadalur			Núpsstadarskógar		
Volc.syst.	Log #		SAR	Log #		SAR	Log #		SAR	Log #		SAR	Log #		SAR	Log #		SAR	Log #		SAR	Log #		SAR
K																						111		87
Grí																			41		150	110		218
Grí																						109		232
K																			40		250			
Grí										1		340	8-17		270							108		259
Ö																						107		278
V-1717										2		430	8-16		310	2-1		290						
Grí										3		450												
I+Grí										4		460	8-15		370									
K										5		470	8-14		380	2-2		380				106		380
Grí										6		470	8-13		380									
Grí													8-12		400				39		360	105		400
Grí										7		472	8-11		490	2-3		410	37		500			
Grí										8		474	8-10		500	2-4		510	36		520	104		500
Grí										9		520	8-9		510	2-5		524						
Bár				08-23		534																103		510
V-1477				08-22		528				10		528	8-8		528	2-6		528	35		528	101		528
Grí										11		550										86		550
Grí				08-21		610							8-7		550	2-7		540	34		600	87		574
K																						88		588
Bár										12+13		580				2-8		590						
Grí										14		640												
Ö-1362	Hkv 1		643	08-20		643				15		643	8-6		643	2-9		643	33		643	89		643
Grí	Hkv 2		650	08-19		660				16		650	8-5		650	2-10		650	32b+c		643	90		660
Grí																2-11		700	32a					
Grí										17		690												
Bár	Hkv 3		710																					
H-bas	Hkv 4		760																					
?	Hkv 5		770																					
K	Hkv 6		780	08-17		750				18		790	8-4		740	2-12		730				92		743
Grí										19		846	8-3		846	2-13		847						
H-1158	Hkv 8		847	08-16		847				20		847	8-2		847	2-13		847						
H-1104	Hkv 9		901										8-135		901									
Grí	Hkv 10		940										8-134		970							93		870
Grí																						94		890
Grí+Bár+?	Hkv 11		970										8-133		980									
Grí										22		950	8-132		1020	2-14		960	31		940	95		980
Grí	Hkv 12		1010	1; 08-15		1080;1080				23		970	8-131		1050	2-15		1010						
Grí				2;08-14		1085;1090																		
Grí																			30		1010	96		1050
K-Eldgjá	Hkv 13		1040																			97		1071
Grí													8-130		1060							98		1073
Grí+Bár				3; 08-13		1100;1100				24		1100	8-129		1100									
Grí							111		1120				8-128		1130	2-16		1130				99		1090
Grí										25		1130										100		1110
Ö-871	Hkv 14		1134	4; 08-12		1134	110		1134	26		1134	8-127		1134	2-17		1134	28		1134	1		1134
Grí	Hkv 15		1140	5; 08-11+10		1135;1135																		
Grí	Hkv 16		1160	6; 08-8		1140;1170	109		1150	27		1140	8-126		1140									
Grí	Hkv 17		1170	7; 08-7		1150;1180										2-18		1170						
Grí										28		1150	8-125		1140				28		1160	2		1160
Bár				8; 08-6		1150;1181	108		1170	29		1190	8-123		1170	2-19		1240						
K	Hkv 18		1190	9; 08-5		1155;1185																3		1170
Bár	Hkv 19		1210	10; 08-4		1160;1190	107		1180				1-122		1170									
Grí	Hkv 20		1220	11		1165	106		1180				1-121		1180	2-20		1260	27		1195	4		1190
Grí	Hkv 21		1220																			5		1200
Grí							105		1180	30		1290	1-120		1190	2-21		1280						
Grí										31		1330												
K													1-119		1210									
Grí							104A		1230															
Bár				12		1170	104		1230	32		1340	1-118		1210	2-22		1300						
K-hrafnkatla	Hkv 22		1250	13		1175	103		1230	33		1350	1-117		1215	2-23		1305	28		1250	6-7		1230
Bár							102		1230	34		1350	1-116		1220	2-24		1310	25		1260			
K				14		1190	101		1260	35		1400	1-115		1260							8		1260
K																						9		1280
Bár							100		1270													10		1285
Bár	Hkv 23		1360																					
Bár	Hkv 24		1410	15		1245	99		1350															
Grí				16		1255													24		1330	11		1290
Grí				17		1260																		
Bár													1-114		1360							12		1390
Grí+Kve													1-113		1380									
Bár																						13		1410
?													1-112		1410									
Bár				18		1580	98		1370				1-111		1440							14		1460
Grí																						15		1510
Grí	Hkv 25		1510	19		1620													23		1390	17		1540
Grí	Hkv 26		1530	20		1630																18		1590
Grí				21		1650	97		1450				1-110		1530				22		1420			
Grí							96		1460				1-109		1550	2-25		1615						
Grí							93+94+95		1465				1-108		1560									
Grí							92																	
Bár	Hkv 27		1630	22		1650																27		1710
K				23		1680	91		1470				1-107		1570	2-26		1620						
Grí							91+		1470				1-105-106		1580	2-27		1630	21		1600			
Grí							90		1470										20		1605			
Bár				24		1700																		
Bár				25		1710																		
Grí	Hkv 28		1660	26		1710	89		1510				1-104		1590				19		1610	28		1710
Grí							88		1590				1-103		1640				18		1970	29		1725
Grí																						30		1750
Grí																						31		1760
Grí																						32		1820
Bár+Kve							87		1620															
Bár				27		1735																		
Bár	Hkv 29		1690	28		1740	86		1660							2-28		1740						
Bár	Hkv 31		1760	29		1740																		
Bár													1-102		1700									
K				30		1750																33		1870
Grí																						34		1890
Grí+?	Hkv 32		1920	31		1950										2-29		1940						
I	Hkv 33		1950																					
K				32		1970	85		1920				1-101		1940							37		1940
G+A	Hkv 34		1995	33		1995	84		1995	A+G		1995	1-100		1995	2-30		1995	17		1995	38		1995
Bár				34		2010																		
Grí							83		2040															
K																						39		2090
K																						40		2130
I				35		2050																41		2150
Bár				36		2060	82		2070				1-99		2080	2-31+32		2265						
Bár							81		2090				1-98		2090	2-33		2100						
Bár													1-97		2130	2-34		2100	16		2030			
Bár																2-35		2120						
Grí													1-97						15		2200	42		2170
Bár							79-80		2110				1-96		2140							43		2200
K	Hkv 36		2065	37		2070																		
K	Hkv 37		2125				78		2120															
K	Hkv 38		2215	38		2170							1-95		2140									
K	Hkv 39		2305	39		2260																		
Bár	Hkv 40		2395	40		2490	77		2150				1-94		2180									
Grí				41		2520																44		2220
Grí				42		2590																		
Bár																						45		2240
I																						46		2260
Kve+?							76		2240				1-92		2260	2-36		2220				47		2265
?							75		2280				1-91		2280	2-37		2230						
Hx																						48		2280
K																						49		2290
Bár							74		2290				1-91		2280	2-37		2230				50		2340
K																						51		2360
Grí													1-90		2300									
Grí							73		2330				1-89		2360							52		2410
K							72		2360	78		2360	1-88		2410	2-38		2290				53		2430
K																2-39		2350						
Grí							71		2370				1-87			2-40		2360				54		2460
Grí							70		2467															
Bár							69		2470	77		2510	1-86		2480	2-41		2430						
H T-layer	Hkv 41		2635	43-44		2670	68		2490				1-85		2500									
Bár							67		2510	76		2610				2-42		2530						
Bár							66			75		2660	1-84		2560	2-43		2535						
Hy							66		2560							2-43; Á3		2535;2710						

	Hreysiskvísl			Nýidalur			Saudárhraukar I			Saudárhraukar II			Kárahnjúkar			Snæfell			Steinadalur			Núpsstadarskógar		
Volc.syst.	Log #		SAR	Log #		SAR	Log #		SAR	Log #		SAR	Log #		SAR	Log #		SAR	Log #		SAR	Log #		SAR
Hy							66		2560							2-43; Á3		2535;2710						
Borrobol-like							65		2610	74		2670	1-83		2590	Á4								
Bár	Hre 41a		2746	45		2700	64		2650	73		2730	1-82		2620	2-44		2600						
Hz										72		2770	1-81		2670							55		2600
K	Hre 41a		2746	46a		2770																56		2620
Grí	Hre 41b		2749	46b		2771																		
Grí							63		2750	71		2800	1-80		2690	2-45		2690						
Grí							62		2760	70		2820	1-79		2710									
Grí													1-78		2720	2-46		2720						
Grí													1-77		2730							57		2770
Grí							61		2810				1-76		2770									
Kve							60		2880				1-75		2810				14		2980			
Bár																						58		2800
Bár+Grí	Hkv 42		2880	47		2900	59		2950				1-74		2850							59		2810
Bár				48		2980	58		2980	69		2940	1-73		2950	2-47		2970						
Grí													1-72		2980							60		2830
Bár							57		3020				1-71		3020				12		3220	61		2840
K-Un																						62		2850
Grí																			11		3280	63		2900
Grí																						64		2970
Grí																						65		3040
Grí																						66		3070
Grí																						67		3120
Hm/n																						68		3130
Grí																						69		3160
H3	Hkv 43		3055	49		3055	56		3055	68		3055	1-70		3055	A5;2-48		3055						
I							55		3070	67		3060	1-69		3060	2-49		3055						
Grí													1-68		3090									
Bár							54		3140	66		3170	1-66		3160				10		3380	70		3200
Bár										65		3170												
Grí													1-65		3200									
Grí																						71		3200
Grí																						72		3220
Grí																						73		3240
K-Ln	HKV 44		3250							63		3390												
Grí	Hreys 44a		3330				53		3150															
Grí																								
Bár							52		3170							2-50		3130				74		3350
Grí+Bár										62		3430												
K	Hreys 53		3400																			75		3560
?							51		3480	60		3490							9		3440			
Bár	Hreys 54		3540																					
Grí	Hreys 55		3646				50		3550				1-61		3590	2-51		3660	8		3560	76		3590
Grí													1-60		3630	2-52		3670						
Grí							49		3590	59		3630	1-59		3660									
Grí										58		3670	1-58		3700									
Grí	Hreys 56		3670										1-57		3710									
Bár	Hreys 57		3700				48		3740	55-57		3805	1-56		3770	2-53		3810						
K	Hreys 58		3740																					
K							47		3760	54		3830				2-54		3830						
Bár										53		3920												
Bár										52		3958												
Bár										51		3960												
Bár	Hreys 59		3790							50		3970												
Bár	Hreys 60		3850				46		3940	49		4000												
Bár	Hreys 61a		4060				45		4030															
Grí	Hreys 61b		4060							48		4020												
Bár										47		4030												
Bár										46		4060												
Grí							44		4070	45		4085												
Grí										44		4090	1-55		3780				7		3710	77		3790
Grí																						78		3860
HS																			6		3860	79		3860
Bár							43		4090	43		4095	1-54		3880	2-55		4060						
Bár													1-53		3900									
K																						80		3920
Grí																						81		4020
K	Hreys 62		4170							42		4130				2-56		4180	V		4060	82		4100
K																						83		4170
Bár										41		4180	1-52		3940	2-57		4230						
Bár+K	Hreys 63		4255				42		4220	40		4220	1-50		4010				5		4060	84		4250
Grí																			4+VI		4100			
Grí																			3+III		4180			
H4	He 29-32		4255				41		4255	39		4255	1-49		4255	70; 2-58		4255	2		4255	85		4255
Bár							40		4300	38		4340	1-48		4300				1og -1		4260			
K	Hre 81		4350													71; 2-59		4370;4480				1-2		4380
Bár																						1-3		4390
Bár	He 6		4390																					
Grí													1-47		4360									
Grí										37		4400	1-46		4630	72		4440	-2		4500	1-4		4580
Bár										36														
Grí																						1-5		4660
K	Hre 82		4420							35		4520												
Grí	Hre 83		4540							34		4670												
Grí	He 8		4580										1-45		4700									
Kve										33		4690												
?																73		4710						
Bár	Hre 84		4650																			1-6		4690
Grí										32		4720												
Grí										31		4740												
Grí	Hre 85		4820							30		4840												
T										29		4910												
K										28		5040										1-7		4760
K	Hre 86		5140							27		5170							-3		4800	1-8		4830
K																						1-9		4860
K																			-4		4910	1-10		4880
H-bas	Hre 87		5195																					
K-N1	Hre 88		5200																					
Kve+Bár	Hre 89		5260							25		5215	1-44		4770	74		4910	-5		4940	1-11		4940
Kve										24		5220	1-43		5130	74b		4990						
Kve										23		5270	1-42		5150									
?	Hre 90		5380																					
K																						1-12		5120
Kve										22		5390				75		5060						
Grí	He 13		5550							21		5420	1-41		5330	76		5140				1-13		5250
Kve										20		5520												
Bár							28		5850	19		5550	1-40		5430							1-14		5320
Kve										18		5580	1-39		5490	77		5330						
Bár	Hre 91		5730				27		5910	17		5610	1-38		5520	78		5360	-6		5260	1-15		5350
Kve										16		5620												
K	Hre 92		5740																			1-16		5430
K																						1-17		5470
Bár							26		5920 5920															
Grí																						1-18		5530
Grí																						1-19		5580
Grí							25		5930	15		5660												
I										14		5670	1-37		5610	79		5440						
Kve							24		5950	13		5680	1-36		5630									
Grí							23		6020	12		5710				80		5500	-7		5300			
Bár	Hre 93		5770				22		6050	11		5750	1-35		5740	81		5570						
Bár	Hre 94		5830				21		6090	10		5800	1-34		5800	82		5590						
Bár	Hre 95		5890							9		5840	1-33		5850	83		5600						
Bár	Hre 96		5910							8		5890	1-32		5920	84		5700						
Bár	Hre 97		5930							7		5930				85		5750						
Bár																86		5810						
K																						1-20		5600
K																						1-21		5630
?																						1-23		5740
Grí																						1-24		5750
Grí	He 17		5967				20		6100	6		5950							-8		5670	1-25a+b		5810
Bár										5		5960	1-31		5990									
Bár+Grí													1-30		6090									
Grí	Hre 98		6000																					
K																88		6010				1-26		5820
K										4		6100										1-28		5870
K	Hre 99		6050																			1-29		5970
Bár	Hre 100		6100				19		6160	3		6150	1-29		6140	89		6100	-9		5690	1-30		5990
K																						1-31		6010
Grí										2		6160				90		6140	-10		6060			
HÓ	Hre 101		6160				18		6160	1			1-28		6160	91; 2-60		6160				1-33		6160

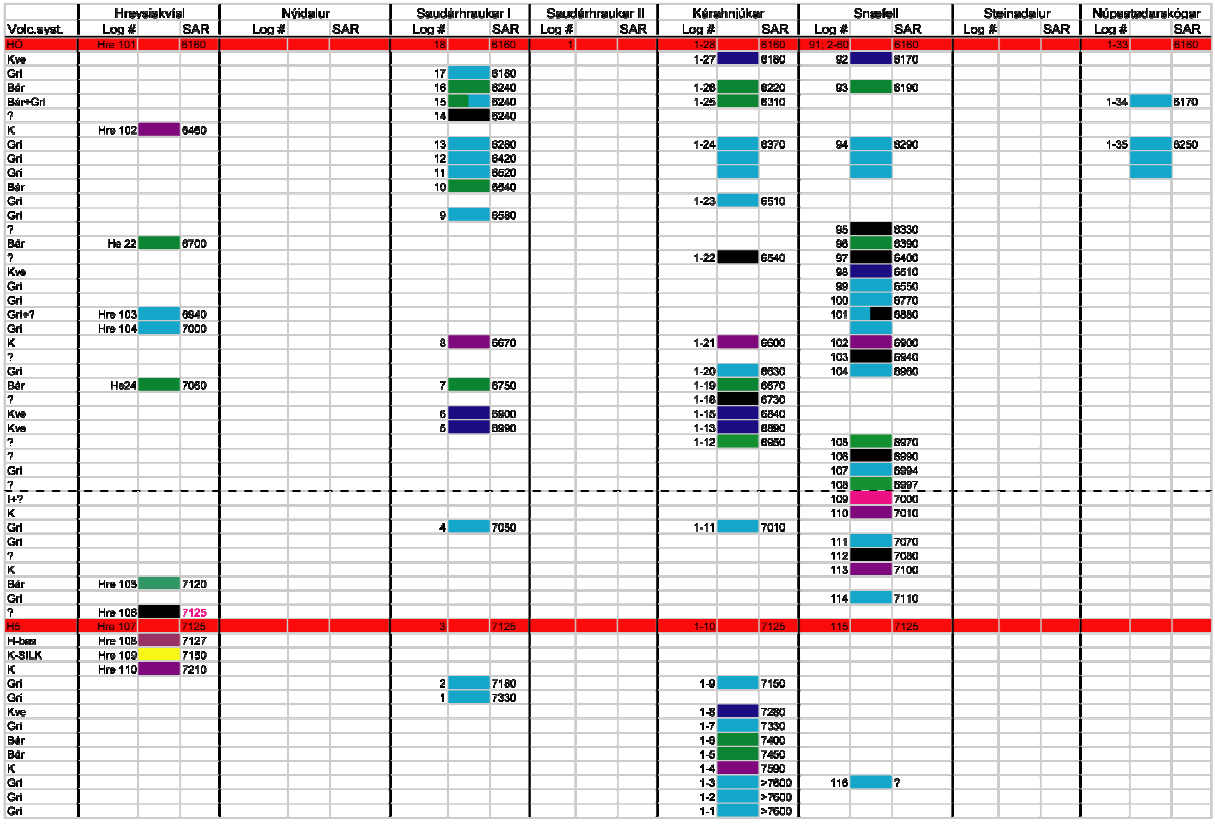

Figure 3 Spread sheet showing correlations of tephra between soil profiles around Vatnajökull. Tephra appearing in the same row represent one and the same eruption and the source volcano is given in the first column where Grí: Grímsvötn, Bár: Bárdarbunga, Kve: Kverkfjöll, K: Katla, H: Hekla, Ö: Öræfajökull, and T: Torfajökull, I: intermediate unknown, and ?: basaltic unknown. The data for each profile is given in three columns where Log # = sample number; colour indicates provenance (for legend see Fig. 1) and SAR = calculated SAR age. Tephra marker layers are highlighted across all columns. Every 1000 years, as depicted from correlated TLF and average SAR, are indicated by broken lines. This division indicates compilation of correlated TLF on Fig. 13 and is the basis for estimated eruption frequency calculations. The layers 35 and 36 in Núpsstadarskógar are not included because they occur below a disturbed (remobilised) soil horizon.

Tephra layer frequency (TLF) in individual profiles (Local TLF)

Stratigraphic logs and TLF histograms of 1000 and 500 year bins from individual profiles are shown in Figures 4-10, Figure 11 gives an overview of the local TLF and detailed descriptions on local TLF are given in Appendix 2. The profiles are selected to represent prehistoric TLF. Additionally, measurements from the historical period at each profile are used to compare the observed TLF with established records of historical eruptions in order to investigate the difference between observed and actual TLF. The obtained preservation ratio of historical eruptions is then used to estimate the prehistoric eruption frequency. Below the TLF information from the seven soil profiles is compared and contrasted.

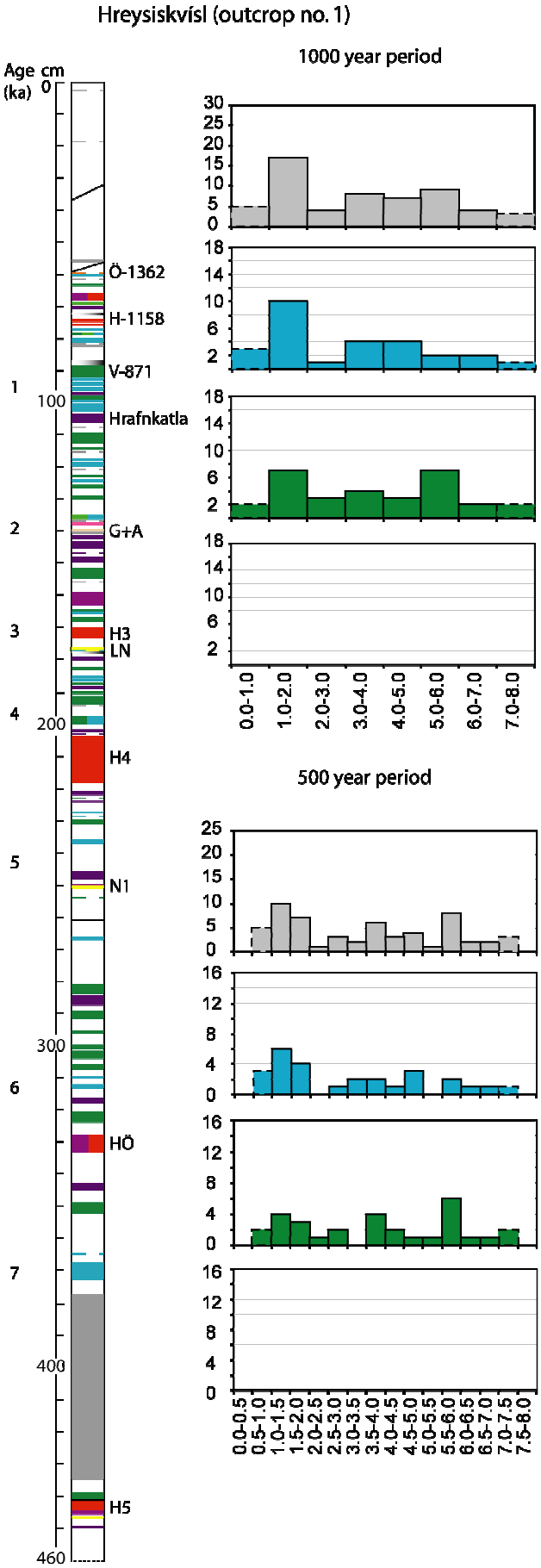

Figure 4 Tephra stratigraphy (log) and tephra layer frequency (TLF) histograms from the Hreysiskvísl profile (no. 1 on Fig. 1). It contains 97 tephra units and covers ~6570 years. The two scales on the left show: 1) age (ka); indicating the beginning of a new millennium, and 2) thickness of tephra and soil in cm. Broken lines in log indicate a discontinuous tephra in profile. Colour indicates tephra provenance as shown in Fig. 1 but for a complete colour code see Fig. 12. Soil horizons are blank. TLF histograms are shown for two bin sizes; 1 ka and 0.5 ka (x-axes) and number of tephra per bin is shown on the y-axis. The top histogram (grey) in each time bin shows the cumulative TLF and the following three histograms give the TLF for each volcano (see colour legend Fig. 1). In this profile Kverkfjöll tephra is absent. Columns highlighted with broken lines represent minimum estimates for the TLF because of incomplete record but the 0-1 ka period only includes ~360 years and the 7-8 ka period ~200 years (see Appendix 2 for further details). Vertical lines on accumulated TLF histograms show location of main tephra marker layers in time, colours indicating provenance. Please note the different scale for accumulated TLF and TLF for individual volcanic systems.

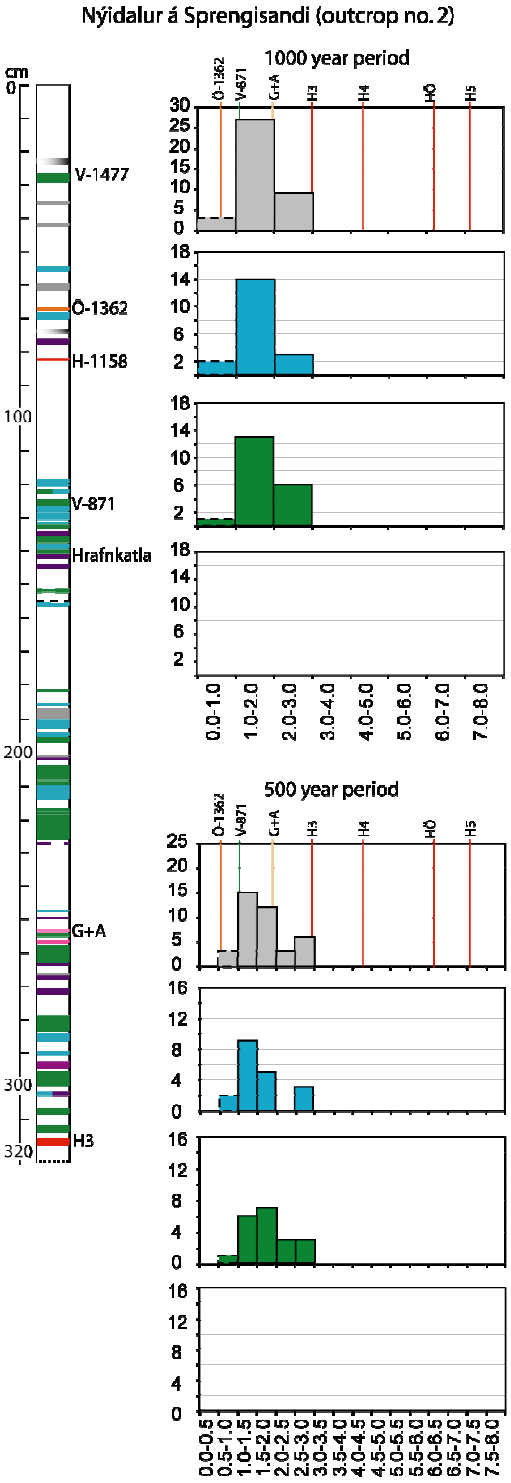

Figure 5 Tephra stratigraphy (log) and TLF histograms from the Nýidalur profile (no. 2 Fig. 1). It contains 56 tephra units and covers ~2500 years. The record included in the first bin (0-1 ka) only covers ~470 years. Legend as in Fig. 4.

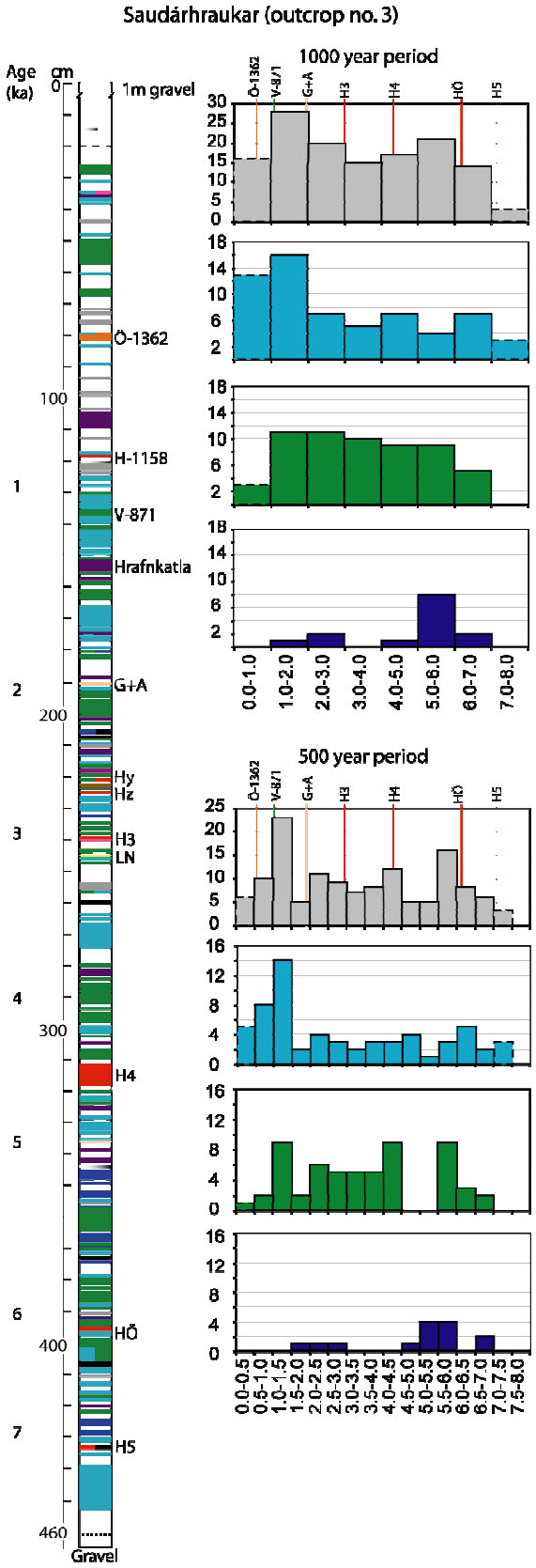

Figure 6 Tephra stratigraphy (log) and TLF histograms from the Saudárhraukar profile (no. 3 Fig. 1). It contains 169 tephra units and covers ~7000 years. The record included in the first bin (0-1 ka) covers ~710 years and the last bin only ~330 years (see Appendix 2 for further details). Legend as in Fig. 4.

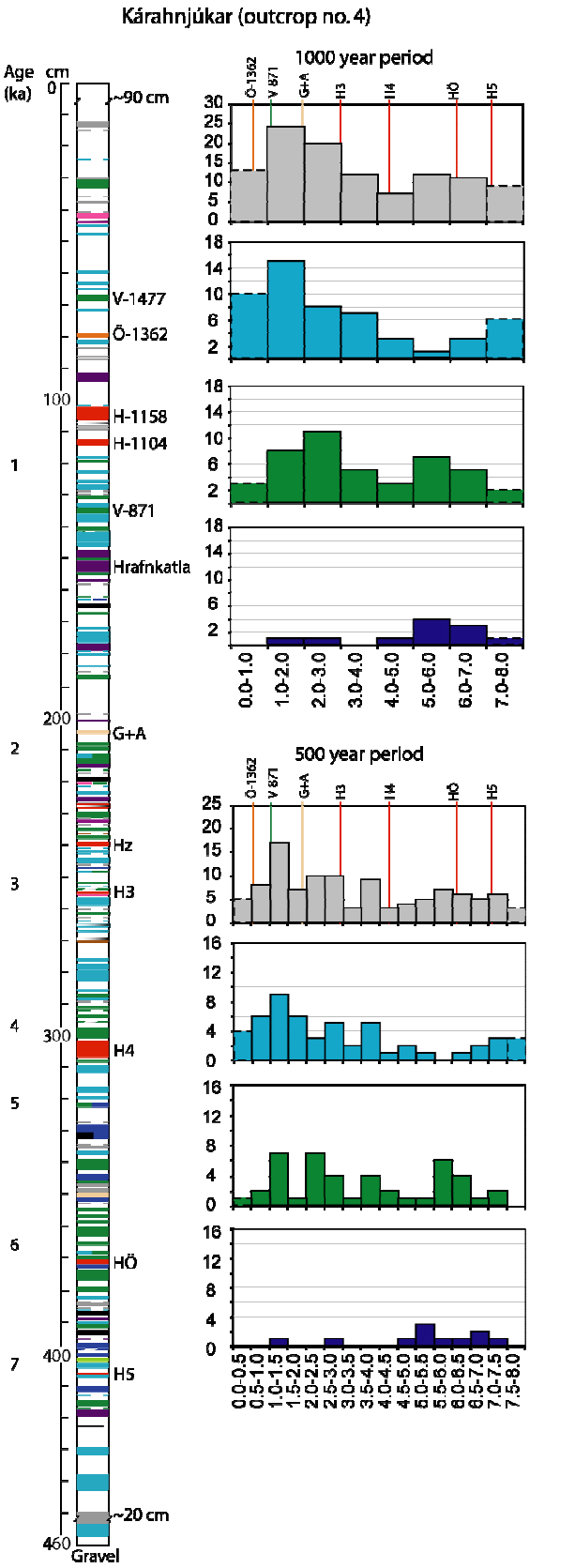

Figure 7 Tephra stratigraphy (log) and TLF histograms from the Kárahnjúkar profile (no. 4 Fig. 1). It contains 139 tephra units and covers ~7300 years. The record included in the first bin (0-1 ka) covers ~730 years and the last bin at least 600 years (see Appendix 2 for further details). Legend as in Fig. 4.

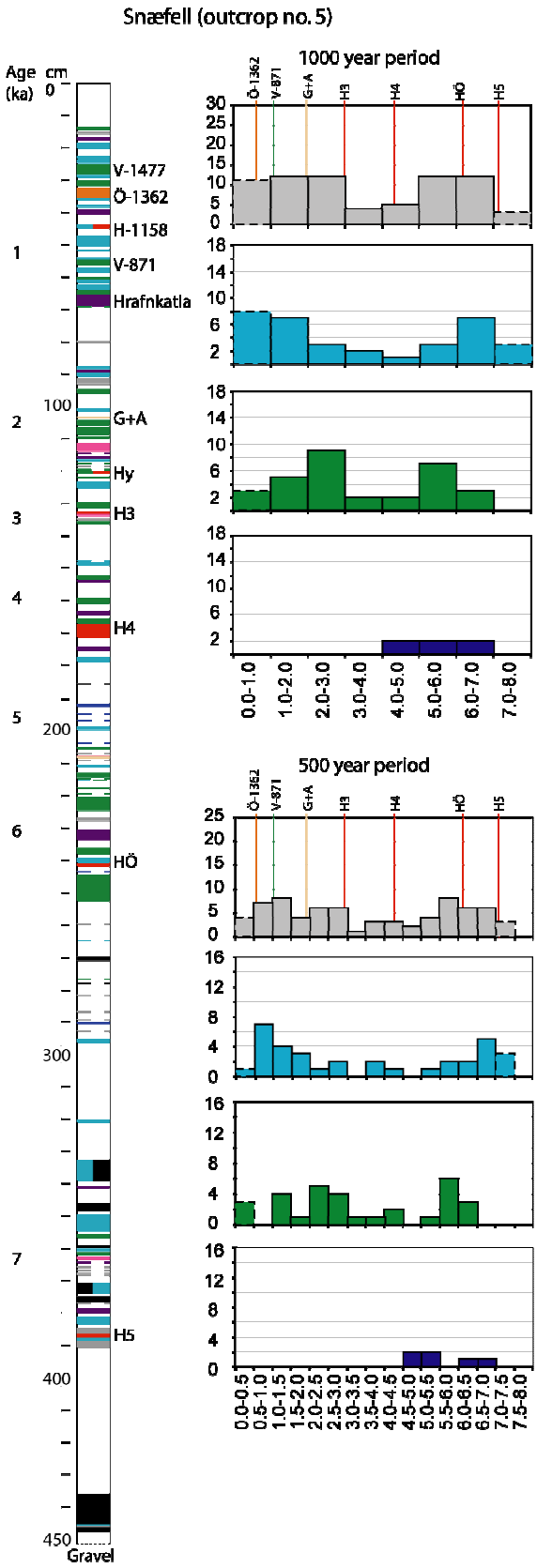

Figure 8 Tephra stratigraphy (log) and TLF histograms from the Snæfell profile (no. 5 Fig. 1). It contains 109 tephra units and covers ~6800 years. The record included in the first bin (0-1 ka) covers ~710 years and the last bin only ~130 years (see Appendix 2 for further details). Legend as in Fig. 4.

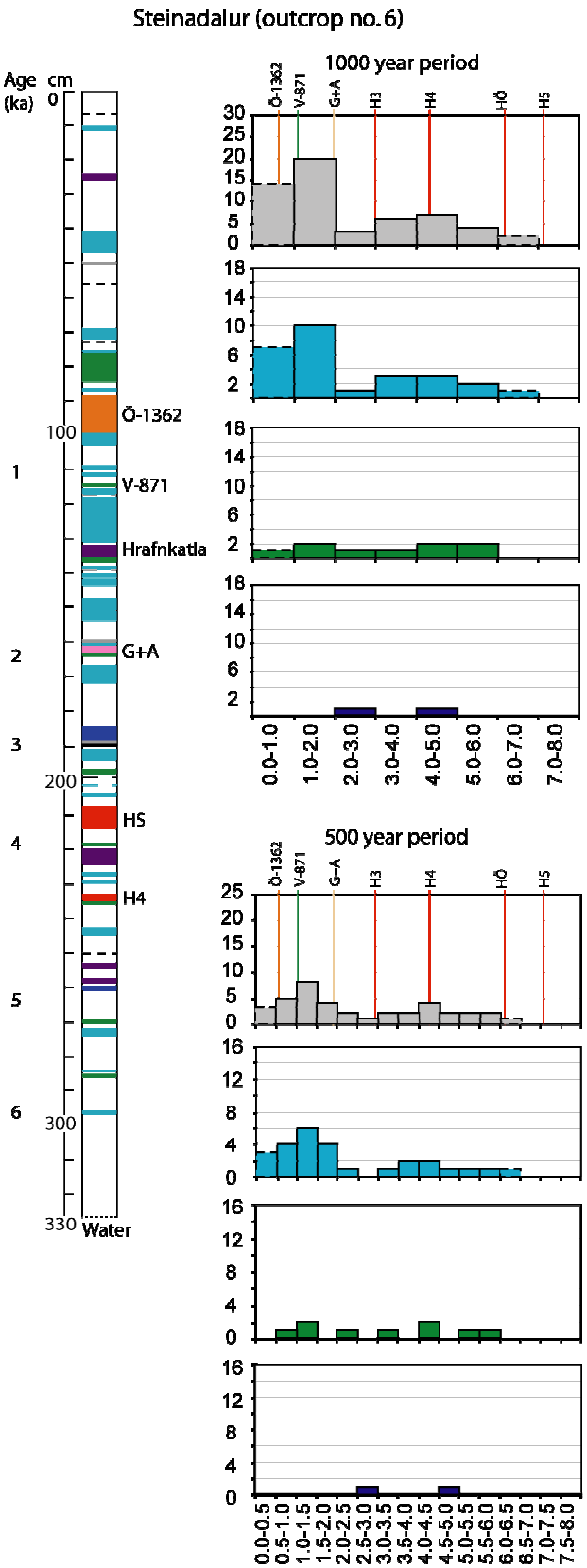

Figure 9 Tephra stratigraphy (log) and TLF histograms from the Steinadalur profile (no. 6 Fig. 1). It contains 50 tephra units and covers ~5800 years. The record included in the first bin (0-1 ka) covers ~850 years and the last bin only ~60 years (see Appendix 2 for further details). Legend as in Fig. 4.

The highest local TLF peak for Grímsvötn tephra is at 2-1 ka in six out of the seven soil sections (Fig 4-11). The exception is the Snæfell profile where it is highest during the last millennium. The last 2000 years in this profile are well constrained by marker tephra layers, which strongly suggests that this diversion at Snæfell is real. This could partly be explained by the thick, iron-rich soil without any preserved tephra below the Hrafnkatla marker layer (see Fig. 12), indicating a temporary change in tephra preservation and lowering the 2-1 ka TLF peak. On the 500 year histogram the Grímsvötn TLF peak is at 1.5-1 ka except at the Núpsstadarskógar profile where it is in the 2.0-1.5 ka bin and at the Snæfell profile where it is shifted to the 1.0-0.5 ka bin. The existence of a correlated TLF maximum in the period 2-1 ka is reinforced by the drop in local TLF in Núpsstadarskógar after 1 ka because this profile contains the most complete record of historical tephra measured in this study, including the youngest tephra layer in Iceland with regional dispersal, the K-1918 layer. The Grímsvötn TLF is low from 6-4 ka in all of the profiles.

The Bárdarbunga TLF generally displays two peaks, one at ~6-5 ka, confined to 6-5.5 ka on the 500 year histogram, and another broader peak 3-1

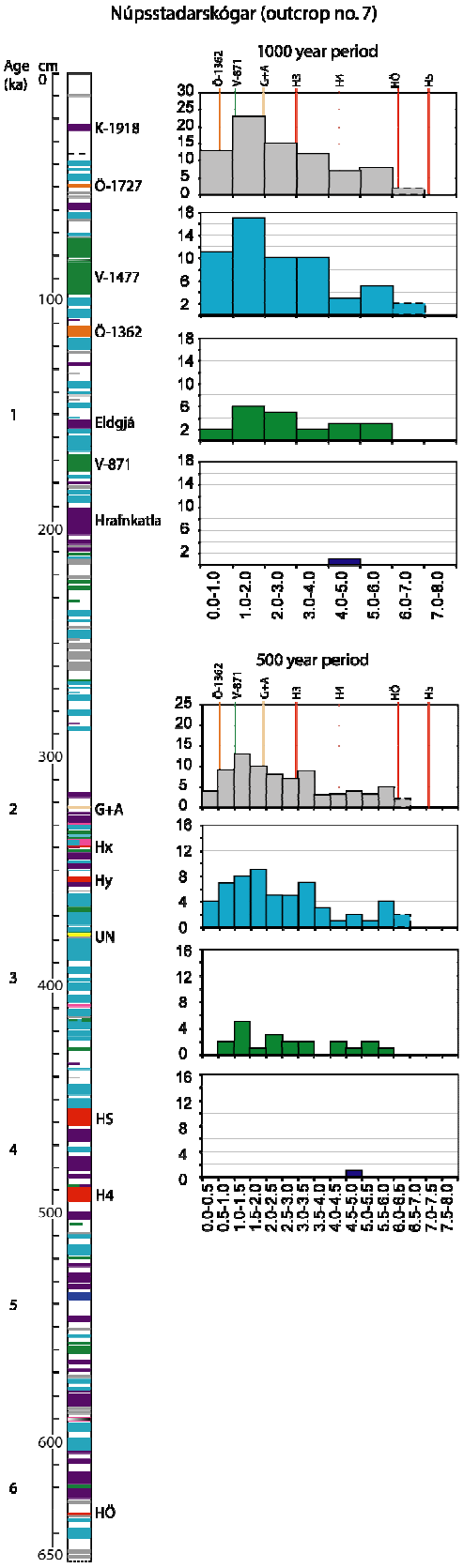

Figure 10 Tephra stratigraphy (log) and TLF histograms from the Núpsstadarskógar profile (no. 7 Fig. 1). It contains 129 tephra units and covers ~6200 years. The record included in the first bin (0-1 ka) covers ~910 years and the last bin only ~250 years (see Appendix 2 for further details. Legend as in Fig. 4.

ka (Figs. 4-10). Within the 3-1 ka peak, the western profiles Hreysiskvísl and Nýidalur exhibit higher local TLF at 2-1 ka while in the eastern profiles of Kárahnjúkar and Snæfell the peak is at 3-2 ka. This is difficult to relate to changes in prevailing wind direction because similar effect is not seen in the local Grímsvötn TLF. However, this could possibly be explained by different seasonality of the eruptions at Grímsvötn and Bárdarbunga in conjunction with eruption intensity. In general the local Bárdarbunga TLF fluctuates more than that of Grímsvötn, but a distinct low is seen 5.5-4.5 ka, similar to Grímsvötn (Fig. 4-10). The Bárdarbunga TLF of last millennium is among the lowest in all profiles.

The Kverkfjöll tephra is best represented in the eastern profiles, i.e. Saudárhraukar, which lies closest to Kverkfjöll, Kárahnjúkar and Snæfell (Figs. 1b, 6-8). In the western profiles, Hreysiskvísl and Nýidalur, which lie farthest away from the volcanic source, no Kverkfjöll tephra is present (Figs. 4-5) and only one and two layers are found in the southern profiles, Steinadalur and Núpsstadarskógar (Figs. 9-10), respectively. Deposition of Kverkfjöll tephra peaks at 6 and 5 ka (Fig.12). This peak coincides with a low in Grímsvötn TLF.

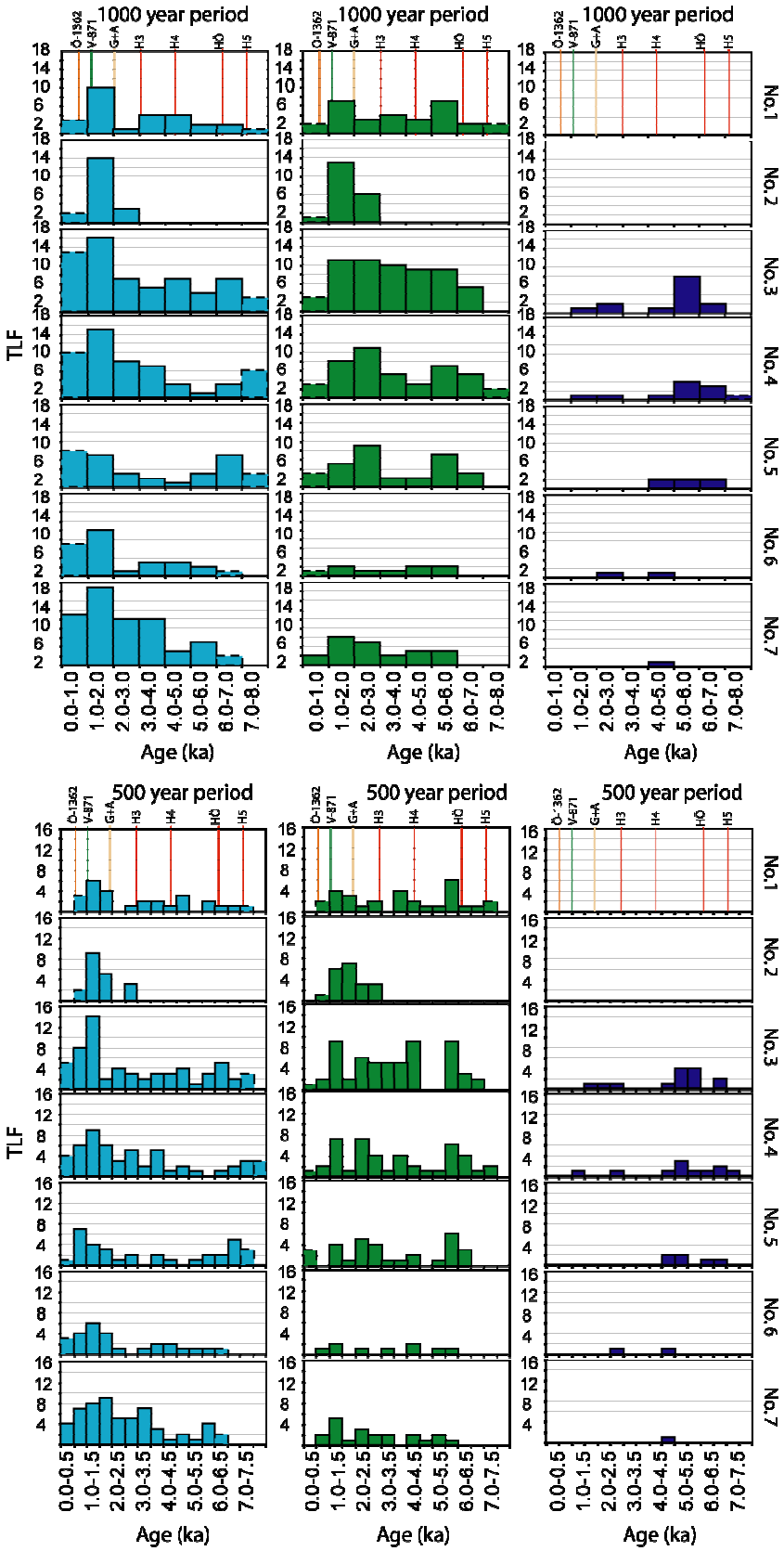

Figure 11 Overview of TLF histograms from the seven soil profiles. Number of tephra per bin is shown on the y-axis and the x-axis shows two bin sizes; 1 ka and 0.5 ka. Location numbers are shown on the right. Legend as in Fig. 4

The zero registration of tephra in time intervals of 4.5-3 ka and from 1-0 ka are present in all profiles and are thus considered periods of repose at the Kverkfjöll volcano.

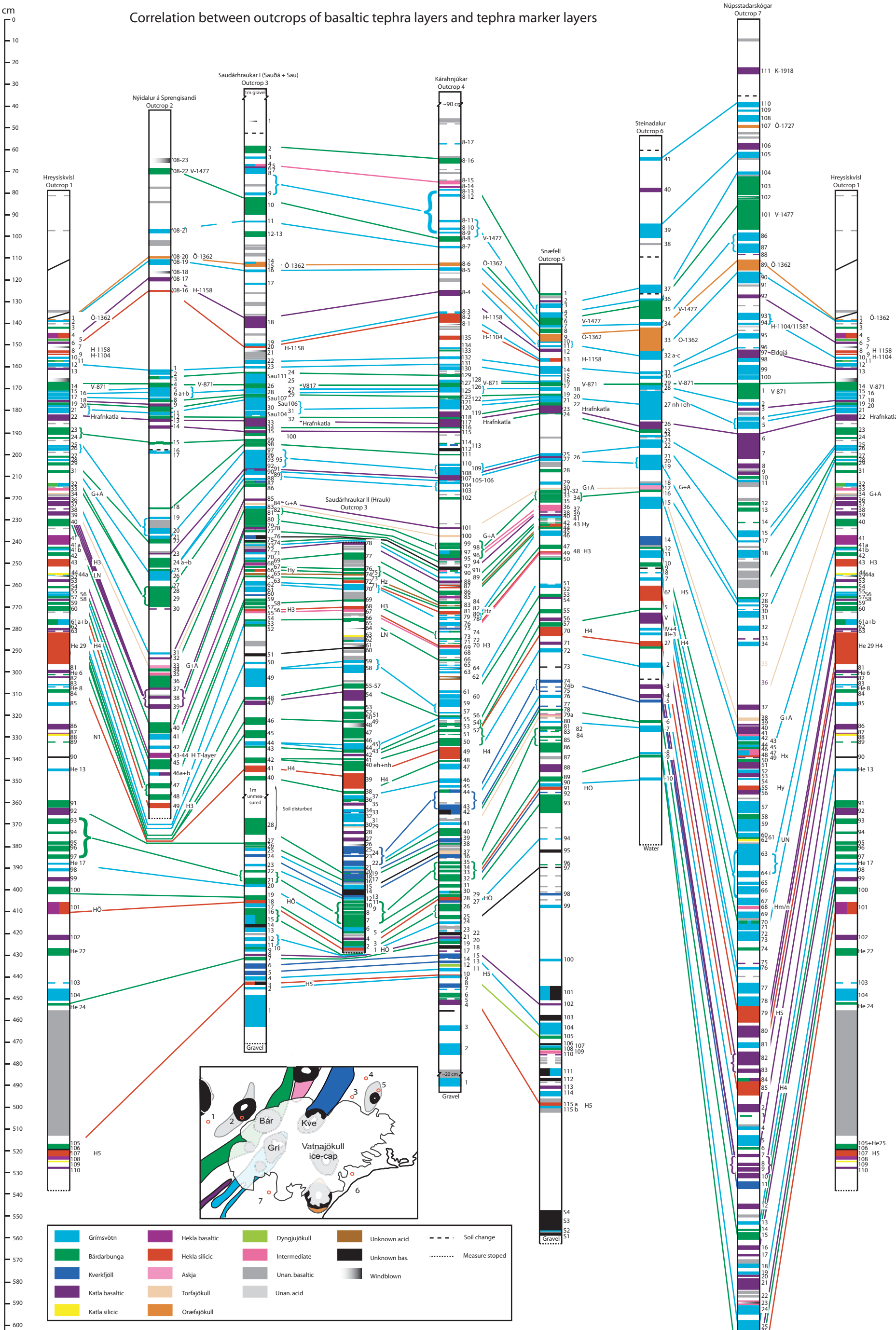

Figure 12 Correlation of tephra between profiles. Thickness of tephra is shown proportionally and colour refers to source volcano (see legend above). Blank intervals represent soil. Numbers to the right of each log show sample numbers and tephra marker layers are indicated by their abbreviated symbol (see Table 1). Layer to layer correlation between profiles is indicated by solid lines and their colour is in accordance with the source volcano code. Tephra series are indicated by "}" symbol. Inset map shows profile locations (see also Fig. 1). Note that the Hreysiskvísl profile is shown twice to close the correlation around the Vatnajökull ice cap and the Saudárhraukar profile is represented by two logs because two sections were measured at that site in order to acommodate for stratigraphic disturbance present in the main profile. These two logs have been combined in Fig. 6.

Combined tephra layer frequency (TLF) after correlation of profiles

The seven profiles were correlated using 1) tephra marker layers, 2) tephra stratigraphy in combination with the calculated SAR age for each tephra unit and 3) chemical composition of the tephra based on the average composition of the tephra units and the associated standard deviations (Fig. 3, Table 4). This correlation enables construction of a combined TLF for the profiles in question or the number of eruptions that have deposited tephra in soils around the Vatnajökull ice cap. At least 348 eruptions have contributed to the tephra record in these profiles (Fig. 3 and 12). Thereof ~70% are from Grímsvötn, Bárdarbunga and Kverkfjöll; 137 from Grímsvötn (39%), 87 from Bárdarbunga (25%) and 18 from Kverkfjöll (5%). Of all Grímsvötn tephra units 52% could be correlated, 58% of Bárdarbunga tephra and 61% of the Kverkfjöll tephra. The Katla volcanic system has produced 16% (57) of the identified tephra, 4% (15) originate from the Hekla system and 1% (4) are other tephra marker layers. About 9% (30) of measured and sampled tephra layers are of unidentified provenance.

The combined TLF can be used to estimate the eruption frequency of the volcanic systems beneath Vatnajökull (Fig. 13). In this context, it is important to recognize that the 8-6 kyr interval is only covered by data from four profiles (Hreysiskvísl, Saudárhraukar, Kárahnjúkar, Snæfell) and the 6-5 kyr interval by five profiles (i.e. the four mentioned above plus Núpsstadarskógar). Consequently, the first 2-3000 years of our record are not as well represented south of the glacier as they are north of it.

The combined TLF histogram exhibits two distinct peaks, from 6-5 ka and 2-1 ka (Fig. 13). When broken down to specific volcanoes, a similar pattern is observed. The Grímsvötn TLF has two peaks, one at 7-6 ka and another at 2-1 ka. Between these two peaks a steady increase in the TLF is observed, from nine layers per 1000 years in the period 6-5 ka to 35 layers at 2-1 ka. The combined TLF of Bárdarbunga shows a rather steady increase to a peak of 20 preserved tephra layers 2-1 ka with a vague lull between 5 and 4 ka. The combined TLF for Kverkfjöll indicates that Holocene explosive eruptions at that volcano are confined to two distinct time intervals; a longer one at 8-5 ka with peak of eight tephra layers between 5-6 ka and another more inconspicuous one at 3-1 ka, represented by four tephra layers.

Table 4 Examples of correlated Bárdarbunga and Grímsvötn tephra from the Kárahnjúkar (Kári) and Saudárhraukar (Shr.) profiles. Correlation is based on stratigraphic position, right below the H4 tephra marker layer (see Fig. 3), and chemical composition of the tephra using the average composition of the tephra units and their associated standard deviations.

Vs.	Log#	Age	SiO_2	TiO_2	Al_2O_3	FeO	MnO	MgO	CaO	Na_2O	K_2O	P_2O_5	Total
Bár	Kári 48		49.54	1.69	14.38	12.05	0.28	7.03	12.09	2.29	0.16	0.20	99.72
Bár	Kári 48		49.84	1.75	14.25	11.80	0.21	6.95	12.17	2.28	0.16	0.12	99.53
Bár	Kári 48		49.54	1.71	14.29	12.30	0.19	6.87	11.80	2.31	0.16	0.13	99.30
Bár	Kári 48		50.00	1.69	14.28	11.54	0.18	6.89	11.97	2.33	0.16	0.14	99.18
Bár	Kári 48		49.99	1.69	14.27	11.78	0.23	6.93	12.06	2.25	0.17	0.11	99.48
Bár	**Mean**	**4300**	**49.78**	**1.71**	**14.29**	**11.89**	**0.22**	**6.93**	**12.02**	**2.29**	**0.16**	**0.14**	**99.44**
Bár	**SD**		**0.23**	**0.03**	**0.05**	**0.29**	**0.04**	**0.06**	**0.14**	**0.03**	**0.00**	**0.03**	**0.21**
Bár	Shr. II 38		48.68	1.64	13.80	12.19	0.22	7.00	12.15	2.17	0.17	0.17	98.19
Bár	Shr. II 38		48.90	1.72	13.72	12.32	0.27	6.83	11.84	2.29	0.18	0.11	98.18
Bár	Shr. II 38		49.69	1.72	14.12	11.80	0.32	7.05	12.11	2.26	0.16	0.09	99.31
Bár	Shr. II 38		48.87	1.75	13.70	12.42	0.27	6.85	11.97	2.17	0.16	0.14	98.31
Bár	Shr. II 38		49.24	1.77	13.90	12.47	0.18	6.62	11.83	2.21	0.18	0.17	98.56
Bár	Shr. II 38		49.05	1.82	13.68	12.31	0.30	6.91	12.05	2.29	0.18	0.17	98.76
Bár	**Mean**	**4340**	**49.07**	**1.74**	**13.82**	**12.25**	**0.26**	**6.88**	**11.99**	**2.23**	**0.17**	**0.14**	**98.55**
	SD		**0.35**	**0.06**	**0.17**	**0.24**	**0.05**	**0.15**	**0.14**	**0.06**	**0.01**	**0.04**	**0.44**
Grí	Kári 46		48.76	2.16	14.11	11.39	0.26	6.77	11.84	2.29	0.31	0.22	98.10
Grí	Kári 46		49.40	2.46	14.04	11.72	0.19	6.51	11.21	2.46	0.34	0.15	98.46
Grí	Kári 46		49.54	2.62	13.88	12.49	0.26	6.15	10.67	2.42	0.36	0.33	98.71
Grí	Kári 46		49.36	2.24	14.25	12.09	0.21	6.93	11.36	2.52	0.30	0.22	99.48
Grí	Kári 46		49.62	2.22	14.34	11.96	0.18	6.90	11.58	2.55	0.30	0.20	99.85
Grí	**Mean**	**4630**	**49.29**	**2.27**	**14.18**	**11.79**	**0.21**	**6.78**	**11.50**	**2.45**	**0.31**	**0.20**	**98.97**
Grí	**SD**		**0.37**	**0.13**	**0.14**	**0.31**	**0.04**	**0.20**	**0.28**	**0.12**	**0.02**	**0.03**	**0.83**
Grí	Shr. II 37		49.25	2.22	14.01	11.80	0.14	6.89	11.58	2.33	0.31	0.17	98.70
Grí	Shr. II 37		49.22	2.31	14.09	12.06	0.27	6.74	11.50	2.34	0.30	0.21	99.04
Grí	Shr. II 37		49.29	2.31	13.79	12.11	0.16	6.78	11.55	2.33	0.31	0.31	98.94
Grí	Shr. II 37		49.42	2.31	13.97	12.25	0.15	6.63	11.51	2.42	0.30	0.26	99.22
Grí	Shr. II 37		49.47	2.33	14.07	11.92	0.27	6.76	11.57	2.48	0.31	0.23	99.42
Grí	Shr. II 37		49.27	2.36	13.99	11.88	0.16	6.81	11.39	2.30	0.33	0.25	98.75
Grí	**Mean**	**4400**	**49.32**	**2.31**	**13.99**	**12.00**	**0.19**	**6.77**	**11.52**	**2.37**	**0.31**	**0.24**	**99.01**
Grí	**SD**		**0.10**	**0.05**	**0.10**	**0.17**	**0.06**	**0.08**	**0.07**	**0.07**	**0.01**	**0.05**	**0.28**

Vs.: Volcanic System. Log# as in Fig. 3. Mean shows the average composition of the six analysed points in each tephra unit. SD is one standard deviation. Age shows calculated SAR age from each soil profile.

5.6 Discussion

Comparison of estimated eruption frequency during historical and prehistoric periods

The eruption history of Grímsvötn and Bárdarbunga during the last eight centuries has been established through tephra studies on outlet glaciers from the Vatnajökull ice cap, soil profiles and written records (e.g. Thorarinsson 1950; 1974; Larsen et al. 1998; Thordarson and Larsen 2007; Larsen and Eiríksson 2008a; b). About 64 Grímsvötn and 19 Bárdarbunga events are identified and confirmed since 1200 AD (Larsen et al. 1998; Thordarson and Larsen 2007), but no historical eruption is known from the Kverkfjöll volcanic system (Thordarson and Höskuldsson 2002).

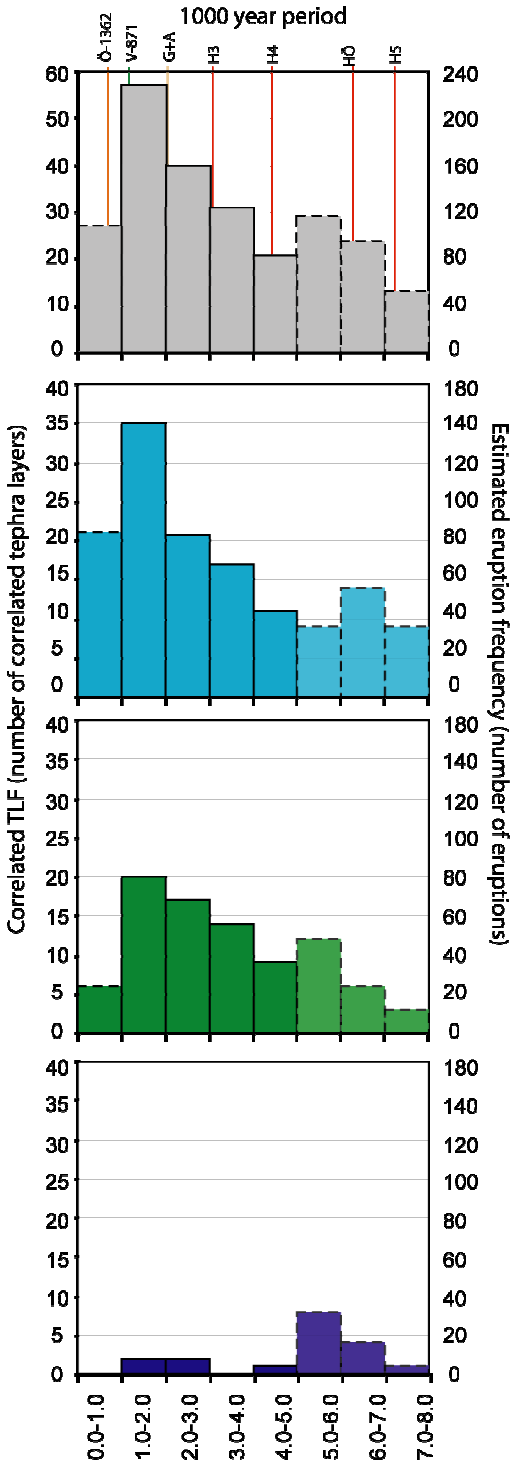

Figure 13 Combined tephra layer frequencies (TLF; scale on left) for the profiles measured around Vatnajökull ice cap along with the estimated eruption frequency (scale on right) after correlation of the seven soil profiles. Time scale is based on SAR calculations (see Fig. 3). Broken lines denote bars based on data from only four to five profiles. Also note, the data for the last time interval, 7-8 ka, is incomplete and only extends back to 7.6 ka (see Figs. 4-10).

Only a fraction of the historical eruptions at volcanoes beneath Vatnajökull have produced tephra that was deposited and preserved in soils outside the ice cap and the barren highland areas (Larsen and Eiríksson 2008a). Recent small eruptions in Grímsvötn, such as those of 1983 and 2004 (Grönvold and Jóhannesson 1984; Oddsson 2007), that have limited tephra dispersal and deposited little or no tephra outside the 8000 km_2 ice cap, are unlikely to leave recognizable layer in soil in distal areas. Larger and more widespread tephra layers, such as those of the 1922 and 1934 Grímsvötn eruptions, are deposited and preserved distally. Therefore, the proportion of preserved tephra layers in the best historical highland profiles used in this study is likely to be somewhat higher than observed in the lowlands. To obtain an estimate on the eruption frequency, a ratio between the number of known eruptions and the correlated number of preserved tephra layers from the last eight centuries of the measured soil sections is calculated. This factor is used for adjusting the estimated eruption frequency in prehistoric time.

Grímsvötn

The combined tephra stratigraphy from the seven soil profiles contains 16 tephra layers from Grímsvötn younger than 1200 AD (Fig. 3), or one-fourth of known eruptions. This is different from the one out of five ratio given by Larsen and Eiríksson (2008a) which was deduced from soil profiles in the lowlands, farther away from the volcanic source. Using the correction factor

obtained in this study, the eruption frequency of Grímsvötn during prehistoric time is ~480 eruptions during the 6500 years covered by the profiles. On average this amounts to ~7 eruptions per century notwithstanding that the correlated tephra stratigraphy (Fig. 13) shows variable activity through time. This is concordant with results of Thordarson and Höskuldsson (2008) even though they use slightly different preservation ratio.

The minimum estimated eruption frequency at Grímsvötn is 36 layers per 1000 years in the periods 8-7 ka and 6-5 ka. However, since the first 2000 years are missing from three profiles (Steinadalur, Núpsstadarskógar, Nýidalur) this assessment probably underestimates the eruption frequency in these periods. The maximum frequency is 140 eruptions in the period 2-1 ka (Fig. 13). In the last millennium (1-0 ka) the eruption frequency is still high but drops to 84 events/1000 yrs which is slightly higher than recently estimated by Thordarson and Larsen (2007) and Larsen and Eiríksson (2008b and references therein) although still within uncertainity limits.

Bárdarbunga

Only five tephra layers from Bárdarbunga, younger than 800 years, are present in the combined tephra stratigraphy (Fig. 3). This gives a preservation ratio of one-fourth as suggested by Larsen and Eiríksson (2008a) from their study at the lowlands and as obtained for Grímsvötn in this study. The total estimated eruption frequency at Bárdarbunga during the 6500 prehistoric years is therefore ~330 eruptions and on average 48 eruptions per 1000 years or ~5 per century.

The distance from source volcano does not seem to affect the preservation ratio for Bárdarbunga tephra as much as was observed for Grímsvötn tephra. Although Grímsvötn shows higher activity than Bárdarbunga only 52% of Grímsvötn tephra layers can be correlated from one profile to another whereas 58% of Bárdarbunga tephra layers are correlated between two or more profiles. This may suggest that the preserved tephra layers from Bárdarbunga have somewhat wider dispersal, and accordingly, could result from larger eruptions than those of Grímsvötn. This could partly explain the lower activity in Bárdarbunga as there is often an inverse relationship between eruption frequency and eruptions sizes where high frequency calls for small eruptions and vice versa (e.g. Vilmundardóttir and Larsen 1986; Simkin and Siebert 1994; Gudmundsson 2000).

As for Grímsvötn, the eruptions at Bárdarbunga are not equally distributed through time (Fig. 4-10). The combined TLF increases rather steadily during the first 7000 years, peaking in the interval 2-1 ka (Fig. 13). The estimated eruption frequency is at minimum at 8-

7 ka (12 eruptions per 1000 years), rising to 80 eruptions at 2-1 ka. Thereafter, the eruption frequency drops considerably to 24 eruptions in the last millennium or to its lowest level in the last 5000 years, yet it accounts for all the 23 confirmed historical eruptions (Thordarson and Larsen 2007).

Kverkfjöll

Kverkfjöll has not produced any historical tephra, thus it is not possible to adjust its eruption frequency as is done for the other volcanoes. However, as the location of Kverkfjöll is similar to Bárdarbunga, both being in the northern part of Vatnajökull ice cap close to the glacier margins and of a similar height (Björnsson and Einarsson 1990), the same preservation ratio is used for Kverkfjöll and Bárdarbunga for estimation of eruption frequency, i.e. one out of every four eruptions is recorded as a tephra layer. After correlation between profiles, the total number of tephra layers originating from Kverkfjöll in prehistoric time is 18, which implies an estimated eruption frequency of ~70 eruptions during the 6500 prehistoric years or 1 event per 100 years on average. However, the TLF indicates that the activity at Kverkfjöll volcano has been episodic during the Holocene with repose periods extending over more than 1000 years, including the current one (~1200 years). At the time of peak activity (6-5 ka) the soil archive contains 8 tephra layers, which leads to an estimate of 32 eruptions per 1000 years (Fig. 13). Ten tephra layers, or about 55%, are found in more than one outcrop.

Temporal variations in the eruption frequency at Grímsvötn, Bárdarbunga and Kverkfjöll – caused by changes in environmental conditions or magma productivity?

Water-magma interaction causes magma fragmentation and explosive eruptions forming wide-spread tephra from the three volcanic systems, emphasizing the primordial role of ice cover on the volcanic source for basaltic tephra formation. Changes in the extent of the ice may therefore influence the observed eruption frequency. Most eruptions taking place on a volcanic system originate in the central volcano whereas eruptions occurring only out on the associated fissure swarm are less frequent (e.g. Gudmundsson 2000). During the last two centuries at least 20 Grímsvötn eruptions are recorded (Thorarinsson 1974; Larsen et al. 1998) of which at least one occurred outside the Grímsvötn central volcano (Þórdarhyrna 1903) and another seven took place outside or partly outside the *caldera* of the central volcano (Larsen and Gudmundsson 1997). In the case of Grímsvötn it can therefore be assumed that the majority of eruptions take place at the central volcano.

The Grímsvötn system is ~100 km long and ice in its area did not melt all at once (Kaldal and Víkingsson 1990). Today Grímsvötn has the largest ice covered area of the three volcanic systems or up to two-thirds (the central volcano and 2/3 of the fissure swarm; Sæmundsson 1978; Jóhannesson and Sæmundsson 1998). The glaciers retreated gradually from the Bárdarbunga system at the end of the last glaciation and the beginning of the Holocene and today about 60 km out of the 190 km long volcanic system is ice covered (Sæmundsson 1978). The fissure swarm of the Kverkfjöll system is mostly ice free (Fig. 1). Nevertheless, all of the central volcanoes are ice covered today and that condition has probably prevailed during all of the Holocene, even during the Holocene Thermal Maximum 8-7 ka (Kaufmann et al. 2004; Ran et al. 2008) when the ice cap probably was significantly smaller. Óladóttir et al. (2007) has demonstrated that the Mýrdalsjökull ice cap survived the Holocene Thermal Maximum supporting the existence of ice cover on the central volcanoes in Vatnajökull during the Holocene.

The cumulative eruption frequency for Grímsvötn, Bárdarbunga and Kverkfjöll is bimodal, one peak at 6-5 ka and another at 2-1 ka (Fig. 13, top), with a low in eruption frequency from 5-2 ka here referred to as the Mid-Holocene low. It could be an artefact caused by greatly reduced ice cover 6-4 ka and consequently less explosive activity on the ice covered parts of Grímsvötn, Bárdarbunga and Kverkfjöll. However, the Holocene Thermal Maximum 8-7 ka (Kaufmann et al. 2004; Ran et al. 2008) precedes the Mid-Holocene low by 1-3 ka making this explanation unlikely. Furthermore, the fact that the minimum is not synchronous on the three volcanic systems makes this possibility improbable. This supports that the observed changes with time in the eruption frequency deduced from the combined TLF are reliable, thus a decrease in volcanic activity causes the Mid-Holocene low.

Abundant magma production at depth due to isostatic rebound and depressurisation is suggested by e.g. Sigvaldason et al. (1992) and Maclennan et al (2002) to trigger intense volcanism at the end and following the last glaciation, as manifested by e.g. large shield volcanoes. However, the eruption frequency during this period is less well constrained. Kaldal (1993) has shown that the margin of the retreating Younger Dryas ice sheet was located 15 km to the west of the SW-trending Bárdarbunga fissure swarm at 10.2 ka, but it was ice free when the large Thjórsá lava emanated from a fissure there 8.6 ka (Hjartarson 1994). Fissure eruptions on the SW-part of the Bárdarbunga system are at least 22 (30 lava units have been mapped, but more than one unit may be attributed to individual eruptions; Vilmundardóttir et al. 2000). The lava flows were dated by the same marker tephra layers as used in the soil sections around Vatnajökull. However, in this area tephra layers older than H5 extend beyond

8.4 ka in soil outside and on top of the oldest lavas, with at least 14 lava flows predating the H5 marker tephra. Of these lavas, five were probably erupted 8-7 ka and the remaining nine, including the large Thjórsá lava flow, 9-8 ka. Hence, the eruption frequency (and productivity) on the ice free SW-part of the volcanic system peaked before 8 ka. The peak in eruption frequency on the ice covered part of the Bárdarbunga system, inferred from the combined TLF at 6-5 ka, occurs 2-3 ka later than the peak on the SW-part of the same volcanic system. If this is looked at as a delay the postulated cause could be a lag in ice melting and resulting pressure release at depth. In that case the 6-5 ka peak could be seen as a response to the Holocene Thermal Maximum when the glaciers were at minimum. However, other causes of spatial variations in eruption frequency must also be considered (see below).

Kverkfjöll shows much lower activity than Grímsvötn and Bárdarbunga, with only single activity peak and long quiet intervals. However, Kverkfjöll is active when eruption frequency is high on the other two systems (Fig. 13) although an inverse relationship is sometimes observed in individual profiles (Fig. 6, 8) with increased local TLF in Kverkfjöll coinciding with local TLF lows in Grímsvötn/Bárdarbunga.

Spatial variations in eruption frequency

The Holocene tephra record clearly shows that Grímsvötn has had the highest eruption frequency of all Icelandic volcanic systems in postglacial times (Fig. 13). The second most active system is Bárdarbunga (Fig. 13) and the prehistoric tephra record from Katla volcano (Óladóttir et al. 2005) show it to be the third most active volcanic system in Iceland. This order of activity is similar to the one obtained for historical time (Thordarson and Larsen 2007). Interestingly, the two volcanic systems located close to the assumed centre of the mantle plume (Fig. 1) are the most active ones whereas Kverkfjöll, located farther from the centre shows much lower activity.

In this context it is worth examining the prehistoric record of the Katla volcano, located on the southern part of the EVZ (Fig.1), which features an event maxima at 8-7 ka and 4-2 ka (Óladóttir et al. 2005; 2008; Fig. 14). The older TLF peak of Katla occurs 1-2000 years prior to the older TLF peak in Bárdarbunga (Fig. 13), but 1000 years later than its LFF peak (Fig. 14). Similarly, the younger Katla TLF peak begins 2000 years prior to that of Grímsvötn and Bárdarbunga. In addition, dated silicic tephra layers from Iceland show event frequency maxima 8-7 ka and 3-2 ka (Larsen and Eiríksson 2008a), similar to the estimated eruption frequency of Katla (Óladóttir et al. 2005) and overall lava age distribution at the EVZ (Jakobsson 1979). The majority of the silicic eruptions occurred at Hekla, Katla, Torfajökull

and Eyjafjallajökull central volcanoes (Larsen and Eiríksson 2008a) located on the southern part of the EVZ and all of which are located far from the surface expression of the assumed centre of the Iceland mantle plume (Wolfe et al. 1997).

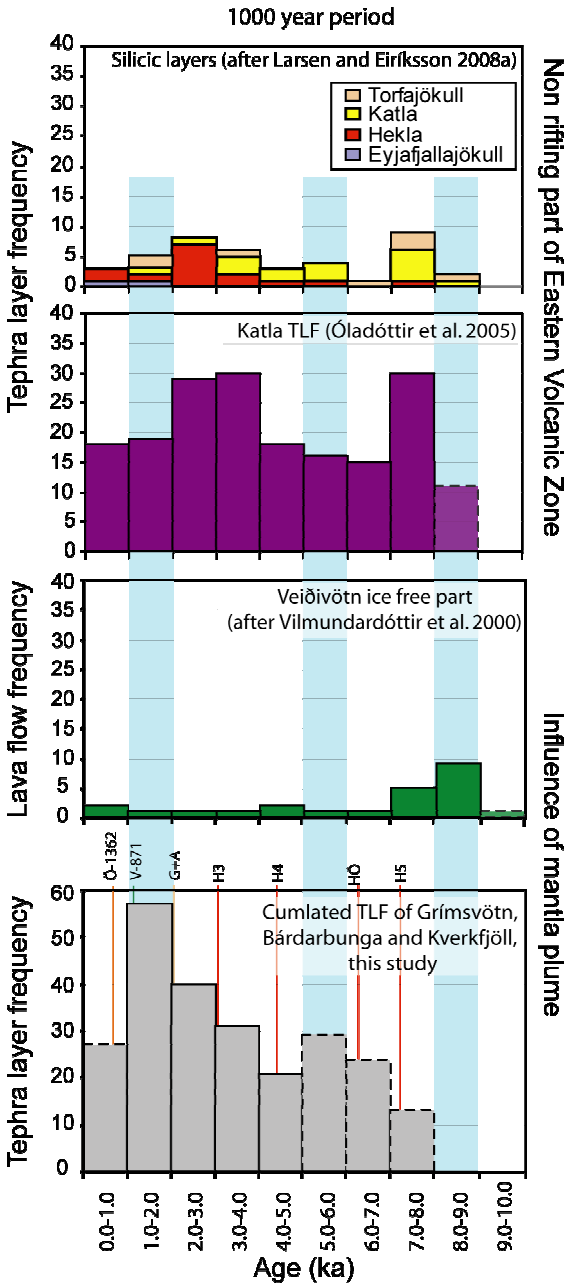

Figure 14 Summarice of eruption frequency peaks observed in volcanic systems on the non-rifting part of the EVZ (top two) and under direct influence of the Icelandic mantle plume (bottom two). Cumulated TLF for the ice covered part of the Grímsvötn, Bárdarbunga and Kverkfjöll volcanic systems in grey, lava flow frequency (LFF) for the ice-free part of the Bárdarbunga system (after Vilmundardóttir et al. 2000) in green, Katla in violet and silicic tephra from Torfajökull, Katla, Hekla and Eyjafjallajökull on the EVZ in tan, yellow, red and blue (after Larsen and Eiríksson 2008a). See further discussion in text.

This age difference in peak eruption frequency at the volcanoes located above the assumed mantle plume centre and those located further to the SW on the propagating rift zone, may suggest that a magma pulse generated during and after the last deglaciation and manifested in high LFF (and large lava volume) at the Bárdarbunga volcanic system at 9-8 ka (Fig. 14), was delayed for 1-2 thousand years farther SW (e.g. Katla TLF peak 8-7 ka), most likely due to less divergent tectonics there. This pattern is repeated when eruption frequency at Katla and the volcanoes on the non-rifting part of the EVZ peaks again 4-2 ka, 1-2 thousand years later than the accumulated TLF peak at 6-5 ka from the three volcanoes under Vatnajökull. Alternatively, magma supply from depth is delayed to the SW where extensional tectonics have not yet developed at the front of the propagating rift segment (e.g. Sæmundsson 1979). Given the clear maximum in eruption frequency above the mantle plume at 2-1 ka, a significant increase in volcanic manifestation could be expected at the volcanoes on the non-rifting part of the EVZ (Katla, Hekla etc.) in the next 1000 years. Taken together, periodic magma generation and delivery from the mantle

plume seem to control the overall eruption frequency at the subglacial Vatnajökull volcanoes, whereas either diverted mantle and melt flow away from the plume core during ascent (Ito 2001) or lithospheric compressional regime could explain the delayed peak activity to the SW.

Temporal variations in eruption frequencies at individual volcanic systems beneath the Vatnajökull ice cap

The vague activity difference between Grímsvötn and Bárdarbunga/Kverkfjöll indicates that pulsing mantle plume is unlikely to account for the finer variations in eruption frequency at a given volcano alone. If deep-seated mantle pulses were entirely responsible for the changes in eruption frequency in these volcanic systems they should be completely synchronised, at least Grímsvötn and Bárdarbunga which maintain similar position relative to the plume centre (Wolfe et al. 1997). Different structure of the magma plumbing system beneath volcanoes has been shown to control eruption frequency in the case of Katla volcano (Óladóttir et al. 2008). There, highest eruption frequency occurs during periods dominated by sill and dyke complexes, and a similar situation appears to influence the individual eruption frequencies at the Vatnajökull volcanoes (Óladóttir et al. Manuscript 3).

5.7 Conclusions

Data obtained from seven soil sections around the Vatnajökull ice cap have revealed the prehistoric eruption history of the ice-covered part of the three volcanic systems, Grímsvötn, Bárdarbunga and Kverkfjöll, going back ~7600 years.

Correlated tephra stratigraphy based on dated marker tephra layers, SAR age calculations and major element chemistry of the volcanic glass, provides a record of 348 prehistorical tephra layers, whereof 137, 87 and 18 were erupted in Grímsvötn, Bárdarbunga and Kverkfjöll, respectively.

The ratio of Grímsvötn and Bárdarbunga tephra layers preserved outside the ice cap during the last 8 centuries of historical time in Iceland was applied to obtain an estimate of the actual eruption frequency in prehistoric time, resulting in a total of 980 eruptions in Grímsvötn, Bárdarbunga and Kverkfjöll during the last ~8000 years.

During historical and prehistoric time total number of eruptions on the ice covered part of the Grímsvötn volcanic system is ~560, making it the most active Icelandic volcanic system in terms of eruption frequency. It has two peaked activity profile showing high activity

7-6 ka with 56 eruptions per 1000 years and again 2-1 ka when in total 140 eruptions took place.

Such increased eruption frequency is also observed in the Bárdarbunga volcanic system, which is the second most active volcanic system with ~350 eruptions during the last ~8000 years. Its activity profile is two peaked and like Grímsvötn the activity is highest 2-1 ka but the older activity peak lags that of Grímsvötn by 1000 years. Both systems show a strong activity decrease during the last millennium.

Kverkfjöll shows considerably less activity and only ~70 eruptions were inferred during the ~6500 years studied during prehistoric time, which is still significantly higher than historical activity which is none. Kverkfjöll was most active 7-5 ka but showed some activity during the first 4 ka observed in this study (8-4 ka) and again 3-1 ka although the activity is low, 4-32 eruptions per 1000 years.

All three volcanic systems show a lull in activity between 5 and 2 ka, referred to as the Mid Holocene low, caused by decrease in volcanic activity that is traced to periodic magma generation and delivery from the mantle plume rather than changes in environmental factors such as changing ice load and ice cover.

Age difference in peak eruption frequency at volcanoes close to the centre of the Iceland mantle plume and volcanoes located on the non-rifting part of the Eastern Volcanic Zone (EVZ) could be explained by diverted flow away from the plume core during ascent, indicating that a significant increase in volcanic manifestation may be expected on the southern EVZ in the future.

5.8 Acknowledgements

This paper is based on a PhD-study at the Laboratoire Magmas et Volcans (LMV), CNRS-Université Blaise Pascal in Clermont-Ferrand and the University of Iceland. It was financed by the Icelandic Science Foundation, Landsvirkjun, Eimskip Fund of the University of Iceland, the French government through a student's grant and the French-Icelandic collaboration programme Jules Verne. Jean-Luc Devidal is specially thanked for his help during major element analyses and Gudmundur Óli Sigurgeirsson and Ester Anna Ingólfsdóttir for priceless field assistance and patience.

5.9 References

Arnalds Ó (2004) Volcanic soils of Iceland. Catena 56(1-3):3-20.

Björnsson A (1985) Dynamics of crustal rifting in NE Iceland. Journal of Geophysical Research 90:10151-10162.

Björnsson H, Einarsson P (1990) Volcanoes beneath Vatnajökull, Iceland: Evidence from radio echo-sounding, earthquake and jökulhlaups. Jökull 40:147-168.

Boygle J (2004) Towards a Holocene tephrochronology for Sweden: geochemistry and correlation with the North Atlantic tephra stratigraphy. Journal of Quaternary Science 19(2):103-109.

Dugmore AJ, Shore JS, Cook GT, Newton AJ, Edwards KJ, Larsen G (1995) The radiocarbon dating of Icelandic tephra layers in Britain and Iceland. Radiocarbon 37(2):379-388.

Dugmore AJ, Newton A (1998) Holocene tephra layers in the Faroe Islands. Fróðskaparrit 46:191-204.

Eiríksson J, Larsen G, Knudsen KL, Heinemeier J, Simonarson LA (2004) Marine reservoir age variability and water mass distribution in the Iceland Sea. Quaternary Science Reviews 23(20-22):2247-2268

Friedman JD, Williams RS, Thorarinsson S, Pálmason G (1972) Infrared emission from Kverkfjöll subglacial volcanic and geothermal area, Iceland. Jökull 22:27-43.

Gíslason SR, Oelkers EH (2003) Mechanism, rates, and consequences of basaltic glass dissolution: II. An experimental study of the dissolution rates of basaltic glass as a function of pH and temperature. Geochimica et Cosmochimica Acta 67(20):3817-3832.

Grönvold K and Jóhannesson H (1984) Eruption in Grímsvötn 1983: Course of events and chemical studies of the tephra. Jökull 34, 1-11.

Grönvold K, Óskarsson N, Johnsen SJ, Clausen HB, Hammer CU, Bond G, Bard E (1995) Ash Layers from Iceland in the Greenland Grip Ice Core Correlated with Oceanic and Land Sediments. Earth and Planetary Science Letters 135(1-4):149-155.

Gudmundsson Á (2000) Dynamics of volcanic systems in Iceland: Example of tectonism and volcanism at juxtaposed hot spot and mid-ocean ridge systems. Annual Review of Earth and Planetary Sciences 28:107-140.

Gudmundsson MT, Björnsson H (1991) Eruptions in Grímsvötn, Vatnajökull, Iceland, 1934-1991. Jökull 41:21-46.

Gudmundsson T, Björnsson H, Thorvaldsson G (2004) Organic carbon accumulation and pH changes in an Andic Gleysol under a long-term fertilizer experiment in Iceland. Catena 56(1-3):213-224.

Haflidason H, Eiríksson J, Van Kreveld S (2000) The tephrochronology of Iceland and the North Atlantic region during the Middle and Late Quaternary: a review. Journal of Quaternary Science 15(1):3-22.

Hammer CU, Clausen HB, Dansgaard W (1980) Greenland ice sheet evidence of postglacial volcanism and its climatic impact. Nature 288:230-235.

Hjartarson Á (1994) Environmental changes in Iceland following the Great Þjórsá Lava Eruption 7800 14C years BP. In: Stötter J, Wilhelm F (eds) Environmental Change in Iceland. Munchen, pp 147-155.

Hreinsdóttir S, Einarsson P, Sigmundsson F (2001) Crustal deformation at the oblique spreading Reykjanes Peninsula, SW Iceland: GPS measurements from 1993 to 1998. Journal of Geophysical Research 106(B7):13803-13816.

Ito G (2001) Reykjanes 'V'-shaped ridges originating from a pulsing and dehydrating mantle plume. Nature 411(6838):681-684.

Jakobsson SP (1979) Petrology of recent basalts of the Eastern Volcanic zone, Iceland. Acta Naturalia Islandica 26:1-103.

Jakobsson SP, Jónasson K, Sigurdsson IA (2008) The three igneous rock series of Iceland. Jökull 58:117-138.

Jóhannesson H, Sæmundsson K (1998) Geological map of Iceland, 1:500,000. Tectonics. Icelandic Institute of Natural History and Iceland Geodetic Survey, Reykjavík.

Jull M, McKenzie D (1996) The effect of deglaciation on mantle melting beneath Iceland. Journal of Geophysical Research-Solid Earth 101(B10):21815-21828.

Kaldal I (1993) Fróðleiksmolar um gamla gjósku í Búdarhálsi. In: Geoscience Society of Iceland Spring meeting. Reykjavík, pp 36-37.

Kaldal I, Víkingsson S (1990) Early Holocene deglaciation in Central Iceland. Jökull 40:51-68.

Kaufmann DS, Ager TA, Anderson NJ, Anderson PM, Andrews JT, Bartlein PJ, Brubaker LB, Coats LL, Cwynar LC, Duvall ML, Dyke AS, Edwards ME, Eisner WR, Gajewski K, Geirsdóttir Á, Hu FS, Jennings AE, Kaplan MR, Kerwin MW, Lozhkin AV, MacDonald GM, Miller GH, Mock CJ, Oswald WW, Otto-Bliesner BL, Porinchu DF, Ruhland K, Smol JP, Steig EJ, Wolfe BB (2004) Holocene thermal maximum in the western Arctic (0-180°). Quaternary Science Reviews 23(5-6):529-560.

Kristjánsdóttir GB, Stoner JS, Jennings AE, Andrews JT, Grönvold K (2007) Geochemistry of Holocene cryptotephras from the north Iceland shelf (MD99-2269): intercalibration with radiocarbon and palaeomagnetic chronostratigraphies. Holocene 17(2):155-176

Lacasse C, Carey S, Sigurdsson H (1998) Volcanogenic sedimentation in the Iceland Basin: influence of subaerial and subglacial eruptions. Journal of Volcanology and Geothermal Research 83(1-2):47-73.

LaFemina PC, Dixon TH, Malservisi R, Árnadóttir Th, Sturkell E, Sigmundsson F, Einarsson P (2005) Geodetic GPS measurements in south Iceland: Strain accumulation and partitioning in a propagating ridge system. Journal of Geophysical Research-Solid Earth 110, B11405, doi:10.1029/2005JB003675.

Larsen G (1982) Gjóskutímatal Jökuldals og nágrennis. In: Thórarinsdóttir H (ed) Eldur er í norðri. Sögufélag, Reykjavík, pp 51-65.

Larsen G (1984) Recent volcanic history of the Veidivötn fissure swarm, Southern Iceland. An approach to volcanic risk assessement. Journal of Volcanology and Geothermal Research 22:33-58.

Larsen G (1992) Gjóskulagið úr Heklugosinu 1158. In: Geoscience Society of Iceland, Spring Meeting 1992. Reykjavík, pp 25-27.

Larsen G, Thorarinsson S (1977) H-4 and other acid Hekla tephra layers. Jökull 27:28-46.

Larsen G, Vilmundardóttir EG (1985) Gjóskurannsóknir á Þjórsársvæði 1983-1984. Orkustofnun (National Energy Authority), Research Report OS-85037/VOD-16B, Reykjavik, pp 20.

Larsen G, Gudmundsson MT (1997) Gos í eldstöðvum undir Vatnajökli eftir 1200 AD. In: Haraldsson H (ed) Vatnajökull. Gos og hlaup 1996. Vegagerðin, Reykjavík., pp 23-36.

Larsen G, Eiríksson J (2008a) Late Quaternary terrestrial tephrochronology of Iceland - frequency of explosive eruptions, type and volume of tephra deposits. Journal of Quaternary Science 23(2):109-120.

Larsen G, Eiríksson J (2008b) Holocene tephra archives and tephrochronology in Iceland - a brief overview. Jökull 58:229-250.

Larsen G, Gudmundsson MT, Björnsson H (1998) Eight centuries of periodic volcanism at the centre of the Icelandic hotspot revealed by glacier tephrostratigraphy. Geology 26:943-946.

Larsen G, Dugmore A, Newton A (1999) Geochemistry of historical-age silicic tephras in Iceland. Holocene 9(4):463-471.

Larsen G, Newton AJ, Dugmore AJ, Vilmundardóttir EG (2001) Geochemistry, dispersal, volumes and chronology of Holocene silicic tephra layers form the Katla volcanic system, Iceland. Journal of Quaternary science 16:119-132.

Larsen G, Eiríksson J, Knudsen KL, Heinemeier J (2002) Correlation of late Holocene terrestral and marine tephra markers north Iceland: implications for reservoir age changes. Polar Research 21(2):283-290.

Maclennan J, Jull M, McKenzie D, Slater L, Grönvold K (2002) The link between volcanism and deglaciation in Iceland. Geochemstry, Geophysics, Geosystems 3(11).

Merlet C (1994) An Accurate Computer Correction Program for Quantitative Electron-Probe Microanalysis. Mikrochimica Acta 114:363-376.

Oddsson B (2007) The Grímsvötn eruption in 2004, Dispersal and total mass of tephra and comparison with plume transport models. Unpublished Masters theses, University of Iceland, Reykjavík, p 112

Óladóttir BA, Larsen G, Thordarson T, Sigmarsson O (2005) The Katla volcano S-Iceland: Holocene tephra stratigraphy and eruption frequency. Jökull 55:53-74.

Óladóttir BA, Thordarson T, Larsen G, Sigmarsson O (2007) Survival of the Mýrdalsjökull ice cap through the Holocene thermal maximum?-Evidence from sulfur contents in Katla tephra layers (Iceland) from the last ~8400 years. Annals of Glaciology 45:183-188.

Óladóttir BA, Sigmarsson O, Larsen G, Thordarson T (2008) Katla volcano, Iceland: magma composition, dynamics and eruption frequency as recorded by Holocene tephra layers. Bulletin of Volcanology 70(4):475-493.

Óskarsson N, Sigvaldason GE, Steinthórsson S (1982) A dynamic model of rift zone petrogenesis and the regional petrology of Iceland. Journal of Petrology 23:28-74.

Óskarsson N, Steinthórsson S, Sigvaldason GE (1985) Iceland Geochemical Anomaly - Origin, Volcanotectonics, Chemical Fractionation and Isotope Evolution of the Crust. Journal of Geophysical Research-Solid Earth and Planets 90(Nb12):11-25.

Ran LH, Jiang H, Knudsen KL, Eiríksson J (2008) A high-resolution Holocene diatom record on the North Icelandic shelf. Boreas 37(3):399-413.

Sæmundsson K (1978) Fissure swarms and central volcanoes of the neovolcanic zones of Iceland. Geological Journal Special Issue 10:451-432.

Sæmundsson K (1979) Outline of the geology of Iceland. Jökull 29:7-29.

Sejrup HP, Sjoholm J, Furnes H, Beyere I, Eide L, Jansen E, Mangerud J (1989) Quaternary tephrochronology on the Iceland Plateau, north of Iceland. Journal of Quaternary science 6:109-114.

Sigmundsson F (2006) Iceland geodynamics: crustal deformation and divergent plate tectonics. Springer; Praxis, Berlin.

Sigurdsson H, Loebner B (1981) Deep sea record of Cenozoic explosive volcanism in the North Atlantic. In: Self S, Sparks RSJ (eds) Tephra Studies. Reidel, Dordrecht, pp 289-316.

Sigvaldason GE, Annertz K, Nilsson M (1992) Effect of glacier loading/deloading on volcanism: Postglacial volcanic production rate of the Dyngjufjöll area, central Iceland. Bulletin of Volcanology 54:385-392.

Simkin T, Siebert L (1994) Volcanoes of the World. Smithsonian Institution, Tuscon, Arizona, p 349.

Simkin T, Siebert L (2000) Earth's Volcanoes and Eruptions: An Overview. In: Sigurdsson H (ed) Encyclopedia of Volcanoes. Academic press, San Diego, pp 249-262.

Sjoholm J, Sejrup HP, Furnes H (1991) Quaternary Volcanic Ash Zones on the Iceland Plateau, Southern Norwegian Sea. Journal of Quaternary Science 6(2):159-173.

Stuiver M, Reimer PJ, Bard E, Beck JW, Burr GS, Hughen KA, McCormac FG, Plicht JVD, Spurk M (1998) INTCAL98 Radiocarbon age calibration 24,000-0 BP. Radiocarbon 40:1041-1083.

Thorarinsson S (1950) Jökulhlaup og eldgos á jökulvatnasvæði Jökulsár á Fjöllum. Náttúrufræðingurinn 20:113-133.

Thorarinsson S (1958) The Öræfajökull eruption of 1362. Acta Naturalia Islandica 2:1-100.

Thorarinsson S (1961) Uppblástur á Íslandi í ljósi öskulagarannsókna. Ársrit Skógræktarfélags Íslands 1960-1961:17-54.

Thorarinsson S (1967) The eruptions of Hekla in historical times. In: Einarsson T, Kjartansson G, Thorarinsson S (eds) The eruption of Hekla 1947-1948. Societas Scientiarum Islandica, Reykjavík, pp 1-177.

Thorarinsson S (1968) Heklueldar. Sögufélagið, Reykjavík, p 185.

Thorarinsson S (1971) Aldur ljósu gjóskulaganna úr Heklu samkvæmt leiðréttu geislakolstímatali. Náttúrufræðingurinn 41:99-105.

Thorarinsson S (1974) Vötnin stríð. Bókaútgáfa Menningarsjóðs, Reykjavík, p 254.

Thorarinsson S, Sæmundsson K (1979) Volcanic activity in historical times. Jökull 29:29-32.

Thordarson T, Höskuldsson Á (2002) Iceland Terra Publishing, Harpenden, UK, p 200.

Thordarson T, Larsen G (2007) Volcanism in Iceland in historical time: Volcano types, eruption styles and eruptive history. Journal of Geodynamics 43(1):118-152.

Thordarson T, Höskuldsson Á (2008) Postglacial volcanism in Iceland. Jökull 58:197-228.

Vilmundardóttir EG, Larsen G (1986) Productivity pattern of the Veiðivötn fissure swarm, southern Iceland, in postglacial time. Preliminary results. In: 17 Nordiska Geologmötet 1986. Helsingfors Universitet, Helsinki, Finnland, p 214.

Vilmundardóttir EG, Snorrason SP, Larsen G (2000) Geological map of subglacial volcanic area soutwest of Vatnajökull ice cap, Iceland, 1:50.000. In: National Energy Authority and National Power Company, Reykjavík.

Wolfe CJ, Bjarnason IT, VanDecar JC, Solomon SC (1997) Seismic structure of the Iceland mantle plume. Nature 385(6613):245-247.

Zielinski GA, Mayewski PA, Meeker LD, Grönvold K, Germani MS, Whitlow S, Twickler MS, Taylor K (1997) Volcanic aerosol records and tephrochronology of the Summit, Greenland, ice cores. Journal of Geophysical Research-Oceans 102(C12):26625-26640.

5.12 Appendix 1 Different length of SAR periods

The SAR in Hreysiskvísl profile ranges from 0.0139 cm/yr between H-1104 and H-1158 to 0.0570 cm/yr between HÖ and N1. The lowest SAR value probably underestimates the accumulation rate because the time period is short and thus more susceptible to slight measurement error. The high SAR below H4 is obtained from soil horizons made up of peat or histosol. Nýidalur profile features the highest SAR of all measured profiles or an average value of 0.1138 cm/yr. However, the range is wide, shifting from 0.0264 to 0.2696 cm/yr. Unusually high SAR values between Ö-1362 and V-1477, as well as between V-871 and H-1158 are primarily an artefact of that gravel is mixed in the soil. In Saudárhraukar the range is 0.0133-0.1435 cm/yr, in and Kárahnjúkar 0.0169-0.1305 cm/yr and in Snæfell the SAR ranges from 0.0139-0.1099 cm/yr, the highest value (time period H5-HÖ) obtained in a horizon of histosol. The lowest SAR value in Steinadalur is 0.0127 cm/yr observed between H4 and HS and the highest observed value is 0.1344 cm/yr from V-1477 to K-1755. The high SAR value for the latter period results from intercalation of aeolian sand layers with the soil during this period. Finally the Núpsstadarskógar profile has SAR numbers from 0.0221-0.0746 cm/yr, the highest value during the youngest time period, from Ö-1727 to K-1918.

5.13 Appendix 2 Further descriptions on local TLF

Hreysiskvísl (profile no. 1; Fig. 4)

The Hreysiskvísl profile lies in the bank of a small tributary discharging into the Hreysiskvísl river in the Central highlands (Fig. 1). The profile was measured and sampled in the 1980's (Larsen and Vilmundardóttir 1985), however, tephra samples were not analysed until this study.

The youngest tephra measured in the profile is Ö-1362 and the oldest one is from Katla, the third one below H5, and has a calculated age of ~7210 years, hence the profile covers ~6570 years and contains 97 tephra units of which Bárdarbunga produced 30.9%, Grímsvötn 26.8%, Katla 23.7%, Hekla 10.3% and the remaining 8.3% are from various volcanic sources (Table 2). No tephra from the Kverkfjöll system is present in the Hreysiskvísl profile.

The Grímsvötn TLF features one peak at 2-1 ka. In the period 2-8 ka the TLF increases steadily until it peaks with one exception, 3-2 ka, where only one tephra unit is observed. The 500 year histogram reveals three separated eruption periods, each with higher TLF than the previous one. From 7.5-5.5 ka one to two units are observed per 500 years, whereas during the period from 5.0-2.5 ka the average is closer to two tephra units per 500 years and during the last period, 2.0-0.5 ka, up to six units are observed during the 500 year period.

Bárdarbunga shows two TLF peaks on the 1000 year histogram, 6-5 and 2-1 ka, each with seven tephra units per 1000 years. The remaining time periods show 2-4 units per 1000 years. The 500 year time periods show that six out of seven units accounting for the older TLF peak are erupted 6.0-5.5 ka whereas the peak from 2-1 ka is made up of tephra units more equally divided through time (three and four eruptions per 500 years). Between 4.0 and 3.5 ka four Bárdarbunga eruptions did produce tephra preserved in Hreysiskvísl but this peak is only vaguely observed on the 1000 year histogram as no Bárdarbunga tephra is observed during the following 500 years.

Nýidalur (profile no. 2; Fig. 5)

The Nýidalur profile lies in a gully cut into thick soil on the lower slopes of Mt. Tungnafellsjökull. A section of the historical part of the profile was disturbed by gravel layers and soil older than H3 was inaccessible making Nýidalur the shortest profile, covering only ~2500 years.

The youngest tephra is the V-1477 marker layer and the oldest one is the H3 tephra. Nevertheless, this profile contains 56 primary tephra units or on average 22.1 per 1000 years which is the second highest observed number of preserved tephra per 1000 years (Table 2). Bárdarbunga has the highest percentage of units, 35.7%, followed by Grímsvötn (33.9%), Katla (19.6%) and Hekla (5.4%). The remaining 5.4% are from various volcanic systems. No tephra from Kverkfjöll was found (Table 2).

Both Bárdarbunga and Grímsvötn show high TLF in Nýidalur during the 2530 years covered by the profile. The trend manifest in the 1000 year time periods is the same for both systems, peaking 2-1 ka. During this time period 13 Bárdarbunga tephra units were deposited whereas only six were deposited in the preceding 1000 years. Grímsvötn more than tripled its TLF, increasing from three units observed 3-2 ka, all erupted during the first 500 years, to 14 tephra units 2-1 ka, of which nine were erupted during the later half of the period. The low TLF during historical time is partly explained by lack of measured data from 0-500 years ago.

Saudárhraukar (profile no. 3; Fig. 6)

Saudárhraukar profile is exposed in a river bank in the proglacial area of Brúarjökull, about 0.5 km north of end moraines left by a glacier surge in 1890 AD. The profile was measured in two sections, a continuous long section with a disturbed portion in the lower half and a supplementary shorter section that covered the disturbed portion. On Figure 6 the two sections are fitted together to show the actual number of tephra while on Figure 3 and 11 the sections are presented separately.

Saudárhraukar profile has 169 preserved tephra units deposited during ~7000 years. The youngest layer is on top of the known V-1717 tephra and the oldest one is from Grímsvötn, two units below H5. The Grímsvötn volcanic system has produced the highest percentage of tephra 36.7%, followed by Bárdarbunga (34.3%) and Katla accounts for 9.5%, Kverkfjöll has produced 8.2% of the tephra units, Hekla 4.7% and the remaining 6.6% are from various volcanic systems (Table 2).

Tephra from Grímsvötn show relatively stable TLF between 8 and 2 ka with three to seven tephra units, or on average 5.5 per 1000 years. This stable TLF is also noticed on the 500 year histograms and as in the Hreysiskvísl profile it can be separated into three periods, i.e. 7.5-5.0, 5.0-2.5 and 2.5-0 ka. The two older periods have low TLF of one to five units per 500 years whereas the last period, from 2.5 ka to the present day, demonstrates considerably higher TLF with up to 14 preserved units per 500 years, peaking from 1.5-1.0 ka.

The Bárdarbunga tephra show interesting distribution through time. On the 1000 year histogram the TLF appears to rise steadily from 7-1 ka and then it suddenly drops from 11 tephra units per 1000 years down to three during the historical 1000 years. This is not merely an artefact owing to poor preservation of the historical part of this soil profile, which is considerably better represented than in the two previously described profiles. This period also shows a high TLF for the Grímsvötn tephra. The 500 year periodicity tells a different story. The TLF peaks 6.0-5.5 ka with nine tephra units per 500 years whereas the preceding period had only 3 units. No tephra is preserved for the following 1000 years but 4.5-4.0 ka another peak with nine tephra units is observed. TLF is then stable during the next 2 ka, followed by a drop 2.0-1.5 ka and then a new peak is observed during the following 500 years with nine tephra units once more.

Kverkfjöll is rather quiet compared to the other two volcanic systems, with one distinct TLF peak 6-5 ka where eight tephra units are found. No tephra is observed during the next 1500 years, to be followed by three units distributed through 1500 years. The TLF peak in Kverkfjöll partly fits into a TLF low in both Grímsvötn and Bárdarbunga (see 500 year histograms).

Kárahnjúkar (profile no. 4; Fig. 7)

The Kárahnjúkar profile comprises thick Andosol exposed in a road-cut south of Fremri-Kárahnjúkur, Eastern Iceland. The soil section was logged and sampled as a key section for the area now submerged below the Hálslón reservoir.

Kárahnjúkar profile contains 139 tephra units divided on ~7300 years. The youngest tephra is from Grímsvötn, on top of the V-1717 tephra layer and the oldest one is also from Grímsvötn but its age is uncertain, although more than 7600 years. The tephra is divided on volcanic systems as follows: Grímsvötn 38.8%, Bárdarbunga 31.7%, Kverkfjöll 7.9%, Katla 7.2%, Hekla 5.8% and 8.6% are from various volcanic systems (Table 2).

Grímsvötn tephra units are scarce between 7-4 ka with only one to three tephra per 1000 years. Prior to this, six units are found during a time period of minimum 600 years as the oldest three units are of uncertain age. The TLF gradually rises to a peak 2-1 ka with 15 tephra units. The 500 year histogram shows a similar low with a 500 years gap with no observed tephra. The TLF fluctuates but slowly increases until it peaks 1.5-1.0 ka with nine tephra units and then it slowly decreases again although remaining high.

A similar trend is observed for Bárdarbunga. The 1000 year histogram shows two peaks, the older one 6-5 ka and the younger one 3-2 ka. The older peak in Bárdarbunga

coincides with a low in Grímsvötn TLF but the younger peak, 3-2 ka, precedes the Grímsvötn peak by 1000 years. The 500 year periodicity shows three peaks, 6.0-5.5, 2.5-2.0 and 1.5-1.0 ka with six to seven tephra units per 500 years and an interesting fall in TLF is observed from 2.0-1.5 ka.

In total 11 tephra units from Kverkfjöll were identified in the Kárahnjúkar profile. Nine were deposited between 8-5 ka with a peak 6-5 ka and two tephra layers were deposited between 3-1 ka.

Snæfell (profile no. 5; Fig. 8)

The Snæfell profile is exposed in a gully cut into a low slope in Saudárdrög north of Mt. Snæfell, eastern Iceland. The upper 1/3 of the soil is dominated by Andosol whereas the lower 2/3 are Histosol.

Snæfell profile holds 109 primary tephra units, the youngest one is the V-1717 layer and the oldest one a Grímsvötn tephra below H5; hence the profile covers ~6800 years. Thick, black tephra deposit at the base of the profile is possibly reworked and not included. The profile holds about the same number of tephra from Grímsvötn and Bárdarbunga, 31.2% and 29.4% respectively, Katla constitutes 11.9% and Kverkfjöll and Hekla 5.5% each. The remaining 16.5% of tephra units are assigned to other volcanic systems, of which 10.1% are basaltic of unidentified origin (Table 2).

Grímsvötn shows two peaks on both the 1000 and 500 year histograms. On the latter the TLF appears very low between 6.5-2 ka with none to two tephra units per 500 years. Compared to Grímsvötn tephra found in other profiles the 2-1 ka time period contains few tephra units or only seven. The preserved part of the historical period (0-1000) contains eight Grímsvötn tephra units resulting in highest observed TLF in the section although it only covers ~710 years.

The TLF from Bárdarbunga is comparable to the one observed in Kárahnjúkar both for the 1000 and 500 year periodicity, peaking 6-5 and 3-2 ka with seven and nine preserved tephra units, respectively, and a sudden fall in TLF 2.0-1.5 ka showing only one tephra unit.

The six tephra units from Kverkfjöll seem to be equally divided over the 3000 years from 7-4 ka but the 500 year histogram shows a "peak" 5.5-4.5 years ago. Interestingly, once again this is during a TLF low in Grímsvötn and Bárdarbunga.

Steinadalur (profile no. 6; Fig. 9)

The Steinadalur profile in Sudursveit, SE of Vatnajökull, has a strong grass cover with old birch trees. It is carved in a riverbank by the glacial river Kaldakvísl that has also covered the

base with gravel. The dominating soil type is Andosol down to the tephra marker layer H4 but below it the soil changes to Histosol.

Steinadalur profile contains the fewest tephra units of the seven measured soil profiles or only 50 even though it covers ~5800 years. The youngest tephra is K-1755 and the oldest one is a Grímsvötn tephra 10 layers below H4 with a calculated SAR age of 6060 years. More than half of the tephra found in Steinadalur originate in Grímsvötn or 56%, 18% are from Bárdarbunga, 10% from Katla, Kverkfjöll and Hekla account for 4% each and the remaining 8% are from various volcanic systems (Table 2).

The Grímsvötn TLF increases until it peaks 2-1 ka with 10 layers per 1000 years, an exception being the time period 3-2 ka with one unit per 1000 years. The TLF then declines but still remains high compared to the older part of the profile, 6-2 ka.

The nine tephra units from Bárdarbunga are fairly equally divided through time showing no distinct peaks. On the 500 year histogram, however, intervals without any tephra deposition appear almost regularly throughout the record.

Two tephra units are found from Kverkfjöll, 4940 and 2980 years old, both of which coincide with lows in the Bárdarbunga and Grímsvötn records, the younger one fitting into the distinctive Grímsvötn low 3-2 ka.

Núpsstadarskógar (profile no. 7; Fig. 10)

The profile at Núpstadarskógar lies in a sloping river bank with rich vegetation including birch and salix. This profile is close to the one logged by Thorarinsson in the 1950's (Thorarinsson 1958). The glacial river Núpsvötn has since then covered the base of the sections with gravel.

The Núpsstadarskógar profile contains the most complete record of the last millennium and the youngest tephra in this study, the K-1918. The oldest measured tephra is from Grímsvötn two units below the HÖ marker tephra; hence the profile covers ~6200 years. It contains in total 129 tephra units, of which 44.2% are from Grímsvötn, 28.7% from Katla, 16.3% from Bárdarbunga, 3.9% from Hekla and the remaining 6.9% from various systems but only one tephra is found from Kverkfjöll (Table 2).

Grímsvötn shows low TLF of two to five preserved tephra units per 1000 years during the first 3 ka with a small peak 6-5 ka. Four thousand years ago the TLF increased to 10 units per 1000 years and further to a peak of 17 layers 2-1 ka, decreasing again to 10 during the last millennium. The 500 year histogram shows that the TLF is highest 2.0-1.5 ka after which it slowly decreases.

The Bárdarbunga tephra is rather equally divided through time with a vague peak 2-1 ka that becomes more distinctive in the 500 year time periods with five tephra units 1500-1000 years ago. Two gaps are apparent, the older one 4.0-3.5 ka and the younger one 0.5-0 ka. The latter cannot be explained by poor preservation of the historical part.

The single Kverkfjöll tephra unit is 4940 years old and falls into the same time period as Kverkfjöll tephra in other profiles. In this profile it once again fits into a low of the other two volcanic systems.

6. Manuscript 3: Origin and ascent of basaltic magma at the subglacial volcanoes beneath northwest Vatnajökull, Iceland

Origin and ascent of basaltic magma at the subglacial volcanoes beneath northwest Vatnajökull, Iceland.

Bergrun Arna Óladóttir[1,2], Olgeir Sigmarsson[1,2] and Gudrun Larsen[2]

1) Université Blaise Pascal, OPGC and CNRS, 5 rue Kessler, 63038 Clemont-Ferrand, France

2) Institute of Earth Sciences, University of Iceland, 101 Reykjavík, Iceland

6.1 Abstract

The subglacial Vatnajökull volcanoes, Grímsvötn, Bárdarbunga and Kverkfjöll are characterised by explosive basaltic eruptions and expulsion of tholeiitic magmas each covering a narrow compositional range. The limited compositional variability reflects magmatic evolution beneath these three volcanic systems revealed by in-situ major and trace element analyses of tephra covering the last ~7.6 ka. Major element concentrations were measured in 280 tephra units from Grímsvötn, 214 from Bárdarbunga and 34 from Kverkfjöll whereas trace elements were analysed in 24, 10 and 11 units, respectively. The tephra from these volcanic systems feature distinct major element compositions although a small overlap occurs between the compositional fields of the Grímsvötn and Kverkfjöll systems. Thus trace element concentrations and ratios, such as Th, La, La/Yb and Sr/Th, were used for source identification of the tephra with composition corresponding to this overlap. Each tephra unit is assigned an age using soil accumulation rate between tephra marker layers of known age. These allow construction of compositional time-series for the three volcanoes over approximately the last eight millennia.

The subtle compositional variations with time are used to infer the structure of the plumbing system at depth. Magmatic evolution in the three volcanic systems is controlled by crystal fractionation and crustal contamination. Co-variations of Ba, Nb and Th concentrations show that only the least evolved basalts from Grímsvötn (G-I; Th <0.9 ppm) and the most primitive Bárdarbunga basalts are consistent with fractional crystallisation alone. More evolved Grímsvötn basalts (G-II; Th >0.9 ppm), Bárdarbunga and Kverkfjöll all form linear arrays which extrapolations intercept at a single value suggesting a common contaminant of evolved basaltic composition with Th and Ba around 2.6 ppm and 130 ppm, respectively. Close inspection of variations of highly compatible versus the most incompatible element concentrations, together with incompatible element ratios, and multi-element spectra, reveal a similar source mineralogy beneath the three volcanoes. This allows an assessment of the relative magma source melting at depth: Bárdarbunga, above the assumed centre of the Iceland mantle plume, produces basalts formed by highest degree of melting whereas the smallest melting is recorded in the Kverkfjöll basalts erupted farther away from the expression of the plume.

A deep magma source appears to have played an important role in the activity of both Grímsvötn and Bárdarbunga, with a sill and dyke complex most active beneath Grímsvötn during a period of highest eruption frequency 2-1 ka. Closer towards the present, when the

eruption frequency lowers again, magma chambers developed again and the compositional variations of basalts from Grímsvötn and Bárdarbunga are consistent with the presence of active magma chambers in their plumbing systems.

6.2 Introduction

Magma production and plate tectonics are closely linked. The most active sites of magma generation are mid-ocean ridges where 75% of the magma volume produced on Earth is formed whereas 20% are generated in subduction zones and the remaining 5% are intraplate magmas (Grove 2000). A lot of the magma produced in the Earth never reaches the surface but crystallizes as sills, dykes and plutons at different depth (Walker 1963; Gudmundsson 1983; 1984) but occasionally all the right conditions are combined and an eruption takes place. The eruption frequency of a volcano, i.e. the rate of recurrence of the right conditions for magma to reach the surface and cause an eruption, is controlled not only by magma generation but also magma transfer through the crust where the type of plumbing system is important (e.g. Óladóttir et al. 2008; Óladóttir et al. Manuscript 2). Several studies have used geochemical variation to decipher geometry, number and sizes of magma chambers as well as plumbing system changes beneath active volcanoes such as Vesuvius, Mt Cameroon, Hekla, Piton de la Fournaise, Mt Etna and Katla (Cortini and Scandone 1982; Fitton et al. 1983; Sigmarsson et al. 1992; Albarede 1993; Condomines et al. 1995; Óladóttir et al. 2008). Here we present major and trace element data of basaltic eruptions from Grímsvötn, Bárdarbunga and Kverkfjöll covering the last ~7.6 ka, obtained through detailed tephra sampling and analyses from measured soil sections around the Vatnajökull ice cap. The magmatic evolution of the three volcanic systems is examined and speculations on the structure of the plumbing systems beneath the central volcanoes are presented.

6.3 Geological context

The three volcanic systems considered here, Grímsvötn, Bárdarbunga and Kverkfjöll, are partly located under the NW-part of the Vatnajökull ice cap in SE Iceland. The central volcanoes of Grímsvötn and Bárdarbunga are close to the assumed centre of the Icelandic mantle plume (Wolfe et al. 1997) and part of the Eastern Volcanic Zone (EVZ), but Kverkfjöll is part of the Northern Volcanic Zone (NVZ) and its central volcano lies farther from the centre of the plume (Wolfe et al. 1997; Fig. 1). Holocene activity of the ice covered part of the systems is characterised by phreatomagmatic activity and all the volcanic systems produce basalts of tholeiitic composition but negligible silicic formations or tephra are known

(Steinthórsson 1977; Jakobsson 1979; Thordarson and Self 1993; Óladóttir et al. Manuscript 1&2).

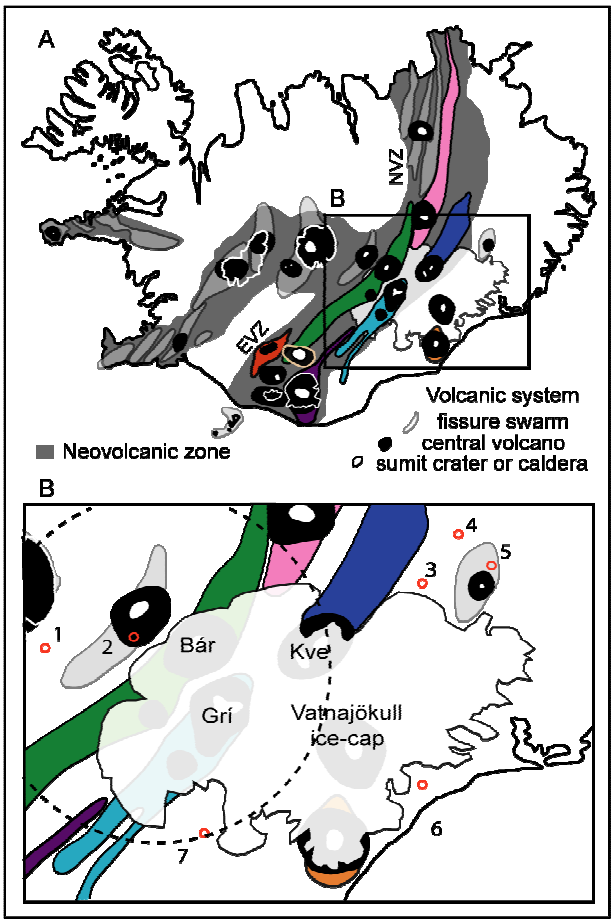

Figure 1 A) The neovolcanic zone and volcanic systems in Iceland concentrating on three volcanic systems: Grímsvötn in sky blue, Bárdarbunga in green and Kverkfjöll in blue. Other volcanic systems of significance for the study are shown in colours: Hekla in red, Katla in violet, Torfajökull in tan, Askja in rose and Öræfajökull in orange. B) Area of study and location of measured and sampled soil sections. Seven soil profiles have been measured and sampled, located around the Vatnajökull ice cap: 1: Hreysiskvísl; 2: Nýidalur; 3: Hraukahreppur; 4: Kárahnjúkar; 5: Snæfell; 6: Steinadalur and 7: Núpsstadarskógar. Circle indicates location of mantle plume at 125 km depth (Wolfe et al. 1997). Abbreviations are as follows: EVZ Eastern Volcanic Zone; NVZ Northern Volcanic Zone; Bár Bárdarbunga central volcano; Grí Grímsvötn central volcano; Kve Kverkfjöll central volcano. Modified after Jóhannesson and Sæmundsson (1998) and Thordarson and Larsen (2007).

During historical time (the last ~1100 years) the Grímsvötn volcanic system has been the most active, Bárdarbunga the second to third alongside Hekla but no historical eruption is known from the Kverkfjöll system (Thordarson and Höskuldsson 2002; Thordarson and Larsen 2007). This order of activity appears also to hold throughout the Holocene and several prehistoric tephra from Kverkfjöll were found (Óladóttir et al. Manuscript 2). Although Grímsvötn has erupted most frequently no data exist on the production rates of the three volcanic systems during the Holocene. However, evidence points toward more wide-spread tephra layers, hence larger eruptions, occurring at Bárdarbunga than Grímsvötn, indicating similar or higher magma production rates at Bárdarbunga than Grímsvötn (Óladóttir et al. Manuscript 2). Additionally more fissure eruptions are known from Bárdarbunga than Grímsvötn (e.g. Vilmundardóttir et al. 2000; Thordarson and Larsen 2007)

Several geophysical studies have been applied for deciphering the internal structure of Grímsvötn central volcano. Gravity and magnetic studies (Gudmundsson and Milsom 1997; Gudmundsson and Högnadóttir 2007) as well as teleseismic inspection (Alfaro et al. 2007) reveal a magma chamber of approximately 10 km^3 at ~3 km depth underneath the central volcano (Alfaro et al. 2007). Measured uplift in Grímsvötn due to inflation prior to the 1998 eruption followed

by subsidence after the eruption is also thought to be related to pressure drop in the assumed magma chamber (Sturkell et al. 2003).

The internal structure of Bárdarbunga central volcano is not as well studied but gravity data are taken to indicate a high density body at depth (Gudmundsson and Högnadóttir 2007). Such bodies are often interpreted as cumulates of gabbro from an overlying magma chamber (e.g. Melengreu et al. 1999; Ablay and Kearey 2000). Bárdarbunga has been one of the most seismically active volcanoes in Iceland showing an abrupt increase in activity since 1974. In 1996 a large earthquake took place in SW Bárdarbunga that migrated towards the Gjálp eruption site, midway between Bárdarbunga and Grímsvötn, this has been interpreted as lateral magma flow from a high level magma chamber beneath Bárdarbunga (Einarsson et al. 1997). Pagli et al. (2007) also relate deflation observed on InSAR data after the Gjálp eruption as a result of a pressure release in an underlying magma chamber. However, geochemical data do not support Bárdarbunga provenance for the magma erupted at Gjálp but rather magma originating at Grímsvötn (Sigmarsson et al. 2000).

The Kverkfjöll central volcano contains two calderas and has not yet enjoyed the attention of the geophysicists but a considerable geothermal activity associated with the northern caldera (Björnsson and Einarsson 1990) points towards the existence of a shallow magma intrusion or a magma chamber.

6.4 Methods

Field work and sample preparation

Samples were taken from tephra, down to less than 1 mm in thickness, from seven soil profiles around the Vatnajökull ice cap, within 30 km from the ice margin (Fig 1b). In total, 921 samples were prepared for thin sections by hand sieving. The 125 µm size fraction was preferred for the 100 µm thick polished thin sections for in-situ measurement in order to have big enough tephra grains for trace element analyses but supplemented if necessary by the 63 and/or 250 µm size fraction.

Analytical techniques

Major element analyses - Electron Microprobe

Electron probe microanalyses (EPMA) of glasses were performed on a WDS Cameca SX100 at the Laboratoire Magmas et Volcans (LMV), Clermont-Ferrand, France. The instrument was calibrated on natural and synthetic mineral standards and glasses. The analytical conditions

used are 15 kV accelerating voltage and 8 nA beam current with a beam diameter of preferably 20 µm but 10 µm where grains were too small. The counting time was 10 s for Na, Ca, Ti, P and Si; 20 s for Mg and Al; 30 s for Mn and finally 40 s for Fe and K, adding up to a total analyses time of 3 min and 40 s for each spot. For felsic grains the beam current was reduced to 4 nA to reduce Na loss and beam diameter had to be reduced to either 10 or 5 µm due to grain size (Óladóttir et al. Manuscript 1). Raw data were corrected by the X-PHI correction procedure (Merlet 1994). Drift and accuracy were assessed by analyzing the international glass standard A99 (Kilauea basalt glass; Jarosewich et al. 1979; Thornber et al. 2002) several times during each analytical session (Óladóttir et al. Manuscript 1).

At least five fresh sideromelane glass grains from each tephra sample were measured. If the analysed points did not show homogeneous major element composition or yielded totals lower than 96.5%, additional analyses were performed in order to have at least 5 homogeneous point analyses with acceptable totals for average calculations (further discussion Óladóttir et al. Manuscript 1).

Trace element analyses with ICP-MS Laser ablation

Trace element concentrations were analysed at Utrecht University, Netherlands, with a Micromass Platform ICP behind a Geolas 193 nm eximer laser ablation system. The laser energy was 9-12 J/cm^2, the pulse repetition rate 10 Hz and the laser beam size 60 µm. Accuracy and overall performance was estimated from repeated analyses of the international glass standard BCR-2G (Colombia River basalt; Wilson 1997; Óladóttir et al. Manuscript 1).

Point analyses were usually made on the 5 grains from each sample previously analysed by the electron microprobe. In a few cases, only 3 grains were analysed due to lack of large enough grains, and up to 7 grains were analysed in samples of heterogeneous major element composition. Weighted mean was calculated from the analysed points representing the trace element composition of a given tephra sample.

6.5 Results

Major elements

In total, major elements were analysed in 921 samples by the electron microprobe from 749 tephra units. Thereof 671 units are of basaltic composition with 79% or 528 units from the subglacial Vatnajökull volcanoes; Grímsvötn, Bárdarbunga and Kverkfjöll. Grímsvötn tephra accounts for 280 tephra units or 53% of the Vatnajökull tephra, Bárdarbunga has produced 214 or 41% and Kverkfjöll is the least active volcanic system of the three with only 34 tephra

units or 6%. The remaining basaltic tephra is mostly from the Katla volcanic system (16%) and the last 5% are from Hekla and unidentified sources; these layers will not be considered any further here. Criteria of fingerprinting for correlating a given tephra to a specific volcano are discussed in Óladóttir et al. (Óladóttir et al. Manuscript 1).

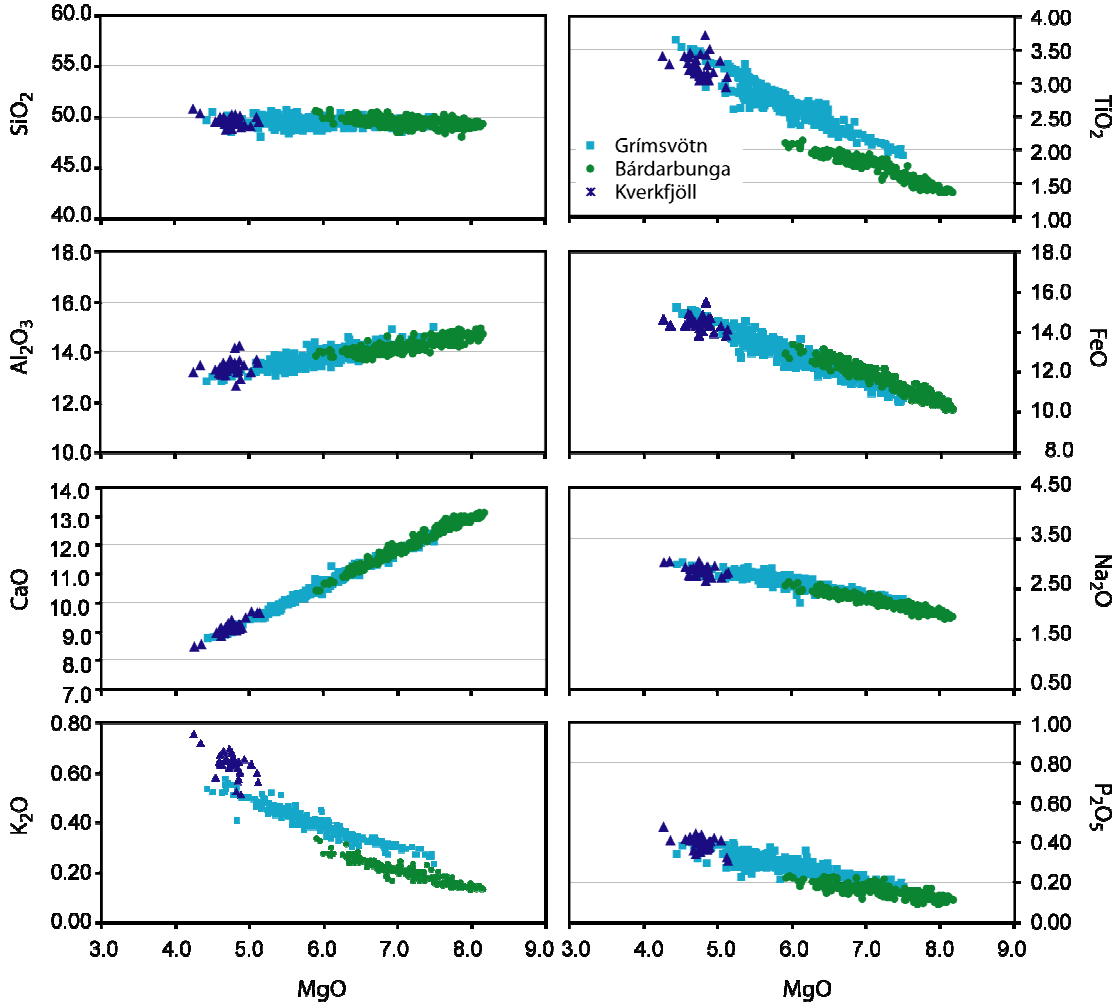

Figure 2 Major element concentrations obtained with EPMA plotted as function of that of MgO. Sky blue squares show tephra with a Grímsvötn composition, green circles Bárdarbunga and blue triangles show Kverkfjöll results. Basalts from all three volcanic systems show liquid-lines-of-descent characteristic for tholeiites but potassium and titanium variations permit to identify different magma roots for each volcano. Analytical error is smaller than the symbol size.

Bárdarbunga produces the least evolved magma (MgO 5.91-8.17 wt%) of the three systems, followed by Grímsvötn (MgO 4.45-7.49 wt%) and Kverkfjöll produces the most evolved magma (MgO 4.26-5.13 wt%; Fig. 2, Table 1). Significant but subtle variations are observed in major element compositions with time (Fig. 3). Grímsvötn yield magma with an average K_2O value of 0.39 wt% and MgO value of 5.92 wt% but during the first ~4200 years, the average K_2O value is 0.37 wt% (range 0.23-0.53 wt%), and the MgO average value is 6.11 wt% (range 4.71-7.49 wt%). Following this period the magma becomes slightly more evolved

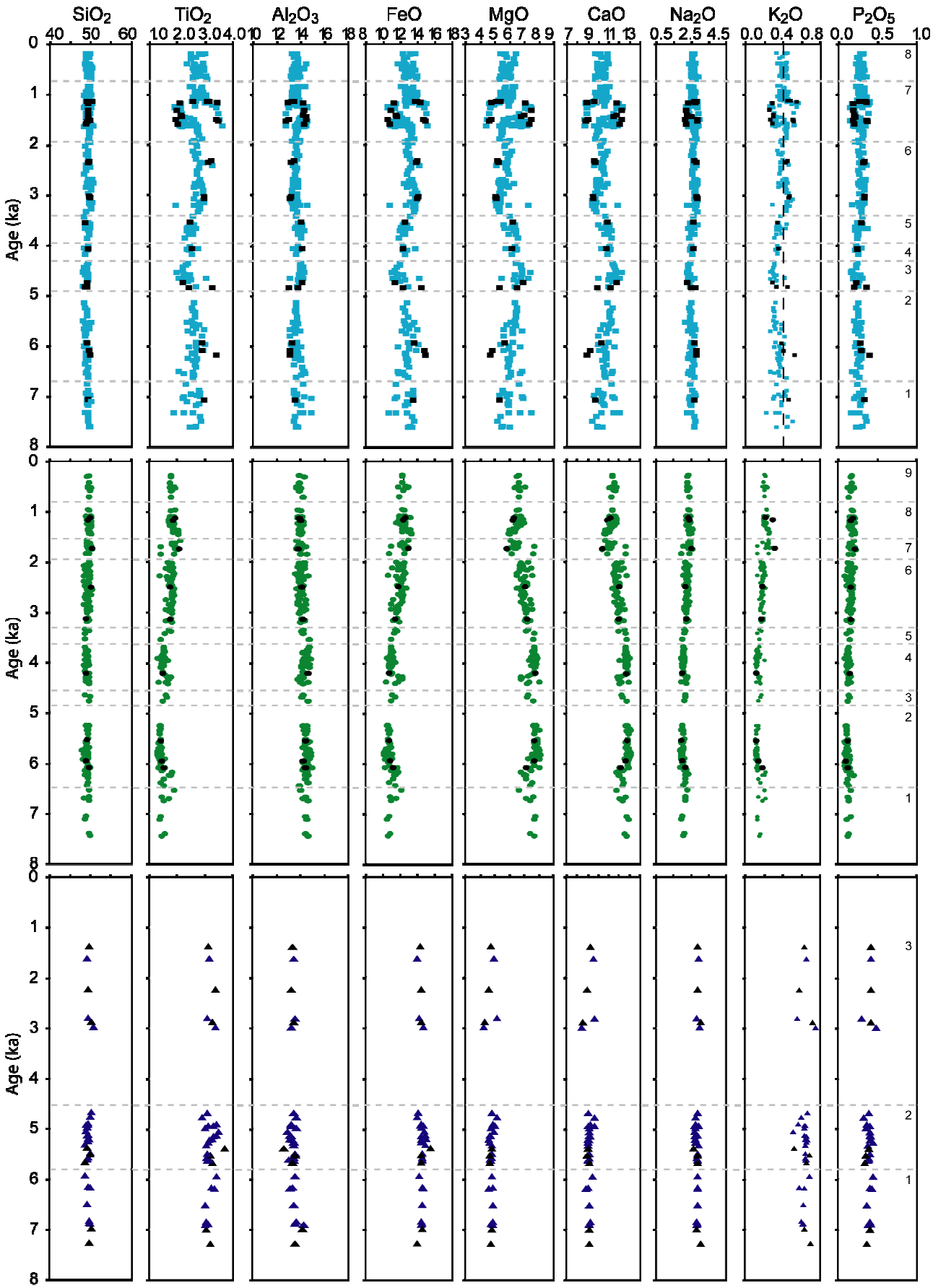

Figure 3 Major element composition plotted against age in thousand years (ka). Age is calculated from soil accumulation rate (Óladóttir et al. Manuscript 2). Analytical error is smaller than the size of symbols. Same symbols as

in Fig. 2 except black symbols represent samples analysed for trace elements concentrations. Activity of each volcanic system is divided into time periods based on observed repose periods shown with broken grey lines and numbered from oldest to youngest period. Grímsvötn shows eight different activity periods, Bárdarbunga nine and Kverkfjöll three. Black broken vertical line in Grímsvötn K_2O shows division in G-I and G-II (G-I<0.4 K_2O<G-II).

during ~750 years with an average K_2O value of 0.42 wt% (range 0.36-0.50 wt%), and an average MgO concentration of 5.60 wt% (range 5.14-6.28 wt%). The next 900 years show again somewhat less evolved magma, although more evolved than those produced during the first ~4200 years, with average of K_2O and MgO of 0.40 and 5.71 wt%, respectively (range 0.34-0.45 and 5.18-6.15 wt%, respectively). The following ~700 years show that Grímsvötn have produced simultaneously two different chemical compositions, both the least (K_2O and MgO average 0.33 and 6.62 wt%, respectively) and most (K_2O and MgO average 0.47 and 5.24 wt%, respectively) evolved basalts erupted from Grímsvötn during the 7600 years under consideration. Similar compositional range is observed before 7 ka but the division in two groups is not as clear as it is from ~1.7-1 ka and the volcanic activity was not nearly as high. The remaining ~1 ka shows major element composition between the two extremes observed in the preceding 700 years with a K_2O and MgO average of 0.40 and 5.90 wt%, ranging from 0.34-0.46 and 5.32-6.48 wt%, respectively. This composition is similar to that formed during the 900 years before the formation of the two extremes.

Bárdarbunga produces basalts with an average composition of 0.19 wt% K_2O and MgO of 7.19 wt% (Fig. 3). During the first ~1300 years the composition scatters with a K_2O range of 0.15-0.23 wt%, averaging at 0.19 wt%, and the MgO value ranges from 6.75-7.80 wt%, with an average of 7.36 wt%. The next ~2800 years are characterised by the least evolved magma produced by the volcanic system, the composition remains stable showing K_2O value close to 0.15 wt% although a few eruptions produced more evolved magma extending the range from 0.12 to 0.23 wt%, the MgO value for the same time period has an average of 7.72 wt% (range 6.86-8.16 wt%). The following ~1200 years show slightly more evolved magma with an average K_2O and MgO value of 0.20 and 7.07 wt%, respectively, (range 0.15-0.24 and 6.60-7.64 wt%, respectively). During 500 years, from 1.8-1.3 ka, the Bárdarbunga volcanic system produced the most evolved basalt observed during the 7.6 ky studied here, with an average value of K_2O of 0.25 wt% (range 0.15-0.33 wt%) and a MgO average value of 6.45 wt% (range: 5.91-7.77 wt%). The remaining ~1000 years show slightly less evolved magma composition but still more evolved than the ~1200 year long period preceding the 500 years. During this time the K_2O average is 0.23 wt% and MgO 6.67 wt%.

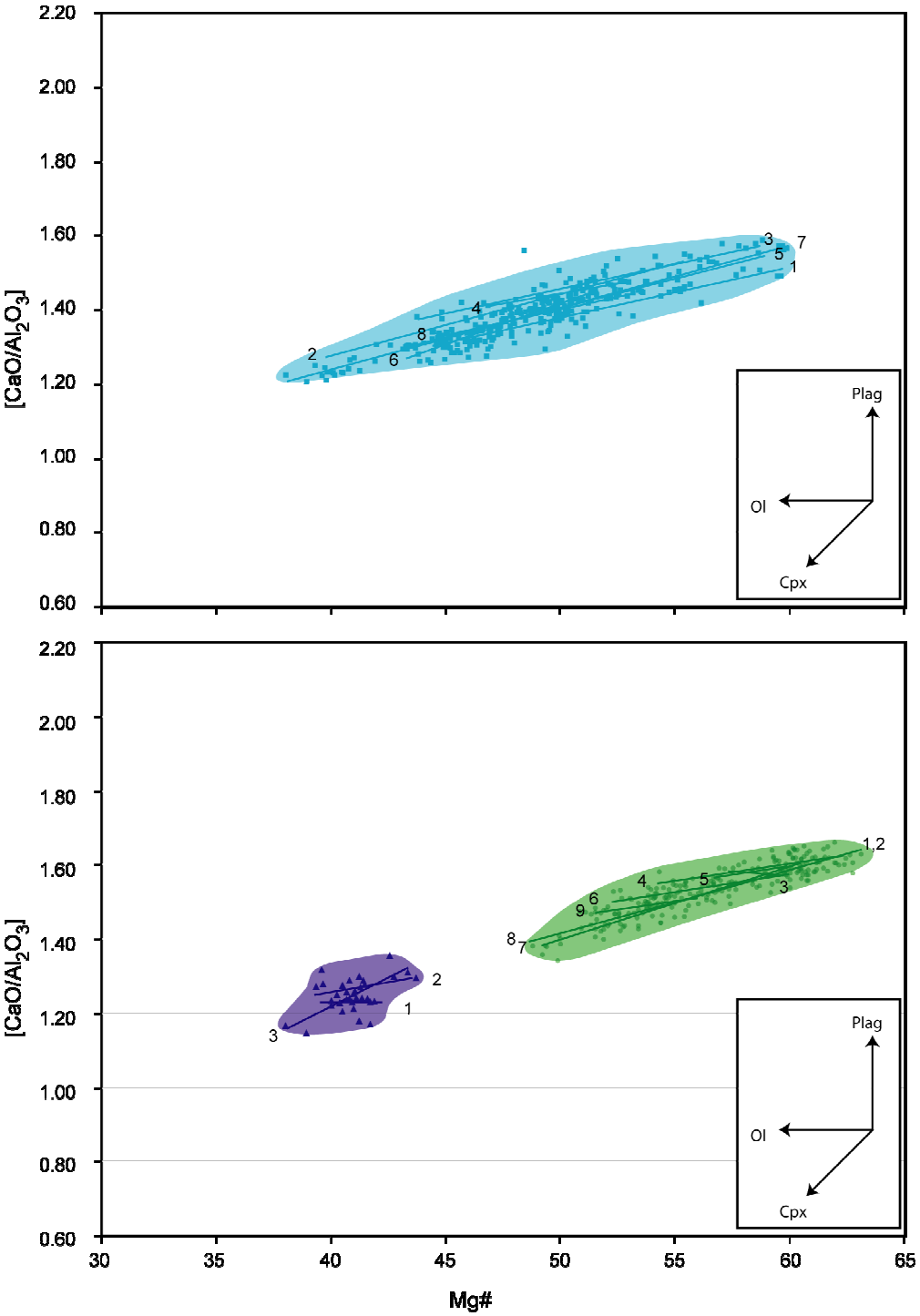

Figure 4 Molar $[CaO]/[Al_2O_3]$ versus Mg#. Compositional fields of the volcanic systems are shown in sky blue, green and blue indicating Grímsvötn, Bárdarbunga and Kverkfjöll, respectively. Inside each compositional field there are numbered lines; representing different time periods (see Fig. 3). Vectors shown in the inset indicate effects of fractional crystallisation of clinopyroxene (Cpx), olivine (Ol) and plagioclase (Plag) on the derived melt composition. The eight different time periods in Grímsvötn display identical slopes indicating similar evolution pattern controlled by Cpx crystallisation. Bárdarbunga shows two main evolution trends, one controlled by Cpx crystallisation and removal (1, 2, 7, 8), and a second one showing increased role of Plag fractionation (4, 5, 6, 9). Kverkfjöll produce more evolved magma with liquid-lines-of-decent indicating stronger role for Cpx fractionation (relative to plag) with time (see text for further discussion). Two sigma error is 3%. Mg# is calculated from the molar proportions of MgO and FeO where FeO is calculated from the total FeO* using the weight ratio $Fe_2O_3/FeO=0.15$.

Kverkfjöll produce the most evolved magma of the three volcanic systems with an average K_2O value of 0.63 wt% (range 0.51-0.75 wt%). The time prior to ~4.7 ka is characterised by production of magma of a similar composition with an average of 0.62 wt% K_2O and an MgO value of 4.78 wt%. However, several eruptions during this time period do produce magma with considerably less evolved magma showing K_2O concentrations as low as 0.51 wt%. Following these ~2900 years a repose period of ~1700 years is observed and the first two eruptions after the repose show the most evolved magma observed during the 7.6 ky under consideration in this study, with K_2O concentration of 0.75 and 0.71 wt%. The following two eruptions show less evolved magma than the average value before, or K_2O values from 0.56-0.57 wt%, but the last two observed eruptions show values close to the average again or 0.65 and 0.62 wt%.

Although the chemical composition produced by the three volcanic systems varies slightly with time these variations are not the principal characteristics of their activity, but rather the irregular repose periods between eruptions. The division into time periods based on repose in activity is shown with grey horizontal broken lines on Fig. 3 and numbered on the right hand side of the figure. Grímsvötn magma is thus divided into eight activity periods; Bárdarbunga has nine and Kverkfjöll three (see Table 2). These periods are indicated with matching numbered lines in Fig. 4 where the molar $[CaO]/[Al_2O_3]$ versus Mg# is shown. The overall variability of Grímsvötn magma composition shows a $[CaO]/[Al_2O_3]$ range from 1.23-1.56 and an Mg# range of 38.1-59.8, whereas Bárdarbunga has somewhat narrower range from 1.35 to 1.65 $[CaO]/[Al_2O_3]$ and Mg# range from 48.7 to 63.0. Kverkfjöll, the least active volcanic system of the three (Óladóttir et al. Manuscript 2.; Fig. 3), has the tightest range of $[CaO]/[Al_2O_3]$ from 1.15 to 1.33 and the Mg# is in the range of 38.1-43.8.

Table 1 Major and trace element compositions samples from Bárdarbunga, Grímsvötn (G-I and G-II) and Kverkfjöll

	Bárdarbunga									
Log#	***Hrau5***	***Hrau19***	***Sau42***	***Kár30***	***Hrau5***	***Sau54***	***Sau67***	***S3-12***	***Sau110***	***S3-29***
Age	***5960***	***5550***	***4220***	***6090***	***5960***	***3140***	***2510***	***1170***	***1134***	***1740***
wt%										
SiO_2	48.90	49.16	49.11	49.70	49.19	48.94	50.21	49.44	50.01	50.55
TiO_2	1.34	1.42	1.52	1.54	1.64	1.77	1.78	1.89	1.94	2.09
Al_2O_3	14.47	14.51	14.71	14.31	13.96	14.31	14.17	14.09	13.94	13.83
FeO	10.25	10.73	10.69	11.23	11.59	11.42	11.81	12.39	12.63	12.89
MnO	0.18	0.21	0.20	0.18	0.23	0.21	0.25	0.22	0.22	0.22
MgO	8.17	7.76	7.83	7.25	7.14	7.26	7.14	6.32	6.35	5.91
CaO	13.01	12.86	12.70	12.18	12.08	11.92	11.93	10.89	11.15	10.38
Na_2O	1.91	1.97	2.00	2.18	2.14	2.26	2.21	2.42	2.37	2.56
K_2O	0.14	0.14	0.14	0.20	0.19	0.20	0.20	0.31	0.24	0.33
P_2O_5	0.11	0.13	0.15	0.13	0.11	0.17	0.17	0.18	0.20	0.22
Total	98.47	98.90	99.06	98.88	98.26	98.45	99.88	98.13	99.04	98.98
ppm										
V	289	306	345	319	334	357	370	337	351	354
Cr	267	205	285	127	87	117	115	38	34	23
Ni	88	73	100	72	62	80	80	46	46	42
Rb	3.2	3.0	3.0	4.1	4.2	4.0	4.4	6.8	4.6	7.2
Sr	143	142	142	138	161	154	155	151	149	154
Y	18.5	16.7	22.8	21.0	21.0	24.3	26.3	31.0	24.8	28.1
Zr	56.4	51.1	65.6	70.7	70.1	81.0	87.1	112.5	87.6	107.7
Nb	6.0	6.0	6.4	7.3	8.5	7.8	8.2	9.9	8.4	10.5
Cs	0.044	0.039	-	0.045	0.045	-	-	0.072	0.057	0.093
Ba	26.9	27.3	28.0	36.6	39.0	36.9	39.0	53.5	42.3	54.0
La	4.65	4.48	5.05	5.95	6.15	6.38	6.52	9.00	7.03	9.05
Ce	11.5	11.9	9.4	15.7	15.7	16.1	17.0	21.3	18.2	22.2
Pr	1.70	1.60	1.88	2.10	2.15	2.34	2.42	3.06	2.50	3.10
Nd	7.25	8.32	9.32	9.88	10.03	11.81	11.61	14.22	12.88	14.05
Sm	2.35	2.54	2.71	3.07	3.13	3.39	3.48	4.15	3.53	4.00
Eu	0.85	0.98	1.02	1.07	1.07	1.17	1.22	1.40	1.27	1.27
Gd	2.45	2.46	2.78	2.98	3.15	3.22	3.28	4.44	3.53	3.94
Dy	3.40	3.24	4.71	3.97	3.71	4.78	5.17	5.90	4.65	5.26
Er	1.80	1.82	2.56	2.29	2.15	2.71	2.95	3.52	2.57	3.05
Yb	2.01	1.99	2.53	2.41	2.45	2.68	2.91	3.43	2.71	3.07
Lu	0.259	0.278	0.406	0.350	0.281	0.395	0.472	0.510	0.371	0.442
Hf	1.32	1.48	2.00	1.98	2.05	2.32	2.43	3.36	2.50	3.09
Ta	0.310	0.348	0.480	0.504	0.445	0.561	0.558	0.720	0.650	0.708
Pb	0.396	0.365	0.413	0.628	0.565	0.540	0.507	0.700	0.790	0.967
Th	0.323	0.307	0.338	0.536	0.415	0.421	0.501	0.950	0.617	0.917
U	0.130	0.100	0.110	0.166	0.148	0.146	0.153	0.277	0.207	0.310
[CaO/Al_2O_3]	1.64	1.61	1.57	1.55	1.57	1.51	1.53	1.41	1.45	1.36
Mg#	62.7	60.4	60.7	57.6	56.5	57.2	56.0	51.8	51.5	49.2
La/Yb	2.32	2.25	2.00	2.47	2.51	2.38	2.24	2.62	2.59	2.95
Rb/Y	0.17	0.18	0.13	0.19	0.20	0.16	0.17	0.22	0.19	0.26
Sr/Th	443	461	420	258	388	365	309	159	242	168

Table 1 Continued

	Grímsvötn G-I										
Log#	***Nups15°***	***Stein24***	***Nups18***	***Sau105***	***Stein22***	***Sau97***	***Hrau31***	***Hrau30****	***Sau50***	***Sau44***	***Hrau6***
Age	***1510***	***1330***	***1590***	***1180***	***1420***	***1450***	***4740***	***4840***	***3550***	***4070***	***5950***
wt%											
SiO_2	49.55	49.44	49.11	49.42	49.48	49.39	49.17	48.86	48.77	49.38	49.22
TiO_2	1.95	2.00	2.02	2.10	2.15	2.16	2.21	2.44	2.48	2.54	2.91
Al_2O_3	14.54	14.32	14.37	14.29	14.29	14.51	14.13	13.87	14.09	14.14	13.30
FeO	10.61	10.97	10.85	11.25	11.51	11.59	11.47	12.33	12.56	12.34	13.64
MnO	0.19	0.23	0.18	0.19	0.15	0.15	0.22	0.19	0.15	0.20	0.21
MgO	7.46	7.46	7.32	7.04	6.98	6.81	6.96	6.51	6.27	6.15	5.67
CaO	12.26	12.26	12.05	11.80	11.72	11.50	11.73	11.15	10.91	10.79	10.30
Na_2O	2.18	2.23	2.23	2.37	2.30	2.51	2.31	2.51	2.66	2.64	2.72
K_2O	0.27	0.26	0.29	0.30	0.31	0.30	0.30	0.33	0.35	0.35	0.38
P_2O_5	0.19	0.19	0.21	0.19	0.21	0.22	0.24	0.21	0.30	0.25	0.29
Total	99.22	99.36	98.62	98.95	99.11	99.16	98.73	98.40	98.53	98.80	98.64
ppm											
V	304	303	294	334	320	349	326	355	367	355	394
Cr	225	258	191	172	155	130	173	102	149	82	52
Ni	70	79	62	72	63	62	66	55	54	44	38
Rb	5.3	5.2	5.5	5.9	6.2	6.7	5.7	6.3	7.3	6.7	7.1
Sr	225	213	209	216	217	216	216	216	211	208	209
Y	21.2	20.0	19.2	25.6	23.5	26.4	22.7	24.2	29.4	26.5	29.2
Zr	89.3	85.0	82.5	108.5	100.9	114.5	100.4	107.3	128.9	121.1	131.6
Nb	10.4	10.2	9.5	10.9	10.8	11.7	11.2	12.8	12.9	13.2	15.4
Cs	0.059	0.051	0.057	-	0.055	-	0.062	0.063	-	-	0.090
Ba	51.6	51.3	50.1	54.7	56.8	58.3	54.4	61.4	65.1	64.4	73.9
La	8.56	8.08	7.76	8.75	9.16	9.41	8.65	9.53	10.73	10.35	11.60
Ce	21.5	20.5	20.1	22.6	22.9	23.4	22.1	24.5	26.5	26.0	28.5
Pr	2.91	2.93	2.90	3.08	3.28	3.31	3.06	3.43	3.70	3.53	3.97
Nd	14.71	13.93	13.39	14.73	15.78	16.09	14.47	16.41	18.45	17.36	19.71
Sm	3.91	3.73	3.68	3.93	4.31	4.70	3.99	4.43	4.75	4.73	5.31
Eu	1.43	1.37	1.46	1.37	1.52	1.67	1.50	1.50	1.65	1.75	1.97
Gd	3.46	3.55	3.59	3.90	4.11	4.27	4.17	4.18	4.53	4.48	5.20
Dy	4.20	4.12	4.06	5.35	4.71	5.40	4.69	4.95	6.08	5.47	6.28
Er	2.22	2.16	2.12	2.75	2.52	2.72	2.46	2.51	3.21	2.83	3.17
Yb	2.13	2.23	2.08	2.60	2.47	2.59	2.50	2.63	3.02	2.85	2.99
Lu	0.324	0.313	0.292	0.373	0.354	0.392	0.320	0.363	0.478	0.427	0.433
Hf	2.34	2.38	2.36	3.09	2.86	3.38	2.48	2.86	3.65	3.23	3.27
Ta	0.650	0.675	0.675	0.728	0.734	0.766	0.707	0.800	0.937	0.808	0.897
Pb		0.698	0.625	0.746	0.761	0.803	0.650	0.819	0.797	0.820	0.885
Th	0.600	0.568	0.546	0.661	0.713	0.738	0.591	0.640	0.773	0.758	0.787
U	0.187	0.225	0.179	0.213	0.232	0.233	0.175	0.240	0.278	0.231	0.247
[CaO/Al_2O_3]	1.53	1.56	1.52	1.50	1.49	1.44	1.51	1.46	1.41	1.39	1.41
Mg#	59.7	58.9	58.7	56.9	56.1	55.3	56.1	52.7	51.3	51.2	46.7
La/Yb	4.02	3.63	3.73	3.37	3.71	3.64	3.46	3.62	3.56	3.63	3.88
Rb/Y	0.25	0.26	0.29	0.23	0.26	0.26	0.25	0.26	0.25	0.25	0.24
Sr/Th	375	375	382	327	305	293	365	337	273	275	266

Table 1 Continued

	Grímsvötn G-II						
Log#	***Kár30***	***Nups66***	***Snæ111***	***Nups65***	***Hrau30****	***Sau109***	***Kár126***
Age	***6090***	***3530***	***7070***	***3520***	***4840***	***1150***	***1140***
wt%							
SiO_2	49.78	49.93	49.59	49.86	49.17	49.76	49.30
TiO_2	2.91	2.96	2.96	2.98	3.04	3.07	3.13
Al_2O_3	13.14	13.15	13.61	13.25	13.14	13.48	13.36
FeO	14.71	14.04	13.52	14.10	14.19	13.78	14.05
MnO	0.20	0.19	0.20	0.20	0.26	0.23	0.28
MgO	4.87	5.11	5.38	5.10	5.58	5.28	5.61
CaO	9.22	9.48	9.72	9.48	10.08	9.73	9.68
Na_2O	2.79	2.85	2.68	2.82	2.78	2.71	2.84
K_2O	0.40	0.46	0.46	0.47	0.40	0.46	0.46
P_2O_5	0.30	0.34	0.33	0.34	0.32	0.35	0.34
Total	98.31	98.52	98.46	98.62	98.96	98.84	99.05
ppm							
V	459	384	385	407	405	417	378
Cr	35	14	68	12	32	62	54
Ni	31	24	41	24	35	41	32
Rb	9.3	9.5	8.2	9.6	8.4	10.0	8.9
Sr	164	207	188	216	222	219	213
Y	39.7	32.9	30.9	34.4	32.2	39.4	30.8
Zr	155.1	152.9	136.3	159.5	150.5	177.7	146.4
Nb	16.5	15.4	15.4	16.6	16.5	18.2	17.6
Cs	0.103	0.089	0.090	0.106	0.064	0.083	0.104
Ba	74.7	80.7	71.9	84.6	77.7	84.6	80.8
La	13.17	12.92	12.28	13.63	12.45	14.38	13.20
Ce	32.2	31.9	30.7	33.9	31.0	35.8	33.8
Pr	4.63	4.30	4.40	4.80	4.30	4.90	4.64
Nd	21.57	21.58	19.60	22.74	21.79	23.73	21.81
Sm	5.96	5.55	5.40	6.24	5.60	6.22	5.88
Eu	2.03	1.98	1.73	2.06	2.00	2.10	1.96
Gd	6.20	5.87	5.51	6.07	5.71	6.20	5.78
Dy	7.73	6.59	6.31	7.18	6.54	8.11	6.49
Er	4.27	3.48	3.57	3.69	3.42	4.32	3.41
Yb	4.33	3.54	3.36	3.72	3.61	4.23	3.38
Lu	0.651	0.490	0.498	0.510	0.487	0.635	0.482
Hf	4.30	4.13	3.54	4.29	3.93	4.95	3.86
Ta	1.057	1.000	0.972	1.120	1.100	1.200	1.080
Pb	1.067	1.200	1.048	1.140	0.950	1.111	1.064
Th	1.167	1.067	0.982	1.106	1.000	1.166	1.040
U	0.357	0.353	0.341	0.359	0.275	0.350	0.333
[CaO/Al_2O_3]	1.28	1.31	1.30	1.30	1.39	1.31	1.32
Mg#	41.1	43.4	45.6	43.3	45.3	44.7	45.7
La/Yb	3.04	3.65	3.66	3.66	3.45	3.39	3.91
Rb/Y	0.23	0.29	0.27	0.28	0.26	0.25	0.29
Sr/Th	141	194	191	195	222	188	205

Table 1 Continued

	Grímsvötn G-II							
Log#	***Kár89***	***S3-7***	***Kár125***	***Sau73***	***Nups15°***	***Sau17***	***S3-11***	***Nups17***
Age	***2360***	***1150***	***1140***	***2330***	***1510***	***6180***	***1165***	***1540***
wt%								
SiO_2	49.44	49.42	49.38	49.68	49.96	50.04	49.41	49.32
TiO_2	3.14	3.14	3.18	3.23	3.40	3.42	3.43	3.47
Al_2O_3	13.19	13.32	13.38	13.53	13.08	13.17	12.98	12.83
FeO	13.83	13.99	14.23	13.97	14.66	14.98	14.30	14.90
MnO	0.49	0.23	0.27	0.22	0.25	0.25	0.23	0.24
MgO	5.26	5.16	5.25	5.18	4.81	4.71	4.78	4.68
CaO	9.73	9.62	9.60	9.61	9.03	8.91	8.93	8.88
Na_2O	2.83	2.77	2.81	2.73	2.85	2.81	2.74	2.88
K_2O	0.43	0.48	0.47	0.45	0.51	0.53	0.55	0.52
P_2O_5	0.33	0.32	0.35	0.34	0.36	0.41	0.36	0.37
Total	98.68	98.44	98.93	98.94	98.91	99.25	97.70	98.09
ppm								
V	445	382	415	407	394	443	411	426
Cr	27	50	63	39	23	10	29	9
Ni	35	30	36	28	22	26	29	20
Rb	9.4	10.0	10.4	9.6	9.7	11.1	11.4	10.3
Sr	219	210	189	224	212	198	216	217
Y	38.1	37.8	34.1	35.7	37.0	42.5	42.2	34.9
Zr	168.0	174.0	138.0	166.7	167.3	199.0	197.0	163.3
Nb	17.0	17.7	16.6	18.6	19.3	20.4	20.4	19.9
Cs	-	0.104	0.108	0.095	0.099	0.134	0.123	0.114
Ba	79.5	85.9	91.5	86.1	87.9	98.7	95.9	89.4
La	13.37	14.81	13.37	14.81	15.19	16.89	17.05	14.51
Ce	33.7	35.5	31.2	35.9	37.0	41.7	41.3	37.9
Pr	4.67	5.03	4.30	5.05	5.23	5.68	5.98	5.18
Nd	23.00	23.10	19.69	25.15	25.70	25.63	27.53	24.92
Sm	6.61	6.25	5.23	6.18	6.39	6.98	7.40	6.40
Eu	2.10	2.10	1.88	2.23	2.21	2.32	2.34	2.38
Gd	6.20	6.57	5.69	6.65	6.37	6.82	7.57	6.69
Dy	7.90	7.29	6.52	7.47	7.62	8.80	8.51	7.12
Er	4.28	4.10	3.60	3.89	4.12	4.64	4.91	3.73
Yb	4.13	3.95	3.71	3.94	3.83	4.69	4.45	3.68
Lu	0.600	0.550	0.524	0.554	0.524	0.635	0.700	0.508
Hf	4.40	4.65	3.70	4.46	4.58	5.41	5.55	4.21
Ta	1.200	1.200	0.957	1.325	1.325	1.400	1.475	1.260
Pb	1.067	1.200	1.175	1.030	1.131	1.265	1.414	1.160
Th	1.100	1.275	1.180	1.125	1.225	1.265	1.496	1.140
U	0.303	0.391	0.343	0.340	0.385	0.431	0.453	0.378
[CaO/Al_2O_3]	1.34	1.31	1.30	1.29	1.26	1.23	1.25	1.26
Mg#	44.5	43.8	43.7	43.9	40.9	39.9	41.3	39.8
La/Yb	3.24	3.75	3.61	3.76	3.97	3.60	3.83	3.94
Rb/Y	0.25	0.26	0.30	0.27	0.26	0.26	0.27	0.29
Sr/Th	199	165	160	199	173	157	144	190

Table 1 Continued

					Kverkfjöll						
Log#	***Kv1***	***Sau5***	***Kv2-2***	***Kv2-1***	***Kári113***	***Hrau20***	***Kár8***	***Sau76***	***Sau60***	***Hrau13***	***Hrau22***
Age		***6990***			***1380***	***5520***	***7280***	***2240***	***2880***	***5680***	***5390***
wt%											
SiO_2	48.73	50.19	49.23	50.09	49.68	49.92	49.84	49.43	50.25	48.72	49.24
TiO_2	2.64	3.06	3.08	3.10	3.11	3.20	3.20	3.38	3.27	3.28	3.69
Al_2O_3	13.82	14.12	13.50	13.68	13.33	13.52	13.49	13. 27	13.45	13.36	12.62
FeO	13.08	14.42	14.65	14.60	14.18	14.40	13.83	14.35	14.31	14.36	15.45
MnO	0.25	0.24	0.23	0.28	0.32	0.24	0.24	0.31	0.23	0.32	0.23
MgO	5.38	4.82	4.80	4.77	4.75	4.66	4.74	4.56	4.34	4.69	4.82
CaO	10.09	9.15	9.15	9.24	9.22	8.94	9.09	8.96	8.52	9.16	9.02
Na_2O	2.77	2.80	2.39	1.94	2.90	2.89	3.03	2.90	3.02	2.88	2.64
K_2O	0.61	0.62	0.64	0.66	0.62	0.68	0.69	0.57	0.71	0.65	0.52
P_2O_5	0.27	0.40	0.44	0.40	0.41	0.35	0.36	0.41	0.41	0.34	0.38
Total	97.65	99.84	98.10	98.76	98.52	98.80	98.52	98.14	98.51	97.75	98.61
ppm											
V	398	434	414	411	344	393	419	464	326	379	404
Cr	20	19	15	15	10	13	20	26		22	14
Ni	34	27	25	24	23	20	25	27	7	27	20
Rb	12.7	13.4	12.6	13.5	12.0	11.4	13.4	14.1	13.4	11.4	11.0
Sr	241	229	230	237	232	228	232	209	248	219	207
Y	30.0	36.4	34.3	35.4	36.6	31.6	34.4	41.3	33.9	25.8	34.8
Zr	160.2	188.5	175.6	180.8	184.2	168.7	182.4	208.7	187.9	139.3	171.8
Nb	17.5	19.3	18.5	19.0	21.4	18.5	19.1	22.4	22.6	19.4	22.4
Cs	0.151	0.120	0.137	0.143	0.119	0.120	0.138	0.153	0.150	0.150	0.118
Ba	113.6	113.7	113.4	118.9	102.0	108.6	119.3	105.8	121.8	108.7	98.7
La	15.13	17.03	16.30	17.31	16.68	16.24	17.35	18.45	17.20	14.76	16.40
Ce	36.2	40.3	39.6	42.5	41.2	36.7	41.7	45.3	41.7	37.0	42.5
Pr	4.88	5.46	5.43	5.90	5.81	5.07	5.65	6.17	5.80	5.05	5.74
Nd	22.64	26.51	25.50	26.83	27.67	23.34	27.37	28.49	26.45	22.45	26.43
Sm	5.56	6.30	6.20	6.90	7.14	6.44	6.85	7.61	7.02	5.62	6.76
Eu	1.89	2.16	2.17	2.37	2.48	1.98	2.19	2.47	2.39	1.81	2.33
Gd	5.40	6.42	6.17	6.67	6.93	6.48	6.48	6.94	6.55	5.60	6.79
Dy	6.58	7.90	7.68	7.96	7.70	6.75	7.06	8.76	7.13	5.53	7.27
Er	3.10	3.85	3.62	4.04	3.97	3.66	3.81	4.58	3.64	2.90	3.99
Yb	3.13	3.96	3.67	4.14	3.82	3.32	3.62	4.56	3.46	2.89	3.89
Lu	0.464	0.560	0.517	0.638	0.530	0.515	0.500	0.681	0.498	0.383	0.529
Hf	4.35	5.10	4.45	4.95	4.83	4.40	4.85	5.84	4.49	3.43	4.55
Ta	1.150	1.238	1.270	1.333	1.396	1.300	1.389	1.533	1.317	1.107	1.290
Pb	1.224	1.400	1.073	1.389	1.297	1.167	1.325	1.422	1.367	1.175	1.350
Th	1.317	1.540	1.386	1.567	1.390	1.400	1.471	1.533	1.533	1.213	1.171
U	0.429	0.442	0.433	0.470	0.457	0.383	0.468	0.503	0.439	0.393	0.440
[CaO/Al_2O_3]	1.33	1.18	1.23	1.23	1.26	1.20	1.23	1.09	1.15	1.25	1.30
Mg#	46.4	41.3	40.9	40.8	41.4	40.6	41.9	36.2	39.0	40.8	39.7
La/Yb	4.83	4.30	4.45	4.19	4.37	4.90	4.80	4.05	4.96	5.11	4.22
Rb/Y	0.42	0.37	0.37	0.38	0.33	0.36	0.39	0.34	0.39	0.44	0.32
Sr/Th	183	149	166	152	167	163	157	136	162	181	177

Table 1 Continued

	Gígöldur		*Unidentified*							
Log#	***D1-2***	***D4-1***	***HKV5***	***Nups4***	***Snæ111***	***Snæ112***	***SnæS1***	***SnæS3***	***SnæS4***	***Hrau60***
Age			***770***	***1190***	***7070***	***7080***				***3490***
wt%										
SiO_2	48.57	49.02	49.01	49.93	49.03	49.21	48.76	48.30	48.57	49.65
TiO_2	1.17	1.35	1.13	3.47	1.82	2.00	1.80	1.88	1.84	1.81
Al_2O_3	14.81	14.34	14.99	13.01	14.76	14.36	14.69	14.68	14.64	14.31
FeO	10.19	11.33	10.42	15.01	10.90	11.39	10.76	11.21	10.75	11.58
MnO	0.22	0.18	0.20	0.22	0.15	0.13	0.19	0.16	0.17	0.20
MgO	8.14	7.33	7.94	4.68	7.54	7.18	7.44	7.40	7.47	6.77
CaO	13.31	12.31	12.76	8.88	12.18	11.76	12.29	12.22	12.12	11.58
Na_2O	1.81	2.06	2.08	2.90	2.19	2.41	2.20	2.25	2.28	2.39
K_2O	0.10	0.18	0.14	0.57	0.23	0.24	0.23	0.24	0.23	0.26
P_2O_5	0.11	0.13	0.07	0.37	0.14	0.15	0.16	0.18	0.20	0.18
Total	98.43	98.23	98.76	99.04	98.95	98.84	98.51	98.53	98.28	98.73
ppm										
V	309	343	293	378	316	309	317	305	305	310
Cr	406	260	323	20	271	131	253	236	224	71
Ni	105	81	93	22	85	66	84	86	76	52
Rb	2.1	3.9	1.3	11.0	4.1	4.3	4.2	4.8	4.3	5.3
Sr	117	142	120	208	209	194	199	195	192	183
Y	19.9	21.6	16.2	36.8	21.5	22.1	20.3	19.7	20.4	18.0
Zr	49.8	59.1	34.7	177.1	83.6	88.6	80.4	83.9	83.4	80.5
Nb	3.8	5.6	2.7	20.7	8.5	8.5	8.3	8.7	8.3	10.2
Cs	-	-	-	0.107	0.069	0.055	0.047	0.052	-	0.068
Ba	18.3	34.7	17.3	95.9	45.6	46.5	43.8	48.1	43.5	47.9
La	3.14	4.84	2.57	16.19	7.27	7.37	6.81	7.30	7.08	8.56
Ce	8.8	11.9	6.8	38.1	18.5	18.7	18.3	18.6	17.8	22.6
Pr	1.37	1.76	1.05	5.44	2.70	2.65	2.58	2.61	2.63	2.96
Nd	6.83	8.82	5.28	25.82	12.67	12.98	12.20	12.37	12.62	13.86
Sm	2.44	2.61	1.90	6.80	3.72	3.59	3.50	3.29	3.42	3.35
Eu	0.88	1.03	0.80	2.26	1.31	1.35	1.32	1.27	1.30	1.24
Gd	2.10	2.63	2.10	6.63	3.60	3.63	3.31	3.40	3.37	3.32
Dy	3.92	3.87	3.11	7.56	4.43	4.50	4.11	4.02	4.13	3.78
Er	2.19	2.42	1.89	3.97	2.33	2.37	2.23	2.18	2.10	1.95
Yb	2.32	2.41	2.02	3.90	2.33	2.27	2.11	2.05	2.03	2.07
Lu	0.384	0.374	0.281	0.568	0.293	0.355	0.298	0.293	0.318	0.282
Hf	1.66	1.82	1.19	4.71	2.37	2.40	2.22	2.25	2.14	2.07
Ta	0.311	0.378	0.184	1.433	0.626	0.583	0.557	0.557	0.558	0.620
Pb	0.396	0.485	0.243	1.486	0.603	0.791	0.676	0.851	0.751	0.664
Th	0.254	0.345	0.149	1.341	0.467	0.513	0.460	0.526	0.502	0.540
U	0.069	0.090	0.054	0.437	0.157	0.169	0.155	0.180	0.180	0.210
[CaO/Al_2O_3]	1.63	1.56	1.55	1.24	1.50	1.49	1.52	1.51	1.50	1.47
Mg#	62.7	57.7	61.6	39.7	59.3	57.0	59.3	58.2	59.4	55.2
La/Yb	1.35	2.01	1.24	4.15	3.12	3.25	3.22	3.56	3.48	4.13
Rb/Y	0.10	0.18	0.08	0.30	0.19	0.19	0.21	0.24	0.21	0.30
Sr/Th	461	413	809	155	449	377	433	371	384	340

° and * two trace element compositions in the same tephra, making the total number of analyses shown in the table 26 even though the total analysed sample number is 24 (see page 11)

Trace elements

Trace elements were analysed in 53 samples of which 45 come from Grímsvötn, Bárdarbunga and Kverkfjöll. Of the 45 analysed samples 24 are from Grímsvötn, 10 from Bárdarbunga and 11 from Kverkfjöll (Óladóttir et al. Manuscript 1; Table 1). For several samples the major element composition is not different enough to tell between evolved Grímsvötn magma and Kverkfjöll magma. Hence, trace elements where analysed in many samples that could either have Grímsvötn or Kverkfjöll composition based on major elements alone. The trace element systematic showed that most of these tephra originated from Grímsvötn (Óladóttir et al. Manuscript 1), explaining why most of the samples analysed for trace elements are from Grímsvötn. Moreover, Grímsvötn basalts clearly form two distinct compositional groups; one (named G-II) that has spectra similar to those of Kverkfjöll on a primitive mantle normalised multi-element diagram. These spectra are characterized by a marked depletion in Sr concentrations and a slight High Field Strength Elements (HFSE) enrichment (Fig. 5). The chondrite normalised REE concentrations confirm the similarities between the G-II basalts and those from Kverkfjöll. Nevertheless, the Kverkfjöll basalts have significantly higher Light Rare Earth Element (LREE) concentrations than G-II basalts whereas Heavy Rare Earth Elements (HREE) are indistinguishable in basalts from the two volcanic systems. In contrast, the less evolved basalts from Grímsvötn (named G-I) have trace element spectra of very similar shape as those from Bárdarbunga. The principal difference is higher concentrations in the most incompatible elements in G-I relative to Bárdarbunga, whereas, again, both volcanic systems produce basalts with very similar HREE concentrations (Fig. 5). Each volcanic system thus clearly has distinct trace element ratios while the Grímsvötn magma division in G-I and G-II is only based on differences in concentrations (G-I>Th=0.9>G-II; Fig. 6; Table 1). The concentrations of the most incompatible elements show a three-fold increase in the whole data set (Table 1), and thus amplify the resolving power for identifying the principal magmatic processes from the compositional variability.

Table 2 Age division of activity periods shown in Fig. 3 and 4 for Grímsvötn, Bárdarbunga and Kverkfjöll.

Activity Periods #	*Bárdarbunga Age (ka)*	*Kverkfjöll Age (ka)*	*Grímsvötn Age (ka)*
1	7.6-6.5	7.6-6.0	7.6-6.8
2	6.5-5.3	5.7-4.7	6.6-5.1
3	4.8-4.7	3.0-1.4	4.8-4.4
4	4.4-3.7		4.2-4.0
5	3.5-3.4		3.9-3.4
6	3.2-2.0		3.3-1.9
7	1.8-1.6		1.9-0.8
8	1.5-1.0		0.7-0.0
9	0.7-0.0		

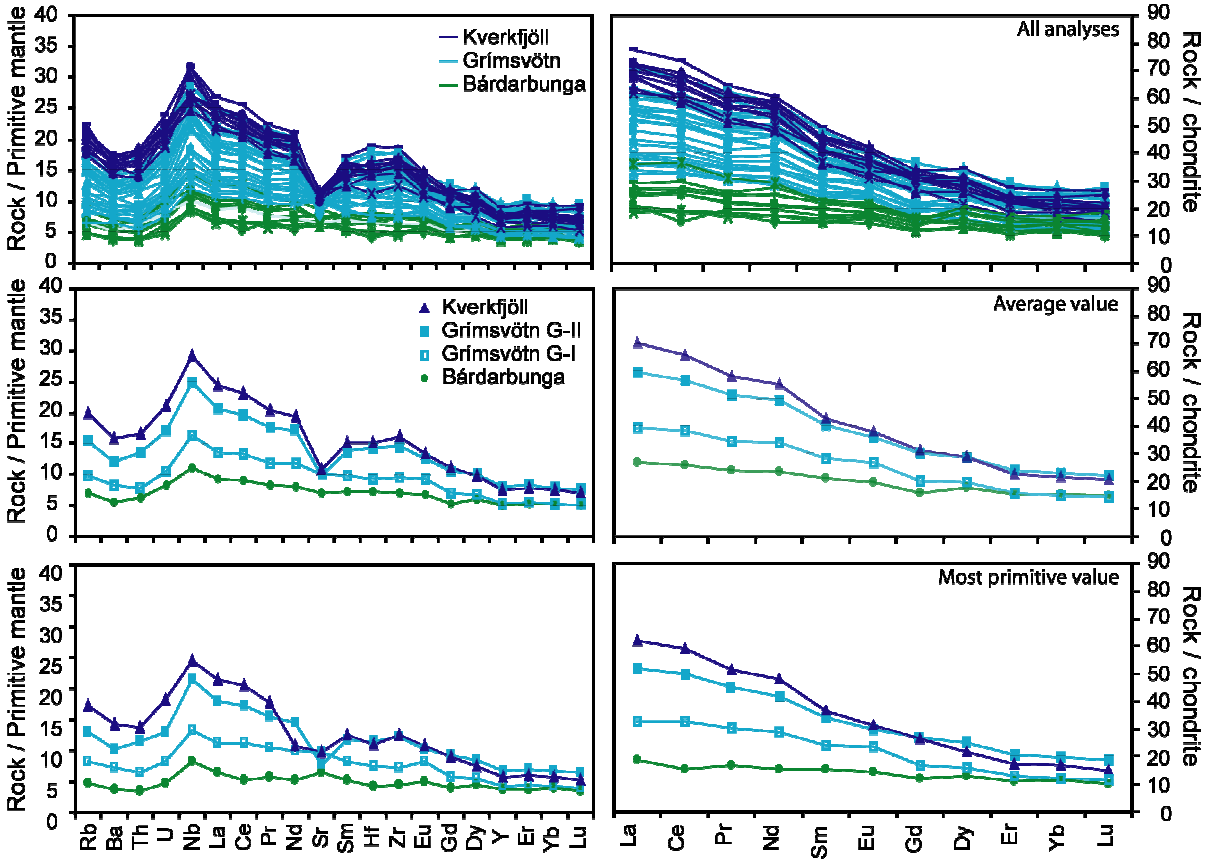

Figure 5 Primitive-mantle normalized multi-element diagrams (to the left; Sun and McDonough 1989) and chondrite normalized REEt (to the right; Sun and McDonough 1989) for Kverkfjöll (blue), Grímsvötn (sky blue) and Bárdarbunga (green). The two uppermost diagrams show results of all analyses obtained, whereas the two in the middle show the average value and the two at the base show the most primitive value of each compositional group. Grímsvötn tephra forms two groups, one that shows a Sr depletion and mimics the Kverkfjöll spectra in all ways (G-II) and another more akin to the Bárdarbunga spectra (G-I). The REE diagram shows LREE enrichment in Kverkfjöll and the G-II Grímsvötn basalt whereas the G-I and Bárdarbunga basalts show less difference between LREE and HREE values when normalised to chondrite. Element order on primitive mantle normalised diagram is from Martin and Sigmarsson (2007).

6.6 Discussion

The Vatnajökull volcanoes produce magma of tholeiitic composition with each of the three volcanic systems producing basalts at somewhat different evolutionary stages despite significant compositional overlap. Bárdarbunga produces the least evolved magma of the three, showing the highest MgO, Ni and Cr concentrations and lowest incompatible element concentration of the three systems, followed by Grímsvötn and the Kverkfjöll basalts are the most evolved (Table 1, Fig. 2, Fig. 7). The true compositional difference between basalts from these three volcanoes can be clearly seen from the concentrations of excluded oxides such as K_2O and TiO_2 for a given MgO concentration, illustrating somewhat different origin of basalts beneath each one of the volcanic system (Fig. 2). This difference is amplified in the trace element compositions that can be used to decipher deep-seated processes at the origin of the different parental magma for each volcanic system. Moreover, at a given volcano the

subtle temporal variations in the major element compositions allow inferences to be drawn on the architecture of the plumbing systems under the central volcanoes.

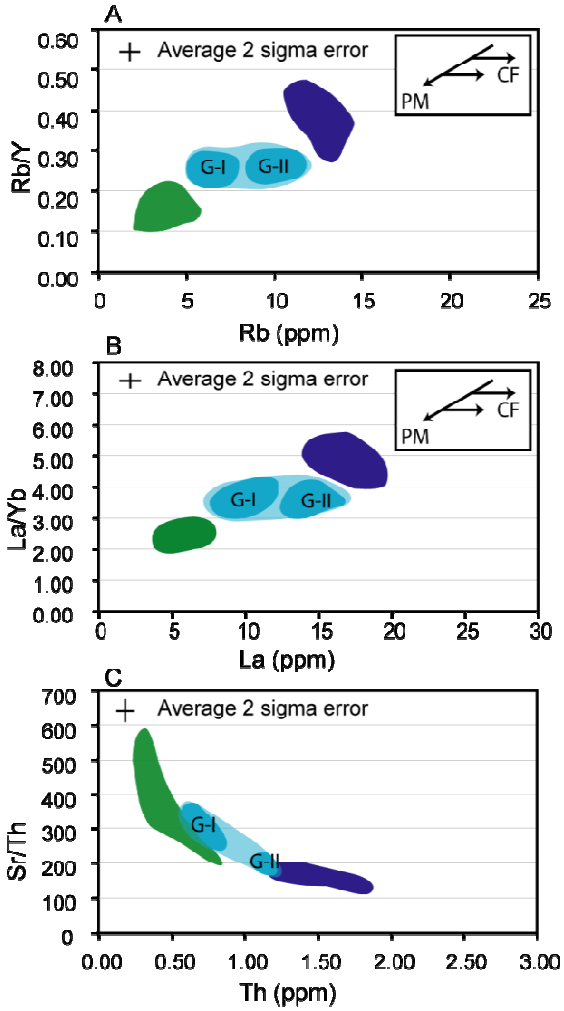

Figure 6 Trace element compositional fields for Grímsvötn (sky blue), Bárdarbunga (green) and Kverkfjöll (blue), shown on three different element ratio plots. The coloured fields show a conservative estimate (enveloping the data and associated 2 sigma error) of trace element composition fields obtained in this study. Grímsvötn magma groups G-I and G-II clearly separates on these plots. The compositional fields of each group are marked with darker sky blue while the whole compositional field of Grímsvötn connects the two groups. *Inset:* Illustration of expected compositional trends caused by crystal fractionation (CF) and partial melting (PM).

Magma origin and evolution – trace element constraints

The evolved basalt composition from Kverkfjöll and its potential link to the underlying mantle plume has been known for decades (Sigvaldason and Steinthórsson 1974), whereas more recent studies, integrating isotope arguments, have inferred significant crustal contamination in the evolved tholeiites of Iceland (e.g. Óskarsson et al. 1982; Hémond et al. 1988; Sigmarsson et al. 1991). Crustal contamination has been examined in details for the Laki 1783-84 basalts, which has a typical G-II composition, and is thought to be dominated by stoping and almost total melting of hydrothermally altered metabasaltic crust (Sigmarsson et al. 1991; Bindeman et al. 2006). For illustrating the importance of crustal contribution to the basalts from the Vatnajökull volcanoes, the behaviour of Ba is scrutinized in Figure 8. The well known fluid-mobile character of Ba makes it an element of choice for tracing the potential composition of the crustal contaminant. From the Ba versus Th concentration plot, it is clear that only the G-I basalts extrapolate through the origin as requested for melts derived from fractional crystallisation only. This is simply due to the fact that the mineral phases extracted contain neither Ba nor Th and will plot at the origin in this diagram. In contrast, best linear-fits through the results from Bárdarbunga, G-II, and Kverkfjöll do not extrapolate through the origin. Instead, these have a common intercept at Ba and Th concentrations equal

to 130 and 2.6 ppm, respectively, corresponding to highly evolved basalt. Further discussion of this contaminant, which may have common characteristics beneath each of the central volcanoes, is outside the scope of this paper and will be discussed elsewhere.

Only the least evolved composition from all volcanoes plot on the fractional crystallisation vector that in turn can be regarded as revised partial melting curve indicating highest melting beneath Bárdarbunga and lowest melting in the roots of Kverkfjöll (Fig. 8). The systematic decrease of incompatible element concentrations from Kverkfjöll basalts, through those from Grímsvötn and to the lowest concentrations in Bárdarbunga, is readily explained by decreasing mantle melting. That is, Kverkfjöll, located farther away from the assumed centre of the mantle plume, produce basalts formed by less mantle melting that in turn may explain lower eruption frequency observed there (Óladóttir et al. Manuscript 2). This idea can be further tested by plotting the concentrations of strongly compatible elements, Ni and Cr, against those of a highly incompatible element, such as Th (Fig. 7). Although little can be affirmed for Kverkfjöll basalts on these diagrams due to dominating effect of fractional crystallisation and crustal contamination (via assimilation-fractional crystallisation (AFC) process), the initial Th values for parental magma composition at both Grímsvötn and Bárdarbunga can be estimated as 0.5 ppm and 0.3 ppm, respectively. If the mantle source is relatively homogeneous beneath the NW Vatnajökull-region, these results strongly indicate significantly higher melting degrees beneath Bárdarbunga. Decreasing La/Yb from Kverkfjöll through Grímsvötn to Bárdarbunga also support the interpretation of increasing melting degrees towards the centre of the mantle plume.

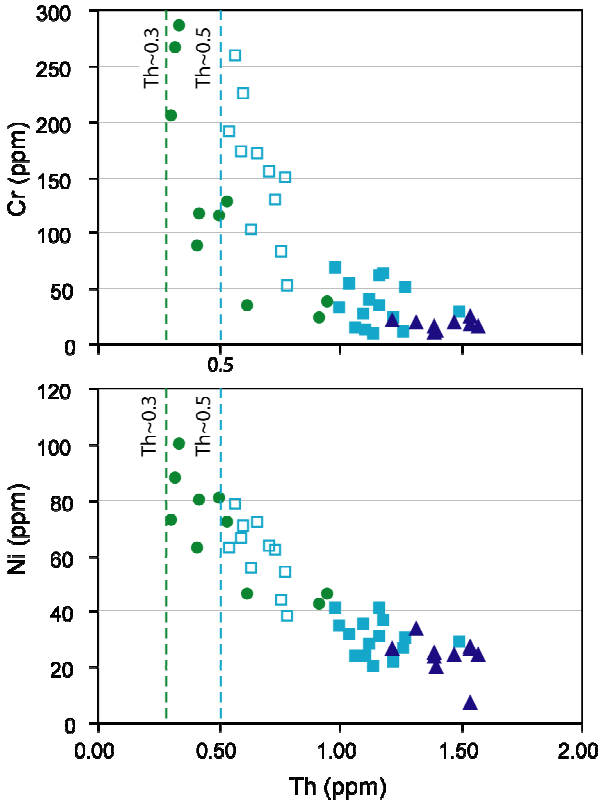

Figure 7 Concentrations of the compatible elements Cr and Ni versus the incompatible Th concentration. The initial Th value for parental magma composition can be estimated as 0.3 ppm in Bárdarbunga and 0.5 ppm in Grímsvötn (broken lines). Colour code as in Fig. 2, G-I is shown with sky blue open squares whereas G-II is shown with filled sky blue squares.

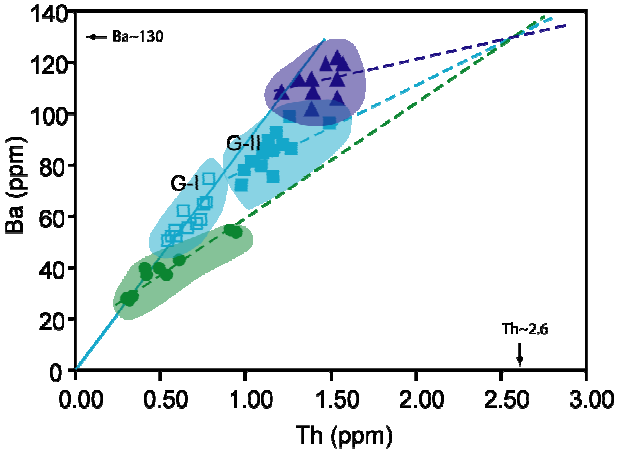

Figure 8 Concentrations of Ba versus Th revealing complex magmatic evolution beneath Vatnajökull volcanoes. Only Grímsvötn G-I is controlled by crystal fractionation alone, having an intercept of a best-fit line at the origin (see text for further discussion). Bárdarbunga, Grímsvötn G-II and Kverkfjöll are all significantly affected by crustal contamination, and their best-fit lines intercepts at Ba and Th close to 130 and 2.6 ppm, respectively (see arrows). This intercepts represent the composition of the crustal contaminant. The most primitive samples from each group (except G-II) plot on the G-I liquid-line-of-decent. This is consistent with increasing mantle melting during the formation of the basalts from Kverkfjöll through Grímsvötn to Bárdarbunga, rather than a common parental magma for all the three volcanoes. According to the location of the three volcanic systems above the assumed centre of the Icelandic mantle plume and on its edge, it is readily understandable that the contaminant appears to be of basaltic composition. High eruption frequency of similar basalts indicates that the magma either lacks time to further differentiate and form acidic magma or that the surrounding country rock is of such elevated temperatures that partial melting of the crust can be high, causing basaltic crustal melt to form rather than silicic one. In this respect it is worth noting that negligible silicic formations are known at these volcanoes and very few tephra with high silica content have been erupted. Compositional fields drawn around data points include 2 sigma SD error of the data points.

The question of mantle homogeneity is fundamental for quantitative estimates of different melting behaviour beneath Vatnajökull and evaluation of possible links between basalt production at depth and eruption frequency observed at surface. Sigmarsson et al. (2000) showed that the historical eruptions of Bárdarbunga and Grímsvötn (G-II compositions) produce basalts with distinct Sr- and O-isotope ratios that may either reflect higher input of metabasaltic crustal melts beneath Grímsvötn or heterogeneous mantle composition. Halldórsson et al. (2008) measured highly variable Sr-isotope ratios in accumulative plagioclase from the large prehistoric lava flows from Bárdarbunga volcanic system, which origin remains unexplained. Before thorough studies of melt inclusions in the most primitive minerals from these volcanic systems, the assessment of mantle homogeneity or heterogeneity must wait further results. Nevertheless, most ratios of highly incompatible elements analyzed in this study (such as Th/U, Ce/Pb, Zr/Hf, Th/Ta, Nb/Ta etc.) are indistinguishable in basalts from the three volcanic systems, and thus support the notion of relative mantle homogeneity. The possibility of a straight link between degree of mantle melting and magma productivity, and hence eruption frequency, can thus be suggested and will be worth examination in further geochemical studies of these basalts. However, changes in the eruption frequency for each volcano is most likely related to the structure of the plumbing system at depth as discussed in next chapter.

Magmatic evolution and plumbing systems - major elements

Based on the molar ratio [CaO]/[Al_2O_3] versus Mg# each volcanic systems shows similar general evolutionary trends when focusing on all the data set or the 7.6 ka being studied (coloured clouds on Fig. 4). However, after dividing the data series from each volcanic system into different activity periods based on repose periods of variable duration (Fig. 3), different evolutionary trends emerge.

Grímsvötn

Grímsvötn is mostly controlled by Cpx crystallisation. It is worth noting that period 7 (~1.9 to ~0.8 ka; Table 2) during which basalts with lowest and highest Mg# are observed corresponds to the episode when magmas of two contrasting compositions were erupted simultaneously from Grímsvötn (Fig. 3).

The less evolved basalt composition, G-I, is likely to originate from further depth than the more evolved G-II basalts, which reflect additional fractionation in colder environment closer to the surface. The G-I composition dominates the first ~4.2 ka or until ~3.4 ka (periods 1-5) although G-II magmas were occasionally erupted as well (Fig. 3). The G-II basalts are principally produced during period 7, possibly in a sill and dyke complex at shallow depth that appears to have played a significant role during the bi-modal magma production beneath Grímsvötn. Just before and after this bi-modal activity (period 7) basalts of intermediate basaltic composition (close to the average of G-I and G-II) dominate the magmatism. Such intermediate basalts are likely to be generated in a small magma chamber that could have formed in the lower part of the hypothetical sill and dyke complex but Michaut and Jaupart (2005) have demonstrated that a sill and dyke complex often merge and form a magma chamber. This sill and dyke complex has been occasionally active during the whole 7.6 ka as suggested by the sporadic G-II eruptions. Judging from the magmatic evolution (slightly increasing K_2O), the magma chamber in which the mixing of G-I and G-II basalts took place became progressively dominant from ~3.4 ka until ~1.9 ka when period 7 starts and the two magma types are contemporaneously erupted either leaving the magma chamber inactive or dominating it. Interestingly, the eruption frequency of Grímsvötn is highest during period 7 (Óladóttir et al. Manuscript 2), which concurs with results from Katla volcano showing highest eruption frequency when magma plumbing system is dominated by a sill and dyke complex (Óladóttir et al. 2008). The magmatic pressure of the G-I basalts from below seems to have been such that these basalts found a way from deeper magma source straight to the surface, either by-passing the sill and dyke complex or destroying part of it. At the same time

the sill and dyke complex is forced to erupt, possibly from increased magma pressure at depth that finally "cleaned out the pipes" and made space for the actual magma chamber to form (period 8 to present day; see conceptual model in Fig. 9).

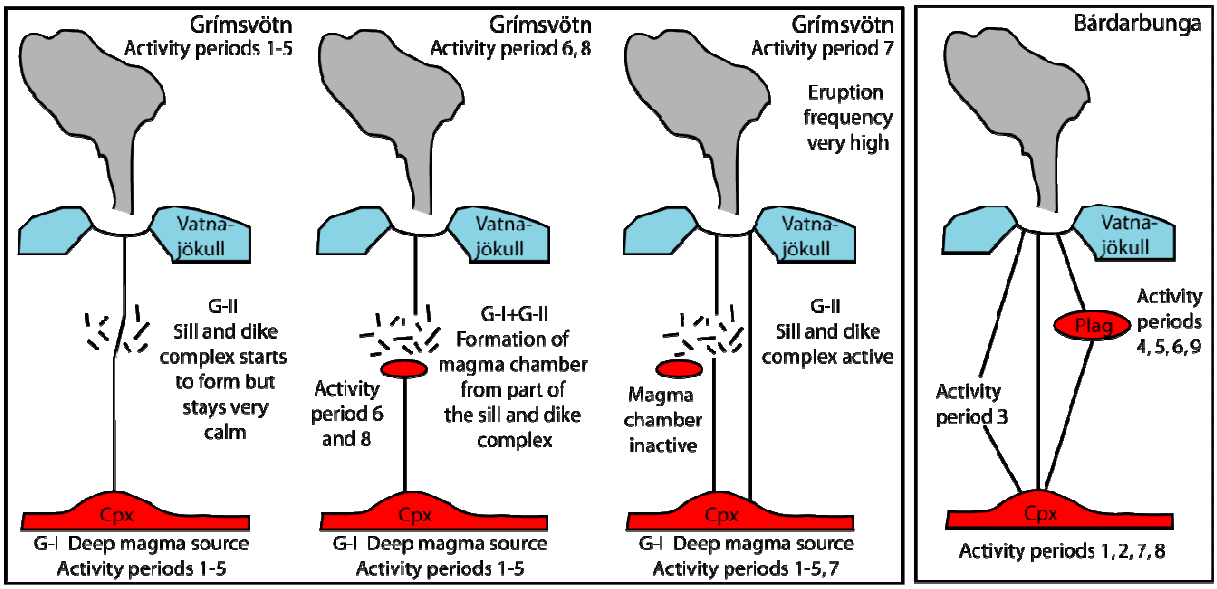

Figure 9 A conceptual evolutionary model for Grímsvötn and Bárdarbunga based on major and trace element composition. Grímsvötn mainly produce magma of G-I composition during the first ~4.2 ka with individual eruptions showing G-II composition, i.e. influence of crustal contamination. With time part of the sill and dyke complex responsible for G-II compositional magma merges to a magma chamber producing magma with a composition intermediate between G-I and G-II. From ~1.7-1 ka, when the eruption frequency in Grímsvötn was at its peak, the magma chamber becomes inactive or is completely over taken by G-I magma from the deep magma source and the sill and dyke complex is activated by high pressures from below. After this high eruption frequency period the magma chamber producing magma with an average composition of G-I and G-II becomes ruling again. Bárdarbunga shows an evolution from a deep magma source until ~5.2 ka when a shallow magma chamber has formed. It remains active until ~2 ka when the eruption frequency of Bárdarbunga peaks and magma from the deep magma source becomes ruling again. The activity remains high during 1 ky or until 1 ka when the magma chamber is reactivated. During the time period 2-1 ka the magma production in the mantle plume seems to have been so high that the plumbing systems beneath Grímsvötn and Bárdarbunga were more or less cleaned out resulting in eruptions of magma generated deep down in the plumbing systems.

Bárdarbunga

Bárdarbunga produces basalts forming two distinct evolutionary trends, one controlled by important Cpx fractionation (lines no. 1, 2, 7, 8; Fig. 4) and the other slightly more influenced by Plag fractionation (lines no. 4, 5, 6, 9; Fig. 4).

Increased Cpx fractionation relative to plagioclase from basalts of similar composition most likely reflects higher pressure of crystallization (Kinzler and Grove 1992a; b), and this fact can be utilized to infer two different magma sources for Bárdarbunga basalt. During periods 1 and 2 the magma erupted comes from the deeper magma source, whereas during period 3 the liquid-line-of-descent reflects the change from the stable deep magma source to a shallower magma storage zone (magma chamber, sill and dyke complex etc.) that was established during period 4 and remained active until the end of period 6. During period 7-8

the deeper magma source takes over again and controls the magmatic evolution in Bárdarbunga until the end of period 8 or until ~1 ka. Interestingly these periods, 7-8, cover the millennia showing the highest eruption frequency observed in Bárdarbunga during the 7.6 ka covered in this study (Óladóttir et al. Manuscript 2). Thousand years ago the eruption frequency decreased again and the shallow magma chamber becomes reactive (see conceptual model Fig. 9). Thus, there appears to be fundamental differences in what controls the eruption frequency at a rift-related volcanic system such as Bárdarbunga, compared with those experiencing little or no rifting, Grímsvötn and Katla, where the type of plumbing system is more controlling in the latter.

Kverkfjöll

Kverkfjöll is by far the least active volcanic system of the three with only 34 identified tephra units making it difficult to speculate much about temporal changes in the plumbing system beneath the volcano. It produces the most evolved magma and the differentiation trends in Figure 4 indicate increasing relative proportion of Cpx fractionation through time. This does not necessarily suggests changing magma source depth as the evolved magma is approaching its eutectic point, crystallising all three phases, Cpx, Ol and Plag together, and relatively larger proportions of Cpx with time. This observation suggests that Kverkfjöll may be in a waning stage unless reactivated with more primitive basalt from depth.

6.7 Conclusions

Results from major and trace element analyses of tephra with provenance in Grímsvötn, Bárdarbunga and Kverkfjöll have revealed difference in magmatic evolution between the volcanic systems located close to the assumed centre of the Icelandic mantle plume. Magma from the volcanic systems shows different amount of mantle melting, Kverkfjöll magma shows the least melting and Bárdarbunga the most. Grímsvötn basalts form two compositional groups, one named G-II that shows Sr depletion and mimics the Kverkfjöll spectra on primitive mantle normalised multi element diagram in all ways. Chondrite normalised REE concentrations further confirm the similarities between G-II and Kverkfjöll. The other Grímsvötn group is named G-I and is more akin to the Bárdarbunga spectra on primitive mantle normalised multi element diagram and chondrite normalised REE concentrations. However each volcanic system has distinct trace element ratios while the Grímsvötn division in G-I and G-II is only based on differences in concentrations.

The magmatic evolution of the three volcanic systems is controlled by crystal fractionation of clinopyroxene, plagioclase and olivine in different ratios but additionally all systems are influenced by crustal contamination from a contaminant of an evolved basaltic composition. However the G-I part of Grímsvötn magma is not affected by the contamination but is controlled solely by crystal fractionation.

The plumbing system beneath Grímsvötn has evolved from a simple plumbing system characterised by magma travelling straight to the surface from a deep magma source although a sill and dyke complex has started to form early in the evolutionary process. Part of this sill and dyke complex has then evolved to a small magma chamber active during ~1.4 ka but was taken over by very high magmatic inflow from below during the period 1.7-1 ka, when the sill and dyke complex is reactivated along with the simple plumbing system during the period of highest eruption frequency observed in Grímsvötn.

Bárdarbunga also shows a simple plumbing system to begin with or until ~5.2 ka. After that a magma chamber evolves that stays active during 1.4 ka or until the eruption frequency of Bárdarbunga reaches a maximum ~2-1 ka and the plumbing system is overfilled with magma originated in the deep magma source characterising the magmatic composition during this period. When the magma chamber is reactivated the eruption frequency lowers again and magma characterised by more plagioclase fractionation becomes dominating.

According to these models the actual plumbing systems beneath both Grímsvötn and Bárdarbunga are characterised by active magma chambers. However, a fundamental difference is observed in what controls eruption frequency in Bárdarbunga, a rift-related volcanic system, and Grímsvötn, a volcanic system experiencing little or no rift, where the type of plumbing system is of much more importance for frequency control in the latter one.

6.8 Acknowledgement

This paper is based on a PhD-study at the Laboratoire Magmas et Volcans (LMV), CNRS-Université Blaise Pascal in Clermont-Ferrand and the University of Iceland. It was financed by the Icelandic Science Foundation, Landsvirkjun, Eimskip and Research Fund of the University of Iceland, the French government student's grant and the French-Icelandic collaboration programme, Jules Verne. Jean-Luc Devidal at LMV and Paul Mason and Gijs Nobbe at the Utrecht University are genuinely thanked for their help during and after EPMA and ICP-MS laser ablation analyses.

6.9 Reference

Ablay GJ, Kearey P (2000) Gravity constraints on the structure and volcanic evolution of Tenerife, Canary Islands. Journal of Geophysical Research-Solid Earth 105(B3):5783-5796.

Albarede F (1993) Residence Time Analysis of Geochemical Fluctuations in Volcanic Series. Geochimica Et Cosmochimica Acta 57(3):615-621.

Alfaro RB, Brandsdóttir B, Rowlands DP, White RS, Gudmundsson MT (2007) Structure of the Grímsvötn central volcano under the Vatnajökull icecap, Iceland. Geophysical Journal International 168:863-876.

Bindeman IN, Sigmarsson O, Eiler J (2006) Time constraints on the origin of large volume basalts derived from O-isotope and trace element mineral zoning and U-series disequilibria in the Laki and Grimsvotn volcanic system. Earth and Planetary Science Letters 245(1-2):245-259.

Björnsson H, Einarsson P (1990) Volcanoes beneath Vatnajökull, Iceland: Evidence from radio echo-sounding, earthquake and jökulhlaups. Jökull 40:147-168.

Condomines M, Tanguy JC, Michaud V (1995) Magma Dynamics at Mt Etna - Constraints from U-Th-Ra-Pb Radioactive Disequilibria and Sr Isotopes in Historical Lavas. Earth and Planetary Science Letters 132(1-4):25-41.

Cortini M, Scandone R (1982) The Feeding System of Vesuvius between 1754 and 1944. Journal of Volcanology and Geothermal Research 12(3-4):393-400.

Einarsson P, Brandsdóttir B, Gudmundsson MT, Björnsson H, Grönvold K, Sigmundsson F (1997) Center of the Iceland hotspot experiences volcanic unrest. Eos Trans. AGU, 78(35):369.

Fitton JG, Kilburn CRJ, Thirlwall MF, Hughes DJ (1983) 1982 Eruption of Mount Cameroon, West-Africa. Nature 306(5941):327-332.

Grove TL (2000) Origin of Magmas. In: Sigurdsson H (ed) Encyclopedia of Volcanoes. Academic press, San Diego, pp 133-149.

Gudmundsson Á (1983) Form and Dimensions of Dykes in Eastern Iceland. Tectonophysics 95(3-4):295-307.

Gudmundsson Á (1984) Formation of dykes, feeder-dykes, and the intrusion of dykes from magma chambers. Bulletin of Volcanology 47:537-550.

Gudmundsson MT, Milsom J (1997) Gravity and magnetic studies of the subglacial Grímsvotn volcano, Iceland: Implications for crustal and thermal structure. Journal of Geophysical Research-Solid Earth 102(B4):7691-7704.

Gudmundsson MT, Högnadóttir T (2007) Volcanic systems and calderas in the Vatnajökull region, central Iceland: Constraints on crustal structure from gravity data. Journal of Geodynamics 43(1):153-169.

Halldórsson SA, Óskarsson N, Grönvold K, Sigurdsson G, Sverrisdóttir G, Steinthórsson S (2008) Isotopic-heterogeneity of the Thjórsa lava-Implications for mantle sources and crustal processes within the Eastern Rift Zone, Iceland. Chemical Geology 255(3-4):305-316.

Hémond C, Condomines M, Fourcade S, Allegre CJ, Óskarsson N, Javoy M (1988) Thorium, Strontium and Oxygen Isotopic Geochemistry in Recent Tholeiites from Iceland - Crustal Influence on Mantle-Derived Magmas. Earth and Planetary Science Letters 87(3):273-285.

Jakobsson SP (1979) Petrology of recent basalts of the Eastern Volcanic zone, Iceland. Acta Naturalia Islandica 26:1-103.

Jarosewich E, Nelen JA, Borberg JA (1979) Electron microprobe reference samples for mineral analysis. In: Fudali RF (ed) Smithsonian Institution Contributions to the Earth Sciences No. 22. Smithsonian Institution Press, Washington, D.C., pp 68-72.

Jóhannesson H, Sæmundsson K (1998) Geological map of Iceland, 1:500,000. Tectonics. Icelandic Institute of Natural History and Iceland Geodetic Survey, Reykjavík.

Kinzler RJ, Grove TL (1992a) Primary Magmas of Mid-Oceanic Ridge Basalts 1. Experiments and Methods. Journal of Geophysical Research 97(B5):6885-6906.

Kinzler RJ, Grove TL (1992b) Primary Magmas of Mid-Oceanic Ridge Basalts 2. Applications. Journal of Geophysical Research 97(B5):6907-6926.

Martin E, Sigmarsson O (2007) Low-pressure differentiation of tholeiitic lavas as recorded in segregation veins from Reykjanes (Iceland), Lanzarote (Canary Islands) and Masaya (Nicaragua). Contributions to Mineralogy and Petrology 154(5):559-573.

Melengreu B, Lénat J-F, Froger J-L (1999) Structure of Réunion Island (Indian Ocean) inferred from the interpretation of gravity anomalies. Journal of Volcanology and Geothermal Research 88(131-146).

Merlet C (1994) An Accurate Computer Correction Program for Quantitative Electron-Probe Microanalysis. Mikrochimica Acta 114:363-376.

Michaut C, Jaupart C (2005) A new model for crystallisation and differentiation in magma chambers. Eos Trans AGU 86(52), Fall Meet Suppl, V11A-03.

Óladóttir BA, Sigmarsson O, Larsen G, Thordarson T (2008) Katla volcano, Iceland: magma composition, dynamics and eruption frequency as recorded by Holocene tephra layers. Bulletin of Volcanology 70(4):475-493.

Óskarsson N, Sigvaldason GE, Steinthórsson S (1982) A dynamic model of rift zone petrogenesis and the regional petrology of Iceland. Journal of Petrology 23:28-74.

Pagli C, Sigmundsson F, Pedersen R, Einarsson P, Árnadóttir Th, Feigl KL (2007) Crustal deformation associated with the 1996 Gjalp subglacial eruption, Iceland: InSAR studies in affected areas adjacent to the Vatnajokull ice cap. Earth and Planetary Science Letters 259(1-2):24-33.

Sigmarsson O, Condomines M, Fourcade S (1992) A Detailed Th, Sr and O Isotope Study of Hekla - Differentiation Processes in an Icelandic Volcano. Contributions to Mineralogy and Petrology 112(1):20-34.

Sigmarsson O, Karlsson HR, Larsen G (2000) The 1996 and 1998 subglacial eruptions beneath the Vatnajokull ice sheet in Iceland: contrasting geochemical and geophysical inferences on magma migration. Bulletin of Volcanology 61(7):468-476.

Sigmarsson O, Condomines M, Grönvold K, Thordarson T (1991) Extreme Magma Homogeneity in the 1783-84 Lakagígar Eruption - Origin of a Large Volume of Evolved Basalt in Iceland. Geophysical Research Letters 18(12):2229-2232.

Sigvaldason GE, Steinthórsson S (1974) Chemistry of tholeiitic basalts from Iceland and their relation to the Kverkfjöll hot spot. In: Kristjánsson L (ed) Geodynamics of Iceland and the North Atlantic Area. D. Reidel, Dordrecht, Holland, pp 155-164.

Steinthórsson S (1977) Tephra layers in a drill core from the Vatnajökull Ice Cap. Jökull 27:2-27.

Sturkell E, Einarsson L, Sigmundsson F, Hreinsdóttir S, Geirsson H (2003) Deformation of Grímsvötn volcano, Iceland: 1998 eruption and subsequent inflation. Geophysical Research Letters 30(4), 1182, doi:10.1029/2002GL016460.

Sun SS, McDonough WF (1989) Chemical and isotopic systematics of oceanic basalts: Implication for the mantle composition and processes. Geological Society, Special Publications 42:313-345.

Thordarson T, Self S (1993) The Laki (Skaftár-Fires) and Grímsvötn Eruptions in 1783-1785. Bulletin of Volcanology 55(4):233-263.

Thordarson T, Höskuldsson Á (2002) Iceland Terra Publishing, Harpenden, UK, p 200.

Thordarson T, Larsen G (2007) Volcanism in Iceland in historical time: Volcano types, eruption styles and eruptive history. Journal of Geodynamics 43(1):118-152.

Thornber CR, Sherrod DR, Siems DR, Heliker CC, Meeker GP, Oscarsson RL, Kauahikaua JP (2002) Whole rock and glass major-element geochemistry of Kilauea Volcano, Hawaii, near-vent eruptive products: September 1994 through September 2001. In: USGS, open file report 02-17.

Vilmundardóttir EG, Snorrason SP, Larsen G (2000) Geological map of subglacial volcanic area soutwest of Vatnajökull ice cap, Iceland, 1:50.000. In: National Energy Authority and National Power Company, Reykjavík.

Walker GPL (1963) The Breiddalur central volcano, eastern Iceland. The Quarterly Journal of the Geological Society of London 119:29-63.

Wilson SA (1997) The collection, preparation, and testing of USGS reference material BCR-2, Columbia River, Basalt. In: U.S. Geological Survey Open-File Report 98-xxx.

Wolfe CJ, Bjarnason IT, VanDecar JC, Solomon SC (1997) Seismic structure of the Iceland mantle plume. Nature 385(6613):245-247.

7. General conclusions

The main objective of this study was to assess the Holocene eruption history and temporal magma evolution of the NW Vatnajökull volcanoes, Grímsvötn, Bárdarbunga and Kverkfjöll through studies of tephra. The location of these volcanoes, close to the assumed centre of the Icelandic mantle plume, makes them particularly interesting as the relationship between the mantle plume and manifested volcanic activity can be evaluated and compared to volcanic activity elsewhere in Iceland, away from its influence.

The project was divided in three parts each one presented in a paper manuscript. The first was to identify primary tephra and confidently trace its provenance. In the second part the focus was on correlation of tephra around the Vatnajökull ice cap and estimating the eruption frequency of the three volcanic systems. The third and last part deals with the magma origin of Grímsvötn, Bárdarbunga and Kverkfjöll and its transfer from source to surface through temporal changing plumbing systems. The principal conclusions of the project are as follows:

1) Field observations, combined with chemical composition of tephra, determine primary volcanic or secondary eolian origin of tephra. Major element composition of primary tephra is sufficient for identifying provenance for most basaltic tephra from Grímsvötn, Bárdarbunga and Kverkfjöll by comparing them to a reference compositional field (RCF) made up of published analyses mostly lava flows of known origin within the three volcanic systems. The data obtained during this study significantly improved the RCF. Nevertheless, the chemical composition fields of the three volcanic systems do slightly overlap. The provenance of 85% of the remaining unknown samples, from the overlapping parts of the compositional fields, is confirmed based on their trace element composition. Both major and trace elements RCF provide good indication of tephra provenance and the new analyses of tephra from the last ~7.6 ky have greatly improved knowledge of the compositional range within each volcanic system.

Four major elements, K_2O, TiO_2, MgO and FeO, and their ratios, mostly tells apart tephra from Grímsvötn, Bárdarbunga and Kverkfjöll volcanic systems and three trace element compositional ratios, Rb/Y, La/Yb and Sr/Th further improve fingerprinting of tephra that plot on two overlapping fields. These results demonstrate the usefulness of combined major and trace element analyses in delineating the provenance of basaltic tephra having similar major element composition.

2) The prehistoric eruption history of the ice-covered part of Grímsvötn, Bárdarbunga and Kverkfjöll going back ~7.6 ky has been revealed using correlated tephra stratigraphy based on dated marker tephra layers. Soil accumulation rate (SAR) age calculations and major element chemistry of the volcanic glass provide a record of 348 prehistorical tephra layers, whereof 137, 87 and 18 were erupted in Grímsvötn, Bárdarbunga and Kverkfjöll, respectively.

The ratio of Grímsvötn and Bárdarbunga tephra preserved outside the ice cap during the last 8 centuries of historical time in Iceland was applied to obtain an estimate of the actual eruption frequency in prehistoric time, resulting in a total of 980 eruptions in Grímsvötn, Bárdarbunga and Kverkfjöll during the last ~8000 years. During historical and prehistoric time total number of eruptions on the ice covered part of the Grímsvötn volcanic system is ~560, making it the most active Icelandic volcanic system in terms of eruption frequency. It has two peaked eruption frequency profile showing high frequency 7-6 ka with 56 eruptions per 1000 years and again 2-1 ka when in total 140 eruptions took place. Such increased eruption frequency is also observed in the Bárdarbunga volcanic system, which is the second most active volcanic system with ~350 eruptions during the last ~8000 years. Its frequency profile is two peaked and like Grímsvötn the eruption frequency is highest 2-1 ka but the older peak lags that of Grímsvötn by 1000 years. Both systems show a strong frequency decrease during the last millennium. Kverkfjöll shows considerably less eruption frequency and only ~70 eruptions were inferred during the ~6500 years studied during prehistoric time, which is still significantly higher than historical activity which is none. Kverkfjöll shows highest eruption frequency 7-5 ka but showed some activity during the first 4 ka observed in this study (8-4 ka) and again 3-1 ka although low, 4-32 eruptions per 1000 years.

All three volcanic systems show a lull in eruption frequency between 5 and 2 ka caused by decrease in volcanic activity that is traced to periodic magma generation and delivery from the mantle plume rather than changes in environmental factors such as changing ice load and ice cover. During prehistoric time a 1-3 thousand years age difference is found between frequency peaks above the mantle plume (Grímsvötn and Bárdarbunga) and at volcanoes located farther SW on the non-rifting part of the Eastern Volcanic Zone (EVZ; e.g. Katla). This lag suggests that a significant increase could be expected in volcanism on this part of the EVZ in the future since the highest observed eruption frequency was only 2-1 ka in Grímsvötn and Bárdarbunga.

3) Results from major and trace element analyses of tephra with provenance in Grímsvötn, Bárdarbunga and Kverkfjöll have revealed difference in magmatic evolution between the

volcanic systems located close to the assumed centre of the Icelandic mantle plume. Magma from the volcanic systems shows different amount of mantle melting, Kverkfjöll magma shows the least melting and Bárdarbunga the most. Grímsvötn basalts form two compositional groups, one named G-II that shows Sr depletion and mimics the Kverkfjöll spectra on primitive mantle normalised multi element diagram in all ways. Chondrite normalised REE concentrations further confirm the similarities between G-II and Kverkfjöll. The other Grímsvötn group is named G-I and is more akin to the Bárdarbunga spectra on primitive mantle normalised multi element diagram and chondrite normalised REE concentrations. However each volcanic system has distinct trace element ratios while the Grímsvötn division in G-I and G-II is only based on differences in concentrations. The magmatic evolution of the three volcanic systems is controlled by crystal fractionation of clinopyroxene, plagioclase and olivine in different ratios but additionally all systems are influenced by crustal contamination from a contaminant of an evolved basaltic composition. However the G-I part of Grímsvötn magma is not affected by the contamination but is controlled solely by crystal fractionation.

The plumbing system beneath Grímsvötn has evolved from a simple plumbing system characterised by magma travelling straight to the surface from a deep magma source although a sill and dyke complex has started to form early in the evolutionary process. Part of this sill and dyke complex evolved to a small magma chamber active during ~1.4 ka, from ~3.3-1.9 ka, but was taken over by very high magmatic inflow from below during the period from 1.7-1 ka, when the sill and dyke complex is reactivated along with the simple plumbing system during the period of highest eruption frequency observed in Grímsvötn.

Bárdarbunga also shows a simple plumbing system to begin with or until ~5.2 ka. After that a magma chamber evolves and stays active during 2.4 ka, from ~4.4-2.2 ka, or until the eruption frequency of Bárdarbunga reaches a maximum from ~2-1 ka and the plumbing system overfilled with magma originated in the deep magma source that characterises the melt composition during this period. When the magma chamber is reactivated the eruption frequency lowers again and magma characterised by more plagioclase fractionation becomes dominating.

According to these models the present plumbing systems beneath both Grímsvötn and Bárdarbunga are characterised by active magma chambers. However, a fundamental difference is observed in what controls eruption frequency in Bárdarbunga, a rift-related volcanic system, and Grímsvötn, a volcanic system experiencing little or no rift, where the type of plumbing system is of much more importance for frequency control in the latter one.

This work has improved the scientific knowledge of temporal variations in chemical composition of three volcanic systems and at the same time extended the chemical reference compositional fields for each system. The study has added vast amount of data on eruption behaviour of the NW Vatnajökull volcanoes allowing more precise predictions about their future behaviour. Additionally, this work has partly revealed the magma origin of the three volcanic systems as well as allowing speculations on factors controlling changing eruption frequency in relation to different geological settings of volcanoes.

8. References

Ablay GJ, Kearey P (2000) Gravity constraints on the structure and volcanic evolution of Tenerife, Canary Islands. Journal of Geophysical Research-Solid Earth 105(B3):5783-5796.

Albarede F (1993) Residence Time Analysis of Geochemical Fluctuations in Volcanic Series. Geochimica Et Cosmochimica Acta 57(3):615-621.

Alfaro RB, Brandsdóttir B, Rowlands DP, White RS, Gudmundsson MT (2007) Structure of the Grímsvötn central volcano under the Vatnajökull icecap, Iceland. Geophysical Journal International 168:863-876.

Alloway BV, Larsen G, Lowe DJ, Shane P, Westgate JA (2007) Tephrochronology. In: Elias SA (ed) Encyclopedia of Quaternary Science. Elsevier, pp 2869-2898.

Arnalds Ó (2004) Volcanic soils of Iceland. Catena 56(1-3):3-20.

Bindeman IN, Sigmarsson O, Eiler J (2006) Time constraints on the origin of large volume basalts derived from O-isotope and trace element mineral zoning and U-series disequilibria in the Laki and Grimsvotn volcanic system. Earth and Planetary Science Letters 245(1-2):245-259.

Bjarnason IT, Wolfe CJ, Solomon SC, Gudmundson G (1996) Initial results from the ICEMELT experiment: Body-wave delay times and shear-wave splitting across Iceland (vol 23, pg 459, 1996). Geophysical Research Letters 23(8):903-903.

Björck S, Ingólfsson Ó, Haflidason H, Hallsdóttir M, Anderson NJ (1992) A high resolution record of the North Atlantic ash zone 1 and the last glacial-interglacial environment changes in Iceland. Boreas 21:15-22.

Björnsson A (1985) Dynamics of crustal rifting in NE Iceland. Journal of Geophysical Research 90:10151-10162.

Björnsson H, Einarsson P (1990) Volcanoes beneath Vatnajökull, Iceland: Evidence from radio echo-sounding, earthquake and jökulhlaups. Jökull 40:147-168.

Boygle J (2004) Towards a Holocene tephrochronology for Sweden: geochemistry and correlation with the North Atlantic tephra stratigraphy. Journal of Quaternary Science 19(2):103-109.

Chauvel C, Hémond C (2000) Melting of a complete section of recycled oceanic crust: Trace element and Pb isotopic evidence from Iceland. Geochemstry, Geophysics, Geosystems 1 Paper number 1999GC000002.

Condomines M, Tanguy JC, Michaud V (1995) Magma Dynamics at Mt Etna - Constraints from U-Th-Ra-Pb Radioactive Disequilibria and Sr Isotopes in Historical Lavas. Earth and Planetary Science Letters 132(1-4):25-41.

Cortini M, Scandone R (1982) The Feeding System of Vesuvius between 1754 and 1944. Journal of Volcanology and Geothermal Research 12(3-4):393-400.

Devidal JL, Sigmarsson O, Óladóttir BA, Larsen G (2008) Sodium loss during electron microprobe analysis of Hekla tephra and empirical corrections. In: IAVCEI 2008 General Assembly. Reykjavík, Iceland, 17-22 August.

Dugmore A (1989a) Tephrochronological studies of Holocene glacier fluctuations in South Iceland. In: Oerlemans J (ed) Glacier Fluctuations and Climate Change. Kluwer Academic, Dordrecht, pp 37-55.

Dugmore AJ (1989b) Iceland volcanic ash in late-Holocene peats in Scotland. Scottish Geographical Magazine 105:169-172.

Dugmore AJ, Newton A (1998) Holocene tephra layers in the Faroe Islands. Fróðskaparrit 46:191-204.

Dugmore AJ, Shore JS, Cook GT, Newton AJ, Edwards KJ, Larsen G (1995) The radiocarbon dating of Icelandic tephra layers in Britain and Iceland. Radiocarbon 37(2):379-388.

Einarsson P (1991) Earthquakes and Present-Day Tectonism in Iceland. Tectonophysics 189(1-4):261-279.

Einarsson P (2008) Plate boundaries, rifts and transforms in Iceland. Jökull 58:35-58

Einarsson P, Brandsdóttir B, Gudmundsson MT, Björnsson H, Grönvold K, Sigmundsson F (1997) Center of the Iceland hotspot experiences volcanic unrest. Eos Trans. AGU, 78(35):369.

Eiríksson J, Larsen G, Knudsen KL, Heinemeier J, Simonarson LA (2004) Marine reservoir age variability and water mass distribution in the Iceland Sea. Quaternary Science Reviews 23(20-22):2247-2268.

Fitton JG, Kilburn CRJ, Thirlwall MF, Hughes DJ (1983) 1982 Eruption of Mount Cameroon, West-Africa. Nature 306(5941):327-332.

Friedman JD, Williams RS, Thorarinsson S, Pálmason G (1972) Infrared emission from Kverkfjöll subglacial volcanic and geothermal area, Iceland. Jökull 22:27-43.

Gehrels MJ, Newnham RM, Lowe DJ, Wynne S, Hazell ZJ, Caseldine C (2006) Towards rapid assay of cryptotephra in peat cores: Review and evaluation of various methods. Quaternary International 178(1):68-84.

Gíslason SR, Oelkers EH (2003) Mechanism, rates, and consequences of basaltic glass dissolution: II. An experimental study of the dissolution rates of basaltic glass as a function of pH and temperature. Geochimica et Cosmochimica Acta 67(20):3817-3832.

Grange LI (1931) Volcanic-ash showers. A geological reconnaissance of volcanic-ash showers of the central part of the North Island. New Zealand Journal of Science and Technology 12:228-240.

Grove TL (2000) Origin of Magmas. In: Sigurdsson H (ed) Encyclopedia of Volcanoes. Academic press, San Diego, pp 133-149.

Grönvold K, Makipaa H (1978) Chemical composition of Krafla lavas. In: Nordic Volcanological Institude Rep. 7816.

Grönvold K, Jóhannesson H (1984) Eruption in Grímsvötn 1983: Course of events and chemical studies of the tephra. Jökull 34:1-11.

Grönvold K, Óskarsson N, Johnsen SJ, Clausen HB, Hammer CU, Bond G, Bard E (1995) Ash Layers from Iceland in the Greenland Grip Ice Core Correlated with Oceanic and Land Sediments. Earth and Planetary Science Letters 135(1-4):149-155.

Gudmundsson Á (1983) Form and Dimensions of Dykes in Eastern Iceland. Tectonophysics 95(3-4):295-307.

Gudmundsson Á (1984) Formation of dykes, feeder-dykes, and the intrusion of dykes from magma chambers. Bulletin of Volcanology 47:537-550.

Gudmundsson Á (1995) Infrastructure and Mechanics of Volcanic Systems in Iceland. Journal of Volcanology and Geothermal Research 64(1-2):1-22.

Gudmundsson Á (2000) Dynamics of volcanic systems in Iceland: Example of tectonism and volcanism at juxtaposed hot spot and mid-ocean ridge systems. Annual Review of Earth and Planetary Sciences 28:107-140.

Gudmundsson MT, Björnsson H (1991) Eruptions in Grímsvötn, Vatnajökull, Iceland, 1934-1991. Jökull 41:21-46.

Gudmundsson MT, Milsom J (1997) Gravity and magnetic studies of the subglacial Grímsvötn volcano, Iceland: Implications for crustal and thermal structure. Journal of Geophysical Research-Solid Earth 102(B4):7691-7704.

Gudmundsson MT, Högnadóttir T (2007) Volcanic systems and calderas in the Vatnajökull region, central Iceland: Constraints on crustal structure from gravity data. Journal of Geodynamics 43(1):153-169.

Gudmundsson T, Björnsson H, Thorvaldsson G (2004) Organic carbon accumulation and pH changes in an Andic Gleysol under a long-term fertilizer experiment in Iceland. Catena 56(1-3):213-224.

Haflidason H, Larsen G, Ólafsson G (1992) The Recent Sedimentation History of Thingvallavatn, Iceland. Oikos 64(1-2):80-95.

Haflidason H, Eiríksson J, Van Kreveld S (2000) The tephrochronology of Iceland and the North Atlantic region during the Middle and Late Quaternary: a review. Journal of Quaternary Science 15(1):3-22.

Halldórsson SA, Óskarsson N, Grönvold K, Sigurdsson G, Sverrisdóttir G, Steinthórsson S (2008) Isotopic-heterogeneity of the Thjorsa lava-Implications for mantle sources and crustal processes within the Eastern Rift Zone, Iceland. Chemical Geology 255(3-4):305-316.

Hammer CU, Clausen HB, Dansgaard W (1980) Greenland ice sheet evidence of postglacial volcanism and its climatic impact. Nature 288:230-235.

Hardarson BS, Fitton JG, Ellam RM, Pringle MS (1997) Rift relocation-a geochemical and geochronological investigation of a palaeo-rift in northwest Iceland. Earth and Planetary Science Letters 153:181-196.

Hards VL (1995) The evolution of the Snæfell volcanic centre, Eastern Iceland. Unpublished PhD theses from the University of Durham, Durham, p 324.

Hémond C, Condomines M, Fourcade S, Allégre CJ, Óskarsson N, Javoy M (1988) Thorium, Strontium and Oxygen Isotopic Geochemistry in Recent Tholeiites from Iceland - Crustal Influence on Mantle-Derived Magmas. Earth and Planetary Science Letters 87(3):273-285.

Hémond C, Arndt NT, Lichtenstein U, Hofmann AW, Óskarsson N, Steinthórsson S (1993) The Heterogeneous Iceland Plume - Nd-Sr-O Isotopes and Trace-Element Constraints. Journal of Geophysical Research-Solid Earth 98(B9):15833-15850.

Hjartarson Á (1994) Environmental changes in Iceland following the Great Þjórsá Lava Eruption 7800 14C years BP. In: Stötter J, Wilhelm F (eds) Environmental Change in Iceland. Munchen, pp 147-155.

Hreinsdóttir S, Einarsson P, Sigmundsson F (2001) Crustal deformation at the oblique spreading Reykjanes Peninsula, SW Iceland: GPS measurements from 1993 to 1998. Journal of Geophysical Research 106(B7):13803-13816.

Hunt JB, Hill PG (1993) Tephra geochemistry: a discussion of some persistent analytical problems. The Holocene 3:271-278.

Hunt JB, Hill PG (2001) Tephrological implications of beam size-sample-size effects in electron microprobe analysis of glass shards. Journal of Quaternary Science 16(2):105-117.

Höskuldsson Á, Imsland P (1998) Snæfell - Eldfjall á gosbelti framtíðar (Geology of Snæfell, an intraplate volcano in Eastern Iceland). Glettingur 8(2-3):22-30.

Ingólfsson Ó, Norddahl H, Haflidason H (1995) Rapid Isostatic Rebound in Southwestern Iceland at the End of the Last Glaciation. Boreas 24(3):245-259.

Ito G (2001) Reykjanes 'V'-shaped ridges originating from a pulsing and dehydrating mantle plume. Nature 411(6838):681-684.

Jakobsson SP (1979a) Outline of the petrology of Iceland. Jökull 29:57-73.

Jakobsson SP (1979b) Petrology of recent basalts of the Eastern Volcanic zone, Iceland. Acta Naturalia Islandica 26:1-103.

Jakobsson SP, Jónasson K, Sigurdsson IA (2008) The three igneous rock series of Iceland. Jökull 58:117-138.

Jarosewich E, Nelen JA, Borberg JA (1979) Electron microprobe reference samples for mineral analysis. In: Fudali RF (ed) Smithsonian Institution Contributions to the Earth Sciences No. 22. Smithsonian Institution Press, Washington, D.C., pp 68-72.

Jóhannesson H (1975) Structure and petrochemistry of the Reykjadalur central volcano and the surrounding areas, Midwest Iceland. Unpublished PhD theses from the University of Durham, Durham, p 273.

Jóhannesson H, Sæmundsson K (1998a) Geological map of Iceland, 1:500,000. Tectonics. Icelandic Institude of Natural History and Iceland Geodetic Survey, Reykjavík.

Jóhannesson H, Sæmundsson K (1998b) Geological map of Iceland, 1:500,000. Icelandic Institude of Natural History and Iceland Geodetic Survey, Reykjavík.

Jull M, McKenzie D (1996) The effect of deglaciation on mantle melting beneath Iceland. Journal of Geophysical Research-Solid Earth 101(B10):21815-21828.

Kaldal I (1993) Fróðleiksmolar um gamla gjósku í Búdarhálsi. In: Geoscience Society of Iceland Spring meeting. Reykjavík, pp 36-37.

Kaldal I, Víkingsson S (1990) Early Holocene deglaciation in Central Iceland. Jökull 40:51-68.

Kaufmann DS, Ager TA, Anderson NJ, Anderson PM, Andrews JT, Bartlein PJ, Brubaker LB, Coats LL, Cwynar LC, Duvall ML, Dyke AS, Edwards ME, Eisner WR, Gajewski K, Geirsdóttir A, Hu FS, Jennings AE, Kaplan MR, Kerwin MW, Lozhkin AV, MacDonald GM, Miller GH, Mock CJ, Oswald WW, Otto-Bliesner BL, Porinchu DF, Ruhland K, Smol

JP, Steig EJ, Wolfe BB (2004) Holocene thermal maximum in the western Arctic (0-180°). Quaternary Science Reviews 23(5-6):529-560.

Keller J (1981) Quaternary tephrochronology in the Mediterranean. In: Self S, Sparks RSJ (eds) Tephra studies. D. Reidel, Dordrecht, pp 227-244.

Kinzler RJ, Grove TL (1992a) Primary Magmas of Mid-Oceanic Ridge Basalts 1. Experiments and Methods. Journal of Geophysical Research 97(B5):6885-6906.

Kinzler RJ, Grove TL (1992b) Primary Magmas of Mid-Oceanic Ridge Basalts 2. Applications. Journal of Geophysical Research 97(B5):6907-6926.

Kokfelt TF, Hoernle K, Hauff F, Fiebig J, Werner R, Garbe-Schonberg D (2006) Combined trace element and Pb-Nd-Sr-O isotope evidence for recycled oceanic crust (upper and lower) in the Iceland mantle plume. Journal of Petrology 47(9):1705-1749.

Kristjánsdóttir GB, Stoner JS, Jennings AE, Andrews JT, Grönvold K (2007) Geochemistry of Holocene cryptotephras from the north Iceland shelf (MD99-2269): intercalibration with radiocarbon and palaeomagnetic chronostratigraphies. Holocene 17(2):155-176.

Lacasse C, Carey S, Sigurdsson H (1998) Volcanogenic sedimentation in the Iceland Basin: influence of subaerial and subglacial eruptions. Journal of Volcanology and Geothermal Research 83(1-2):47-73.

Lacasse C, Sigurdsson H, Jóhannesson H, Paterne M, Carey S (1995) Source of Ash-Zone-1 in the North-Atlantic. Bulletin of Volcanology 57(1):18-32

LaFemina PC, Dixon TH, Malservisi R, Árnadóttir Th, Sturkell E, Sigmundsson F, Einarsson P (2005) Geodetic GPS measurements in south Iceland: Strain accumulation and partitioning in a propagating ridge system. Journal of Geophysical Research-Solid Earth 110, B11405, doi:10.1029/2005JB003675.

Larsen G (1981) Tephrochronology by microprobe glass analysis. In: Self S, Sparks RSJ (eds) Tephra Studies. D. Reidel, Dordrecht, pp 95-102.

Larsen G (1982) Gjóskutímatal Jökuldals og nágrennis. In: Thórarinsdóttir H (ed) Eldur er í norðri. Sögufélag, Reykjavík, pp 51-65.

Larsen G (1984) Recent volcanic history of the Veidivötn fissure swarm, Southern Iceland. An approach to volcanic risk assessement. Journal of Volcanology and Geothermal Research 22:33-58.

Larsen G (1992) Gjóskulagið úr Heklugosinu 1158. In: Geoscience Society of Iceland, Spring Meeting 1992. Reykjavík, pp 25-27.

Larsen G (1996) Gjóskutímatal og fjóskulög frá tíma norræns landnáms á Íslandi. In: Grímsdóttir GÁ (ed) Um landnám á Íslandi. Vísindafélag Íslendinga (Societas Scientarum Islandica), Reykjavík, pp 81-106.

Larsen G (2000) Holocene eruptions within the Katla volcanic system, south Iceland: Characteristics and environmental impact. Jökull 49:1-28.

Larsen G, Thorarinsson S (1977) H-4 and other acid Hekla tephra layers. Jökull 27:28-46.

Larsen G & Vilmundardóttir EG (1985) Gjóskurannsóknir á Þjórsársvæði 1983-1984. Orkustofnun (National Energy Authority), Research Report OS-85037/VOD-16B, Reykjavik, pp 20.

Larsen G, Gudmundsson MT (1997) Gos í eldstöðvum undir Vatnajökli eftir 1200 AD. In: Haraldsson H (ed) Vatnajökull. Gos og hlaup 1996. Vegagerðin, Reykjavík., pp 23-36.

Larsen G, Eiríksson J (2008a) Late Quaternary terrestrial tephrochronology of Iceland - frequency of explosive eruptions, type and volume of tephra deposits. Journal of Quaternary Science 23(2):109-120.

Larsen G, Eiríksson J (2008b) Holocene tephra archives and tephrochronology in Iceland - a brief overview. Jökull 58:229-250.

Larsen G, Gudmundsson MT, Björnsson H (1998) Eight centuries of periodic volcanism at the centre of the Icelandic hotspot revealed by glacier tephrostratigraphy. Geology 26:943-946.

Larsen G, Dugmore A, Newton A (1999) Geochemistry of historical-age silicic tephras in Iceland. Holocene 9(4):463-471.

Larsen G, Newton AJ, Dugmore AJ, Vilmundardóttir EG (2001) Geochemistry, dispersal, volumes and chronology of Holocene silicic tephra layers form the Katla volcanic system, Iceland. Journal of Quaternary science 16:119-132.

Larsen G, Eiríksson J, Knudsen KL, Heinemeier J (2002) Correlation of late Holocene terrestral and marine tephra markers north Iceland: implications for reservoir age changes. Polar Research 21(2):283-290.

Le Bas MJ, Le Maitre RW, Streckeisen A, Zanettin B (1986) A chemical classification of volcanic rocks based on the total alkali-silica diagram. Journal of Petrology 22:745-750.

Longerich H, Diegor W (2001) Introduction to Mass spectrometry. In: Sylvester P (ed) Laser-Ablation-ICPMS in the Earth Sciences Principles and Applications. Mineralogical Association of Canada, St. John's Newfoundland, pp 1-21.

Maclennan J, Jull M, McKenzie D, Slater L, Grönvold K (2002) The link between volcanism and deglaciation in Iceland. Geochemstry, Geophysics, Geosystems 3(11).

Mangerud J, Furnes H, Johanssen J (1986) A 9000 year old ash bed on the Faroe Islands. Quaternary Research 26:262-265.

Mangerud J, Lie SE, Furnes H, Kristianssen IL, Lomo L (1984) A Younger Dryas ash bed in western Norway and its possible correlation with tephra in cores from the Norwegian Sea and the North Atlantic. Quaternary Research 21:85-104.

Martin E, Sigmarsson O (2007) Low-pressure differentiation of tholeiitic lavas as recorded in segregation veins from Reykjanes (Iceland), Lanzarote (Canary Islands) and Masaya (Nicaragua). Contributions to Mineralogy and Petrology 154(5):559-573.

Melengreu B, Lénat J-F, Froger J-L (1999) Structure of Réunion Island (Indian Ocean) inferred from the interpretation of gravity anomalies. Journal of Volcanology and Geothermal Research 88:131-146.

Merlet C (1994) An Accurate Computer Correction Program for Quantitative Electron-Probe Microanalysis. Mikrochimica Acta 114:363-376.

Meyer PS, Sigurdsson H, Schilling JG (1985) Petrological and geochemical variations along Iceland's Neovolcanic zones. Journal of Geophysical Research 90:10043-10072.

Michaut C, Jaupart C (2005) A new model for crystallisation and differentiation in magma chambers. Eos Trans AGU 86(52), Fall Meet Suppl, V11A-03.

Miyashiro A (1978) Nature of alkalic volcanic rock series. Contributions to Mineralogy and Petrology 66:91-104.

Nicholson H (1990) The magmatic evolution of Krafla, NE Iceland. Unpublished PhD theses from the University of Edinburgh, Edinburgh, p 286.

Nielsen CH, Sigurdsson H (1981) Quantitative Methods for Electron Micro-Probe Analysis of Sodium in Natural and Synthetic Glasses. American Mineralogist 66(5-6):547-552.

Norddahl H, Haflidason H (1992) The Skógar Tephra, a Younger Dryas Marker in North Iceland. Boreas 21(1):23-41.

Oddsson B (2007) The Grímsvötn eruption in 2004, Dispersal and total mass of tephra and comparison with plume transport models. Unpublished Masters theses from the University of Iceland, Reykjavík, p 112.

Óladóttir BA, Larsen G, Thordarson T, Sigmarsson O (2005) The Katla volcano S-Iceland: Holocene tephra stratigraphy and eruption frequency. Jökull 55:53-74.

Óladóttir BA, Thordarson T, Larsen G, Sigmarsson O (2007) Survival of the Mýrdalsjökull ice cap through the Holocene thermal maximum?-Evidence from sulfur contents in Katla tephra layers (Iceland) from the last ~8400 years. Annals of Glaciology 45:183-188.

Óladóttir BA, Sigmarsson O, Larsen G, Thordarson T (2008) Katla volcano, Iceland: magma composition, dynamics and eruption frequency as recorded by Holocene tephra layers. Bulletin of Volcanology 70(4):475-493.

Óskarsson N, Sigvaldason GE, Steinthórsson S (1982) A dynamic model of rift zone petrogenesis and the regional petrology of Iceland. Journal of Petrology 23:28-74.

Óskarsson N, Steinthórsson S, Sigvaldason GE (1985) Iceland Geochemical Anomaly - Origin, Volcanotectonics, Chemical Fractionation and Isotope Evolution of the Crust. Journal of Geophysical Research-Solid Earth and Planets 90(Nb12):11-25.

Pagli C, Sigmundsson F, Pedersen R, Einarsson P, Árnadóttir Th, Feigl KL (2007) Crustal deformation associated with the 1996 Gjálp subglacial eruption, Iceland: InSAR studies in affected areas adjacent to the Vatnajökull ice cap. Earth and Planetary Science Letters 259(1-2):24-33.

Persson C (1971) Tephorchronological investigation of peat deposits in Scandinavia and on the Faroe Islands. Geological Survey of Sweden C 656:34.

Potts PJ (1987) A Handbook of Silicate Rock Analysis. Blackie Academic & Professional, Wiltshire, p 622.

Pyle DM (1999) Widely dispersed Quaternary tephra in Africa. Global and Planetary Change 21(1-3):95-112.

Ran LH, Jiang H, Knudsen KL, Eiríksson J (2008) A high-resolution Holocene diatom record on the North Icelandic shelf. Boreas 37(3):399-413.

Reed SJB (1996) Electron Microprobe and Scanning Electron Microscopy in Geology. Cambridge University Press, Cambridge.

Saunders AD, Fitton JG, Kerr AD, Norry MJ, Kent RW (1997) North Atlantic Province. In: Mahoney JJ, Coffin MF (eds) Large igneous provinces: continental, oceanic, and planetary flood volcanism. Geophysical Monograph 100, American Geophysical Union, Washington DC, pp 44-93.

Schuessler JA, Schoenberg R, Sigmarsson O (2009) Iron and lithium isotope systematics of the Hekla volcano, Iceland - Evidence for Fe isotope fractionation during magma differentiation. Chemical geology 258:78-91.

Sejrup HP, Sjoholm J, Furnes H, Beyere I, Eide L, Jansen E, Mangerud J (1989) Quaternary tephrochronology on the Iceland Plateau, north of Iceland. Journal of Quaternary Science 6:109-114.

Shane P (2000) Tephrochronology: a new Zealand case study. Earth-Science Reviews 49(1-4):223-259.

Sigmarsson O, Condomines M, Fourcade S (1992) A Detailed Th, Sr and O Isotope Study of Hekla - Differentiation Processes in an Icelandic Volcano. Contributions to Mineralogy and Petrology 112(1):20-34.

Sigmarsson O, Karlsson HR, Larsen G (2000) The 1996 and 1998 subglacial eruptions beneath the Vatnajökull ice sheet in Iceland: contrasting geochemical and geophysical inferences on magma migration. Bulletin of Volcanology 61(7):468-476.

Sigmarsson O, Condomines M, Grönvold K, Thordarson T (1991) Extreme Magma Homogeneity in the 1783-84 Lakagígar Eruption - Origin of a Large Volume of Evolved Basalt in Iceland. Geophysical Research Letters 18(12):2229-2232.

Sigmundsson F (2006) Iceland geodynamics: crustal deformation and divergent plate tectonics. Springer; Praxis, Berlin.

Sigurdsson H, Loebner B (1981) Deep sea record of Cenozoic explosive volcanism in the North Atlantic. In: Self S, Sparks RSJ (eds) Tephra Studies. Reidel, Dordrecht, pp 289-316.

Sigvaldason GE, Steinthórsson S (1974) Chemistry of tholeiitic basalts from Iceland and their relation to the Kverkfjöll hot spot. In: Kristjánsson L (ed) Geodynamics of Iceland and the North Atlantic Area. D. Reidel, Dordrecht, Holland, pp 155-164.

Sigvaldason GE, Annertz K, Nilsson M (1992) Effect of glacier loading/deloading on volcanism: Postglacial volcanic production rate of the Dyngjufjöll area, central Iceland. Bulletin of Volcanology 54:385-392.

Simkin T, Siebert L (1994) Volcanoes of the World. Smithsonian Institution, Tuscon, Arizona, p 349.

Simkin T, Siebert L (2000) Earth's Volcanoes and Eruptions: An Overview. In: Sigurdsson H (ed) Encyclopedia of Volcanoes. Academic press, San Diego, pp 249-262.

Sjoholm J, Sejrup HP, Furnes H (1991) Quaternary Volcanic Ash Zones on the Iceland Plateau, Southern Norwegian Sea. Journal of Quaternary Science 6(2):159-173.

Spudis PD (2000) Volcanism on the Moon. In: Sigurdsson H (ed) Encyclopedia of Volcanoes. Academic press, San Diego, pp 697-708.

Steinthórsson S (1977) Tephra layers in a drill core from the Vatnajökull Ice Cap. Jökull 27:2-27.

Steinthórsson S, Óskarsson N, Sigvaldason GE (1985) Origin of alkali basalts in Iceland : a plate tectonic model. Journal of Geophysical Research 90((B12)):10027-10042.

Stuiver M, Reimer PJ, Bard E, Beck JW, Burr GS, Hughen KA, McCormac FG, Plicht JVD, Spurk M (1998) INTCAL98 Radiocarbon age calibration 24,000-0 BP. Radiocarbon 40:1041-1083.

Sturkell E, Einarsson L, Sigmundsson F, Hreinsdóttir S, Geirsson H (2003) Deformation of Grímsvötn volcano, Iceland: 1998 eruption and subsequent inflation. Geophysical Research Letters 30(4), 1182, doi:10.1029/2002GL016460.

Sun SS, McDonough WF (1989) Chemical and isotopic systematics of oceanic basalts: Implication for the mantle composition and processes. Geological Society, Special Publications 42:313-345.

Sæmundsson K (1978) Fissure swarms and central volcanoes of the neovolcanic zones of Iceland. Geological Journal Special Issue 10:451-432.

Sæmundsson K (1979) Outline of the geology of Iceland. Jökull 29:7-29.

Sæmundsson K (1991) Jarðfræði Kröflukerfisins (Geology of the Krafla volcanic system). In: Garðarsson AÓ, Einarsson Á (eds) Náttúra Mývatns. Hið Íslenska náttúrufræðifélag, Reykjavík.

Thorarinsson S (1944) Tefrokronologiska studier pa Island. Geografisca Annaler 26:1-217.

Thorarinsson S (1950) Jökulhlaup og eldgos á jökulvatnasvæði Jökulsár á Fjöllum. Náttúrufræðingurinn 20:113-133.

Thorarinsson S (1952) Hverfjall II. Aldur Hverfjalls og myndun (Hverfjall: Age and formation). Náttúrufræðingurinn 22(4):146-172.

Thorarinsson S (1958) The Öræfajökull eruption of 1362. Acta Naturalia Islandica 2:1-100.

Thorarinsson S (1961) Uppblástur á Íslandi í ljósi öskulagarannsókna. Ársrit Skógræktarfélags Íslands 1960-1961:17-54.

Thorarinsson S (1967) The eruptions of Hekla in historical times. In: Einarsson T, Kjartansson G, Thorarinsson S (eds) The eruption of Hekla 1947-1948. Societas Scientiarum Islandica, Reykjavík, pp 1-177.

Thorarinsson S (1968) Heklueldar. Sögufélagið, Reykjavík, p 185.

Thorarinsson S (1971) Aldur ljósu gjóskulaganna úr Heklu samkvæmt leiðréttu geislakolstímatali. Náttúrufræðingurinn 41:99-105.

Thorarinsson S (1974) Vötnin stríð. Bókaútgáfa Menningarsjóðs, Reykjavík, p 254.

Thorarinsson S (1980) Langleiðir gjósku úr þremur Kötlugosum. Jökull 31:65-73.

Thorarinsson S (1981) Tephra studies and tephrochronology: A historical review with special reference to Iceland. In: Self S, Sparks RSJ (eds) Tephra Studies. D. Reidel Publishing Company, Dordrecht, Holland, pp 1-12.

Thorarinsson S, Sæmundsson K (1979) Volcanic activity in historical times. Jökull 29:29-32.

Thordarson T, Self S (1993) The Laki (Skaftár-Fires) and Grímsvötn Eruptions in 1783-1785. Bulletin of Volcanology 55(4):233-263.

Thordarson T, Höskuldsson Á (2002) Iceland Terra Publishing, Harpenden, UK, p 200.

Thordarson T, Larsen G (2007) Volcanism in Iceland in historical time: Volcano types, eruption styles and eruptive history. Journal of Geodynamics 43(1):118-152.

Thordarson T, Höskuldsson Á (2008) Postglacial volcanism in Iceland. Jökull 58:197-228.

Thornber CR, Sherrod DR, Siems DR, Heliker CC, Meeker GP, Oscarsson RL, Kauahikaua JP (2002) Whole rock and glass major-element geochemistry of Kilauea Volcano, Hawaii,

near-vent eruptive products: September 1994 through September 2001. In: USGS, open file report 02-17.

Uragami K, Yamada S, Nagamura Y (1933) Studies on the volcanic ashes in Hokkaido. Bulletin of Volcanological Society of Japan 1:79-90.

van Achterbergh E, Ryan CG, Jackson SE, Griffin W (2001) Data reduction software for La-ICP-MS. In: Sylvester P (ed) Laser ablation ICP-MS in Earth Science Principles and Applications. Mineralogical Association of Canada, pp 239-243.

van den Bogaard C, Schminke HU (2002) Linking the North Atlantic to central Europe: a high-resolution Holocene tephrochronological record from northern Germany. Journal of Quaternary science 17:3-20.

Vilmundardóttir EG, Larsen G (1986) Productivity pattern of the Veiðivötn fissure swarm, southern Iceland, in postglacial time. Preliminary results. In: 17 Nordiska Geologmötet 1986. Helsingfors Universitet, Helsinki, Finnland, p 214.

Vilmundardóttir EG, Snorrason SP, Larsen G (2000) Geological map of subglacial volcanic area soutwest of Vatnajökull ice cap, Iceland, 1:50.000. National Energy Authority and National Power Company, Reykjavík.

Waagstein R, Jóhansen J (1968) Tre vulkanske askelag fra Færøerne. Meddelser fra Dansk Geologisk Forening 18:257-264.

Walker GPL (1963) The Breiddalur central volcano, eastern Iceland. The Quarterly Journal of the Geological Society of London 119:29-63.

Wallace P, Anderson Jr. AT (2000) Volatiles in magmas. In: Sigurdsson H (ed) Encyclopedia of Volcanoes. Academic press, San Diego, pp 149-170.

Wastegard S (2005) Late Quaternary tephrochronology of Sweden: a review. Quaternary International 130:49-62.

Wastegard S, Turney CSM, Lowe JJ, Roberts SJ (2000) New discoveries of the Vedde Ash in southern Sweden and Scotland. Boreas 29(1):72-78.

White RS, Bown JW, Smallwood JR (1995) The Temperature of the Iceland Plume and Origin of Outward-Propagating V-Shaped Ridges. Journal of the Geological Society 152:1039-1045.

Wilson SA (1997) The collection, preparation, and testing of USGS reference material BCR-2, Columbia River, Basalt. In: U.S. Geological Survey Open-File Report 98-xxx.

Wolfe CJ, Bjarnason IT, VanDecar JC, Solomon SC (1997) Seismic structure of the Iceland mantle plume. Nature 385(6613):245-247.

Zielinski GA, Mayewski PA, Meeker LD, Grönvold K, Germani MS, Whitlow S, Twickler MS, Taylor K (1997) Volcanic aerosol records and tephrochronology of the Summit, Greenland, ice cores. Journal of Geophysical Research-Oceans 102(C12):26625-26640.